UNIVERSITY OF GHANA

COLLEGE OF BASIC AND APPLIED SCIENCES

TOLERANCE OF *PLASMODIUM FALCIPARUM* TO ARTEMETHER-LUMEFANTRINE IN THE GAMBIA

A THESIS SUBMITTED TO THE BOARD OF GRADUATE STUDIES, UNIVERSITY OF GHANA, LEGON, IN PARTIAL FULFILMENT OF THE REQUIREMENTS FOR THE AWARD OF DOCTOR OF PHILOSOPHY IN MOLECULAR CELL BIOLOGY OF INFECTIOUS DISEASES

BY

HADDIJATOU MBYE

(10601182)

WEST AFRICAN CENTRE FOR CELL BIOLOGY OF INFECTIOUS PATHOGENS

DECEMBER 2020

DECLARATION

I hereby declare that the work presented in this thesis was done by me, Haddijatou Mbye after registration for a PhD at the Department of Biochemistry, Cell and Molecular Biology, University of Ghana under the supervision of Dr. Alfred A. Ngwa (Medical Research Council at London School of Hygiene and Tropical Medicine), Prof. Neils B. Quashie (West African Centre for Cell Biology of Infectious Pathogens, University of Ghana) and Dr. Marcus Lee (Wellcome Sanger Institute).

All references have been duly cited.

…… ……

Haddijatou Mbye (Student) Dr. Alfred A. Ngwa (Supervisor)

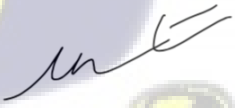

…… ……

Prof. Neils B. Quashie (Co-supervisor) Dr. Marcus Lee (Co-supervisor)

ABSTRACT

Antimalarial drug resistance contributes significantly to obstacles in reducing the global burden of malaria especially in sub-Saharan Africa (sSA) where the disease is most prevalent. Resistance to artemisinin-based combination therapies (ACTs), the only recommended frontline drugs for the treatment of uncomplicated malaria is now widespread in South East Asia (SEA). However, ACTs remain efficacious in sSA though *in vivo* delayed parasite clearance and *in vitro* reduced susceptibility to both components of the drug has been reported. Resistance to ACTs is therefore anticipated especially with its sustained use in endemic regions and the recent report of the emergence of *de novo Pfk13* mutation that is now spreading in Rwanda. In The Gambia where artemether-lumefantrine (AL) is the first-line drug used for over 10 years, a steady increase in parasite tolerance to lumefantrine (LUM) was observed over a period of 4 years which strongly correlated with reported directional selection on a cysteine desulfarase gene *(Pfnfs1)*. These findings are concerning and require continuous drug surveillance to track spontaneous development of AL resistant parasites and determine pathways to resistance development.

This study therefore sought to investigate the prevalence and mechanisms of parasite tolerance to AL in The Gambia. A novel *ex vivo* drug susceptibility assay suitable to simultaneously assess parasite responses to both drugs used in AL was developed and used to assess drug susceptibility profiles of circulating parasites in western Gambia. This assay was then used to confirm identified potent compounds from the Medicines for Malaria Venture pathogen box effective against the erythrocytic stages of the parasite for future development into new antimalarial drugs. The prevalence of known drug resistance markers was assessed and novel markers that could be associated with drug resistance identified using both regression analysis and GWAS approach. Finally, CRISPR-Cas9 genome editing was used to functionally validate *Pfnfs1* for its involvement in LUM tolerance using gene editing approaches.

Results generated from this study revealed that LUM and dihydroartemisinin tolerant *P. falciparum* parasites are circulating in western Gambia. Three hit compounds from the MMV pathogen box were also identified using the PSRA and these showed to be more potent than CQ, two of which have higher potencies than the fast-acting DHA. These compounds should be prioritised and exploited as therapeutic agents. The present work also revealed that wildtype *Pfmdr1* variants selected by LUM are seen to be increasing in the western Gambia population which could be as a result of continuous pressure from AL. Surprisingly, mutant *Pfcrt* haplotypes remained at more than 50% in the population, probably driven by the unofficial use of chloroquine available from private vendors or mefloquine which is used in combination with artesunate as the first-line drug in neighbouring Senegal, with whom there is significant human migration. sulfadoxine-pyrimethamine (SP) resistant markers are in fixation, and these are continuously selected for by the use of SP in seasonal malaria chemotherapy and intermittent preventive treatment in pregnancy. Several regions on the *P. falciparum* genome were observed to be under recent signatures of selection and a number of alleles, including a cluster of invasion loci on chromosome 10 were observed to be weakly associated with drug response, warranting further investigation. Finally, the association of *Pfnfs1* with LUM tolerance could not be established as recombinant parasites of interest were not recovered possibly due to fitness cost associated with the non-synonymous SNP.

Keywords:

Malaria, antimalarial drug resistance, *ex vivo* drug assays, high throughput screening genotyping, functional analysis, association studies

ACKNOWLEDGEMENT

After many years of hard work, I would like to first and foremost thank God the Almighty for giving me life and giving me the ability and strength to pursue my educational career all through the way. During this long and challenging but exciting journey, a lot of people stood by my side, day in and day out, never relenting in their duties. Today this success story that is about to be written in the annal of our history is all due to their support, steadfastness and encouragement.

My sincere thanks and gratitude first and foremost goes to my supervisor Dr Alfred A. Ngwa, who has never relented in guiding, encouraging and supporting me. You have always taken your time to give me the necessary support. To my co-supervisor, Prof. Neils Quashie, your support and input has been invaluable. I am sincerely grateful to Dr. Marcus Lee, Dr. Sophie Adjalley and all the laboratory members in the Malaria Programme for their support and guidance and for making my time at the Wellcome Sanger Institute a fantastic one. To my mentors, Dr Effua Usuf and Dr Joseph Okebe, thank you for your continuous guidance and encouragement.

The University of Ghana through my professors, colleagues and friends really made it an exceptional experience. To my colleagues, you made life in Ghana very exciting and a lively one for me. I say thank you so much! I am especially grateful to the Malaria Population Biology team at MRCG from whom I have gained so much knowledge and experience. Your support has been immeasurable. You all have been there throughout for me. Thank you!

In the Wolof culture, there is an adage that says, "If the dance of a baby is exciting, it is because the mother holds the arms of the baby". All the success that I am registering today could not have happened without the support of my family. To my mother Yaboye, you are a confidant, a strong pillar of support, a shoulder to cry on and a person that I can always run back to. To

my siblings, you have also been very supportive and have been there throughout for me. I am especially grateful to my husband for his invaluable support throughout this journey. You have gone a long way out to make sure that this thesis is completed.

Finally, I would like to acknowledge the study participants and their parents/guardians for providing the samples that enabled me to successfully perform a part of this study. To all those who have contributed toward the realisation of this work, I say THANK YOU!

TABLE OF CONTENTS

DECLARATION ..... *i*

ABSTRACT ..... *ii*

ACKNOWLEDGEMENT ..... *iv*

TABLE OF CONTENTS ..... *vi*

LIST OF FIGURES ..... *xi*

LIST OF TABLES ..... *xiii*

1.0 General introduction *1*

1.1 Background **1**

1.2 Conceptual framework **7**

1.3 Aim and specific objectives **9**

1.3.1 Specific objective 1 9

1.3.1.1 Hypothesis 1 9

1.3.1.2 Hypothesis 2 9

1.3.1.3 Rationale 10

1.3.2 Specific objective 2 11

1.3.2.1 Hypothesis 11

1.3.2.2 Rationale 11

1.3.3 Specific objective 3 12

1.3.3.1 Hypothesis 12

1.3.3.2 Rationale 13

2.0 Literature review *14*

2.1 Malaria epidemiology **14**

2.2 Malaria biology **17**

2.2.1. *Plasmodium* parasites 17

2.2.2 *Plasmodium falciparum* life-cycle 17

2.3 Malaria immunity and vaccine development 22

2.4 Malaria control and intervention strategies 23

2.4.1 Vector control 23

2.4.2 Malaria chemotherapy and chemoprevention 24

2.4.2.1 The history of antimalarial drugs 25

2.4.2.1.1 MMV compound libraries for antimalarial drug development 29

2.5 Threats to the control of malaria 30

2.5.1 Insecticide resistance 30

2.5.2 Antimalarial drug resistance 31

2.5.2.1 Evolution, spread and mechanisms of antimalarial drug resistance 31

2.5.2.2 Artemether-lumefantrine resistance development 36

2.5.2.3 Lumefantrine and cysteine desulfurase gene 37

2.6 Tools for surveillance of antimalarial drug efficacy status 40

2.6.1 CRISPR-Cas9 genome editing 40

3.0 Tolerance of Gambian Plasmodium falciparum to Dihydroartemisinin and Lumefantrine detected by Ex vivo Parasite Survival Rate Assay (PSRA) 43

3.1 Abstract 43

3.2 Introduction 44

3.3 Materials and Methods 46

3.3.1 Sample collection 46

3.3.2 Parasite processing for drug assays 48

3.3.3 Parasite Survival Rate Assay (PSRA) 49

3.3.4 Ring-stage survival assay (RSA) 52

3.3.5 Genotyping of selected drug resistance loci 52

3.3.6 Statistical analysis of drug survival rates 53

3.4 Results 54

3.4.1 Ring stage survival rates of field isolates by Microscopy and Flow cytometry . 55

3.4.2 *P. falciparum ex vivo* survival decreases with longer drug exposure..... 57

3.4.3 Distribution of PSRA sensitivities to AL..... 61

3.4.4 Consistent clusters of survival rate patterns to both DHA and LUM..... 64

3.4.5 Frequencies of drug resistance alleles from western Gambia in 2017 67

3.5 Discussion..... 70

4.0 Antimalarial activities of compounds in the MMV pathogen box 75

4.1 Abstract..... 75

4.2 Introduction..... 76

4.3 Materials and methods..... 78

4.1.1 *P. falciparum in vitro* parasite culture 78

4.1.2 Compounds from the MMV pathogen box 78

4.1.3 IC_{50} determination assay 78

4.1.4 Parasite survival rate assay (PSRA) 79

4.1.5 Statistical analysis..... 79

4.4 Results..... 80

4.1.6 Primary screen of compounds with antimalarial activity from the pathogen box reveals highly potent compounds..... 80

4.1.7 Re-evaluation of IC_{50} of compounds with high potencies 84

4.1.8 Parasite survival patterns following exposure to potent compounds 84

4.1.9 Parasite growth following 72 hours of drug exposure..... 88

4.5 Discussion..... 90

5.0 Linked variants across signatures of positive selection in the Plasmodium falciparum genome are associated with in vitro responses to artemisinin derivatives and partner drugs..... 94

5.1 Abstract 94

5.2 Introduction 95

5.3 Methods 97

5.3.1 Samples and populations 97

5.3.2 Population genetic analysis 97

5.3.3 *Ex vivo* drug susceptibility assay 99

5.3.4 Association analysis of *in vitro* drug sensitivity with genome-wide SNPs and regions of IBD 99

5.4 Results 100

5.4.1 Highly related regions of the genomes of recent *P. falciparum* population 100

5.4.2 Drug resistant allele frequencies from western Gambia in 2008 and 2014/15 . 103

5.4.3 Genome-wide association analysis 104

5.4.4 Relatedness and linkage between markers of selection with phenotypes 106

5.5 Discussion 108

6.0 Functional validation of Plasmodium falciparum cysteine desulfurase gene for its involvement in lumefantrine tolerance 110

6.1 Abstract 110

6.2 Introduction 111

6.3 Materials and methods 112

6.3.1 Guide RNA design and cloning 112

6.3.2 Donor design and assembly 116

6.3.3 *In vitro P. falciparum* parasite culture 118

6.3.4 Parasite transfections and drug selection 118

6.3.5 DNA extraction and screening of recombinant parasites 119

6.3.6 Drug susceptibility assays 120

6.4 Results 121

6.4.1 gRNA design and validated cloning into pDC2-cam-coCas9-U6.2-hDHFR plasmid 121

6.4.2 Cloning of guide oligonucleotides into pDC2-cam-coCas9-U6.2-hDHFR plasmid 121

6.4.3 Gibson assembly of donor into pDC2-cam-coCas9-U6.2-hDHFR^{guide} plasmid 122

6.4.4 Recovery of 3D7 and Dd2 *P. falciparum* parasite transfections 126

6.4.5 Confirmation of successful *Pfnfs1* K/Q65 editing 126

6.4.6 Confirmation of recombinant parasite 128

6.4.7 Susceptibility of recombinant parasites to antimalarial drugs 130

6.5 Discussion 133

7.0 General discussion, conclusion, limitations and recommendation 136

7.1 General discussion 136

7.2 General conclusion 141

7.3 Limitations and recommendations 142

7.0 REFERENCES 144

8.0 APPENDICES 177

LIST OF FIGURES

Figure 1.1: Conceptual Framework for monitoring antimalarial drug resistance 7

Figure 2.1: Global map of *P. falciparum* malaria incidence in 2017..... 16

Figure 2.2: The life-cycle of *P. falciparum*..... 18

Figure 2.3: Illustration of events that follow treatment with ART. 28

Figure 2.4: Chromosomal location of the cysteine desulfurase (*Pfnfs1*). 39

Figure 2.5: Schematic representation of CRISPR Cas9 gene editing..... 42

Figure 3.1: Map of The Gambia with study location. 47

Figure 3.2: Schematic representation of *ex vivo* PSRA. 51

Figure 3.3: Parasite responses following exposure to drugs using RSA and PSRA..... 56

Figure 3.4: Individual trajectories of 41 isolates following drug exposure..... 58

Figure 3.5: Parasite log responses following exposure to DHA, LUM and DMSO-treated control at 24-, 48- and 72- hours of drug exposure with PSRA. 59

Figure 3.6: Individual profiles of 41 isolates..... 62

Figure 3.7: (a) Re-invasion parasitaemias and (b) log response rates from mixed model analysis of four laboratory adapted isolates 63

Figure 3.8: Grouped profiles of 41 isolates following exposure to DHA and LUM. 65

Figure 3.9: Correlation analysis between initial patient parasitaemia at day 0 prior to assay set-up and parasite survival rates of isolates..... 66

Figure 3.10: Allele frequencies and association analysis of field isolates from 2017. 69

Figure 4.1: -log10 IC_{50} values of 125 compounds from the MMV pathogen box. 81

Figure 4.2: Representative graph of dose response curve of seven potent compounds..... 85

Figure 4.3: Individual responses of 10 *P. falciparum* field isolates 87

Figure 4.4: Percentage re-invasion parasitaemia of 10 *P. falciparum* field isolates..... 89

Figure 5.1: -log10 *P* value of calculated iR using isoRelate within each population. 101

Figure 5.2: -log10 *P* value of calculated iR using isoRelate between population pairs..... 102

Figure 5.3: Box and whisker plots of -log10 *P* values of genome-wide SNP association with 4 antimalarial drugs. 106

Figure 5.4: Genotype-phenotype interaction networks across the *P. falciparum* genome. . 107

Figure 6.1: pDC2-cam-coCas9-U6.2-hDHFR plasmid..... 114

Figure 6.2: CRISPR Cas-9 gene editing strategy used for *Pfnfs1* 115

Figure 6.3: a. One percent (1%) agarose gel electrophoresis 124

Figure 6.4: a. Schematic representation of targeted gene editing of *Pfnfs1* using CRISPR-Cas9. 125

Figure 6.5: PCR amplification of *Pfnfs1* gene fragment..... 128

Figure 6.6: Sequence analysis of wild-type and recombinant parasites..... 129

Figure 6.7: IC_{50} estimates for *P. falciparum* wild-type and recombinant parasites..... 131

LIST OF TABLES

Table 2.1: Widely used antimalarial drugs with their modes of action, years of introduction and resistance development and their associated markers of resistance 34

Table 3.1:Effect of drug exposure on predicted responses of the treatment groups (DHA, LUM, DMSO-control) and exposure times (24-, 48- and 72- hours) 60

Table 3.2: Allele frequencies of drug resistance genes for 41 parasite isolates with drug phenotypic data (PSRA and RSA) in 2017..... 67

Table 4.1: IC_{50} values of 125 compounds with antimalarial activity and 3 known drugs from the MMV pathogen box. 82

Table 4.2: IC_{50} values and 95% confidence intervals of seven compound with high potencies against 3D7..... 86

Table 5.1: Allele frequencies of known drug resistance genes for 56 *P. falciparum* isolates collected from 2014 and 2015 malaria transmission seasons..... 103

Table 5.2: IC_{50} values of 56 samples assayed against AMD, LUM, DHA and ARM in 2014/15 transmission season..... 105

Table 6.1: Guide oligonucleotide sequences designed for *Pfnfs1* gene modification..... 121

Table 6.2: List of primers used for genotyping and sequencing..... 123

Table 6.3: Dd2 and 3D7 transfected parasites using both guides (gRNA-1 and gRNA-2) and both donors (K65 and Q65) of the *Pfnfs1* gene..... 127

Table 6.4: IC_{50} values of parent and recombinant parasite lines 132

Table A.1: Loci with significant IBD within populations..... 177

Table A.2: Loci with significant IBD between populations 203

Table A.3: Loci significantly associated with drugs using parametric test..... 221

Table A.4: Loci presented as outliers with association to drugs using the MLM model.... 229

LIST OF ABBREVIATIONS

5' CAM	*P. falciparum* calmodulin promoter
ACT	artemisinin combination therapy
AL	artemether-lumefantrine
AMD	amodiaquine
Amp	ampicillin
ARM	artemether
ARS	artesunate
ART	artemisinin
ASAQ	artesunate-amodiaquine
ASMQ	artesunate-mefloquine
ASSP	artesunate- sulfadoxine/pyrimethamine
AV	atovaquone
Cas9	CRISPR-associated gene 9
CNV	Copy number variation
CQ	chloroquine
CRISPR	clustered regularly interspaced short palindromic repeats
DBS	dried blood spots
DDAO-SE	7-hydroxy-9H-(1,3-dichloro-9, 9-dimethylacridin-2-one) succinimidyl ester
DHA	dihydroartemisinin
DHA-PIP	dihydroartemisinin-piperaquine
DHFR	dihydrofolate reductase
DHPS	dihydropteroate synthetase
DMSO	dimethyl sulfoxide
DSB	Double stranded break

DV	digestive vacuole
FDR	false discovery rate
Fe-S	iron – sulfur
GAPIT	Genomic Association and Prediction Integrated Tool
gDNA	genomic DNA
gRNA	guide RNA
GTS	global technical strategy
GWAS	genome-wide association studies
hDHFR	human dihydrofolate reductase
HF	halofantrine
HRM	high-resolution melting
HTS	high throughput screening
IBD	identity by descent
IC_{50}	50% inhibitory concentration
IE	intra-erythrocytic
INI	initial parasitaemia
IPTp	intermittent preventive treatment in pregnancy
IPTp-SP	intermittent preventive treatment with sulfadoxine-pyrimethamine
iRBC	infected red blood cells
IRS	indoor residual spraying
LB	luria-Bertani
LLINs	long lasting insecticide-treated nets
LUM	lumefantrine
MAF	minor allele frequency
MDA	mass drug administration

MFQ	mefloquine
MLM	mixed linear model
MMV	Medicines for Malaria Venture
MSP	merozoite surface protein
NE	non-exposed
netGWAS	network-based Genome-Wide Association Studies
NMCP	National Malaria Control Programme
PAM	protospacer adjacent motif
PBS	phosphate buffered saline
PE	pre-erythrocytic
Pfaat1	*P. falciparum* amino acid transporter
Pfap2-mu	*P. falciparum* adaptor protein complex 2 mu subunit
Pfcdpk1	*P. falciparum* calcium-dependent protein kinase 1
Pfcrt	*P. falciparum* chloroquine resistant transport
Pfdhfr	*P. falciparum* dihydrofolate reductase
Pfdhps	*P. falciparum* dihydropteroate synthase
Pfef2	*P. falciparum* translational elongation factor 2
Pfk13	*P. falciparum* kelch 13
Pfmdr1	*P. falciparum* multidrug resistant protein 1
Pfmrp	*P. falciparum* multidrug resistance-associated protein
Pfmsp	*P. falciparum* merozoite surface protein
Pfnfs1	*P. falciparum* cysteine desulfurase
Pfpk7	*P. falciparum* protein kinase 7
Pfpm	*P. falciparum* plasmepsin
PI4K	phosphatidylinositol 4-kinase

PIP	piperaquine
PQ	primaquine
PSA	piperaquine survival assay
PSRA	parasite survival rate assay
PV	parasitophorous vacuole
PVFA	parasite viability fast assay
PYR	pyrimethamine
QN	quinine
R&D	Research and Development
RBC	red blood cells
RSA	ring-stage survival assay
rSAP	shrimp alkaline phosphatase
SD	sulfadoxine
SEA	South-East Asia
SMC	seasonal malaria chemoprevention
SNP	single nucleotide polymorphism
SP	sulfadoxine-pyrimethamine
sgRNA	single-guide RNA
sSA	sub-Saharan Africa
SURFIN	surface-associated interspersed protein
TES	therapeutic efficacy study
uRBC	uninfected red blood cells
VCF	variant call file
WHO	World Health Organisation

CHAPTER 1

1.0 General introduction

1.1 Background

Malaria remains a global health concern, with 229 million reported cases and 409,000 deaths in 2019 (WHO, 2020a). Children under 5 years of age and pregnant women are the most vulnerable groups accounting for 67% of all malaria related deaths worldwide (WHO, 2020a). The main region affected by malaria is sub-Saharan Africa (sSA), with over 90% of cases and deaths caused by the most virulent *Plasmodium* species, *P. falciparum*. Five other malaria parasite species infect humans of which *P. vivax* is geographically the most widespread, resulting in about 75% of malaria infections outside of sSA (WHO, 2019). Of the remaining four species that infect humans, *P. knowlesi* has zoonotic origins and is restricted to Malaysia and parts of Indonesia, while *P. malariae*, *P. ovale curtisi* and *P. ovale wallikeri* are considered benign as they mostly cause less significant morbidities (White et al., 2014).

Malaria incidence declined drastically over the last decade due to global scale-up of various control intervention strategies including long lasting insecticide-treated nets (LLINs) and indoor residual spraying (IRS) targeting the mosquito vectors, seasonal malaria chemoprevention (SMC) and the deployment of artemisinin-based combination therapies (ACTs) for prevention and treatment of *P. falciparum* infections respectively (WHO, 2020a). This is considered a significant progress although about half the world's population remain at risk of getting infected by malaria parasites. Indeed, progress in malaria control has slowed globally since 2015, with several countries recording an increase in malaria cases (WHO, 2017). Accelerating control interventions and overcoming the challenges that impede progress towards malaria control and elimination are therefore crucial.

The World Health Organization (WHO) has set targets to reduce 90% of global mortality rates associated with malaria by 2030 compared to 2015, and eliminate malaria from a minimum of 35 countries through harnessing innovation and research expansion (WHO, 2017). With an increase in global funds towards malaria elimination in recent years and the availability of effective control interventions, the global technical strategy (GTS) for malaria 2016-2030 milestone set by WHO for a malaria-free world can be achieved. This milestone was based on three pillars: (1) ensuring universal access to prevent, diagnose and treat malaria (2) increasing efforts to eradicate malaria and attain a malaria free status, and (3) transforming malaria surveillance into a key strategy (WHO, 2015a). However, several factors threaten progress towards malaria elimination such as the inevitable development of insecticide resistance by mosquito vectors and drug resistance by parasites, as well as the lack of an effective vaccine. In most endemic countries, the two major mosquito vector species that transmit malaria are resistant to the best class of insecticide available, pyrethroids (Hemingway et al., 2016). More challenging is the development of parasite resistance to the most potent antimalarial drugs, artemisinin (ART) derivatives, which has been established and is widespread in South-East Asia (SEA) (Müller et al., 2019).

There has been reported resistance by *P. falciparum* to all classes of antimalarial drugs, a significant challenge in malaria control. Several factors influence the development of drug resistant parasites including the pharmacodynamic properties of the drug, the parasite load in the human host and the level of host immune responses (Capela et al., 2019). Historically, antimalarial drug resistance has mostly emerged from the Greater Mekong sub-region in SEA, spreading to other endemic areas. Resistance to chloroquine (CQ), sulfadoxine-pyrimethamine (SP), mefloquine (MFQ), and more recently to piperaquine (PIP) and the current frontline ARTs, all emerged in SEA (Fairhurst et al., 2016). The reason for this phenomenon is currently not known. It has been suggested that in low transmission settings such as in SEA, infected

individuals have low immunity and are more likely to develop symptoms, and treatment with monotherapies or mismanagement of drugs may have led to the selection of resistant parasites (Miotto et al., 2013). In addition, high rates of monoclonal infections and lower levels of genetic diversity in these low transmission settings result in low crossover rates during meiosis, reducing the dilution effect of wild-type while favouring resistance development and spread of mutants (Lopera-Mesa et al., 2013; Takala-Harrison et al., 2015).

CQ was considered the most successful antimalarial drug ever deployed before its emergence of resistance at the Thai-Cambodia border in 1957, which spread to SEA and later to sSA (Awasthi et al., 2013). SP was then deployed to replace CQ as first-line treatment in 1993, but *P. falciparum* shortly developed resistance to the drug combination (Mwendera et al., 2016; Pinichpongse et al., 1982). SP was later replaced by ACTs in the mid 2000s across most endemic countries and this remains the only recommended first-line treatment available globally. ART derivatives in ACTs are currently the most potent and fast-acting antimalarial drugs to date, yet resistance to these have been characterised clinically as an increase in parasite clearance half-life following treatment and the presence of non-synonymous mutations in the Kelch-13 propeller domain (*Pfk13*) (Fairhurst et al., 2016; Menard et al., 2015). These non-synonymous mutations on *Pfk13* that have been associated with ART resistance in SEA include the change from cysteine to tyrosine at codon 580 (C580Y), isoleucine to threonine at codon 543 (I543T), tyrosine to histidine at codon 493 (Y493H) and arginine to threonine at codon 539 (R539T) (Ariey et al., 2014). Till date, these *P. falciparum* major K13 mutations associated with clinical resistance or delayed parasite clearance are uncommon in Africa, though several other non-synonymous single nucleotide polymorphisms (SNPs) have been reported across the continent. Recently the *Pfk13* R561H mutation was reported to have emerged independently and spread in Rwanda, though this was not associated with treatment failure (Uwimana et al., 2020). ACTs therefore remain widely efficacious in sSA, despite cases of treatment failure or

reduced *in vitro* susceptibility to ACT drugs reported in numerous regions (Plucinski et al., 2015; WHO, 2017). Their effectiveness for malaria control and elimination especially in Africa requires the sustained efficacy of the ARTs as well as partner drugs (Witkowski, Khim, et al., 2013).

Reduced parasite sensitivity to artemether - lumefantrine (AL), the most common ACT used in Africa have been reported by studies in multiple countries (Borrmann et al., 2011; Dama et al., 2017). The efficacy of ACTs heavily depend on the efficacy of the partner drug, as evident from failure of dihydroartemisinin - piperaquine (DHA-PIP) following widespread PIP resistance in SEA (Saunders et al., 2014). Thus ACT treatment failures might be driven by reduced efficacy of either the ART component or the partner drug (Abdulla et al., 2015). Treatment failure against ART monotherapy was reported in Africa over 15 years ago, while lumefantrine (LUM) resistant parasites were successfully generated *in vitro* before its use in AL (Mwai et al., 2012). In The Gambia, an increasing trend in tolerance to LUM was observed *ex vivo* over a period of 4 years suggesting that parasites might be evolving towards a state of LUM tolerance and resistance (Amambua-Ngwa et al., 2017). Hypothetically, resistance to LUM may occur before ART resistance in high endemic regions given that parasites are exposed to LUM for a longer time during treatment due to its long half-life. This thereby increases the risk of exposure to sub-optimal doses and consequently resistance selection as the drug is slowly metabolised (Tilley et al., 2016). Therefore, determining the differences in parasite responses to ART derivatives such as dihydroartemisinin (DHA) (the active component of all ART derivatives) and LUM, used in combination as the first-line treatment for uncomplicated malaria in Africa is essential. With LUM resistance anticipated, it will be valuable to identify genetic markers associated with tolerance and determine mechanisms of resistance development. This will facilitate drug resistance monitoring across the transects of malaria transmission, strengthening timely updates of treatment policies (Djimde et al., 2015).

Antimalarial drug surveillance is recommended by the WHO to constantly monitor the efficacy of drugs and effectively detect changes in parasite responses and associated genetic markers. This is achieved through clinical therapeutic efficacy studies (TES), *in vitro/ex vivo* drug assessment and molecular surveillance for prevalence of drug resistant markers (Nsanzabana, Ariey, et al., 2018). *In vitro*/*ex vivo* drug assays are frequently used to determine parasite drug susceptibility profiles, useful for the early detection of resistance development. However, with the use of combination therapies, assessing antimalarial drug efficacy is now complex as the drugs used in combination are of different classes and potencies. In addition, the current assays in place such as the 50% inhibitory concentration (IC_{50}) determination assay and Ring-stage Survival Assay (RSA) are not standardised, leading to inconsistency in results being generated in different laboratories. Assays that will allow for systematic and simultaneous monitoring of all drug classes are therefore needed. Aside from drug resistance surveillance, it is also important to identify and validate candidate genetic markers associated with drug resistance (van Tyne et al., 2011). This will be beneficial for determining drug resistance mechanisms as well as tracking its development and spread.

To preserve the efficacy of currently used drugs and replace resistant ones, it is imperative to identify novel lead compounds and transform them to clinical candidates. Multiple strategies exist for discovery and development of novel antimalarial drugs. Most of the new drug classes were identified using the traditional drug discovery approach of high throughput screening (HTS) of compound libraries (Flannery et al., 2013). Due to the lack of comprehensive understanding of the parasite biology, it is reasonable to identify highly potent compounds that will successfully go through all phases of clinical trials without understanding their mechanism of action and target (Nzila, 2006). Alternatively, HTS is also used to screen for compound activities against identified drug targets (Delves et al., 2018). The Medicines for Malaria Venture (MMV) have released two compound libraries with activity against malaria parasites

resulting to numerous candidates under clinical trials which can be found on the MMV website (www.mmv.org/mmv-open/pathogen-box) (Ashley et al., 2018). An ideal antimalarial drug should target multiple stages of the parasite life-cycle with a long half-life.

1.2 Conceptual framework

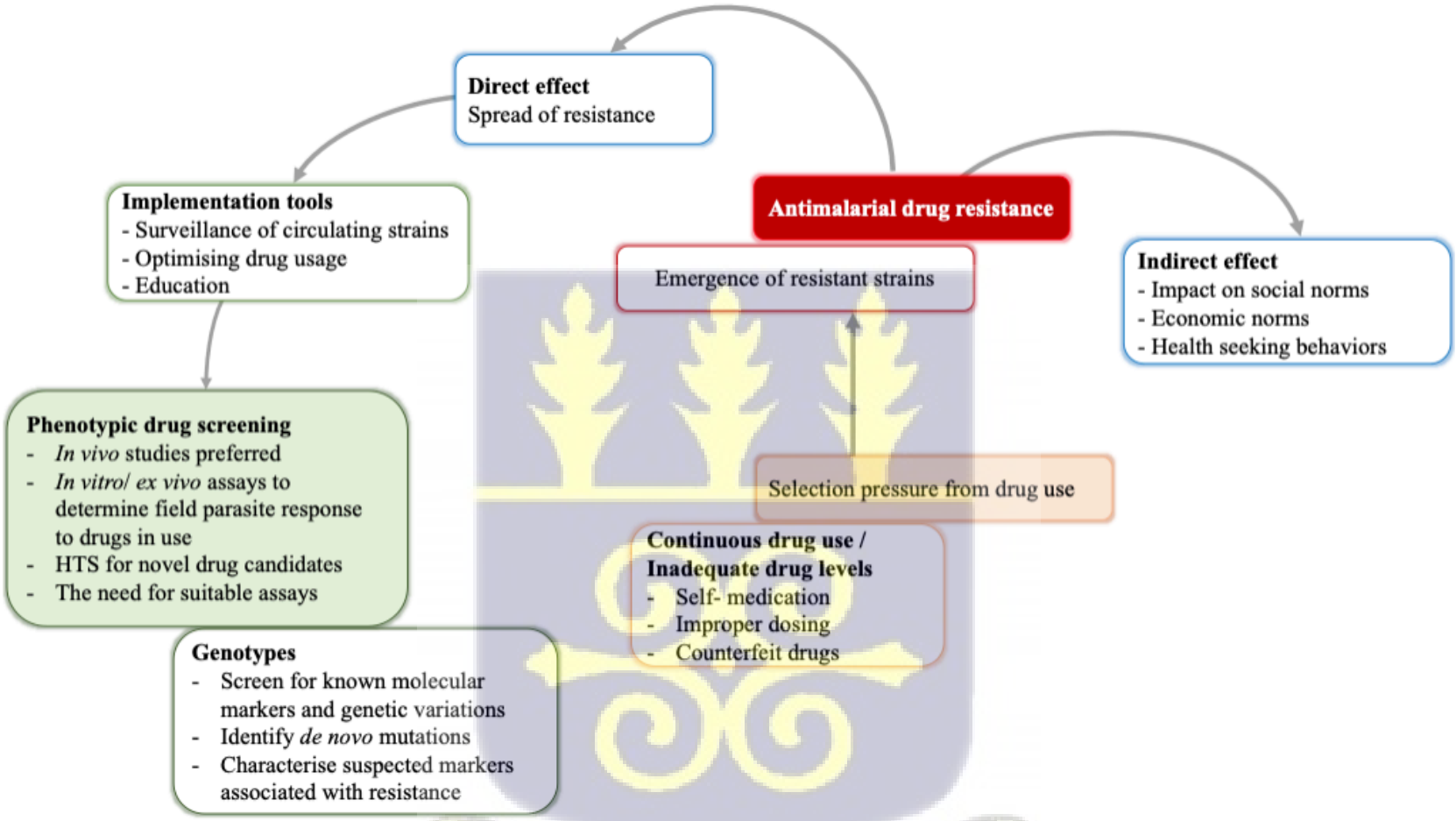

Figure 1.1: Conceptual framework for monitoring antimalarial drug resistance.

Drug pressure from continuous drug use in a population and the inadequate use of drugs results in selection pressure on the parasite genome (Ndiaye et al., 2021). Residual antimalarial drug that is present following drug use e.g. from the long half-life partner drugs such as LUM in AL can persist in the blood for a long time, selecting for resistant parasites. This can lead to the emergence and spread of drug resistant parasites having both direct and indirect effects as depicted in Figure 1.1 (Nsanzabana, 2019). Multiple tools can be used to combat or slow down the development and spread of antimalarial drug resistance.

Surveillance of circulating parasite strains in a population is important in determining evolving resistance strains. The gold standard for determining drug efficacy is by doing *in vivo* TES which is continuously carried out by the National Malaria Control Programmes (NMCP) (Nsanzabana, Djalle, et al., 2018). Additionally, *in vitro* and *ex vivo* drug susceptibility assays are carried out to assess drug susceptibility profiles away from interference by host, and this is valuable for characterising drug resistance and developing new drugs. Different *in vitro* drug susceptibility assays have been used to assess the efficacy of antimalarial drug to parasites, however, as stated in sub-section 1.1 above and in more detail in sub-section 1.3.1.3 below, theses assays cannot be used to simultaneously assess drugs of all classes (De Lucia et al., 2018). Hence, there is the need to develop a sensitive assay which can be used for all drug classes. This assay will also be useful in screening identified compounds for their antimalarial activities which is a starting point for antimalarial drug discovery and development.

It is important to determine resistance before it becomes clinically evident and as such, surveillance of known molecular markers of antimalarial drug resistance should be continuously done (Packard, 2014). It is however apparent that molecular markers that are associated with artemisinin resistance in SEA are not the same as those observed in sub-Saharan Africa as discussed in sub-sections 1.3.2.2 and 5.2. Therefore, it is required to identify

de novo mutations associated with resistance to ARTs and partner drugs, and also validate suspected molecular markers.

1.3 Aim and specific objectives

Overall Aim

This study sought to determine the prevalence and mechanisms of parasite tolerance to AL used in combination as the first-line treatment of uncomplicated malaria in The Gambia.

1.3.1 Specific objective 1

To develop a sensitive novel phenotypic assay to detect differences in parasite responses to AL and lead compounds from the MMV pathogen box.

1.3.1.1 Hypothesis 1

In vitro tolerance to AL by *P. falciparum* will occur in The Gambia following its use as first-line treatment for uncomplicated malaria for over a decade.

1.3.1.2 Hypothesis 2

Compounds with structural similarities to previously used antimalarial drugs will be less active against *P. falciparum* parasites.

1.3.1.3 Rationale

Malaria incidence in The Gambia has declined over the last 15 years (Broekhuizen et al., 2021). These achievements are partly due to increased use of the ACT, AL. However continuous and high drug pressure on dwindling parasite populations could potentially select for AL tolerant parasites. Resistance to ARTs have not yet emerged in The Gambia and across the sub-region although delayed parasite clearance to AL has been reported in a number of countries (Ashley et al., 2014; Dama et al., 2017). In The Gambia, a steady increase in parasite tolerance to LUM was observed over a period of 4 years, and this might evolve to a persistent state of LUM resistance (Amambua-Ngwa et al., 2017). With decreased sensitivity to LUM, the efficacy of AL will be threatened as residual parasites will not be cleared out following AL based treatment. To effectively assess the efficacy of both artemether (ARM) and LUM, an assay that is suitable for both drugs is needed. The current drug assays available: IC_{50} and RSA, cannot be consistently applied to estimate parasite sensitivity to both drugs used in combination. In addition to inconsistency in results generated, the IC_{50} assay is suited for slow-acting drugs and therefore cannot be used to assess fast acting ARTs. RSA on the other hand was designed to assess the efficacy of ART derivatives following a short pulse of drug exposure to not more than 3-hour old rings and is insensitive to slow acting drugs. This study was therefore designed to assess the efficacy status of AL in western Gambia using a novel flow cytometry-based assay. The assay was also used to assess the efficacy status of potent compounds from the MMV pathogen box against Gambian *P. falciparum* population.

1.3.2 Specific objective 2

To determine prevalence of known drug resistant markers and novel molecular markers of LUM tolerance.

1.3.2.1 Hypothesis

Increased use of AL in The Gambia over the past decade will directionally select for genetic markers of adaptation to LUM in parasite populations.

1.3.2.2 Rationale

P. falciparum has a highly variable genome. Resistance to all previously used antimalarial drugs have been associated with specific genetic variants selected following sustained drug pressure (Zhao et al., 2019). Hence, the selection pressure exerted on the parasite from the use of AL and other ACTs could result in the selection of standing or *de novo* genetic variants leading to drug adaptation. Molecular surveillance of drug resistant markers is therefore needed to determine temporal changes in drug resistant allele frequencies and how these changes affect AL tolerance. Already, SNPs and copy number variation (CNV) at the *P. falciparum* multidrug resistance protein 1 gene locus (*Pfmdr1)* have been associated with reduced susceptibility to AL and these polymorphisms have also historically been associated with CQ and amodiaquine (AMD) resistance. Isolates carrying the wild-type *Pfmdr1*, N allele *at* codon 86 (86N) and *P. falciparum* CQ resistance transporter (*Pfcrt*) at codon 76 (76K) are more tolerant to LUM but sensitive to CQ (Raman et al., 2019; Veiga et al., 2016). Since the introduction of AL in Africa, the prevalence of *Pfmdr1* alleles have been fluctuating and regions with previously high prevalence of mutant 86Y variant associated with CQ resistance now predominantly have 86N variant (Achieng et al., 2015; Kateera et al., 2016). A similar reversal to the wild-type has been

reported for *Pfcrt* 76K, though the pattern remains heterogeneous across Africa. For example, The Gambia still reports high prevalence (mean frequency of >70% across the country) of *Pfcrt* 76T resistant variant despite the use of AL for over 15 years (Amambua-Ngwa et al., 2017). Hence the dynamics of temporal variance in these resistance-associated loci is probably determined by more complex biological and environmental factors than just the drugs used. It is therefore important to temporally characterise the evolution of known and putative drug resistance markers currently circulating in different populations which might serve as a backbone for de novo mechanisms of resistance. These and novel markers evolving directionally could be associated with adaptation to ACT components such as LUM. Already, temporal analysis of *P. falciparum* isolates from The Gambia pre- and post- ACT introduction (2008 vs 2014) reported directional selection on a cysteine desulfurase gene *(Pfnfs1)* associated with increased *ex vivo* tolerance (increased IC_{50}s) to LUM (Amambua-Ngwa et al., 2018). The mechanism of resistance to LUM has not been clearly determined. *Pfnfs1* amongst other markers might be driving LUM tolerance, warranting further characterisation.

1.3.3 Specific objective 3

To functionally validate SNPs in *Pfnfs1* as markers of LUM tolerance using CRISPR-Cas9 genome editing approach

1.3.3.1 Hypothesis

Genetic editing of *P. falciparum* cysteine desulfurase using CRISPR-Cas9 will generate LUM resistant parasite lines.

1.3.3.2 Rationale

Functional genomic tools can be used for site-directed gene editing to confirm the role of identified markers of drug resistance (Straimer et al., 2012). *Pfnfs1* which encodes cysteine desulfurase, is thought to be under directional selection, probably due to LUM pressure in The Gambia (Amambua-Ngwa et al., 2018). Cysteine desulfurases deliver sulfur to numerous metabolic pathways, including the iron-sulfur (Fe-S) complex biogenesis which are modulated in apicomplexan cell development, stress conditions and drug resistance (Gao, 2020). Fe-S clusters play a significant role in many biological processes and are targeted by antimalarial drugs. Additionally, iron homeostasis which is essential for the development of erythrocytes is involved in the mechanism of action of quinolines (Lalève et al., 2016). With a consistent increase in allele frequency of *Pfnfs1* 65K in western Gambia since the introduction of AL, the current study sought to functionally validate *Pfnfs1* as a potential marker of LUM tolerance to gain further insights into the mechanisms of LUM resistance development.

CHAPTER 2

2.0 Literature review

2.1 Malaria epidemiology

Malaria is one of the deadliest infectious diseases caused by unicellular protists of the *Plasmodium* genus, with over half of the world population at risk of infection. Globally, an estimated 229 million malaria cases were reported in 2019 alone with about 409,000 deaths primarily in children under 5 years of age (WHO, 2020a). Malaria is closely associated with poverty, with the populations most affected having limited access to effective prevention, diagnosis and treatment services. The majority of malaria related cases and deaths occur in low-income African countries as depicted in Figure 2.1, accounting for 93% and 94% of all cases and deaths respectively. The prevalence is heterogeneous across the continent, with hot regions of transmission of the deadliest *P. falciparum* in Nigeria and Democratic Republic of Congo. In west Africa, transmission remains generally high despite successes in the most coastal countries of Mauritania, Senegal, Gambia and Guinea Bissau in reducing transmission levels towards pre-elimination (Diouf et al., 2022). Despite the significant decline in malaria over the last 15 years, the number of confirmed cases and deaths remain relatively significant, with The Gambia for examples, officially recording 53,386 cases and 41 deaths in 2019 (WHO, 2020a).

Global malaria incidence significantly declined between 2010 and 2018, with a 22% reduction in Africa (WHO, 2019). Such gains were primarily attributed to the effective use of control interventions such as LLINs, IRS and ACTs. Several endemic countries are currently focusing their efforts on eliminating malaria, which can be accomplished following a 3-year cycle of interrupted indigenous cases with the ability to halt re-establishment of transmission with all

human malaria species (WHO, 2019). In 2015, the GTS for malaria 2016 to 2030 set a goal for the elimination of malaria by 2030 in at least 10 endemic countries.

The progress towards global malaria control has been remarkable though the pace has slowed in recent years and the global malaria burden remains enormous (over ~400,000 deaths). Several factors threaten the progress towards malaria elimination and the achievement of goals set by GTS, including, inadequate funding and more significantly, the continued emergence and spread of insecticide resistant mosquitoes and drug resistant parasites.

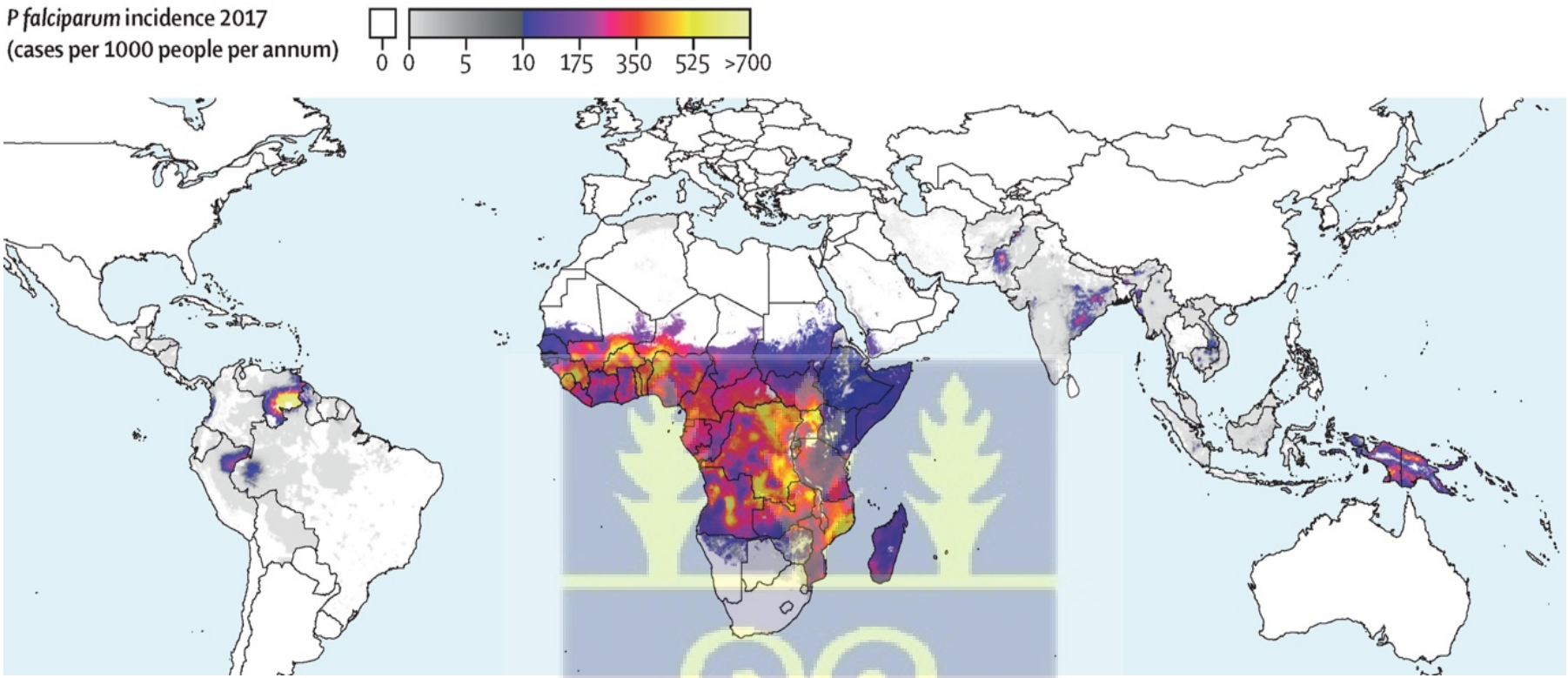

Figure 2.1: Global map of P. falciparum malaria incidence in 2017. Adapted from (Weiss et al., 2019).

2.2 Malaria biology

2.2.1. *Plasmodium* parasites

The *Plasmodium* genus consists of several parasite species with specific host preferences and virulence, six of which cause human malaria infections (White et al., 2014). *P. falciparum* is the most virulent of the malaria parasite species responsible for > 90% of all malaria infections and predominates in Africa where the disease has the highest burden. *P. vivax* is considered to cause severe illness, and deaths from *vivax* malaria are claimed to be underestimated globally (Cowman et al., 2016; Naing et al., 2014). *P. knowlesi*, a zoonotic species, is known to thrive in Malaysia and other parts of SEA, and also causes severe disease in humans (Ahmed et al., 2015). The remaining three species, *P. malaria*, *P. ovale curtisi* and *P. ovale wallikeri* cause less significant disease.

2.2.2 *Plasmodium falciparum* life-cycle

The life-cycle of *Plasmodium* species are complex, alternating between the female Anopheles mosquito which is the vehicle of transmission and the human host (Cowman et al., 2016). Within the mosquito vector, the parasite undergoes sexual reproduction, while its asexual phase occurs in the human host.

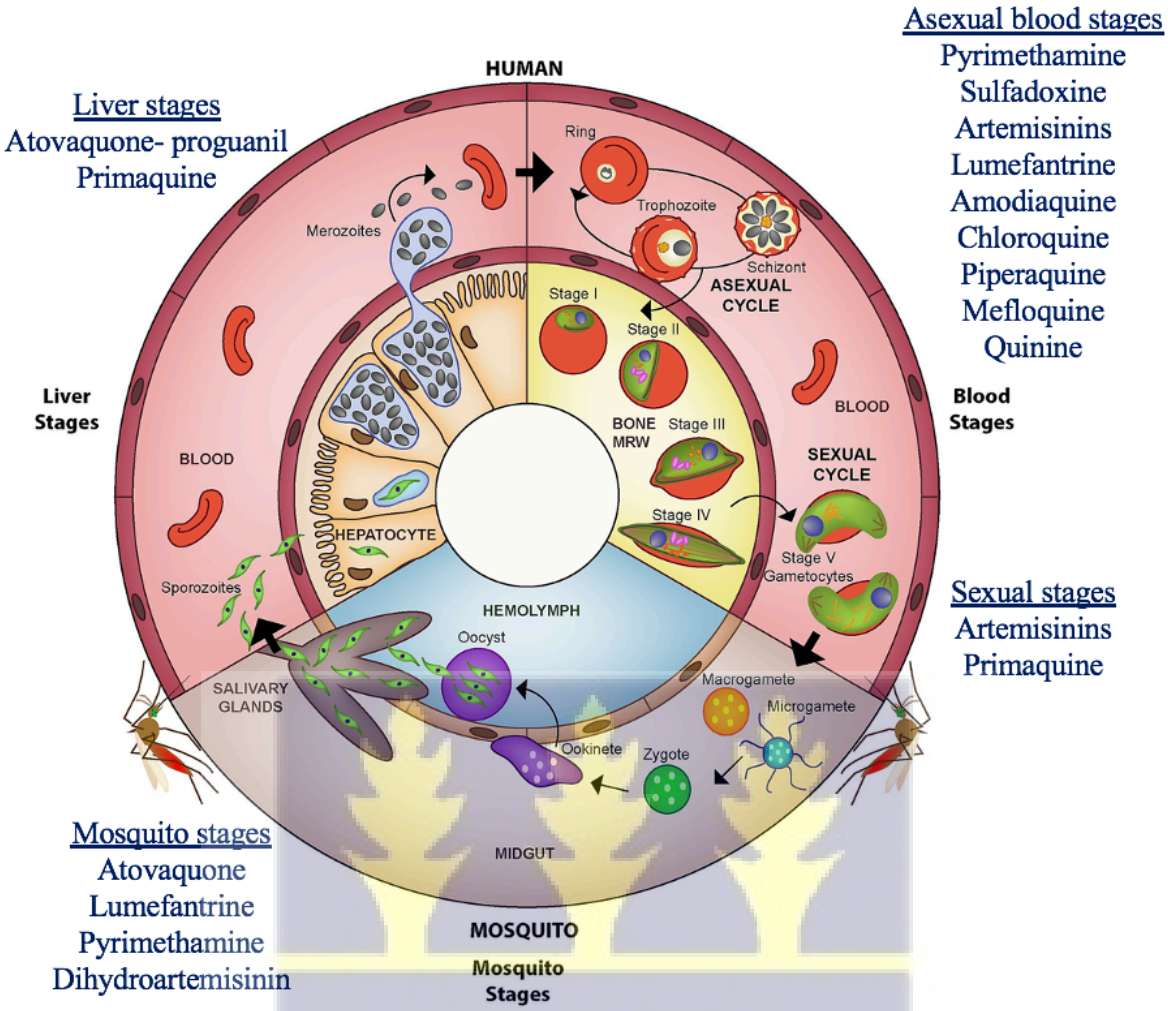

Figure 2.2: The life-cycle of *P. falciparum* with the stages targeted by the most widely used antimalaria drugs. Adapted from (Nilsson et al., 2015).

Infection within the human host begins when an infected female Anopheles mosquito probes for a blood meal, injecting motile sporozoites into the skin (White et al., 2014). Sporozoites can remain in the dermis for up to 3 hours after inoculation before entering the blood circulation via random movement (Vaughan et al., 2017). As they reach the blood capillaries in the liver sinusoid, sporozoites migrate through the liver sinusoidal endothelial cells or the liver resident macrophages: Kupffer cells, allowing entry into the parenchyma, ultimately infecting hepatocytes. A single sporozoite invades one hepatocyte, protected by a parasitophorous

vacuole (PV) membrane within which it further develops (Figure 2.2) (Kaushansky et al., 2015). Sporozoites undergo schizogony, a process that takes 2 to 10 days, replicating their genome to approximately 10^4 to 10^5 times. *P. falciparum* liver stage development takes an average of 6.5 days and can yield up to 90,000 hepatic merozoites from a single schizont. These merozoites are packed in membrane bound vesicles called merosomes that bud-off infected hepatocytes and are not effectively recognised by human immune mechanisms (Vaughan et al., 2012). The pre-erythrocytic (PE) phase of the life-cycle is asymptomatic and cannot be easily detected in humans (Vaughan et al., 2017). It represents a bottleneck for drug interventions that can prevent parasites from progressing to the intra-erythrocytic (IE) stages. Currently, the PE parasite stages can be targeted by atovaquone (AV)/proguanil (Malarone), primaquine (PQ) (Figure 2.2), and a number of investigational drug candidates (Raphemot et al., 2016).

When hepatic schizonts rupture, they release merozoites into the hepatic circulation, initiating the process of IE developmental cycle. These free merozoites rapidly invade erythrocytes through essential and specific ligand-receptor interactions that lead to multiple processes (Bhatt et al., 2015; Burns et al., 2019). These stepwise processes for a successful merozoite invasion include, initial attachment of the merozoite to the red blood cell (RBC) surface, re-orientation of merozoite apical end for contact with the RBC surface, tight junction formation between merozoite and host cell, invasion of merozoite into RBC membrane and finally, resealing of RBC membrane (Cowman et al., 2016). As these steps progress, merozoites are vulnerable to direct exposure from drugs (Burns et al., 2019).

Following invasion of RBCs, merozoites develop into ring stage parasites within 6 hours, the stage at which the PV is formed, and progress into metabolically active trophozoites (Perrin et al., 2021). In the digestive vacuole (DV), toxic heme residues from haemoglobin digestion is converted to haemozoin. At 33 to 36 hours post-invasion, schizogony (nuclear division without

cell division) occurs, resulting from multiple rounds of DNA replication and asynchronous nuclei fission to yield a multi-nucleated, polyploid schizont (mitotic division) (Simon et al., 2021). Segmentation and cytokinesis of each nucleus occur, resulting in the formation of 16 to 32 haploid daughter merozoites. At about 48 hours post-invasion, these merozoites are released when the schizont bursts, completing the human host phase of the life-cycle (Venugopal et al., 2020). The parasites undergo regular cycles of RBC re-invasion, replication and egress, multiplying exponentially in susceptible individuals to over 10^{12} parasites resulting in symptomatic disease (Von Seidlein et al., 2012).

The symptoms often associated with malaria are as a result of sequestration of late stages in microvasculature of vital organs and schizont rupture (Reviewed by (Zekar et al., 2021)). Malaria symptoms are typically non-specific including fever, headache, nausea and muscle pains, which mostly resolve within a few days when treated with effective antimalarial drugs (Bartoloni et al., 2012). A proportion of malaria infections progress to severe diseases with pathologies ranging from metabolic alterations, liver dysfunction, renal failure and placental malaria, all of which can lead to death (Katsoulis et al., 2021). The risk of developing severe malaria varies with age and transmission intensity, immune status and various genetic susceptibility factors (Nguetse et al., 2019). Most drugs such as quinolines target the erythrocytic stages of the parasite life-cycle, acting against haemozoin formation (Figure 2.2) (Reviewed by (Kumar et al., 2018)). Complete treatment with ACTs should resolve the infection caused by *P. falciparum* sensitive parasites, as ARTs act broadly at all stages but mostly the rings (Krungkrai et al., 2016).

During schizogony, some parasites commit to gametocytogenesis, a process of sexual differentiation into male and female gametocytes (Figure 2.2) (Kafsack et al., 2014). Although less than 10% of schizonts commit to sexual differentiation, it is an important phase in the life-

cycle of the parasite as it guarantees continuous transmission to the mosquito vector (Liu et al., 2011). The triggers of gametocytogenesis and the timing of parasite commitment to sexual differentiation are not well understood. Exposure of parasites to various environmental stressors such as drug treatment or high parasitaemia, has been associated with an increase in *in vitro* commitment to gametocytogenesis (Portugaliza et al., 2020). Studies have established the transcription factor AP2-G as a master regulator of gametocytogenesis, which is absolutely essential for gametocyte formation (Kafsack et al., 2014). Gametocyte development in *P. falciparum* occurs in five morphologically distinct stages that lasts for 10 to 14 days (Reviewed by (Nixon, 2016)). Stage I gametocytes resemble trophozoites morphologically while all other stages have a characteristically crescent shape. Apart from stages I and V gametocytes found in the periphery, all other stages are sequestered in the bone marrow, a mechanism to avoid clearance by the spleen (Joice et al., 2014). Mature gametocytes can survive in the bloodstream for days prior to mosquito ingestion, a stage that can be targeted by drugs (Chawla et al., 2021). Drugs targeting gametocytes including PQ and ARTs are important for malaria control programmes as they can prevent ongoing transmission (Camarda et al., 2019).

Sexual and asexual reproduction of gametocytes occur in the mosquitoes (Figure 2.2). When a mosquito probes for a bloodmeal, the PV membrane of the RBCs rupture, facilitating egress of gametocytes (Sologub et al., 2011). Activated gametocytes develop into male and female gametes within the mosquito midgut (Bennink et al., 2016). Male gametocytes undergo three rapid rounds of DNA replication and flagella assembly, forming eight flagellated and highly motile microgametes, a process known as exflagellation. Female gametocytes do not replicate but develop into a single macrogamete (Reviewed by (Ngotho et al., 2019)). Each haploid microgamete binds and fuses to a macrogamete, generating a diploid zygote. The zygote goes through nuclear fusion followed by DNA replication and meiosis (Guttery et al., 2012). The zygote grows into a motile ookinete that migrates through the mosquito midgut epithelium and

develops into oocysts where asexual replication occurs to generate sporozoites. Motile sporozoites released following oocyst rupture migrate to and reside in the mosquito's salivary glands, ready for transmission to the next human host, completing the life-cycle of the parasite (Cowman et al., 2016). AV and DHA amongst others are effective against the parasite's mosquito stages (Figure 2.2) (Delves et al., 2012).

2.3 Malaria immunity and vaccine development

Malaria immunity in humans is complex, affected by host and parasite genetic factors as well as environmental factors. Malaria immunity is non-sterile where anti-disease immunity can be acquired, but infections can persist and become asymptomatic (Crompton et al., 2014). Immunity develops with time and exposure, acquired after years of parasite exposure and infections in malaria endemic regions (Barua et al., 2019). The degree of innate immune response influences the magnitude of adaptive immune response (Schrum et al., 2018) and repeated exposure contributes to the production of antibodies against all parasite life-cycle stages (Rodriguez-Barraquer et al., 2016). Acquired immunity affects treatment outcomes with antimalarial drugs by facilitating parasite clearance and improving treatment efficacy (O'Flaherty et al., 2017). The possibility to develop immunity against malaria makes it possible for an effective vaccine to be developed. The search for a highly effective vaccine remains a top priority to achieve the ultimate goal of eliminating malaria.

The greatest challenge to an effective vaccine has been the physiological and genetic complexity of the parasite. First, the genome of the parasite has about 5300 genes, most of which have unknown function (Gardner et al., 2002). In addition, a large number of antigens with strong immunogenicity in *P. falciparum* are highly polymorphic (Osier et al., 2014). Efforts to develop vaccines target candidates expressed at the PE, IE and sexual stages of the

parasite life-cycle (Cowman et al., 2016). The most promising vaccine strategy would target various antigens at different stages of the life-cycle. The most advanced candidate for a malaria vaccine is the anti-sporozoite vaccine RTS,S/AS01. However, RTS,S/AS01 fails to provide long term protection (Greenwood et al., 2016; RTS S Clinical Trials Partnership, 2015). Though phase 3 trials showed allele specific efficacy, the RTS,S/AS01 has been approved and is now being implemented in rollout EPI trial phase in Ghana, Malawi and Kenya (Han et al., 2017). Due to the modest efficacy of RTS,S/AS01, development of vaccines with improved efficacy status remains a priority for the malaria elimination end-game. A broad pipeline of vaccine candidates, including irradiated sporozoites and subunit vaccines are currently under development (Draper et al., 2018). Due to the lack of an effective vaccine, control interventions largely depend on insecticides and drugs.

2.4 Malaria control and intervention strategies

Malaria control strategies mainly target the mosquito vectors with insecticides or the human stages of the parasites with drugs. New drug approaches are now emerging that target the vector.

2.4.1 Vector control

This is an essential component in the drive towards the elimination of malaria. The prevention of malaria transmission relies almost entirely on insecticide use for vector control (Hemingway et al., 2016). The use of ITNs and IRS has decreased human-mosquito contact thereby reducing transmission, a factor that has contributed to a two-third reduction of malaria cases in Africa between 2000 and 2015 (Bhatt et al., 2015). LLINs, the most widely used and cost-effective ITN, retain their efficacy even after more than 20 washes and can be used for up to 3 years as

recommended by WHO. Over the last two decades, the use of IRS and LLINs increased significantly to achieve the target of universal coverage. Their use in low and middle income malaria endemic countries account for the biggest reduction in malaria burden in the 21st century (Killeen et al., 2017). For more than a decade now, the WHO has recommended the use of pyrethroids as the only chemical class of effective and safe insecticides for vector control. Several new classes have been developed, but resistance has been reported against all classes. New approaches such as the use of Ivermectin and genetically engineered mosquitoes remain under investigation though showing promise in reducing the density of mosquitoes in endemic communities (The Ivermectin Roadmappers, 2020).

2.4.2 Malaria chemotherapy and chemoprevention

In order to prevent the progression of uncomplicated malaria to severe forms, prompt diagnosis and effective treatment within the first 24 to 48 hours of the onset of symptoms is needed (WHO, 2015a). Currently, ACTs are used for the treatment of uncomplicated malaria globally. Complicated malaria is usually treated with intravenous or intramuscular artesunate (ARS), ARM or quinine (QN) followed by oral treatment with the recommended ACTs (WHO, 2012a, 2015b).

Beyond treatment, malaria chemoprevention is applied to children and pregnant women, who are most vulnerable to severe disease. SMC is a strategy used to reduce the burden of malaria in children under 5 years of age in malaria endemic regions at the start of every transmission season. It was recommended by the WHO in 2012 to administer a complete dose of SP plus AMD at monthly intervals for up to 4 months to prevent malaria related morbidity and mortality in children (WHO, 2013). This is with the objective of maintaining therapeutic concentrations of the drugs in the blood throughout the transmission season.

In 2012, the WHO also recommended the use of intermittent preventive treatment (IPTp) with SP in pregnant women (IPTp-SP) from the second trimester to minimise episodes of malaria during pregnancy and the possible consequences (WHO, 2014a). This was shown to effectively reduce episodes of malaria among pregnant women, maternal and foetal anaemia, improve birth weight and minimise neonatal mortality (Bouyou-Akotet et al., 2016).

The ACT, DHA-PIP is used for mass drug administration (MDA) campaigns which administers a therapeutic dose to an entire population despite infection status to treat asymptomatic infections and prevent re-infection, rapidly decreasing malaria prevalence and incidence, and interrupt transmission within a short term (Deng et al., 2018; WHO, 2015a).

2.4.2.1 The history of antimalarial drugs

Antimalarial drugs have been the cornerstone of malaria control and prophylaxis since the isolation of QN from the bark of the Cinchona tree in the 1820s (Table 2.1) (Greenwood, 1992). QN became the standard drug for intermittent fever from the early 17th century and has been used for over 300 years for the treatment of both uncomplicated and severe forms of malaria. However, as a result of its adverse effects, the use of QN was later limited to treatment of severe malaria (Achan et al., 2011). Following the discovery of QN, the active search and development of other potent antimalarial drugs followed, resulting in the synthesis and screening of thousands of compounds for their activity against malaria in the early 20th century (Pérez-Moreno et al., 2016). Several other antimalarial drugs have been introduced for malaria treatment, all of them from 3 main drug classes: quinolines, antifolates and ARTs (WHO, 2015b). Quinoline containing drugs include CQ, AMD, PQ, halofantrine (HF), MFQ, PIP, pyronaridine and LUM. CQ, a 4-aminoquinoline which is less toxic and more rapidly produced than QN was introduced in 1945, considered to be the most effective and successful

antimalarial drug used globally (Sáenz et al., 2012) (Table 2.1). CQ was the main drug deployed in the WHO Global Eradication campaign in the 1950s and an important component in malaria control and elimination programmes (Nájera et al., 2011). CQ and related quinoline drugs are blood schizonticides that act inside of the DV by interfering with the formation of toxic heme moieties. CQ accumulates in the DV and inhibits haemozoin formation when heme is released following haemoglobin digestion by the parasite. Free heme is toxic to the parasite and lyses the parasite membrane resulting in its death (Herraiz et al., 2019) The mechanisms by which other quinoline related drugs interact with heme remains unclear.

Antifolates include proguanil, pyrimethamine (PYR) and sulfadoxine (SD) which were considered to be an almost ideal class of antimalarial drugs (Verhoef et al., 2017). These drugs are used as various combinations because they easily develop resistance when applied as monotherapies. They are highly synergistic to each other and with other drugs and are highly potent (Costanzo et al., 2011). In 1967, the most widely used antifolate combination, SP was introduced and deployed as the first-line drug for treatment in many sSA countries following widespread resistance to CQ (Table 2.1) (Achan et al., 2018). These are also blood schizonticides that interfere with folate metabolism, essential for parasite survival. SD inhibits dihydropteroate synthetase (DHPS) activity, which is needed for folate biosynthesis, decreasing the synthesis of dihydropteroate. PYR inhibits the activity of dihydrofolate reductase (DHFR), an essential enzyme required for the parasite's folic acid pathway (Costanzo et al., 2011). Inhibiting these two enzymes results in the inhibition of pyrimidine and purine biosynthesis as well as certain amino acids.

Artemisia annua has been used by the Chinese as herbal remedy to treat haemorrhoids for at least 2000 years and to treat fever since 1596 (Aftab et al., 2014). Its active ingredient was purified in 1971 (Table 2.1) , named qinghaosu and is now widely used for the treatment of

malaria (Faurant, 2011; White et al., 2015). Between the 1980s – 90s, ART derivatives were widely used in China, Thailand and Vietnam. The use of ART as monotherapy resulted in high failure rates but its combination with quinolines resulted in a highly effective therapy for the treatment of uncomplicated malaria (WHO, 2014b). ART is a sesquiterpene trioxane lactone with a peroxide bridge that is essential for its activity (Tilley et al., 2016). ART is reduced to form DHA which is more potent than ART *in vivo* (Bridgford et al., 2018). A number of other ART derivatives have been synthesised from DHA, some of which are used in ACTs including ARM and ARS. Different mechanisms of ART action have been proposed. Activation of the endoperoxide bridge of ARTs by Fe^{2+}-heme is necessary for antimalarial activity (Tilley et al., 2016) (Figure 2.3). ART in its active state is lethal to very early ring and trophozoite stage parasites presumably resulting from alkylation of biomolecules including lipids, proteins and heme which in turn cause oxidative stress and parasite death (Figure 2.3) (Tilley et al., 2016).

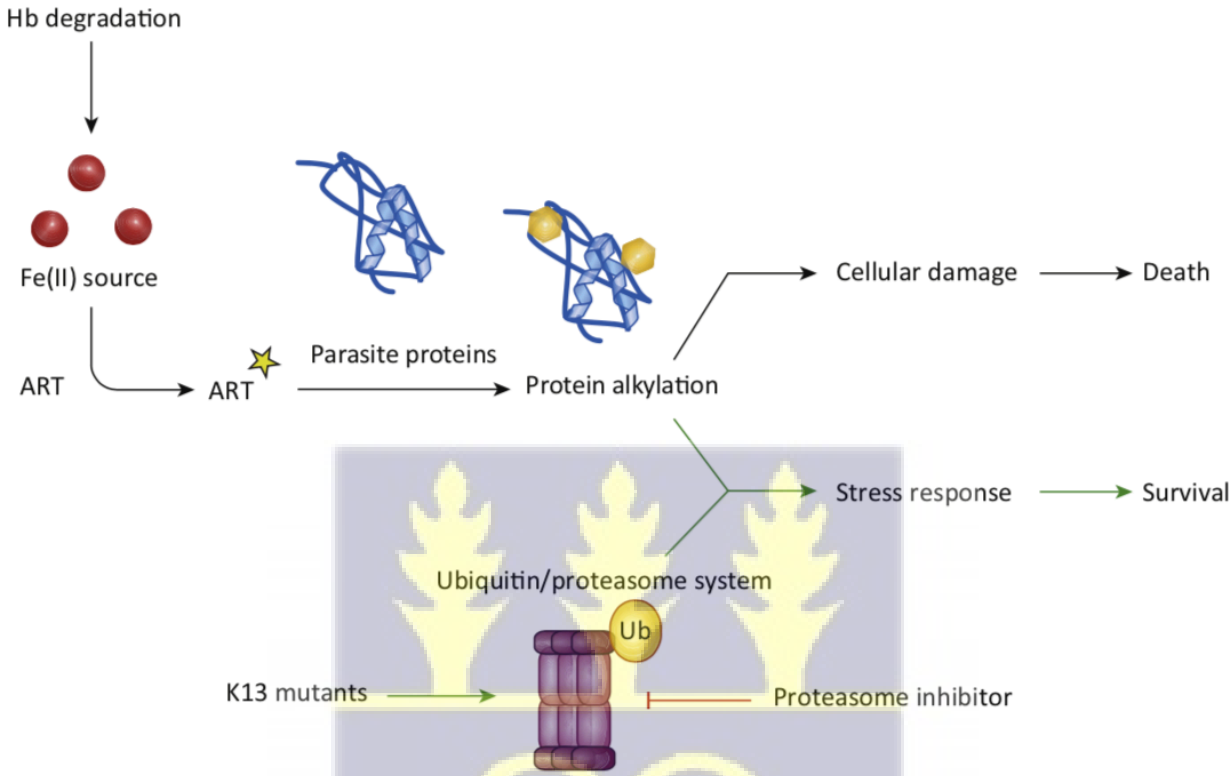

Figure 2.3: Illustration of events that follow treatment with ART. ART derivatives are activated by a reduced iron source which is mostly heme that is released from haemoglobin degradation. Activated ART* reacts with parasite proteins, leading to parasite damage and eventually parasite death. Alternatively, resistant parasites mount a stress response using the unfolded protein response that includes ubiquitin/proteosome system resulting to surviving parasites. Proteasome inhibitors have been proposed to dampen stress response, thus promoting cell death (Adapted from (Tilley et al., 2016)).

Currently, ACTs are the mainstay treatment for uncomplicated malaria, a combination of an ART derivative and a 4-aminoquinoline or amino-alcohol as the partner drug. The partner drugs used include AMD, PIP, pyronaridine, MFQ and LUM and SP (Phillips et al., 2017). There are 5 combination therapies approved by the WHO that have proven to be highly effective in clinical trials, with > 94% of patients clearing up parasites by day 28: artesunate-SP (ASSP), AL, artesunate-amodiaquine (ASAQ), artesunate-mefloquine (ASMQ) and DHA-PIP (WHO, 2015a). Among these, AL is the most widely used ACT in malaria endemic regions and several studies have shown its efficacy against multidrug resistant parasite strains (Thu et al., 2017).

2.4.2.1.1 MMV compound libraries for antimalarial drug development

The MMV is actively involved in supporting the discovery and development of novel antimalarial drugs. Currently, nine drugs are under product development, another nine under translational phase and 15 candidates under research phase ("MMV-supported projects," 2020). With the persistent emergence and spread of drug resistant parasites, there is the need to continuously screen for compounds with antimalarial activities to replace ineffective drugs and preserve the efficacy of potent ones. Numerous approaches are currently being used to classify compounds with high potency against *P. falciparum*. These include drug repurposing, identifying compounds that act against new discovered drug targets, exploring natural products for antimalarial activity and developing analogues of existing drugs (Mishra et al., 2017). A detailed understanding of the mode of action of drugs being developed would be ideal, but the exact modes of action of drugs used for decades are still not fully understood. None of the antimalarial drugs were rationally developed with the intention of inhibiting a specific drug target (Kumar et al., 2018). For most antimalarials with known drug targets, their potencies were first identified *in vitro* or in animal models and their modes of action and targets subsequently identified.

2.5 Threats to the control of malaria

The emergence of mosquito resistance to the most effective insecticides limits the efficacy of IRS and LLINs. On the other hand, parasite resistance to antimalarial drugs is also widespread, with resistance to all classes of antimalarial drugs established. These together are major threats to malaria control particularly in highly endemic regions of Africa (Lindsay et al., 2021; Menard et al., 2017).

2.5.1 Insecticide resistance

Pyrethroid resistance has developed in the two main groups of vectors prevalent in most endemic regions: *Anopheles gambiae sensu lato* and *Anopheles funestus* (Hemingway et al., 2016). With only one class of insecticide available for LLINs and the campaign for universal LLIN coverage, major challenges exist. Alternative insecticides have been proposed for IRS but resistance to these is also increasing (Hemingway et al., 2016; Sougoufara et al., 2020). In addition to developing insecticide resistance, the effectiveness of bed-nets is compromised by several factors such as their inappropriate use for fishing or farming activities and changes in mosquito behaviours such as biting times and resting habits (Ojuka et al., 2015). The WHO therefore has developed a global plan for the management of insecticide resistant malaria vectors with proposed approaches to preserve the effectiveness of vector control interventions (WHO, 2012b). The use of interventions in combination and the rotation of insecticides are two major strategies available.

2.5.2 Antimalarial drug resistance

2.5.2.1 Evolution, spread and mechanisms of antimalarial drug resistance

The continued emergence and spread of drug resistant parasites pose a major challenge to malaria control. The plasticity of *P. falciparum* gives it the ability to develop resistance to antimalarial drugs, affecting the efficacy of all drugs that have ever been developed till date (Lukens et al., 2014). This has been one of the greatest challenges in malaria control, reversing major gains made globally in the past two decades. The WHO defines drug resistance as the ability of parasite strains to survive and/or multiply after the administration of drugs at recommended therapeutic doses or higher (WHO, 2015a). Resistance emerges due to parasite adaptation following drug pressure accompanied by genetic changes with unique mutations that confer drug resistance (Ray et al., 2017). In low transmission settings such as SEA with low parasitaemia monoclonal infections, the need for treatment is high due to low acquired immunity, contributing to increased drug use. This may explain why the Thai-Cambodia border is the historic epicentre of antimalarial drug resistance (Ashley et al., 2014).

QN resistance was first reported in SEA in 1967 although it had remained at low rates in both SEA and Africa (WHO, 2014c). It was replaced by CQ which developed resistance at a relatively slower rate compared to other antimalarial drugs after almost 20 years of its extensive use. Global use of CQ was curtailed in early 1960s after resistance emerged in the Thai-Cambodian border in 1957 (Table 2.1), spreading to SEA and later to sSA in 1970, and this became widespread all over sSA by 1980 (Packard, 2014). Parasite resistance to CQ results in reduced accumulation of CQ in the DV, preventing the drug from reaching therapeutic doses, and thus not lethal (Alam Saifi et al., 2013). Several studies have shown that the reduced accumulation of CQ in the DV is due to a decreased accumulation of CQ and not the export of the drug from the DV (Lehane et al., 2011; Roepe, 2014). Resistance to other quinolines is

proposed to occur in a similar manner. The genetic determinant of CQ resistance are mutations in the *Pfcrt* gene that were first described in 2000 (Fidock et al., 2000). *Pfcrt* is located on chromosome 7 of the *P. falciparum* genome and is highly polymorphic with at least 20 variations in its exon resulting in more than 20 unique protein sequences recorded (Reviewed by (Parida et al., 2016)). The key amino acid change associated with the CQ-resistant phenotype is K76T in *Pfcrt* and is consistently associated with at least three other amino acid changes (Ecker et al., 2012). As resistance to CQ emerged, massive drug screening programs followed, identifying three novel antimalarial drugs: AMD which is a 4-aminiquinoline, MFQ a quinolinemethanol, and HF a phenathrene methanol (Tse et al., 2019). Unfortunately, resistance to all three drugs emerged (Table 2.1) and became widespread in many parts of the world, with multidrug resistance seen in some regions where no effective quinoline drugs could be used (Reviewed by (Callaghan et al., 2017)). Many other genes have been associated with resistance to quinolines, including *Pfmdr1* and the multidrug resistance-associated protein 1 gene (*Pfmrp1*) (Gil et al., 2021). *Pfmdr1* is thought to be involved in the export of hydrophobic compounds from the DV including MFQ, HF and other unrelated drugs such as ART derivatives(Reiling et al., 2015). Amino acid variations in *Pfmdr1* at N86Y and Y184F are similarly associated with CQ resistance, with N86Y also contributing to AMD resistance while rendering parasites sensitive to LUM, MFQ and DHA (Veiga et al., 2016). Increase in copy numbers of gene clusters encoding plasmepsin 2 (*Pfpm2*) and *Pfpm3* proteins are associated with PIP resistance (Table 2.1) (Leroy et al., 2019).

CQ was replaced by SP as the first-line drug in many African countries in the 1990s, however resistance to SP emerged shortly afterwards and became widespread. Antifolate resistance is associated with mutations in *P. falciparum* dihydrofolate reductase *(Pfdhfr)* and *P. falciparum* dihydropteroate synthase (*Pfdhps)* at codons 16, 51, 59, 108 and 164 of *Pfdhfr* resulting in PYR resistance and codons 436, 437, 540, 580 and 613 of *Pfdhps* leading to sulphadoxine resistance

(Patel et al., 2017). These mutations are attributed to reduced binding efficiency of the drugs to the parasite enzymes and an increase in the number of mutations is associated with increased levels of resistance (Mbugi et al., 2006).

ACT resistance was first observed in the Thai-Cambodia border with ASMQ in 2002 (Chenet et al., 2016). This was attributed to ART resistance, primarily mediated by mutations in the propeller domain of *Pfk13*. ART resistance has not been established in Africa though there has been isolated reports from imported cases (Lu et al., 2017; Sutherland et al., 2017). The emergence and spread of ART resistance in Africa would be disastrous for malaria control.

Table 2.1: Widely used antimalarial drugs with their modes of action, years of introduction and resistance development and their associated markers of resistance

Chemical class	Drug name	Year of introduction	Mode of action	Year of resistance development	Drug resistant markers
Quinoline derivatives (Amino alcohols)	QN	1820	Inhibits heme detoxification	1967	SNPs in *Pfmdr1, Pfmrp, Pfnhe1*, CNV in *Pfmdr1*
	HF	1988	Inhibits heme detoxification	1993	SNPs and CNV in *Pfmdr1*
	LUM	1976	Inhibits heme detoxification	-	SNPs and CNV in *Pfmdr1*
	MFQ	1977	Inhibits heme detoxification	1982	SNPs and CNV in *Pfmdr1*
Quinoline derivatives (4-aminoquinolines)	CQ	1945	Inhibits heme detoxification	1957	SNPs in *Pfcrt*, Pfmdr1 and *Pfmrp* genes
	AMD	1948	Inhibits heme detoxification	1971	SNPs and CNV in *Pfmdr1*
	PIP	1978	Inhibits heme detoxification	1982	Amplification of *Pfpm2* and *Pfpm3*
Quinoline derivatives (Naphthoquinone)	AV	1996	Inhibits parasite respiratory reaction	1996	SNP in *Pfcytb*

Antifolate derivatives	SP	1967	Inhibits DHPS/ DHFR activity	1967	SNPs in *Pfdhps* and *Pfdhfr*
Artemisinin derivatives / ACTs	ART monotherapy	1971	Heme/protein alkylation	1980	SNPs in *Pfk13* propeller domain
	ARS monotherapy	1975	Heme/protein alkylation	2008	Not known
	AL	2001	Heme/protein alkylation	2006	SNPs in *Pfk13* propeller domain
	ASAQ	2006	Heme/protein alkylation	-	SNPs in *Pfk13* propeller domain
	ASMQ	2000	Heme/protein alkylation	2002	De-amplification of *Pfmdr1* copy number
	Artesunate-SP	2006	Heme/protein alkylation	2012	SNPs in *Pfk13* propeller domain
	DHA-PIP	2002	Heme/protein alkylation	2007	SNPs in *Pfk13* propeller domain
	AS-PY	2012	Heme/protein alkylation	2012	SNPs in *Pfk13* propeller domain

QN = Quinine, HF = Halofantrine, LUM = Lumefantrine, MFQ = Mefloquine, CQ = Chloroquine, AMD = Amodiaquine, PIP = Piperaquine, AV = Atovaquone, SP = Sulfadoxine/Pyrimethamine, ART = Artemisinin, ARS = Artesunate, AL = Artemether-lumefantrine, ASAQ = Artesunate-amodiaquine, ASMQ = Artesunate-mefloquine, DHA-PIP = Dihydroartemisinin-piperaquine, AS-PY = Artesunate-Pyronaridine

2.5.2.2 Artemether-lumefantrine resistance development

Studies have shown that the use of ACTs does not prevent the selection of molecular markers associated with partner drug resistance, particularly if its resistance has previously been identified in that region (Arya et al., 2021; Nsanzabana, 2019). The wild-type alleles *Pfmdr1-86N* and *Pfcrt-76K* have been associated with LUM tolerance. It has been shown that parasites carrying the wild-type *Pfmdr1-86N* allele are more likely to recrudesce following AL treatment compared to the *Pfmdr1-86Y* mutant allele and can tolerate higher concentrations of LUM if they also carry the *Pfmdr1-184F* and *Pfmdr-1246D* wild-type alleles (NFD haplotype) (Malmberg, Ferreira, et al., 2013; Venkatesan et al., 2014). An increase in *Pfmdr1* copy number is associated with AL treatment failure in SEA and could result in AL resistance development in sSA. A number of African countries already reported reduced parasite sensitivity to AL, raising concerns about the drug's efficacy, especially given that it is the most widely used in Africa (Davlantes et al., 2018; Plucinski et al., 2015). The emergence of LUM tolerant parasites increase the burden of clearing the parasite load on ARM, which in turn has the potential to increase the risk of developing resistance, threatening the sustained efficacy of AL (Raman et al., 2019). In high transmission settings, parasites are more exposed to drugs particularly those with longer half-lives, thus increasing their chances of being selected for resistance. Resistance to LUM may therefore arise prior to the development of resistance to the ART counterpart in Africa (Conrad et al., 2019). The mechanisms of LUM resistance are of interest in this study and will be further discussed.

2.5.2.3 Lumefantrine and cysteine desulfurase gene

LUM is an aryl amino alcohol with structural similarity to QN, MFQ and HF, with the chemical name: 2-dibutylamino-1-[2,7-dichloro-9-(4-chlorobenzylidene)-9H-fluoren-4-yl]-ethanol. It is a blood schizonticide active against *P. falciparum* blood stage parasites with a half-life of about 4 to 5 days. Until its introduction in combination with ARM in the late 1990s, LUM was never used as monotherapy. LUM is highly effective against CQ resistant parasites, although its exact mechanism of action, as with most antimalarial drugs, remains unresolved (Reviewed by (Tse et al., 2019)). It is proposed to bind to ferriprotoporphyrin IX (hemin) produced during haemoglobin breakdown in the DV of the parasite to prevent the conversion of toxic heme to haemozoin (Combrinck et al., 2013).

Ex vivo drug efficacy studies in The Gambia showed a steady increase in parasite tolerance to LUM from 2012 to 2015. Also, temporal analysis of parasites collected before and a few years after the introduction of AL showed the strongest signature of directional selection in the cysteine desulfurase gene, which correlated with *ex vivo* increase in LUM IC_{50}s (Amambua-Ngwa et al., 2018). Cysteine desulfurase, consisting of the enzymatic subunit: NFS1, is found in the mitochondria of the parasite. It functions by catalysing the conversion of cysteine into alanine and elemental sulfur for Fe-S cluster biogenesis (Maio et al., 2016). Fe-S clusters are small inorganic cofactors involved in a number of biological processes and proteins with Fe-S clusters are modulated during cell development, stress conditions and drug resistance(Gisselberg et al., 2013). In addition, iron homeostasis which is required for erythrocytic development, is implicated in the mechanisms of action of quinolines, the same drug family as LUM (Rishi et al., 2017). With these implications, the validation of *Pfnfs1-65k* is therefore important for its association with LUM tolerance. The cysteine desulfurase gene is located on chromosome 7 of *the P. falciparum* genome. The gene (PF3D7_0727200) is

approximately 1.7 kb in size (Figure 2.4) with no introns and one single exon encoding 553 amino acids (https://plasmodb.org/plasmo/app/record/gene/PF3D7_0727200). The reference allele codes for the polar charged lysine (K) and the alternative allele codes for the polar-uncharged glutamine (Q).

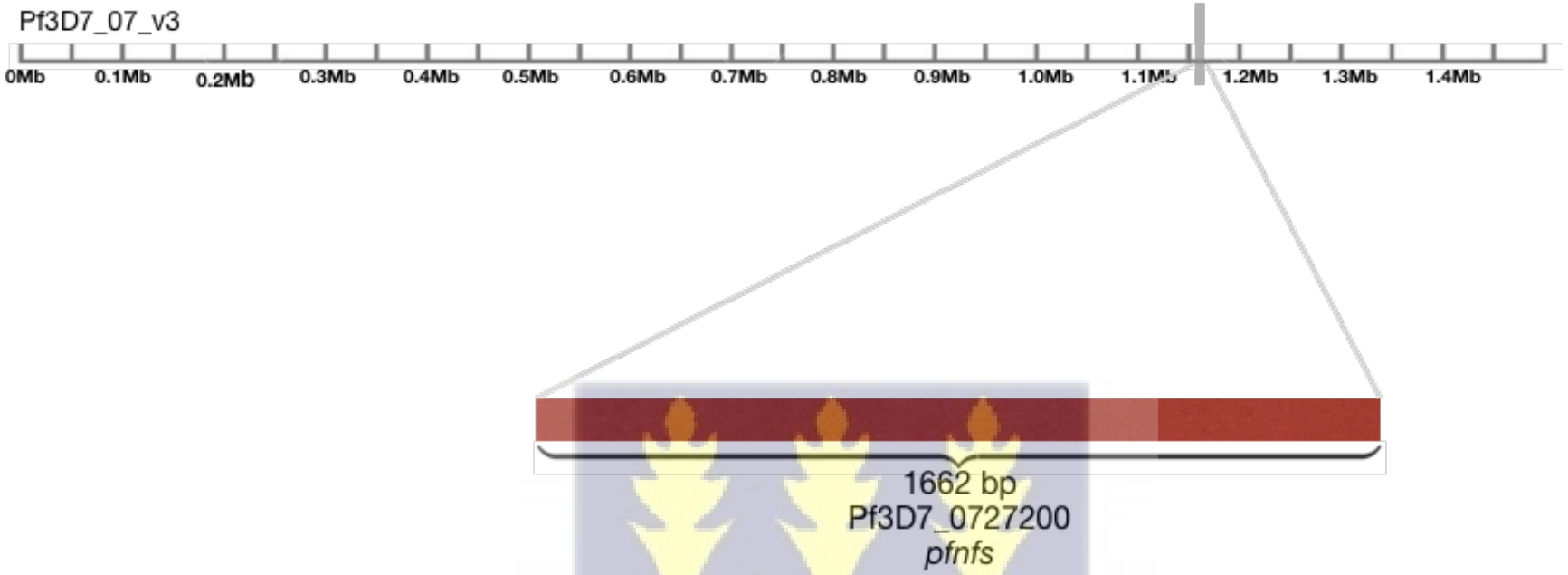

Figure 2.4: Chromosomal location of the cysteine desulfurase.

2.6 Tools for surveillance of antimalarial drug efficacy status

Monitoring the effectiveness of antimalarial drugs is recommended by the WHO for the timely detection of the emergence and spread of drug resistant parasites. Currently, three main approaches are used to assess the susceptibility of antimalarial drugs, including *in vivo* TES, *in vitro/ex vivo* drug efficacy tests and molecular assays to identify validated markers of drug resistance (WHO, 2009). These methods are complementary and provide valuable information on the spread of drug resistance. However, these tools lack standardisation, particularly for *in vitro/ex vivo* drug assays. The development of new assays for antimalarial drug efficacy studies which will provide reliable results to track the emergence of resistance is thus needed (Nsanzabana, Ariey, et al., 2018). It would also be useful to identify and validate novel markers of drug resistance. The advent of technological advancement in cell and molecular genetics such as next generation sequencing and CRISPR-Cas9 gene editing allow for improved approaches towards understanding of the biology of the parasite and unfold mechanisms of drug resistance.

2.6.1 CRISPR-Cas9 genome editing

Until recently, generating transgenic *P. falciparum* parasites has always been complex and laborious. The traditional genome editing approach is a laborious process that involves multiple rounds of parasite culture and drug selection in hopes of generating random DNA breaks in the regions of interest (Muralidharan et al., 2011). Zinc finger nucleases on the other hand introduce site-specific double stranded breaks (DSBs) on the region of interest, generating targeted mutations (Straimer et al., 2012). This method is highly efficient, however, it is not widely implemented due to its high cost and laborious process (Ghorbal et al., 2014). Recently, clustered regularly interspaced short palindromic repeats (CRISPR)/CRISPR-associated gene

9 (Cas9) has been successfully implemented in *P. falciparum* (Kudyba et al., 2018). This has revolutionised the ability to edit the genome of *P. falciparum* efficiently and has now become a widely used tool for gene editing of the parasite (Ghorbal et al., 2014). It allows the specific targeting of genes through the use of customised guide RNAs (gRNAs) that are homologous to the target gene. The gRNA forms a complex with Cas9 endonuclease as depicted in Figure 2.5, directing it to the target locus to introduce a double stranded break three nucleotides upstream of the Protospacer adjacent motif (PAM) site, initiating the parasite's repair mechanism (Lee et al., 2019). *P. falciparum* lacks the canonical non-homologous end joining machinery; hence it relies on its homologous repair machinery (Ng et al., 2019). A DNA template with homology regions upstream and downstream of the cleavage site is thus required for repair which brings in an added advantage of designing a customised donor template that incorporates specific mutations of interest (Bollen et al., 2018).

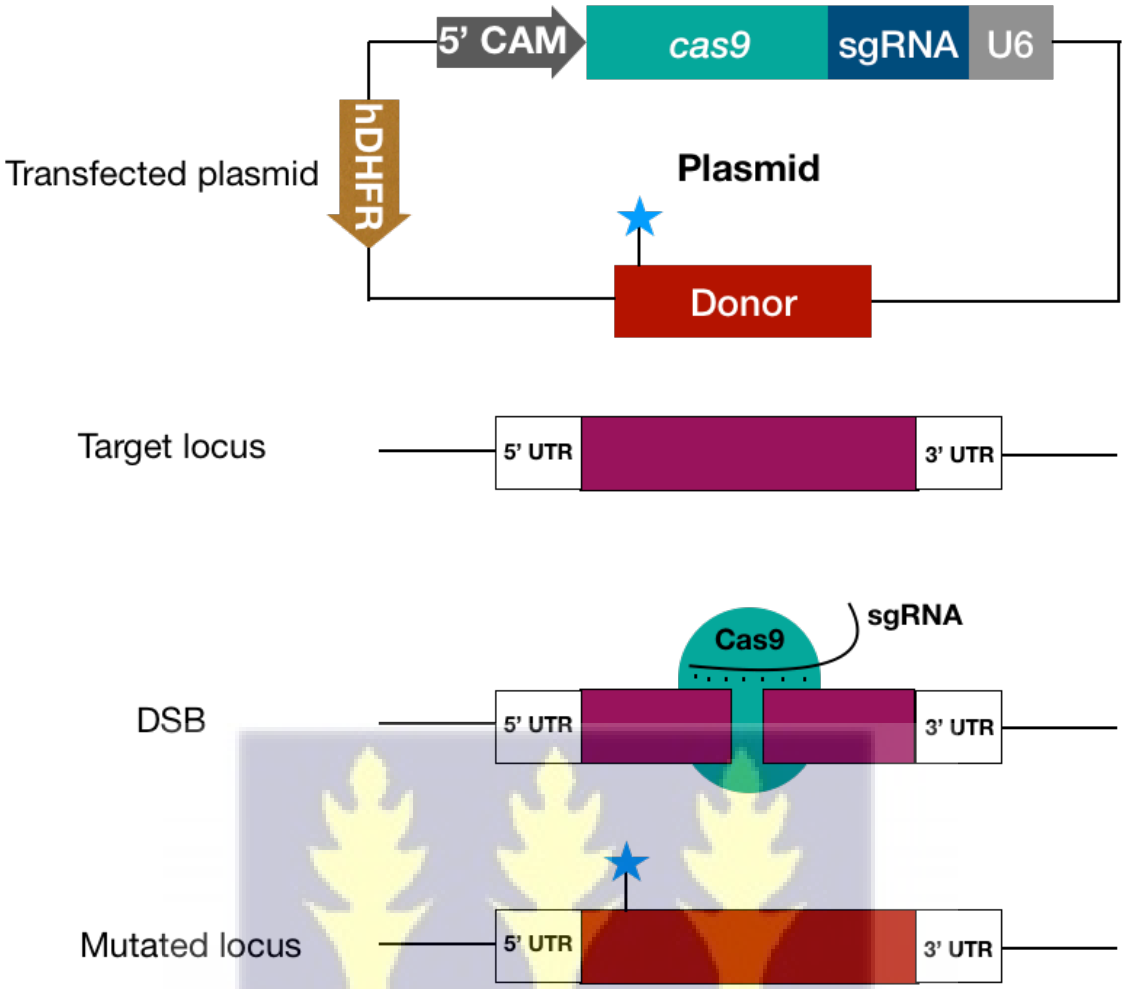

Figure 2.5: Schematic representation of CRISPR Cas9 gene editing of a single nucleotide used in this study. It consists of a single plasmid expressing the single-guide RNA (sgRNA) driven by RNA polymerase III dependent U6 promoter (U6), the Cas9 endonuclease driven by *P. falciparum* calmodulin promoter (5' CAM), a human dihydrofolate reductase (hDHFR) selectable marker and a donor template. The target locus is shown, and a double stranded break is introduced by Cas9 which is coupled with the sgRNA. The resultant mutated locus carries the desired modification on the gene of interest.

CHAPTER 3

3.0 Tolerance of Gambian *Plasmodium falciparum* to Dihydroartemisinin and Lumefantrine detected by *Ex vivo* Parasite Survival Rate Assay (PSRA)

Published in Antimicrobial Agents and Chemotherapy, 2019

DOI: 10.1128/AAC.00720-20.

3.1 Abstract

Monitoring of *P. falciparum* sensitivity to antimalarial drugs in Africa is vital for malaria elimination. However, the commonly used *in vitro/ex vivo* IC_{50} test is inconsistent for several antimalarials, while the alternative RSA for ART derivatives has not been widely adopted. Here, an alternative two-colour flow-cytometry based parasite survival rate assay (PSRA) was applied to detect *ex vivo* antimalarial tolerance in *P. falciparum* isolates from The Gambia.

PSRA infers parasite viability from quantifying re-invasion of uninfected red blood cells (uRBCs) following 3 consecutive days of drug exposure using 10-fold the IC_{50} drug concentration of field isolates. The drug survival rate for each isolate is obtained from the slope of the growth/death curve. PSRA of 41 isolates for DHA and LUM was obtained out of 51 infections tested by RSA against DHA. The genotypes for known drug resistance genetic loci in *Pfdhfr, Pfdhps, Pfmdr, Pfcrt* and *Pfk13* genes was also determined.

The PSRA for 41 Gambian isolates showed faster killing and lower variance by DHA compared to LUM, despite a strong correlation between both drugs. Four and three isolates were respectively tolerant to DHA and LUM, with continuous growth during drug exposure. Isolates with the *Pfmdr1*-Y184F mutant variant had increased LUM survival though this was

not statistically significant. SP resistance markers were fixed, while all other variants associated with antimalarial drug resistance were prevalent in more than 50% of the population.

The PSRA detected *ex vivo* antimalarial tolerance in Gambian *P. falciparum.* This calls for its wider application and increased vigilance against resistance to ACTs in this population.

3.2 Introduction

The WHO currently recommends regular efficacy testing of the locally used antimalarials in humans, complemented by *in vitro* (laboratory-based) assessment of parasite growth in response to drug exposure (WHO, 2016). Comparing the *in vitro* efficacy of ACTs is complex as the components have different mechanisms of action (WHO, 2018). Moreover, most of the existing drug susceptibility assays were developed when treatment was based on monotherapies (Noedl et al., 2003; Sinha et al., 2017). The most common assays are based on the IC_{50}; drug concentrations required to inhibit parasite growth by half under a set of experimental conditions (De Lucia et al., 2018). This approach is sensitive to variations in drug concentrations used and inconsistency in data analysis. IC_{50} assays also do not assess the temporal course of parasite viability following drug exposure, and are not suited for ART derivatives with characteristically shorter half-lives (De Lucia et al., 2018).

New *in vitro* methods assessing the efficacy of fast-acting drugs such as the RSA (Witkowski, Amaratunga, et al., 2013), Piperaquine survival assay (PSA) (Duru et al., 2015) and Parasite Viability Fast Assay (PVFA) (Linares et al., 2015) are now available. RSA and PSA determine parasite survival following drug exposure and withdrawal, while the PVFA aims at discriminating fast-acting antimalarial drugs by assessing parasite killing kinetics over time. There are still critical gaps in these assays; RSA was designed solely for fast-acting drugs and therefore cannot be used for slow-acting antimalarials with longer half-lives (Witkowski,

Amaratunga, et al., 2013). The PVFA has only been used in antimalarial development for screening candidate drugs.

Besides *in vitro* assessment of drugs, molecular surveillance is recommended to monitor the emergence and spread of resistance by determining the proportion of isolates in a given population with resistance associated alleles (Grais et al., 2018). While the *Pfk13* molecular markers of ART resistance have not been identified in sSA (Taylor et al., 2015), resistant alleles in *Pfcrt* and *Pfmdr1* for both current and previously used drugs, including partners in ACTs, are in circulation (Ehrlich et al., 2021). For instance, the use of LUM in the ACT: AL has been associated with an increase in copy numbers, the frequency of N86 allele, and the N86/184F/D1246 haplotype of *Pfmdr1* (Malmberg, Ferreira, et al., 2013; Mbaye et al., 2016; Venkatesan et al., 2014). Additionally, SP used in SMC and IPTp select for mutant *Pfdhfr* and *Pfdhps* alleles (Ndiaye et al., 2013). Combining molecular surveillance with *in vitro* surveillance can therefore provide an early warning signal on the emergence of drug tolerant parasites. This is critical for a parasite population that is exposed to substantial pressure by drug and vector control interventions such as in The Gambia, where malaria transmission and prevalence are low to very low. The Gambia together with neighbouring Senegal is driving for malaria elimination by deploying SMC, while mass drug treatments with ACTs are being contemplated (Faye et al., 2018).

Therefore, the goal of this study was to evaluate the PSRA to estimate *ex vivo* drug sensitivity of *P. falciparum* from The Gambia to the currently used ACT: AL. The PSRA mimics 3 days of exposure to an ACT, measuring parasite survival rates over this period. The assay assesses the survival and re-invasion potential of parasites following exposure to LUM and DHA; prototypes of slow- and fast-acting components of ACTs used in most endemic countries. The approach offers significant advantages over the standard IC_{50} determination assay due to its

higher sensitivity in measuring parasite viability based on the production of invasive merozoites after drug exposure; an index of susceptibility or drug tolerability.

3.3 Materials and Methods

3.3.1 Sample collection

Ethical clearance for this study was obtained from the Gambia Government/MRCG at LSHTM Joint Ethics committee and further approved by the Gambian Ministry of Health (Ethical review number: SCC 1631). The study was conducted as part of a TES of AL in collaboration with the NMCP at the Brikama Health Centre (western Gambia) (Figure 3.1) in 2017. Patients were included in the study following diagnosis of *P. falciparum* infection with a parasite density of at least 1000/µL. An informed consent or assent was obtained from eligible patients. Two millilitres (2 ml) of venous blood samples were collected at day 0 of the TES into EDTA tubes and blood spots made on Whatman filter papers (Scientific Laboratory Supplies). Filter papers were air dried and stored in sealed sample bags with silica gel desiccants. Samples were transported on ice to the MRCG at LSHTM culture facility and processed within 4 hours of collection.

Figure 3.1: Map of The Gambia with study location. The black shaded circle shows Brikama study site which is in western Gambia.

3.3.2 Parasite processing for drug assays

Thin blood smears were made for all samples to identify parasite life-cycle stages. For each sample, 50 µL was used to estimate parasite density using a C6 flow cytometer (BD Accuri™, BD Biosciences) after DNA staining with SYBR Green I DNA intercalating dye (Applied Biosystems). To eliminate white blood cell populations from the analysis, gating was done on the RBC population only using forward and side scatter parameters followed by gating of the SYBR Green I positive population which effectively delineates infected red blood cells (iRBCs). Plasma was separated from blood cells following centrifugation for 5 minutes at 1500 rpm. An equal volume of incomplete media (RPMI 1640 (Sigma-Aldrich, UK) supplemented with 35 mM HEPES (Sigma, St. Louis, MO), 24 mM $NaHCO_3$, 1 mg/l of hypoxanthine (Sigma), 5µg/ml of gentamicin (Gibco-BRL)) was added to the cell pellet and layered on 6 ml of lymphoprep (Axis-Shield, UK). The layered sample was centrifugated for 20 minutes at 2,500 rpm and leukocytes aspirated. The RBCs were washed thrice by re-suspending the pellet in incomplete media and centrifugated for 5 minutes at 1,500 rpm. The washed pellet was re-suspended in growth media: incomplete media with 0.5% Albumax (Gibco-BRL). The parasitaemia was normalized to 0.5% (1000 parasites / µL) for all samples with parasitaemia higher than 0.5% and 2% haematocrit using O^+ heterologous uRBCs prior to PSRA and RSA. Four laboratory adapted strains were used as internal controls: 3D7, Dd2 and MRA-1239 which are sensitive to both LUM and DHA, and MRA-1241 which is sensitive to LUM but resistant to DHA. The isolates were routinely cultured with fresh O^+ uRBCs and maintained at 2% haematocrit with growth media under standard incubation conditions of 37°C, 90% N_2, 5% O_2, and 5% CO_2. All laboratory adapted strains were synchronized twice with 5% D-sorbitol to obtain ≥ 80% ring stages prior to assay set-up. One hundred and seventy samples were obtained from Brikama Health Centre in 2017.

3.3.3 Parasite Survival Rate Assay (PSRA)

The PSRA is based on re-invasion of surface stained O^+ uRBC by merozoites emerging from ruptured schizonts that developed after drug exposure of infected samples. This was a modification of the protocol described (Linares et al., 2015). Here, target uRBCs were pre-stained with the amine-reactive fluorescent dye: 7-hydroxy-9H-(1,3-dichloro-9, 9-dimethylacridin-2-one) succinimidyl ester (DDAO-SE; 10 µM; Invitrogen); a far-red cell dye as described (Theron et al., 2010). A 2% haematocrit suspension of the uRBCs in incomplete media with 10 µM DDAO-SE was made and incubated at 37°C for 2 hours while shaking. The suspension was washed once, re-suspended with incomplete media and re-incubated for a further 30 minutes. DDAO-SE stained uRBC suspension: $uRBC^{DDAO\text{-}SE}$ were washed and reconstituted with growth media for a final haematocrit of 2%.

PSRAs were set up using laboratory isolates of ≥ 80% rings (*in vitro*) and field isolates within 4 hours of sample collection (*ex vivo*). The assays were done in triplicate for sensitivity to concentrations that were 10-fold higher than the median IC_{50} of the respective drugs determined in a previous study (Amambua-Ngwa et al., 2017). Briefly, 100 µL of parasite suspension at 0.5% parasitaemia and 4% haematocrit was added to 48-well microtiter plates pre-coated with 100 µL of the respective drugs at twice the target concentration:

$$(10\text{-fold median } IC_{50}) \times 2$$

This resulted in a final drug concentration of 10-fold median IC_{50} of DHA (8.1 nM) and LUM (398 nM) at 2% haematocrit. A no-drug control, substituted with 0.1% dimethyl sulfoxide (DMSO) (Sigma-Aldrich, UK) was assayed for each sample. The samples in the microtiter plates were incubated for 24-, 48- and 72- hours respectively using standard incubation conditions. Drugs were refreshed every 24 hours after washing cells by incubating twice for 5

minutes with incomplete media. Fifty microliters of the drug-free suspension was transferred to a fresh 96-well microtiter plate containing 100 µL of uRBC$^{DDAO-SE}$ (1 in 3 dilution) which was further incubated for 48 hours (Figure 3.2).

Each sample was then washed and counterstained with 1:10,000 dilution of SYBR Green I in phosphate buffered saline (PBS). For this, 100 µL of diluted stain solution was added to each assay well of the microtiter plate and incubated in the dark at room temperature with shaking for 20 minutes. Stained cells were washed twice and re-suspended with 200 µL of PBS. A further 1 in 4 dilutions with PBS was done prior to flow cytometric counting using BD Accuri™ C6 flow cytometer. For acquisition, the fluorescence emission peak for SYBR Green I and DDAO-SE were set at 520nm and 657nm for the green and red channels respectively. For each assay well, 100,000 events were acquired and data analysed using the BD Accuri™ C6 software. All ex vivo assays were performed in triplicates.

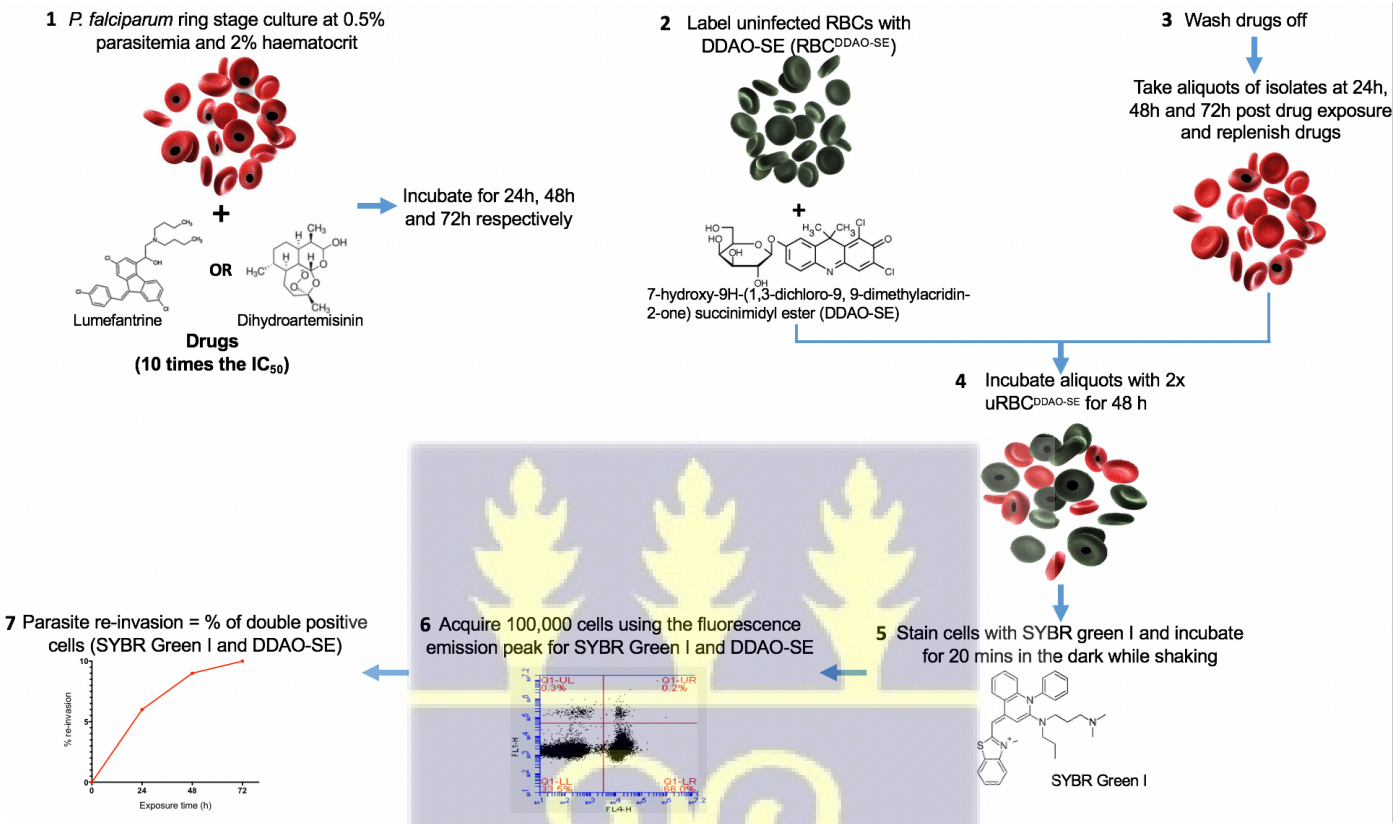

Figure 3.2: Schematic representation of *ex vivo* PSRA. (1) iRBCs at 0.5% parasitaemia and 2% haematocrit are incubated with 10-fold median IC_{50}s of DHA and LUM for 24-, 48- and 72-hour timepoints. (2) uRBCs are stained with the intracellular dye: DDAO-SE ($uRBC^{DDAO-SE}$). (3) Drugs are washed off from step 1 every 24 hours, aliquots taken, and drugs replenished. (4) Post-exposure drug free aliquots are incubated with 2 X $uRBC^{DDAO-SE}$ for a further 48 hours. (5,6) These are then counterstained with SYBR Green I for flow cytometric analysis where 100,000 cells are acquired (7) and double positive stained cells analysed.

3.3.4 Ring-stage survival assay (RSA)

A modification of the RSA protocol (Amaratunga et al., 2014; Witkowski, Amaratunga, et al., 2013) was carried out to assess the re-invasion potential of parasites exposed to 700nM of DHA, replacing microscopy with two-colour flow cytometry similar to the PSRA protocol above. Leukocyte depleted iRBCs were set up in duplicates at 0.5% parasitaemia and 2% haematocrit. Each isolate was exposed to 700 nM of DHA and 0.1% DMSO as control for exactly 6 hours under standard incubation conditions. DHA and DMSO were then washed off using incomplete media and parasites re-suspended with drug-free growth media. Fifty microliters of this suspension was added to 100 µL uRBC$^{DDAO-SE}$ in a separate 96-well microtiter plate and both plates incubated for a further 66 hours. Thin blood smears were then made and stained with Giemsa following the standard RSA protocol. Ring-stage survival rates were determined microscopically using the initial parasitaemia before drug exposure (initial parasitaemia: INI), DMSO control (non-exposed: NE) and DHA-exposed (DHA). Ring-stage survival was calculated for isolates with growth rate of ≥ 1% using the published formula:

$$\text{Percentage survival (\%)} = (\text{DHA}/\text{NE}) \times 100$$

The cells incubated with uRBC$^{DDAO-SE}$ were counterstained as above with SYBR Green I and acquired using BD Accuri™ C6 flow cytometer to determine parasite re-invasion rates. All *ex vivo* assays were performed in triplicates.

3.3.5 Genotyping of selected drug resistance loci

Genotyping of isolates from western Gambia in 2017 was done by locus specific high-resolution melt (HRM) assays with parasite DNA extracted from filter paper dried blood spots (DBS). To recover parasite DNA, DBS were punched onto 96-deep well plates, using punchers

and forceps that were rinsed in 1% bleach and alpha-Q water after each sample to limit cross-contamination. For each plate, 4 negative and 4 positive controls were included. Genomic DNA was manually extracted using the QIAamp® 96 DNA Blood Kit (Qiagen, Hilden, Germany) with manufacturer's instructions. The DNA concentration of the eluates were quantified using a Nanodrop 1000 (Thermo Scientific) and stored at -20°C until use. One micromolar (1 µM) of gDNA of approximately 10 pg/uL - 1 ng/uL, was used for genotyping assays. HRM genotyping reactions were performed for the following alleles: *Pfcrt* C72/M74/N75/K76, *Pfmdr1* N86, *Pfmdr1* Y184, *Pfdhps* S436/A437, *Pfdhfr* N51/C59 and *Pfk13* C580 on the LightCycler® 96 Real-Time PCR System (Roche). The primers and probes used for PCR reactions with 2.5X LightScanner master-mix (Biofire) were as previously described (Daniels et al., 2012). Each reaction had a final forward and reverse primer concentration of 0.05 µM and 0.2 µM respectively (asymmetric PCR) and 0.2 µM for allele specific probes. The PCR conditions and analysis method used are as previously described (Daniels et al., 2012).

3.3.6 Statistical analysis of drug survival rates

The analysis aimed mainly at evaluating the effect of drug exposure from the magnitude of decline in growth by re-invasion with time of exposure compared to drug free controls, i.e. LUM Vs no-drug and DHA Vs no-drug. The study also aimed to explore patterns of variation in response to drug exposure between isolates. To first assess the effect of time of exposure on survival (growth), the re-invasion rates were log-transformed for normality and these values were used for descriptive statistics on responses at each time-point. Linear mixed effect models were then fitted to examine the heterogeneity in drug susceptibility allowing for interaction between time and drug treatment group (LUM or DHA) with random effects on subjects. Since there were three discrete time points of measurement, an indication of potential non-linear

relationship between treatment response and time, time was used as categorical variable comparing differences in effect of treatment for 48- and 72- hours against 24 hours as reference. As such, the effect of longer exposure could be examined. To explore the difference in susceptibility to each drug per isolate, the drug effect was first obtained from the difference between drug exposed and no-drug control at each time point. A linear trend was the fitted across timepoints for each isolate, deriving patterns of individual growth decay slopes. These estimated slopes represent individual parasite survival (or death) rates. Based on the derived decay patterns (individual trajectories), an isolate was assigned to one of the four classes: linear decrease (---), linear increase (+++), non-linear increase/decrease (+-+) and non-linear decrease/increase (-+-). In addition, the relationship between individual trajectories and their corresponding genotypes were assessed. All analyses were performed using the R package (RStudio version 1.2.5001) and Stata 14 (StataCorp, College Station, TX, USA). A *P* value of < 0.05 was considered significant. Other plots were explored using Prism (GraphPad Prism version 7.0a).

3.4 Results

P. falciparum isolates collected from patients with uncomplicated malaria cases recruited across the malaria transmission season in 2017 from western Gambia were analysed. A total of 79 out of 170 (46.5%) isolates had a parasitaemia of ≥ 0.5% and these were set up for both PSRA and RSA assays. Analysis data was obtained for 41 (52%) and 51 (64.6%) samples which had a drug free *ex vivo* growth rate of ≥ 1% for PSRA and RSA respectively. Apart from the field isolates used in this study, the PSRA was tested against a panel of previously characterized isolates, including an ART resistant parasite line: MR4-1241 with the *Pfk13* I543T mutation (Figure 3.7).

3.4.1 Ring stage survival rates of field isolates by Microscopy and Flow cytometry

Ring stage survival rates of 51 isolates were determined using conventional microscopy as per the initial RSA protocol (Witkowski, Amaratunga, et al., 2013) and modified using uRBC$^{DDAO-SE}$ and SYBR Green I for flow cytometric analysis. Following pulse exposure to DHA, 31 isolates (61%) had surviving parasites observed by microscopy, ranging from 0.05 to 1.2% (Figure 3.3a). Flow cytometric counting of re-invasion in pre-stained uRBCs was more sensitive, showing all isolates to have post-drug exposure survival ranging from 0.14 to 1.53%. The mean survival rates determined by flow cytometric analysis was statistically higher than microscopy (P <0.0001). Despite this, there was a strong positive correlation between the two analysis methods, with R= 0.83 and P = 2.7 x 10^{-14} (Figure 3.3b). However, isolates with the highest ring survival rates by flow cytometry were not the same observed by microscopy. Based on flow cytometry only, % ring survival after 6 hours of exposure to 700nM of DHA significantly correlated with parasite survival rates following PSRA analysis (R = 0.53, P = 0.00038), (Figure 3.3c). Overall, the median cumulative rates of survival over the 72 hours of exposure was not significantly different between DHA (-0.051 to 0.029) and LUM (-0.048 to 0.037), (P = 0.35) though the responses to LUM had a wider distribution (Figure 3.3d).

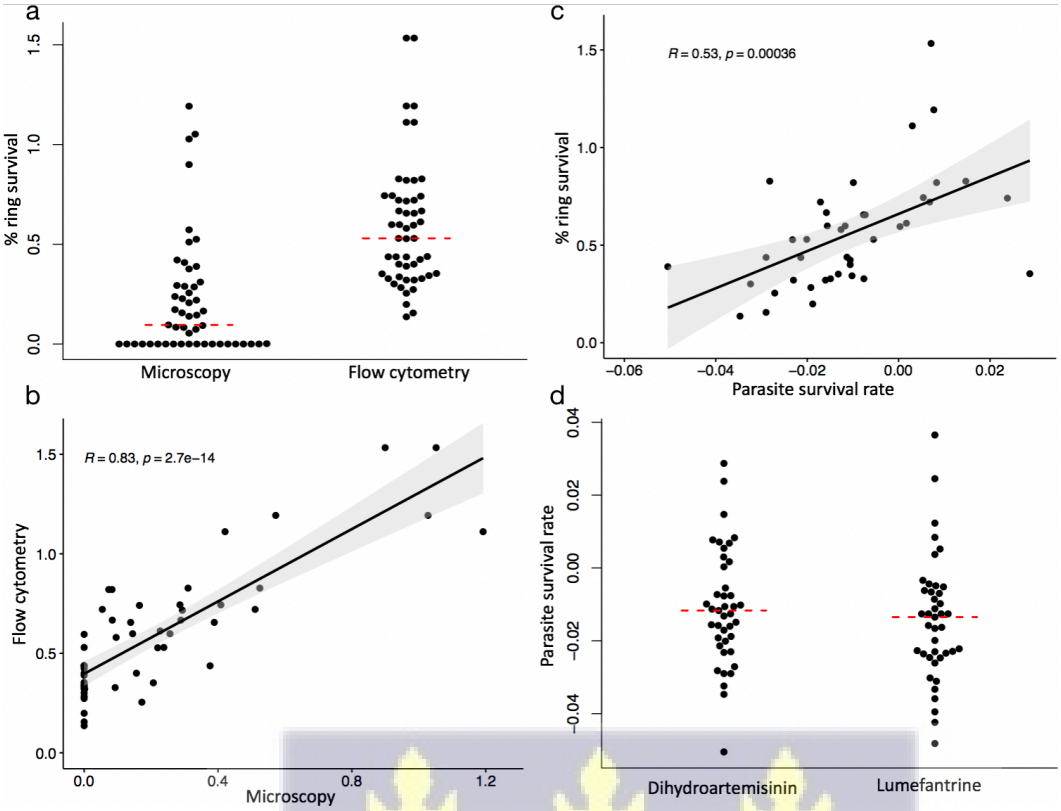

Figure 3.3: Parasite responses following exposure to drugs using RSA and PSRA. (a) Percentage ring survival of 51 isolates using conventional microscopy to assess viable parasites and flow cytometry to assess the number of re-invaded parasites following pulse exposure and withdrawal of DHA with RSA. Each point on the plot represents an isolate. The median survival rates of the isolates for each method are shown as the red broken lines. T-test statistics gave a *P* value of < 0.0001 using Wilcoxon rank sum test. (b) Correlation analysis of percentage ring survival using flow cytometry and microscopy with a Pearson correlation coefficient of R = 0.83 and *P* = < 0.0001 and (c) correlation analysis of percentage ring survival using RSA and parasite survival rates using PSRA analysis. Pearson correlation coefficient gave an R value of 0.53 and a *P* value of 0.00036. (d) Distribution of the parasite survival rates of 41 isolates treated with DHA and LUM at 3 timepoints over 72 hours with PSRA. Each point shows the rate at which each isolate survives following drug exposure with reference to DMSO-treated control. The red dotted lines are the median survival rates for both drug treatments with *P* = 0.35. *P* value of < 0.05 represents statistical significance.

3.4.2 *P. falciparum ex vivo* survival decreases with longer drug exposure

By comparing log of survival rates between isolates with different durations of drug exposure, the overall survival declined with increased exposure time for both drugs, whereas there was an increasing growth trend in the drug-free group over time (Figure 3.4 and 3.7). The mean differences between treatment and control groups were always significant and increased with time as treatment groups appeared to show a marked decline in predicted survival particularly after 72 hours (Figure 3.5). Pairwise comparison between the drug-treated groups against drug-free group showed significant differences at all three timepoints (Table 3.1). Using 24 hours as the reference, differences in predicted responses were seen for both DHA and LUM at 72 hours post drug exposure. At 48 hours, the differences in predicted responses were not statistically significant when compared to 24 hours. This could be due to the exponential increase in merozoite iRBCs following a complete *P. falciparum* growth cycle (Murray et al., 2017), potentially resulting to the high responses seen at 48 hours in the control group (Figure 3.4c and 3.7).

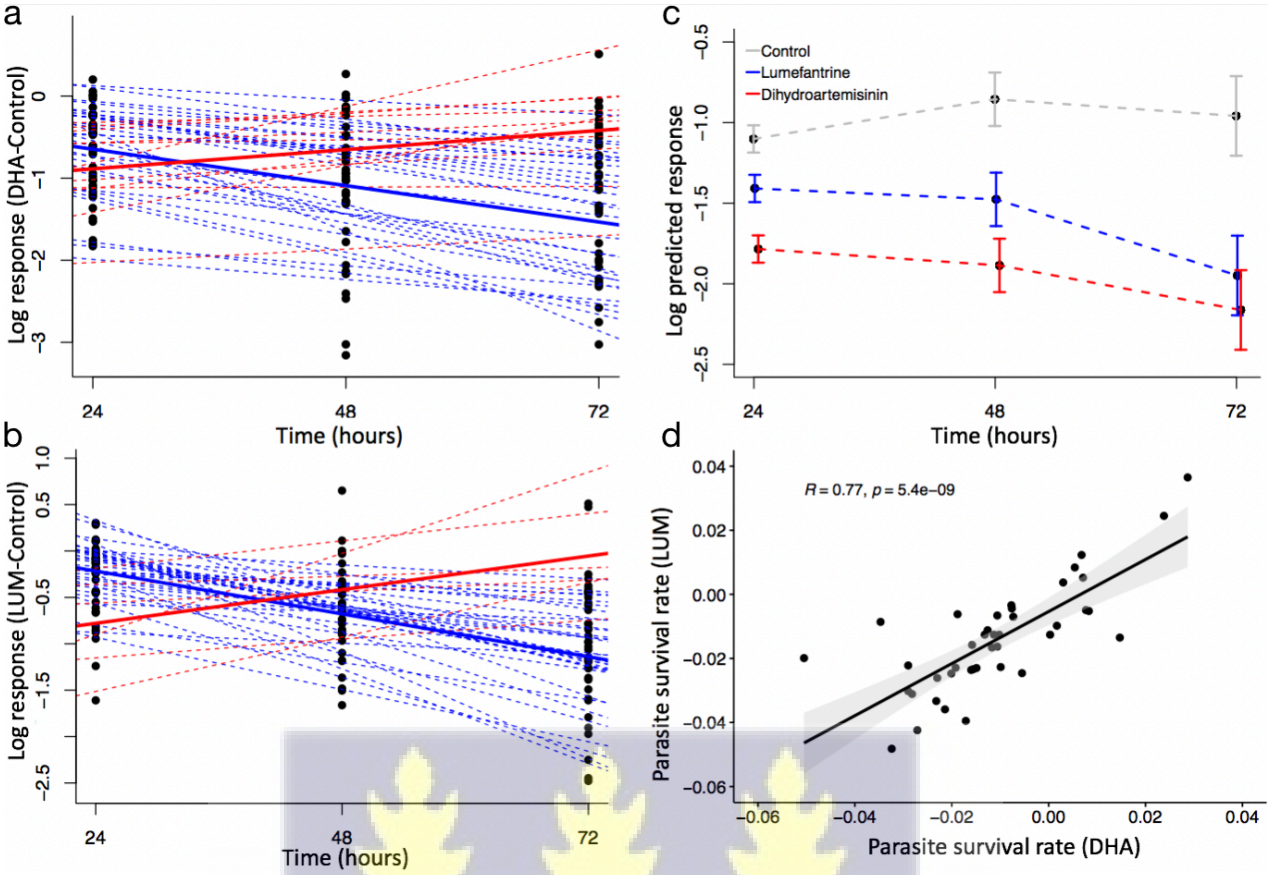

Figure 3.4: Individual trajectories of 41 isolates following drug exposure. (a) DHA and (b) LUM relative to DMSO treated control at 24-, 48-, and 72- hour timepoints. Linear mixed effect model was used, and a linear trend fitted for each isolate across timepoints. The blue and red dotted lines show the isolates with decreasing and increasing responses over time respectively. The thick blue and red lines represent the mean log response of isolates with decreasing and increasing responses respectively. (c) Mean predicted parasite responses of all isolates following exposure to DHA (red broken line), LUM (blue broken line) and DMSO control (grey broken line) with the SEM shown as bars. (d) Correlation between parasite survival rates of isolates treated with DHA and LUM with R = 0.77 and $P < 0.001$.

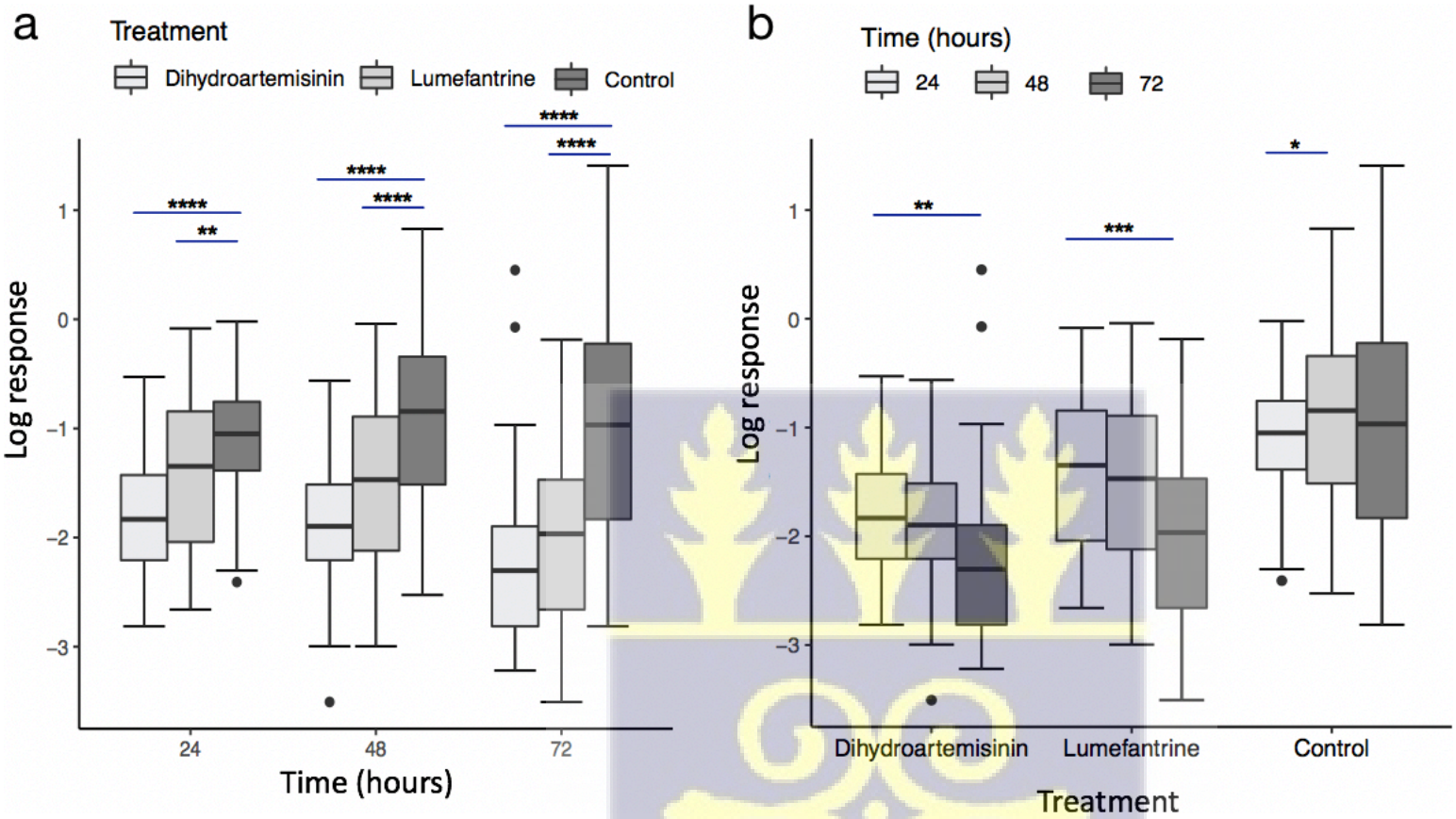

Figure 3.5: Parasite log responses following exposure to DHA, LUM and DMSO-treated control at 24-, 48- and 72- hours of drug exposure with PSRA. Mixed model for log response and interaction between group and time with random intercept was fitted. Mean responses comparing the log response of (a) the three treatment groups at each timepoint and (b) the three timepoints for each treatment groups. $P < 0.05$ was considered significant.

Table 3.1:Effect of drug exposure on predicted responses of the treatment groups (DHA, LUM, DMSO-control) and exposure times (24-, 48- and 72- hours) for *P. falciparum* isolates analysed by PSRA.

Treatment groups	**Difference (95%CI)**	***P* value**
(DHA vs Control) 24h	-0.68 (-0.90, -0.47)	**<0.0001**
(DHA vs Control) 48h	-1.03(-1.25, -0.81)	**<0.0001**
(DHA vs Control) 72h	-1.20 (-1.42, -0.99)	**<0.0001**
(LUM vs Control) 24h	-0.31 (-0.52, -0.09)	**0.005**
(LUM vs Control) 48h	-0.62(-0.84, -0.41)	**<0.0001**
(LUM vs Control) 72h	-0.99 (-1.21, -0.77)	**<0.0001**
(48h vs 24h) Control	0.25 (0.01, 0.48)	**0.04**
(48h vs 24h) DHA	-0.10 (-0.33, 0.13)	0.39
(48h vs 24h) LUM	0.07 (-0.30, 0.16)	0.57
(72h vs 24h) Control	0.14 (-0.13, 0.42)	0.31
(72h vs 24h) DHA	-0.38 (-0.65, -0.10)	**0.007**
(72h vs 24h) LUM	-0.54 (-0.81, -0.27)	**0.0001**

*24h = 24 hours; 48h = 48 hours; 72h = 72 hours; DHA = Dihydroartemisinin treatment; LUM = Lumefantrine treatment; Control: DMSO treatment.

Values in bold are significant *P* values determined by pairwise comparisons.

3.4.3 Distribution of PSRA sensitivities to AL

Individual responses to each drug were derived from fitting a linear model on the differences in predicted responses between the drug treated and control with time. These *ex vivo* parasite survival rates ranged from -0.051 – 0.029 for DHA and from -0.048 – 0.037 for LUM. The majority of isolates had a negative slope with consistently reducing survival with time (Figure 3.4a and 3.4b). This was seen for 30 isolates for DHA and 35 for LUM representing 73% and 85% of isolates treated respectively. Conversely, 27% (11/41) and 15% (6/41) had a net increase in growth despite 72 hours of exposure to DHA and LUM, with similar or higher predicted responses under drug conditions compared to the controls with DMSO (Figure 3.4a and 3.4b, Figure 3.6a and 3.6b). Interestingly, one isolate had a net increase following exposure to both DHA and LUM. The overall response and rates of growth decline was higher for DHA compared to LUM (Figure 3.4c). However, the survival rates between DHA and LUM showed a strong positive correlation (R = 0.77, P = 5.4e-09), (Figure 3.4d).

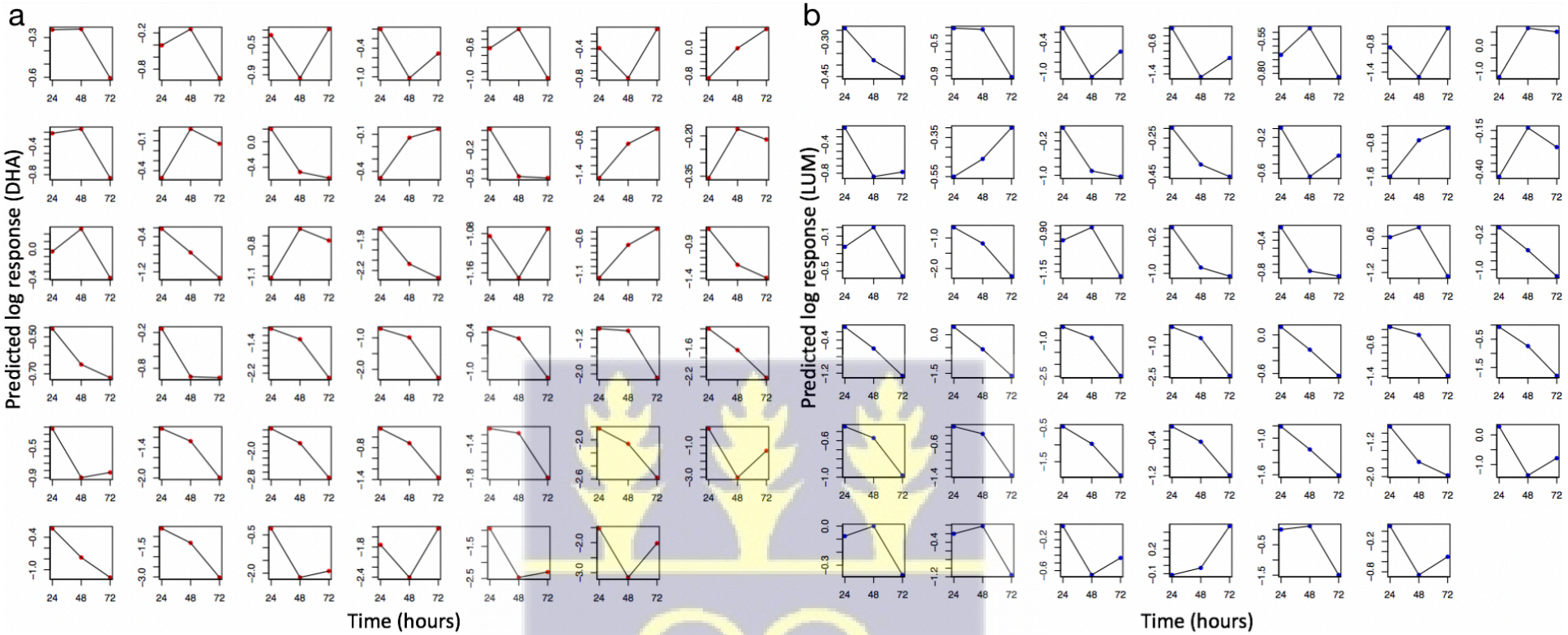

Figure 3.6: Individual profiles of 41 isolates following exposure to (a) DHA and (b) LUM at 24-, 48- and 72- hours with PSRA. Each point on the individual plots represent the difference between the predicted response of the DMSO-treated control and drug treatment. The connecting lines give an indication of the response pattern of each isolate.

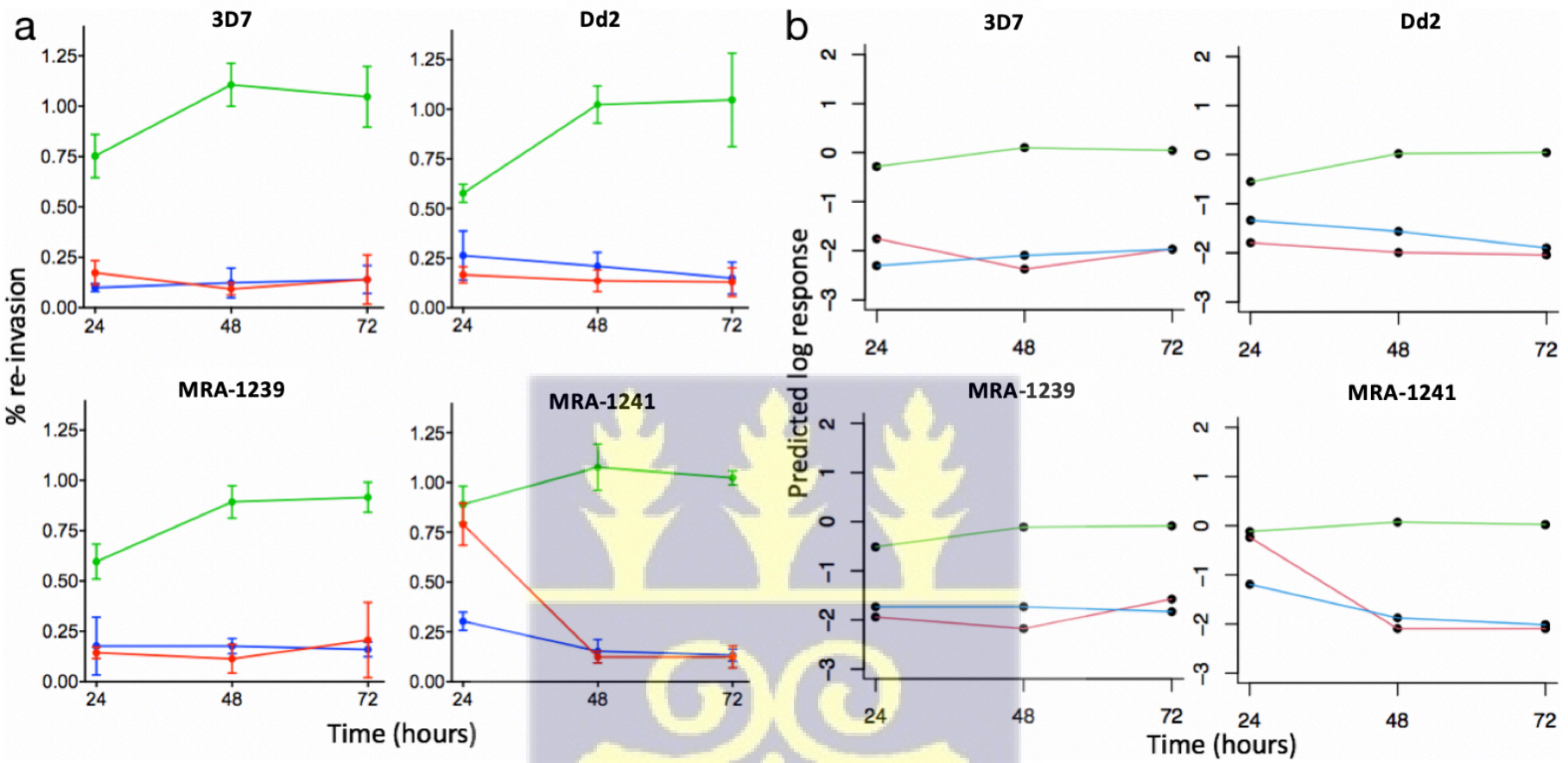

Figure 3.7: (a) Re-invasion parasitaemias and (b) log response rates from mixed model analysis of four laboratory adapted isolates following exposure to DHA (red lines), LUM (blue lines) and DMSO-control (green lines) at 24-, 48- and 72- hours with PSRA. In (a), the confidence intervals of % re-invasions for 3 replicates of 3 independent experiments are shown in bars.

3.4.4 Consistent clusters of survival rate patterns to both DHA and LUM

Four patterns of responses were identified based on the growth vs time curve for both drugs (Figure 3.8a and 3.8b). The most common pattern was a continuous decline in survival with increase in time of exposure. This first group of isolates defined as linear decrease (designated as "---" on figure 3.8) represented 46% (19/41) and 51% (21/41) of isolates tested against DHA and LUM respectively. The second group of isolates had a peak in growth at 48 hours of drug exposure ("-+-") and these represented 19.5% (8/41) and 22% (9/41) of isolates tested. The third group were isolates with consistently linear increase ("+++") despite drug exposure, with 9.75% (4/41) and 7.3% (3/41) identified for DHA and LUM, and the fourth pattern were isolates with the lowest survival timepoint at 48 hours ("+-+") representing 24% (10/41) and 20% (8/41) of isolates. These patterns did not correlate with initial parasitaemia (Figure 3.9) or other patient demographic information.

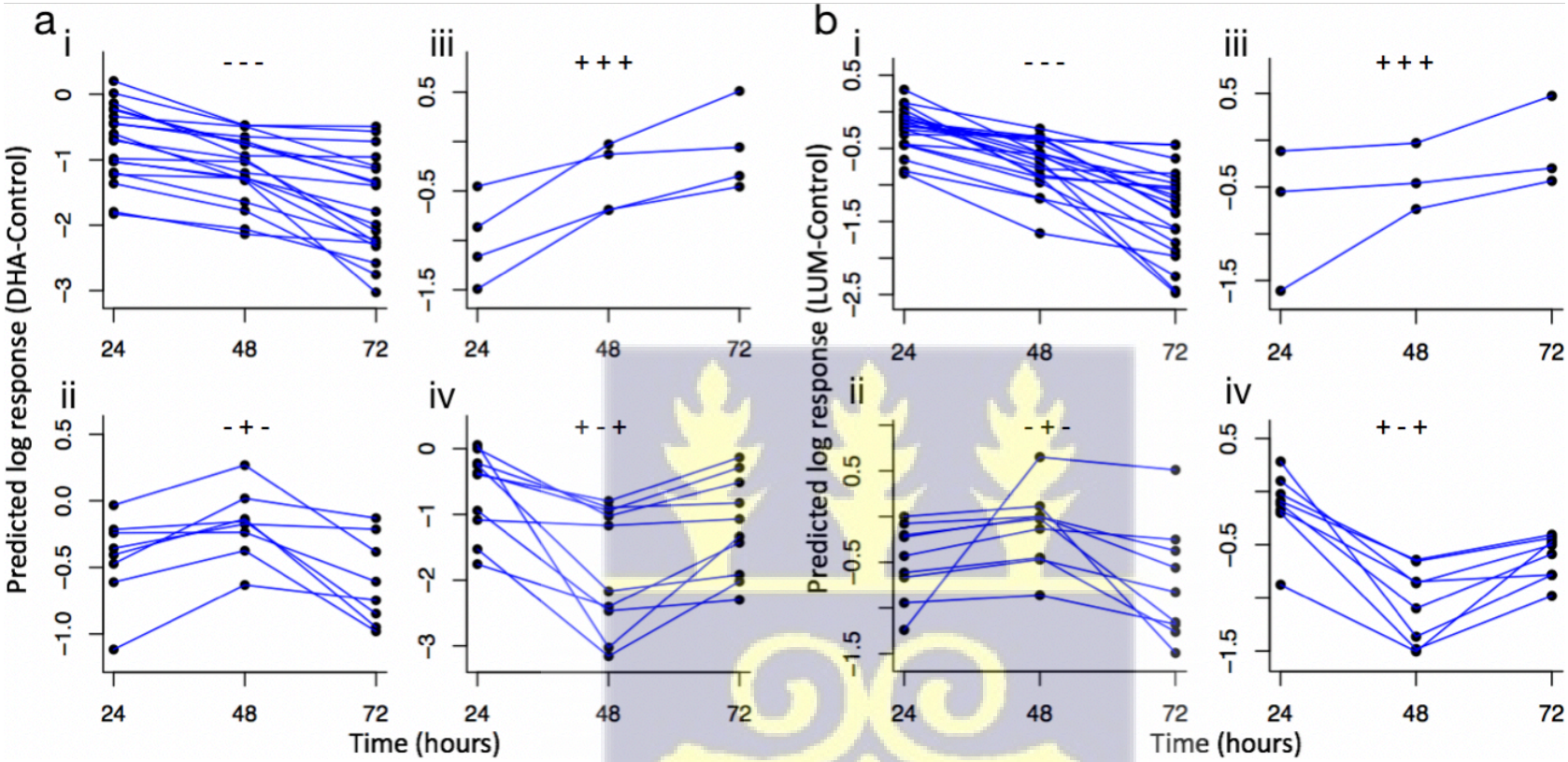

Figure 3.8: Grouped profiles of 41 isolates following exposure to DHA and LUM at 24-, 48- and 72- hours with PSRA. Each point in the individual plots represent the difference between the predicted response of the (a) DHA treated and control and (b) LUM treated and control. The connecting lines give an indication of the response pattern of each isolate. The isolates are grouped based on their response profiles. (i) linear decrease (---), (ii) non-linear decrease/increase (-+-), (iii) linear increase (+++), (iv) non-linear increase/decrease (+-+).

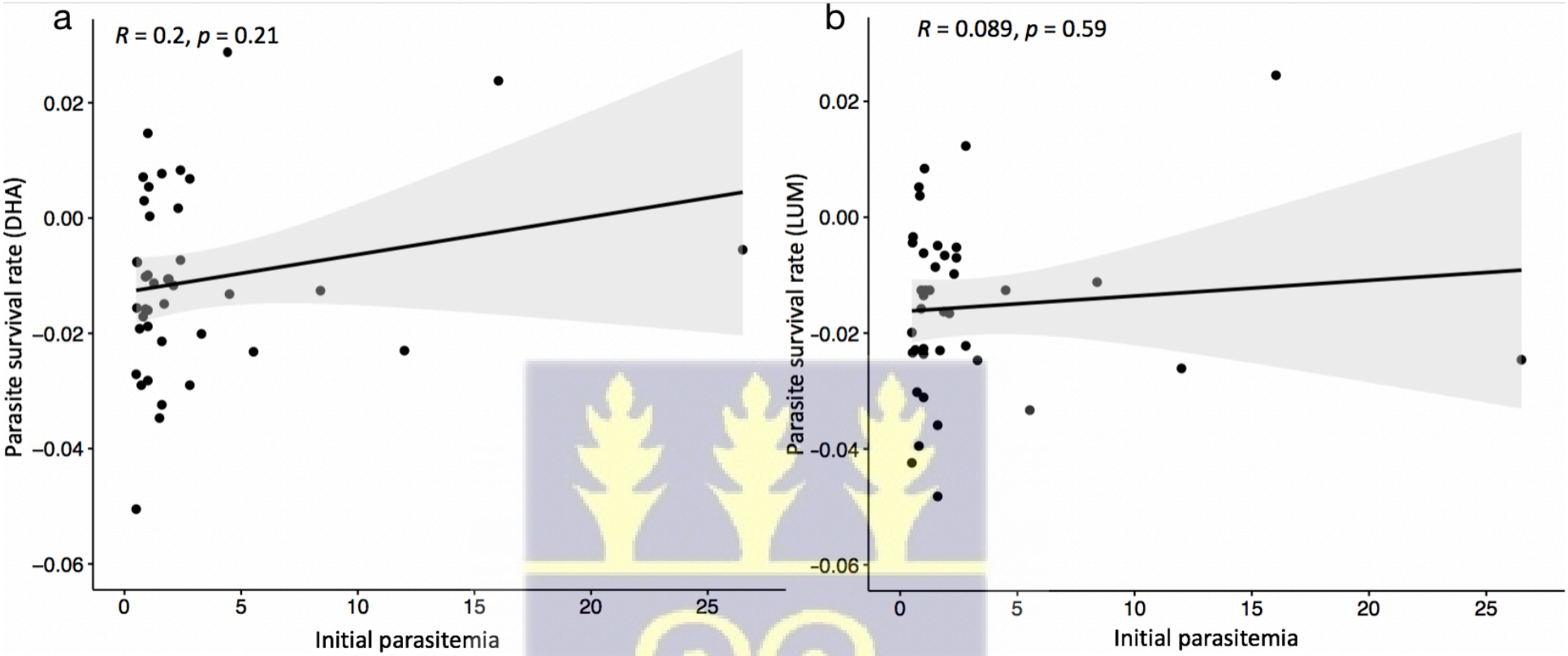

Figure 3.9: Correlation analysis between initial patient parasitaemia at day 0 prior to assay set-up and parasite survival rates of isolates treated with (a) DHA with a Pearson correlation coefficient of R = 0.2 and *P* = 0.21 and (b) LUM with R = 0.089 and *P* = 0.59.

3.4.5 Frequencies of drug resistance alleles from western Gambia in 2017

Genotypes were obtained for at least 39 isolates for *Pfcrt* C72/M74/N75/K76, *Pfmdr1* N86, *Pfmdr1* Y184, *Pfdhps* S436/A437, *Pfdhfr* N51/C59 and *Pfk13* C580 (Table 3.2 and Figure 3.10). The *Pfcrt* mutant haplotype was found in 79% of isolates with 2% of mixed infections. Ninety-three percent (93%) of isolates were wild-type for *Pfmdr1* N86 and 5% mixed, while 57% were mutant for *Pfmdr1* Y184 and 12% mixed. For antifolate markers, 90% of isolates had mutant variants at *Pfdhps* S436/A437 while all isolates were mutated for *Pfdhfr* N51/C59. The analysis for the *Pfdhfr* alleles: IT/NC was excluded as the scoring of the melting curves were ambiguous, showing up to 55% of mixed allele calls. *Pfk13* C580 was wild-type for all isolates. Given the almost fixed frequencies of either wild-type or mutant at these loci tested, no association with the PSRA patterns could be determined. However, for *Pfmdr1* codon 184, higher LUM responses were observed for isolates with the 184F mutant allele though the mean differences were not significant between these and isolates with Y184 wild-type variant (Figure 3.10c. ii).

Table 3.2: Allele frequencies of drug resistance genes for 41 parasite isolates with drug phenotypic data (PSRA and RSA) in 2017.

Gene	Alleles	Codons	Frequency
Pfcrt	C72, M74, N75, K76	CMNK (wild-type)	0.17
		CIET (mutant)	0.79
		CMNK/CIET (mixed)	0.02
Pfmdr1	N86	N (wild-type)	0.93

		Y (mutant)	0
		N/Y (mixed)	0.05
	Y184	Y (wild-type)	0.29
		F (mutant)	0.57
		Y/F (mixed)	0.12
Pfdhps	S436/A437	SA (wild-type)	0.02
		SG (mutant)	0.88
		FG (mutant)	0.02
		SA/SG (mixed)	0.05
		FG/SA/SG (mixed)	0.02
Pfdhfr	N51/C59	NC (wild-type)	0
		IR (mutant)	0.26
		IT/NC (mixed)	-
		IR/NR (mixed)	0.12
		NR/NC (mixed)	0.02
Pfk13	C580	C (wild-type)	1
		Y (mutant)	0

Pfcrt = *P. falciparum* chloroquine resistance transporter; *Pfmdr1* = *P. falciparum* multidrug resistance gene 1; *Pfdhps* = *P. falciparum* dihydropteroate synthase; *Pfdhfr* = *P. falciparum* dihydrofolate reductase; *Pfk13*= *P. falciparum* kelch 13

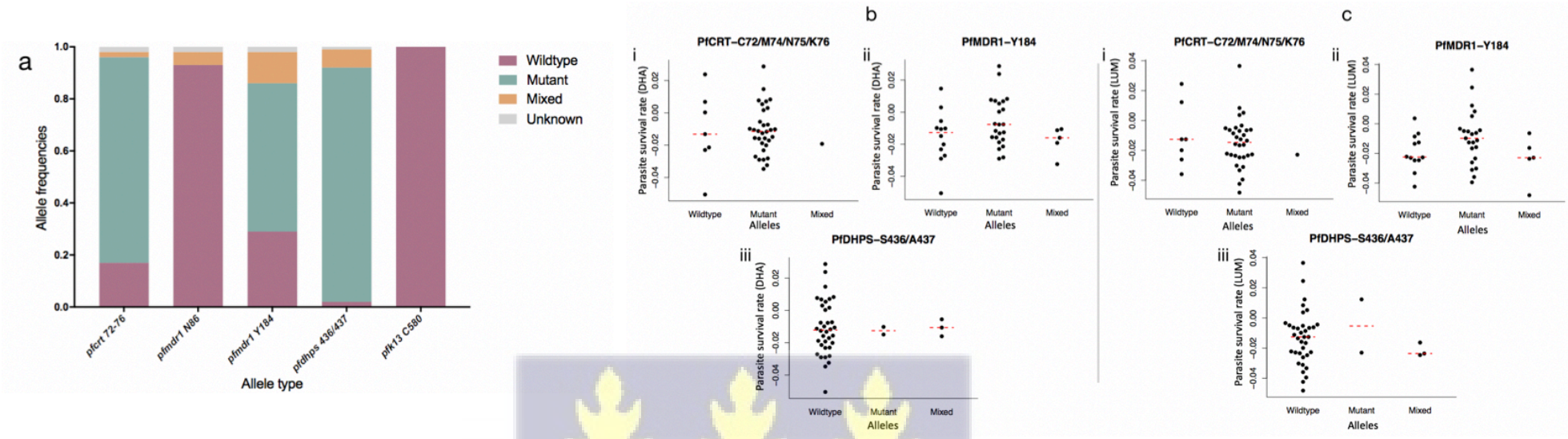

Figure 3.10: Allele frequencies and association analysis of field isolates from 2017. (a) Allele frequencies of 41 field isolates for the drug resistant genes: *Pfcrt* C72/M74/N75/K76, *Pfmdr1* N86, *Pfmdr1* Y184, *Pfdhps* S436/A437 and *Pfk13* C580. Parasite survival rates of (b) DHA and (c) LUM for isolates with wild-type, mutant and mixed alleles for *Pfcrt* C72/M74/N75/K76, *Pfmdr1* Y184 and *Pfdhps* S436/A437. Each point in the graphs represent the parasite survival rate of an isolate. The broken red lines indicate the median survival rates of the isolates with the same alleles.

3.5 Discussion

This study describes the *ex vivo* susceptibility rates of natural isolates from The Gambia, where transmission has declined, and increasing *ex vivo* tolerance to LUM by IC_{50} was seen as well as modest survival rates (26%) to DHA by RSA. These rates were obtained against DHA and LUM with a flow cytometry-based PSRA, with potential application to other drugs and antimalarial candidates. The potency of these drugs depend on the drug concentrations used and the length of exposure, with the assumption that cytotoxicity occurs when parasites are exposed to the active component of the drug for a prolonged time (Tilley et al., 2016). Here, drug concentrations that are 10-fold higher than the median IC_{50} of the respective drugs obtained from the assessment of field isolates from western Gambia in 2015 was used (Amambua-Ngwa et al., 2017). The use of 10-fold higher drug concentrations, though much lower than serum concentrations, proved to be the optimal concentration to determine the rate of kill of slow, medium and fast acting drugs. This concentration is sub-optimal, allowing for gradual effect of the drugs on the parasites (Sanz et al., 2012).

The PSRA provided several advantages over the IC_{50} and RSA assays; it determines the effect of drugs over 72 hours of exposure and measures both parasite growth and viability by determining re-invasion even at low parasite densities. Unlike RSA, there is no requirement for assaying early rings which can be difficult to ascertain for natural isolates from malaria patients, thereby eliminating the need for further stressing isolates by synchronizing them with sorbitol (Mata-Cantero et al., 2014). Similar to the *in vivo* parasite clearance rate assay for determining the efficacy of ART derivatives, the PSRA determines clearance rates from the rate of *ex vivo* inhibition of growth over 72 hours of drug exposure (White, 2017). This duration of exposure allows rings that emerge from tolerant isolates over the first cycle (48 hours) to experience another round of drug exposure for 24 hours, followed by recovery in drug free

medium. The overall outcome is the kinetics of parasite killing by the test drug over 72 hours. This assay is therefore a variant of the PVFA (Linares et al., 2015; Sanz et al., 2012). Like PVFA, the PSRA does not assess parasite metabolic activity or other parasite molecules to quantify survival or death indirectly (Linares et al., 2015). It quantifies viability from a direct count of viable merozoites that emerge from drug-exposed schizonts and invade pre-stained uRBCs: uRBC$^{DDAO-SE}$. Flow cytometry provided increased sensitivity by individually counting cells and distinguishing new autologous and heterologous infected cells. With a 2 to 1 ratio of uRBC$^{DDAO-SE}$ to non-stained RBCs, higher numbers of pre-stained uRBCs are present, skewing re-invasion to occur in these cells. As merozoites emerge after drug exposure, active re-invasion is proof of viability. This gives a good estimate of the number of parasites that survive following drug exposure. The rate of death is therefore intrinsic to the level of drug tolerance by each isolate. Autologous re-invasion of unstained RBCs are excluded from the analysis as they cannot be differentiated from dead and arrested cells.

Unlike RSA, the PSRA uses a much lower concentration of drug but potent enough to kill isolates and to induce the delayed clearance phenotype in RSA control isolate (MRA-1241). Hence, there was a high positive correlation between PSRA and flow-cytometry modified RSA. With strong correlation with microscopy but improved throughput, flow cytometry-based RSA and PSRA should allow for robust detection of emerging drug tolerance in natural isolates. Future and wider application of this method is warranted in Africa where drug pressure is substantial. This is the case for The Gambia where the ACT: AL is used as first line treatment and other ACTs are being considered for mass administration after several clinical trials.

Most of the isolates tested by PSRA in The Gambia had decreasing parasite survival with increasing days of exposure to drugs. However, four and three isolates continued to grow in the presence of DHA and LUM respectively and were considered potentially tolerant, with one

isolate surviving in the presence of both drugs. The number of tolerant isolates would be higher if these included those that showed reduced growth after 48 hours of exposure to both drugs, then a rebound of viable isolates after 72 hours. These suggest a state of reduced drug sensitivity, allowing parasite growth and re-invasion to occur in the presence of sub-lethal drug concentrations (De Lucia et al., 2018). The seven surviving isolates could be on a path towards a persistent state of drug insensitivity that may result in resistance and should be closely monitored. Extending the assay time to 96 hours could also reveal clearer response profiles for the isolates with non-linear responses over the 72-hour period. Importantly, the weak correlation between initial patient parasitaemia and parasite response suggests that the responses seen are not driven by the rate at which parasites grew in the patient (*in vivo*). Most isolates had similar response patterns for both drugs and their survival rates correlated positively. This could be an indication of common mechanisms that enable survival to several drugs, a factor that could lead to multidrug resistance.

Multidrug resistance to ART derivatives and partners has been confirmed in SEA (Hamilton et al., 2019). A consistent increase of LUM tolerance between 2012 and 2015 was already shown in The Gambia (Amambua-Ngwa et al., 2017). In the same study, 26% of the isolate in the 2015 population from western Gambia showed viable parasites by microscopy-based RSA for DHA. The presence of surviving parasites in this current study though at different proportions with both assays, suggests sustained low level of DHA tolerance and requires further investigation. These parasites survived and replicated in high concentration and prolonged length of DHA pressure with RSA and PSRA respectively. Malaria transmission in western Gambia has reduced drastically in the last decade, with prevalence of infection lower than 5% overall and in 2019 (https://data.worldbank.org/indicator/). Despite this, various ACTs remain widely available and accessible through private and public vendors. While it is officially required that ACTs should be prescribed only upon a positive malaria diagnosis, this is hardly

sustained given regular short supplies of Rapid Diagnostic Test kits. Therefore, it can be speculated that the emergence of tolerant parasites is being driven by high drug pressure against low transmission which is hypothesized to be one of the main drivers in the emergence of antimalarial drug resistance in SEA. This calls for improved vigilance across Africa as elimination programs are implemented. ACT resistance has been shown to emerge on a backbone of known drug resistance including *Pfmdr1* and *Pfcrt* selected by LUM. The WHO recommends surveillance for known and emerging markers of resistance in natural populations.

Isolates assayed were genotyped for alleles at *Pfmdr1, Pfcrt, Pfdhfr, Pfdhps* and *Pfk13* loci that have been implicated in quinoline, antifolate or ART resistance. High levels of resistance loci against the antifolates was seen, an expected result given the use of SP by SMC and IPTp. High levels of *Pfmdr1* N86, the wild type allele selected by LUM was also revealed, a result aligning with what was previously shown for this population (Amambua-Ngwa et al., 2017). On the contrary, the *Pfcrt* 72-76 mutant haplotype was in over 80% of isolates, indicating continuous selection by CQ. CQ had been withdrawn for treatment of malaria raising the question as to which drugs are driving selection at *Pfcrt* but not *Pfmdr1* (Ocan et al., 2019). Selection of *Pfcrt* may be driven by AMD which is available in combination with ARS accessible from private vendors in The Gambia and is the ACT of choice in neighbouring Senegal with whom there is significant human migration. More insights should be gained on this considering current extensive temporal and spatial genome sequencing for these parasite population. With the high levels of mutant or wild-type alleles at drug resistant genes, an analysis of genetic association for the four different parasite PSRA profiles was not possible. However, higher survival rates against LUM were seen for isolates with the mutant variant at *Pfmdr1* 184F though this was not significantly different from the distribution of rates in isolates with wild-type alleles.

The responses observed for samples carrying multiple strains is assumed to be a combined effect of the different strains present and the six isolates that survived following exposure to either of the two drugs have specific molecular signatures influencing their phenotypes which should be further investigated. Despite the number of isolates showing growth after 72 hours of exposure to DHA, no mutant alleles of *Pfk13* C580 were found in the population. ART associated *k13* variants are rare in African populations but high frequencies of other non-synonymous SNPs on *Pfk13* had been observed for isolates from The Gambia (Ménard et al., 2016). These further buttresses the need for routine and in-depth surveillance of this population.

This study highlights early signs of *ex vivo* drug tolerance of parasites from western Gambia to the most common ACT components. These were derived by PSRA which provides a significant advancement in approaches for the determination of parasite susceptibility. A wider application of this approach across sSA to distinguish drug tolerance and resistance will support current and future chemoprevention and chemotherapeutic strategies against malaria.

CHAPTER 4

4.0 Antimalarial activities of compounds in the MMV pathogen box

4.1 Abstract

Development of drug resistance in malaria is inevitable, necessitating the need for prompt discovery of novel antimalarial drugs. The MMV has made it feasible for fast and effective screening and identification of compounds with activities against neglected diseases. A library of 400 compounds was developed and 125 of these have antimalarial activity. The present work aimed at assessing parasite susceptibility to compounds from the MMV pathogen box using the newly developed PSRA to assess its potential in differentiating parasite responses to these compounds. Parasites from the field were used to verify the potencies of these compounds, an approach that has not previously been done.

The CQ sensitive laboratory adapted isolate, 3D7 was used for initial screening of all 125 compounds with antiplasmodial activities found in the pathogen box using the IC_{50} determination assay. Six compounds with higher potency than CQ were selected for further analysis. Of these six, three of the compounds were further tested against parasite isolates from the field using the newly developed PSRA.

MMV667494 was more potent than all 125 compounds using both the IC_{50} and PSRA assays. MMV010576 was identified to be slow acting but more potent than DHA at 72 hours of exposure to parasites. Finally, though MMV634140 was identified to be more potent than CQ, some isolates were able to survive and replicate in its presence, a risk for future resistance development. Some of the compounds screened in this study have previously been characterised and their targets identified. More work should be done to determine their

pharmacokinetic properties which is necessary for them to progress in the drug development pipeline.

4.2 Introduction

Several antimalarial drugs used are structurally related with similar modes of action, most of which fall under three major classes. The quinolines which are active against the erythrocytic stages of the parasite life-cycle (Alam Saifi et al., 2013), antifolates which are active against asexual forms of the parasite and the ART derivatives, most active against very early ring stages and are considered to be the most potent class of antimalarial drugs to date (Heller et al., 2019). As these compounds are chemically related, resistance to one drug can accelerate the development of resistance to other closely related drugs. A well-known example is the cross resistance observed between the two 4-aminoquinolines: CQ and AMD (Diawara et al., 2017). It has been suggested that parasites that develop resistance to multiple drugs are genetically more plastic, enabling them to rapidly evolve and develop resistance to any novel drug regardless of chemical class (cross resistance) (Reviewed by (Thu et al., 2017)). The mechanisms with which this occurs, if understood, can explain the rapid development of multidrug resistance in SEA (Hamilton et al., 2019).

The use of monotherapies easily contributed to the development of drug resistance in parasite populations. Resistance can develop following parasite exposure to sub-therapeutic concentrations of drugs in the circulation *in vivo* (Tilley et al., 2016). This could be as a result of a number of factors including long half-life characteristics of some drugs, incomplete treatment course by an infected individual or fake/counterfeit drug use with sub-therapeutic drug doses, resulting in parasite recrudescence post treatment (Ross et al., 2019). The use of antimalarial drugs in combination as in ACTs, was introduced to prevent parasite

recrudescence and slow down the rate at which antimalarial resistance develop. ART and its derivatives in ACTs are able to rapidly kill parasites, reducing parasite load in an infected individual by 10,000 folds in 48 hours. However, these drugs have a relatively short half-life and are required to be active in the patient's blood for at least 3 to 4 parasite life-cycles in order to effectively clear out all parasites in circulation (Wells et al., 2015).

As a result, ART derivatives are inefficient for use as monotherapy and are therefore used in combination with partner drugs with relatively longer half-lives such as quinolines. The two drugs used in combination have different mechanisms of actions and pathways to target parasites resulting in better clearance efficiency than monotherapies (Tilley et al., 2016). However, following about a decade of use, resistance to ACT components developed and ACT treatment failure was reported across SEA (Witkowski, Khim, et al., 2013). The threat of this occurring or spreading to Africa, which bears the greatest burden from malaria, will spell doom for malaria elimination. Hence, novel antimalarial drugs should be developed to replace inefficient drugs and protect the efficacy of existing ones.

Efforts to develop new antimalarial drugs use HTS methods to assess the antimalarial activity of compound libraries. Here, 125 compounds with anti-plasmodial activity were screened from the MMV pathogen box containing a total of 400 compounds against neglected tropical diseases. The novel PSRA which is highly sensitive was used to confirm the potencies of the most potent compounds. The ideal antimalarial drug should be highly potent with a long half-life, maintaining a plasma concentration above sub-therapeutic concentrations for up to 4 parasite life-cycles (Reviewed by (Wells et al., 2015)).

4.3 Materials and methods

4.1.1 *P. falciparum in vitro* parasite culture

P. falciparum laboratory adapted isolate: 3D7 was continuously cultured using standard culture conditions as described in section 3.3.2. Thin blood smears were made and stained with Giemsa to determine parasite stages and parasitaemia.

4.1.2 Compounds from the MMV pathogen box

The pathogen box compounds were obtained from MMV in sealed plates consisting of 400 compounds at a concentration of 10 mM dissolved in DMSO. Information about the pathogen box can be accessed via the MMV website (www.mmv.org/mmv-open/pathogen-box). Compounds were diluted to 1 mM concentration in 100% DMSO, aliquots made in 96 well microtiter plates and stored at -80°C.

4.1.3 IC_{50} determination assay

All 125 compounds with activity against *P. falciparum* were serially diluted 5-fold resulting in a final concentration range of 20 µM to 0.05 nM with nine concentrations in 96-well microtiter plates. These were tested against laboratory-maintained 3D7 isolates at 1% parasitaemia and 2% haematocrit for growth inhibition over 72 hours using standard incubation conditions. Following incubation, cells were stained with 100 µL of 1 in 5000 SYBR Green I intercalating dye in lysis buffer containing 0.005% SDS. Fluorescence was measured at 450 nm using the Fluoroskan™ Microplate Fluorometer.

A subset of the compounds identified as most potent were screened using more stringent compound concentrations as follows: 2-fold serial dilutions resulting to 10 concentrations ranging from 25 nM to 0.05 nM for MMV634140, MMV010576, MMV085499; 3-fold serial dilutions of 10 concentrations ranging from 25 nM to 0.001 nM for MMV024443, MMV023985 and MMV010545; and 2-fold serial dilutions of 18 concentrations ranging from 25 nM to 0.20 nM for MMV667494. Following exposure for a full growth cycle, infected cells were stained with SYBR green I and invaded cells counted using BD Accuri™ C6 flow cytometer as described (Mbye et al., 2020).

4.1.4 Parasite survival rate assay (PSRA)

Survival rates of 10 field isolates were assessed following exposure to 10-fold higher IC_{50} of 3 selected compounds from the pathogen box: MMV667494, MMV634140, and MMV010576, together with DHA and LUM as described in section 3.3.3. Parasites were harvested at an additional time of 6 hours post drug/compound exposure resulting in a time-course profile of four timepoints.

4.1.5 Statistical analysis

All statistical analyses were performed using GraphPad Prism v7.0 and graphs prepared from GraphPad and R software. All assays were set up in triplicates and data normalised. IC_{50} values were calculated using a four-parameter nonlinear regression fit against the log drug concentrations. A P value of < 0.05 was considered significant.

4.4 Results

4.1.6 Primary screen of compounds with antimalarial activity from the pathogen box reveals highly potent compounds

An initial screen of 125 compounds with antimalarial properties from the MMV pathogen box showed a wide range of IC_{50} responses against the CQ sensitive 3D7 laboratory isolate (Figure 4.1, Table 4.1). The reference drugs QN, CQ and AMD with known antimalarial properties were also screened as controls with IC_{50} values of 41.72 nM, 35.14 nM and 45.38 nM respectively. The IC_{50} values of the 125 compounds ranged between 0.02 nM and 9702 nM with a median of 804.40 nM. A total of 16 compounds showed potencies similar to or higher than CQ with their IC_{50}s ranging from 0.02 nM to 30.98 nM. The IC_{50}s of the remaining 109 compounds with lower potency than CQ ranged between 36.39 nM to 9702 nM. The median IC_{50} of the 16 compounds with higher potencies than CQ was 3.85 nM and that of the remaining compounds with lower potencies relative to 3D7 was 1197 nM.

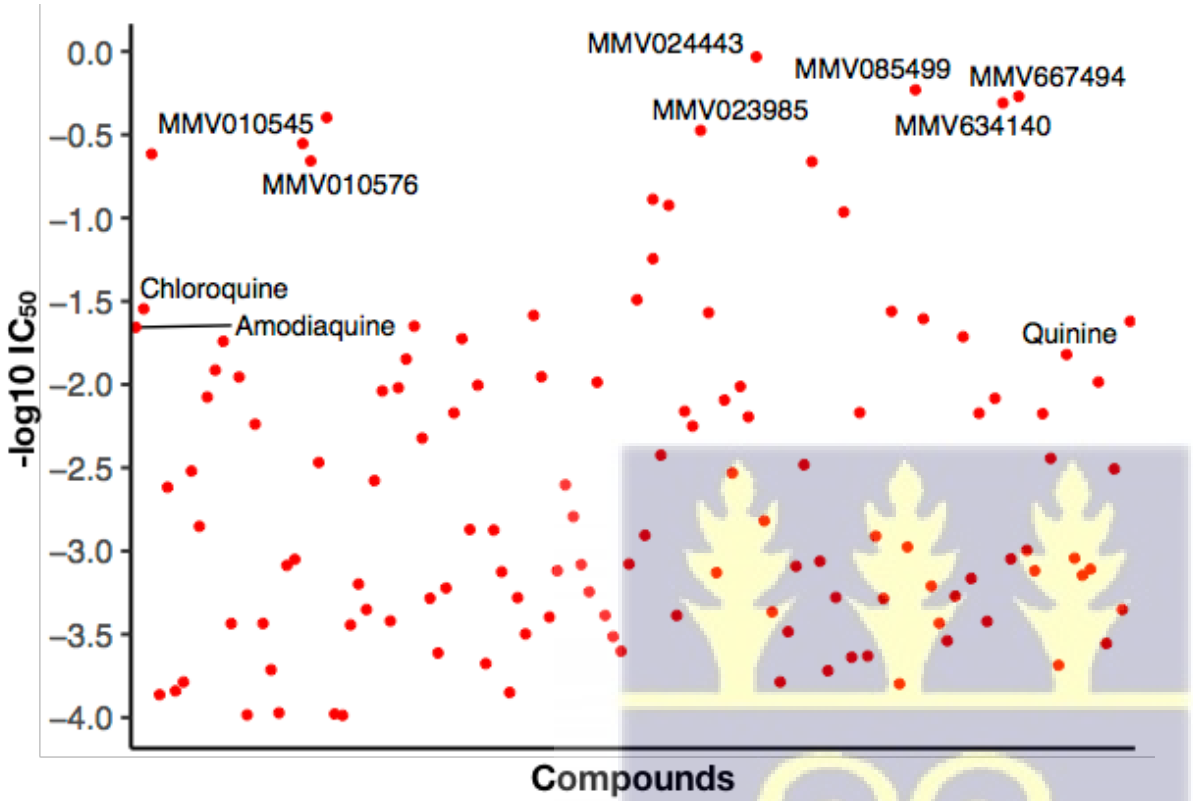

Figure 4.1: -log10 IC_{50} values of 125 compounds from the MMV pathogen box. These compounds were screened using 3D7 laboratory adapted isolate and the IC_{50} determination method. The labelled compounds were identified as hits and subjected to further analysis. Known drugs used as controls are also labelled on the plot.

Table 4.1: IC_{50} values of 125 compounds with antimalarial activity and 3 known drugs from the MMV pathogen box.

Compound	IC_{50} value (nM)	Compound	IC_{50} value (nM)	Compound	IC_{50} value (nM)
Amodiaquine	45.38	**MMV020120**	742.7	**MMV026468**	303.2
Chloroquine	35.143	**MMV020136**	100.9	**MMV026490**	4.588
Quinine	41.72	**MMV020152**	4740	**MMV026550**	1152
MMV000016	4.131	**MMV020165**	748.4	**MMV028694**	5231
MMV000023	7285	**MMV020289**	1332	**MMV030734**	1897
MMV000858	413.8	**MMV020291**	7065	**MMV031011**	9.212
MMV000907	6910	**MMV020320**	1904	**MMV032967**	4344
MMV001059	6114	**MMV020321**	3147	**MMV032995**	147.6
MMV006239	330.6	**MMV020388**	38.44	**MMV062221**	4269
MMV006372	710.7	**MMV020391**	89.87	**MMV084603**	814.7
MMV006741	119	**MMV020512**	2491	**MMV084864**	1925
MMV006833	81.91	**MMV020517**	1313	**MMV085071**	36.39
MMV006901	55.04	**MMV020520**	400.2	**MMV085210**	6278
MMV007133	2726	**MMV020591**	621.7	**MMV085230**	945.9
MMV007471	90.19	**MMV020670**	1207	**MMV085499**	1.701
MMV007625	9639	**MMV020982**	1758	**MMV1019989**	40.31
MMV007638	173.2	**MMV021057**	96.96	**MMV1028806**	1624
MMV007803	2723	**MMV021375**	2438	**MMV1029203**	2714
MMV007920	5166	**MMV022029**	3267	**MMV1030799**	3459
MMV008439	9382	**MMV022236**	3995	**MMV1037162**	1866
MMV009054	1220	**MMV022478**	1197	**MMV1088520**	51.67

MMV009135	1122	**MMV023183**	30.98	**MMV392832**	1461
MMV010545	3.572	**MMV023227**	804.4	**MMV393144**	148.7
MMV010576	4.545	**MMV023233**	7.718	**MMV407834**	2645
MMV010764	293.9	**MMV023233**	17.57	**MMV560185**	121.1
MMV011229	2.494	**MMV023370**	265.4	**MMV634140**	2.039
MMV011511	9514	**MMV023388**	8.389	**MMV663250**	1115
MMV011691	9702	**MMV023860**	2438	**MMV667494**	1.861
MMV011765	2776	**MMV023949**	144.7	**MMV676260**	990
MMV011903	1579	**MMV023953**	177.9	**MMV676269**	1314
MMV016136	2246	**MMV023985**	2.981	**MMV676270**	149.8
MMV016838	377.7	**MMV024035**	37.07	**MMV676350**	277.8
MMV019087	109.4	**MMV024101**	1348	**MMV676358**	4846
MMV019189	2629	**MMV024114**	124.1	**MMV676380**	66.12
MMV019234	104.5	**MMV024195**	340.1	**MMV676442**	1104
MMV019551	70.39	**MMV024397**	102.8	**MMV676528**	1397
MMV019721	44.66	**MMV024406**	156.6	**MMV676605**	1283
MMV019742	210.1	**MMV024443**	1.078	**MMV676877**	96.6
MMV019790	1922	**MMV024829**	658.5	**MMV676881**	3587
MMV019807	4097	**MMV024937**	2321	**MMV687246**	321.1
MMV019838	1669	**MMV026020**	6115	**MMV687794**	0.02277
MMV019993	148.3	**MMV026313**	3049	**MMV688980**	2245
MMV020081	53.13	**MMV026356**	1234		

nM = nanomolar, IC_{50} = 50% inhibitory concentration

4.1.7 Re-evaluation of IC_{50} of compounds with high potencies

Seven compounds with high potencies screened using more stringent compound concentrations were re-analysed for their IC_{50}s. The IC_{50} concentrations of these compounds ranged between 0.01 nM and 0.52 nM (Figure 4.2, Table 4.2) with MMV667494 being the most potent of all compounds with antimalarial activity in the MMV pathogen box (Table 4.2).

4.1.8 Parasite survival patterns following exposure to potent compounds

Three compounds out of the seven potent compounds were randomly selected. These are MMV667494 and MMV634140 with very low IC_{50}s and MMV010576 with a relatively higher IC_{50}. LUM and DHA were also included and the PSRA test conducted. Their killing rates were tested against 10 fresh natural isolates from The Gambia (BK19-1 to BK19-10) with a growth rate of more than 1% observed from the DMSO treated groups. Isolates BK19-1, BK19-3 and BK19-4 were relatively more sensitive to DHA and MMV634140. BK19-2 and BK19-10 showed similar sensitivity to all drugs and compounds. Parasites from BK19-3 remained viable with increasing re-invasion trend despite exposure to LUM, comparable to the DMSO control. All samples had very low but measurable re-invasion rates following exposure to the test compounds for 72 hours. For most samples, a peak was observed at 48 hours post drug/compound exposure (Figure 4.3).

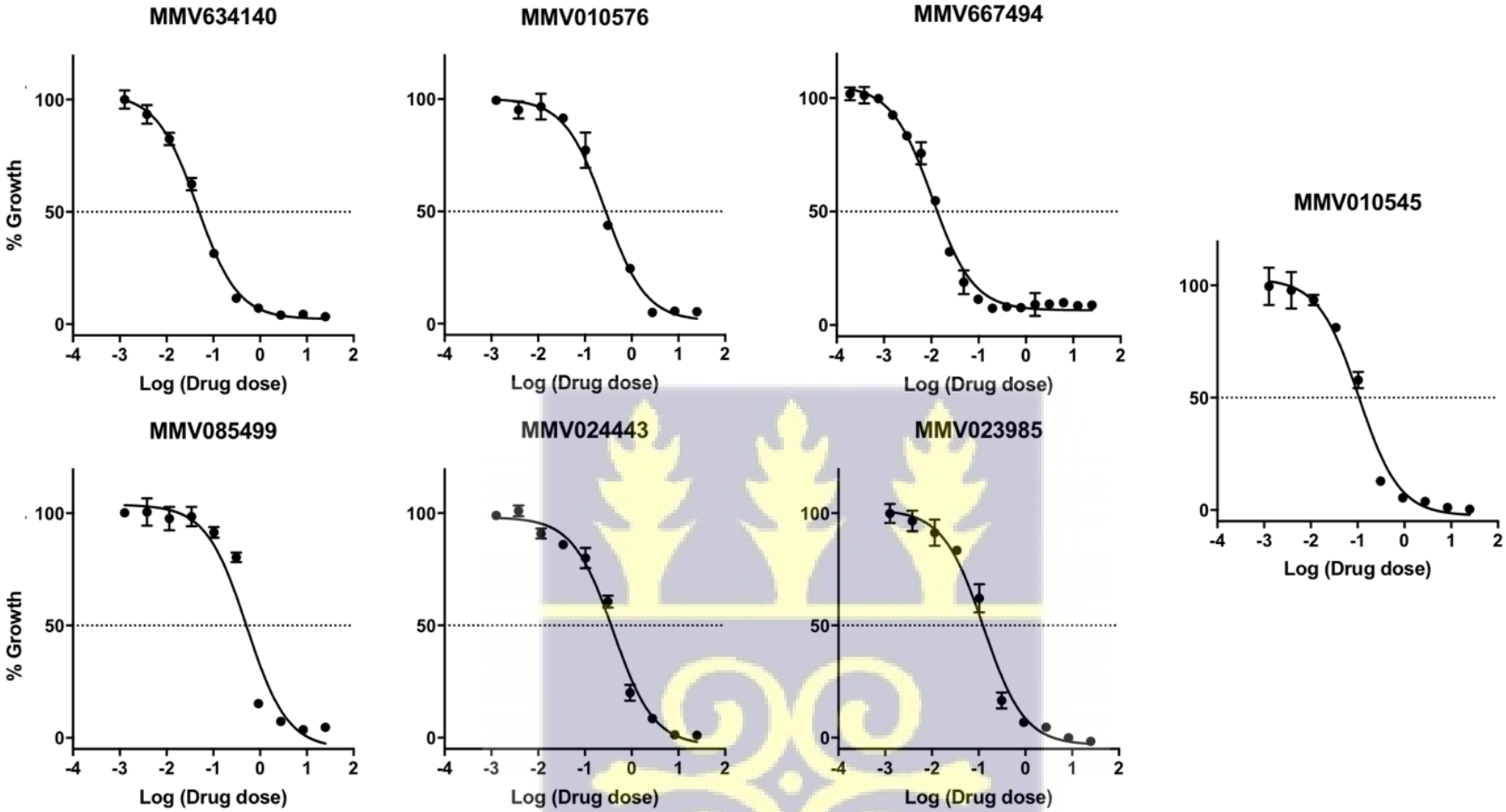

Figure 4.2: Representative graph of dose response curve of seven potent compounds. The error bars represent standard deviations for 3 replicates of each drug concentration tested. The dotted lines show the concentration at which 50% of the parasite population was inhibited by the compound.

Table 4.2: IC_{50} values and 95% confidence intervals of seven compound with high potencies against 3D7.

Compounds	IC_{50}s (nM)	95% CI
MMV634140	0.04537	0.03912 to 0.05259
MMV010576	0.2707	0.216 to 0.3394
MMV667494	0.01046	0.008786 to 0.01245
MMV085499	0.518	0.3298 to 0.8121
MMV024443	0.4034	0.3124 to 0.52
MMV023985	0.1275	0.09583 to 0.1694
MMV010545	0.1064	0.07911 to 0.1428

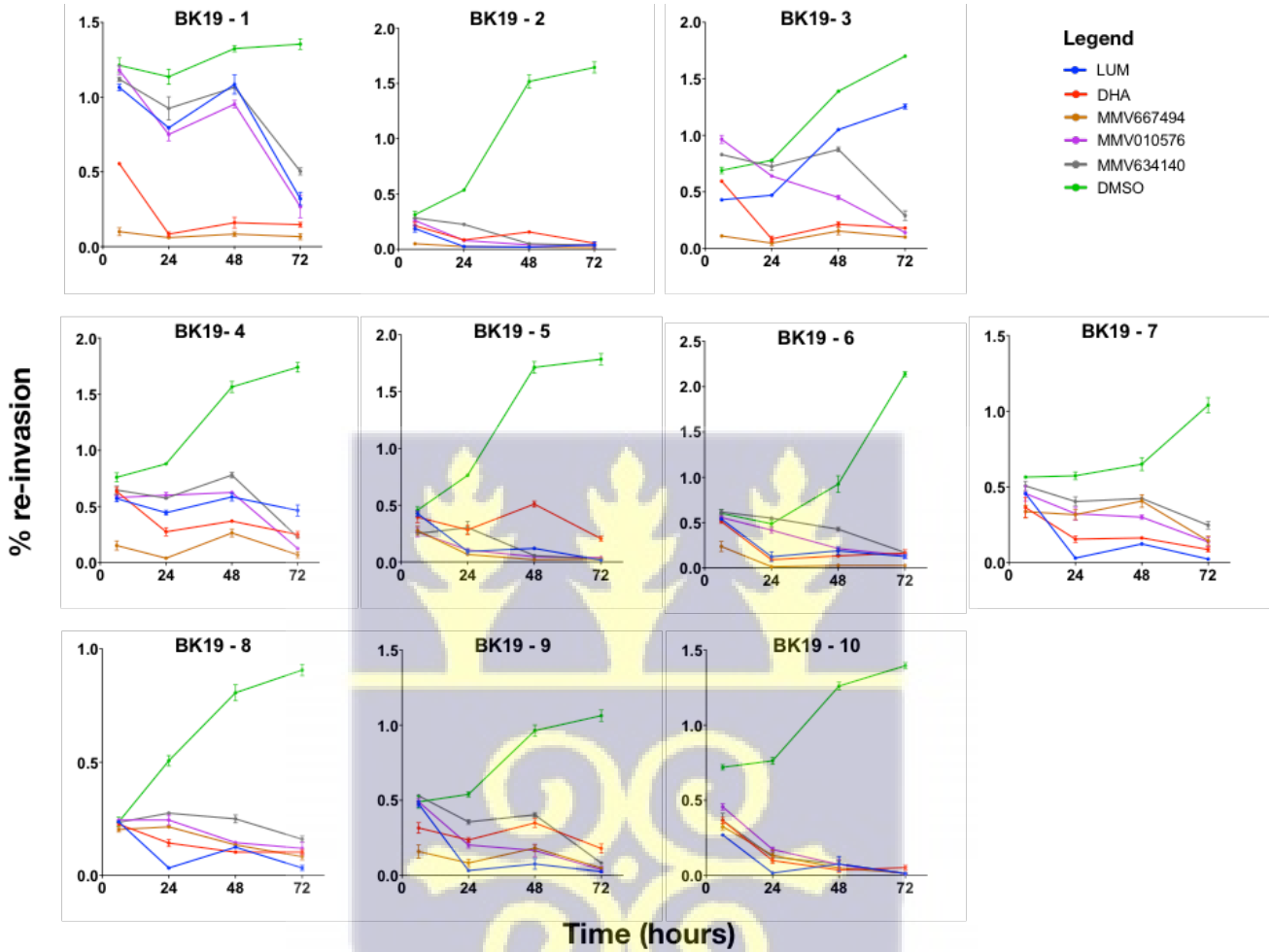

Figure 4.3: Individual responses of 10 *P. falciparum* field isolates following exposure to LUM, DHA, MMV667494, MMV010576, MMV634140 and a no-drug DMSO control at 6-, 24-, 48- and 72-hours. The responses are shown in percentage re-invasion parasitaemia and the error bars represent standard deviations of 3 individual replicates.

4.1.9 Parasite growth following 72 hours of drug exposure

Three and two samples analysed showed a re-invasion parasitaemia of > 0.2% following 72 hours of exposure to LUM and DHA respectively (Figure 4.4a, 4.4b). From the MMV compounds tested, one and four samples had a re-invasion parasitaemia of > 0.2% following 72 hours exposure to MMV010576 and MMV634140 respectively (Figure 4.4d, 4.4e) whilst all samples had re-invasion parasitaemias of < 0.2% following exposure to MMV667494. All samples showed higher sensitivity to MMV667494 (Figure 4.4c). Overall, the highest re-invasion parasitaemia were observed with LUM exposure with a mean re-invasion parasitaemia of 0.23% followed by MMV634140 with a mean of 0.18% (Figure 4.4f). The rest of the compounds had mean re-invasion parasitaemia of 0.14% for DHA, 0.06% for MMV667494 and 0.11% for MMV010576. The no-drug DMSO control had a mean re-invasion parasitaemia of 1.48%, 25 folds higher than observed for MMV667494. Two isolates showed higher levels of tolerance to drugs; BK19-1 had a re-invasion parasitaemia of > 0.2% for LUM, MMV010576 and MMV634140, while BK19-4 had > 0.2% re-invasion parasitaemia for LUM, DHA and MMV634140. BK19-3 had a re-invasion parasitaemia of > 1% following exposure to LUM.

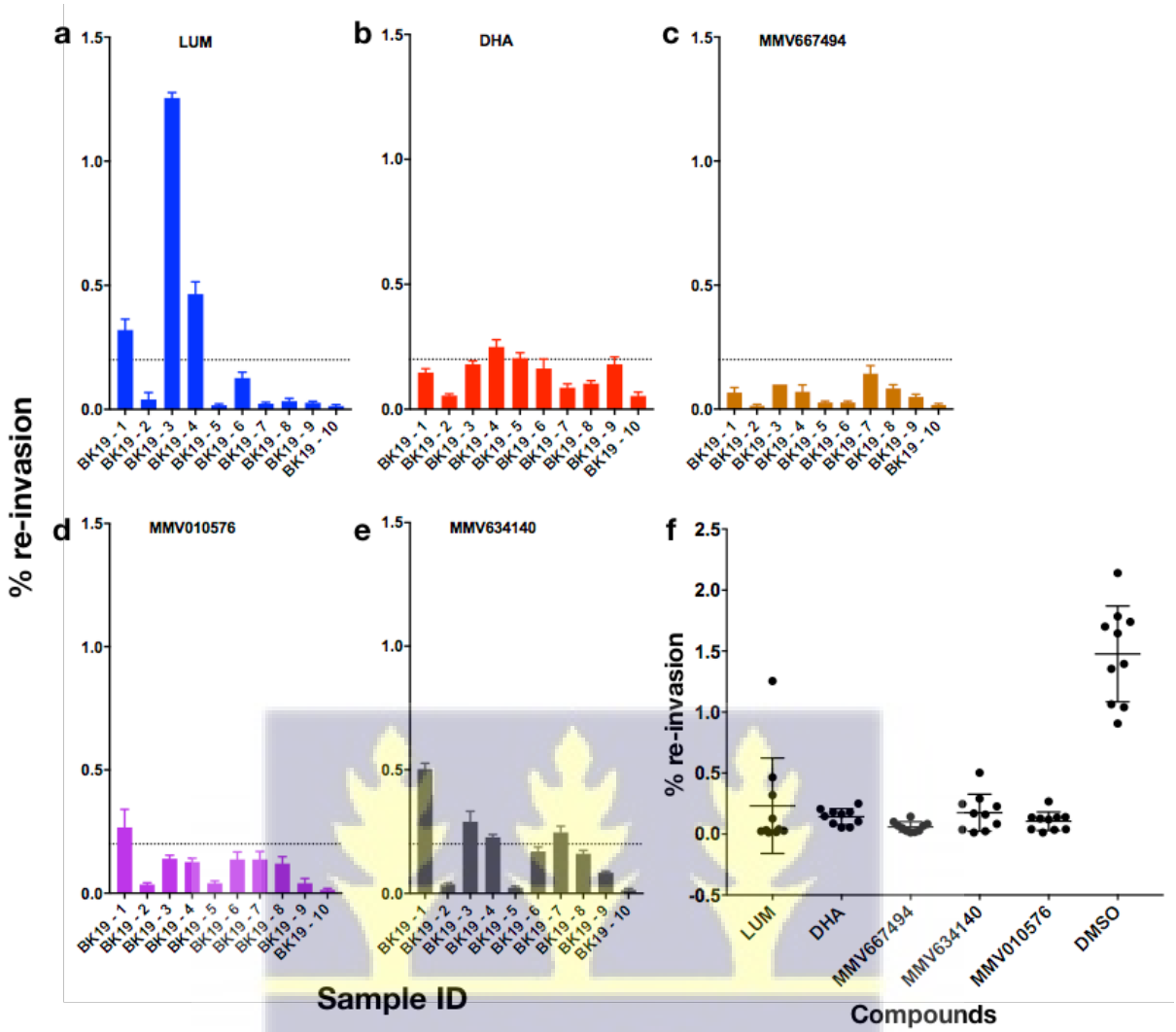

Figure 4.4: Percentage re-invasion parasitaemia of 10 *P. falciparum* field isolates analysed against (a) LUM, (b) DHA, (c) MMV667494, (d) MMV634140, and (e) MMV010576 at 72 hours post exposure. (f) Responses of 10 field isolates following 72 hours exposure to drugs, test compounds and no-drug DMSO control. The error bars represent standard deviations from three replicates.

4.5 Discussion

The MMV pathogen box provides a major opportunity to identify lead compounds for a variety of pathogens. This report describes the use of the standard high throughput IC_{50} determination assay to screen compounds from the MMV pathogen box for their activity against *P. falciparum* parasites and the novel PSRA to confirm its application to other drugs and antimalarial candidates and to verify the potencies of these compounds. Currently, majority of studies that assess parasite susceptibility to available drugs and novel compounds use reference laboratory strains which have gone through many cycles of culturing in laboratory environments (Leba et al., 2015). Though the use of laboratory strains gives relevant and insightful results, analysis using field isolates and *ex vivo* assay set-ups will give results that could be more comparable to *in vivo* drug efficacy (Leba et al., 2015). In this study, the use of field isolates that have undergone selection following several years of exposure to various antimalarial drugs revealed differences in responses to identified potent compounds. This has allowed the identification of potential lead compounds that are active against ring stage *P. falciparum* laboratory and field isolates from The Gambia.

Lead compound identification is carried out in the early stages of MMV's Research and Development (R&D) process to classify drug-like compounds with desired biological and pharmacological activities that could potentially lead to the development of novel clinically relevant compounds (Duffy et al., 2017). Varying levels of *P. falciparum* inhibitory activities were observed in the primary screening of the compounds, with 16 compounds identified to have similar or higher killing potencies than CQ. Subsequent analysis of a subset of the most potent compounds revealed some that are highly effective against the laboratory adapted 3D7 isolate, a CQ sensitive parasite line.

Three compounds were tested *ex vivo* against 10 field isolates in order to assess their effectiveness against parasites from infected individuals, mimicking drug effectiveness *in vivo*. Four out of the 10 isolates were seen to be sensitive to all compounds and known drugs. However, following 72 hours of exposure to LUM and DHA respectively, three and two isolates had re-invasion parasitaemias of > 0.2%. The cut-off of 0.2% was selected as the median re-invasion parasitaemia following 72 hours drug exposure to 41 samples in 2017 (Mbye et al., 2020). Two isolates exceeding 0.5% after 72 hours exposure to LUM can be classed as tolerant. These isolates need to be further investigated as they seem to be developing resistance to LUM as previously reported for isolates from The Gambia (Amambua-Ngwa et al., 2017). It is important to note that one of these LUM tolerant isolate was also tolerant to MMV010576, while two of them showed relatively lower sensitivities to MMV634140. This observed phenotype could be as a result of the isolates developing resistance to multiple drugs, which gives them the propensity to have tolerant/resistant phenotypes for novel drugs (Thu et al., 2017).

The complexity of the *P. falciparum* parasites makes it challenging to have compounds with activity against all life-cycle stages, which also makes it difficult to identify and characterise drug targets. Compounds described as being highly potent in this study have previously been studied with their targets characterised or hypothesised (Duffy et al., 2017). Of the seven compounds selected for subsequent analysis, MMV667494 and MMV634140 were previously classified as quinoline-carboxamides, related to quinolines, the reason for observed cross resistance with LUM and MMV634140. These two compounds are proposed to inhibit *P. falciparum* translational elongation factor 2 (*Pfef2*), required for protein synthesis (Baragana et al., 2016). The activities of these compounds against multiple stages of the *P. falciparum* life-cycle including the PE, IE, gametocyte and ookinete stages have been confirmed *in vitro* and *in vivo* using animal models. In the current analysis, MMV667494 showed higher killing

potency than all MMV compounds using both the IC_{50} determination assay and the PSRA. Even at 6 hours following drug exposure, this compound was seen to inhibit parasites at higher rates than DHA. MMV667494 could therefore be a promising antimalarial candidate. Given its high potency and the ability to inhibit multiple parasite stages, it should be further explored to assess its pharmacokinetic properties towards antimalarial drug development.

MMV010576, one of the top hits, is a 2-amino pyridine derivative that has previously been optimised, resulting in the synthesis of the clinical candidate MMV390048 with inhibitory activity against phosphatidylinositol 4-kinase (PI4K) (Paquet et al., 2017). This compound has previously been reported to effectively inhibit schizont maturation at sub-micromolar concentrations (Patra et al., 2019). PSRA analysis showed that MMV010576 is more potent than DHA after 72 hours of drug exposure which conforms with its characterisation as an egress inhibitor (Patra et al., 2019). Nevertheless, it seems to be a slow acting compound, with little activity seen after 6 hours of exposure. For ring stages within 6 hours of exposure, MMV085499 was identified as a potent candidate. It is a 2-amino pyrazine also with PI4K activity, that targets the IE stages of the parasite (Duffy et al., 2017). In a recent screen of the pathogen box, MMV023985 and MMV010545 were classified as imidazopyridazines that inhibit *P. falciparum* calcium-dependent protein kinase 1 (*Pfcdpk1*) and *P. falciparum* protein kinase 7 (*Pfpk7*) (Duffy et al., 2017). MMV024443, an indole-2-carboxamide has also been shown to target *Pfcdpk1* which is required for parasite invasion and development and is expressed throughout the IE stages of the parasite. MMV024443 has been shown to have excellent egress inhibition activity (Patra et al., 2019).

Overall, three compounds were identified that are highly potent against *P. falciparum* laboratory adapted isolates, confirmed using natural isolates from the field and the PSRA. This confirms the application of the PSRA to other drugs and antimalarial candidate to determine

parasite susceptibility. This work opens up opportunities to exploit these compounds as therapeutic agents. Based on their recent target identification, determining their pharmacokinetic and toxicity properties is essential for progression through the drug development pipeline. The remaining compounds with hypothetical targets should be further explored in order to inform on their structure-activity relationship and improve their performance, pharmacokinetics and toxicity. Field isolates should be increasingly used to better assess the range of responses that will be seen for different drugs and compounds, and more confidently identify potent compounds. A major limitation of *in vitro* assays is that compounds such as PQ which requires metabolic activation are likely to be omitted and therefore it is necessary to carry out assays that would detect all synthesised compounds (Reader et al., 2015).

CHAPTER 5

5.0 Linked variants across signatures of positive selection in the *Plasmodium falciparum* genome are associated with *in vitro* responses to artemisinin derivatives and partner drugs

Accepted for publication in Journal of Antimicrobial Chemotherapy, 2022

5.1 Abstract

Though AL is still highly effective in The Gambia, treatment failure following its use has been reported and *ex vivo* LUM tolerance has been shown to be increasing in recent years. Several regions on the genome of *P. falciparum* were also recently identified to be under recent positive directional selection using samples collected pre- and post- introduction of AL which could be as a result of selection pressure from drugs.

To confirm the relationship between AL and differentiating loci observed, re-analysis of the genomes of parasite isolates with drug sensitivity phenotypes from western Gambia was done. Identity-by-descent (IBD) analysis was done to identify highly related loci which was followed by Genome-Wide Association Studies (GWAS) and regression analysis to determine associations between markers of recent selection and drug phenotypes.

Results show several regions, including a cluster of gene on chromosome 10, with high IBD, indicating recent signatures of selection. These also include *Pfcrt* and *P. falciparum* amino acid transporter (*Pfaat1)* drug resistant-associated loci. Both GWAS and regression analysis revealed several loci that are associated with drug responses. CG1 protein (PF3D7_0709100) which is in proximity with *Pfcrt* and SURFIN 14.1 (PF3D7_14776000) was identified to be associated with LUM responses. *Pfmrp2* (PF3D7_1229100) and SURFIN 4.2

(PF3D7_0424400) was associated with responses to DHA. The involvement of these genes in drug susceptibility should be further investigated.

5.2 Introduction

Resistance to all current partner drugs have been previously described, including LUM and PIP which had never been implemented as monotherapy (Baliraine et al., 2011; Eastman et al., 2011). The cases of reduced ACT efficacy in sSA has mostly been reported against AL, a combination including LUM (Dama et al., 2017; Ebohon et al., 2019). As the sustained efficacy of ACTs depends on the continuous potency of both the ARTs and the long-acting ACT partner drug, accurate monitoring of the efficacy to all currently used drugs is vital as a strategy for drug policy in different regions. This can be accompanied by surveillance of associated molecular markers. Unfortunately, the molecular markers for LUM, the partner in the most popular AL have not been validated (Ehrlich et al., 2020). Identification of these markers would facilitate drug resistance monitoring following over a decade of ACT use in most endemic countries.

Genomic analysis of SEA parasites identified key mutations in the *Pfk13* locus associated with delayed clearance, the ART resistance phenotype. These major variants are rare in Africa, though the *Pfk13* R561H mutant has emerged *de novo* and spread within Rwanda (Uwimana et al., 2020). Thus, ART resistance could emerge independently in Africa and this could involve alternative mechanisms from those dominant in SEA. Already, analysis of the genomes of isolates from imported infections in the UK that failed to respond to treatment found polymorphisms in the *P. falciparum* adaptor protein complex 2 mu subunit (*Pfap2-mu*) locus, *Pfap2-mu* I568T, which have now been functionally shown to lead to increased *in vitro* ring survival of *P. falciparum* against ART (Henrici et al., 2019). As ACTs continue to be applied

in routine treatment and contemplated for MDA, continuous monitoring of their efficacy and identification of local markers of selection is vital, especially for population where transmission has become low, population antimalarial immunity is low and cases of drug failure have been reported, such as The Gambia (Amambua-Ngwa et al., 2017).

Malaria incidence has reduced significantly in The Gambia thanks to intensified interventions (Mwesigwa et al., 2019). While ACTs remain highly efficacious across the country, isolated cases of reduced treatment efficacy against AL have been reported in the low transmission regions. Recent genome scans of *P. falciparum* isolates from these populations showed signature of selection at drug resistance loci but also recent directional selection in temporal populations that may be due to the use of AL since 2007. Between 2008 and 2014, a small number of loci also differentiated, the most significant of which was around *Pfnfs1* on chromosome 7 (Amambua-Ngwa et al., 2018). One of the alleles in this locus, the 65Q mutant was present in isolates with higher LUM IC_{50}s, suggesting increased tolerance. The same study also showed significant differentiation at the *Pfcrt* region between the low transmission populations and higher transmission regions in the east.

Hypothetically, the western low transmission populations could be evolving towards higher drug tolerance and the relationship between evolving genetic markers and antimalarial susceptibility is not known. Here, genomes of isolates from the west of the Gambia were re-analysed for which *ex vivo* drug susceptibility has been determined using the standard IC_{50} assay. Both mixed regression models were applied to determine genome-wide loci that associated with drug susceptibility. High level of quinoline resistance markers were found and new regions of selection on chromosome 10 invasion gene cluster identified, with shared ancestry to isolates from SEA that are putatively associated with drug tolerance.

5.3 Methods

5.3.1 Samples and populations

P. falciparum infected blood samples were collected during the 2014 and 2015 malaria transmission season as described in section 3.3.1.

Whole genome sequences of *P. falciparum* isolates generated from isolates in collaboration with malariaGEN consortium at the Wellcome Sanger Institute (projects; 1103-PF-PDN-GMSN-NGWA, 1136-PF-GM-NGWA, 1137-PF-GM-DALESSANDRO) were also analysed. Paired-end reads were aligned to the *P. falciparum* 3D7 reference genome (v3) as previously described (Miotto et al., 2015). Variations in the genome were called using in-house variant calling algorithms as described (Amambua-Ngwa et al., 2018). Freely available Gambian genome data from 2008 and those from Cambodia from 2010 populations were obtained from previous publications and the Pf3K project (https://www.malariagen.net/projects/pf3k).

5.3.2 Population genetic analysis

Variant Call Files (VCF) of a total of 78 samples collected in 2008, 152 samples in 2014/2015 and 570 samples from Cambodia were used in this study. The DEploid program was used to determine clonality of the Cambodian isolates extracted from the WSI Pf3K database and monoclonal infections were selected for further analysis. The VCF of all isolates from The Gambia and Cambodia were merged, biallelic SNPs extracted and filtered based on the following conditions: Minor allele frequency (MAF) ≥ 1%, RMS mapping quality (MQ) ≥ 20, read depth (DP) ≥ 5 and VQSLOD ≥ 3. All loci satisfying these conditions but with a percentage of missing genotypes of > 20% of the total number of samples in the data were

subsequently discarded. Isolate with > 20% missing SNP calls were also removed from the final dataset.

Missing genotypes and mixed calls were imputed and phased respectively as previously described (Amambua-Ngwa et al., 2019). Briefly, genotypes were phased at all mixed loci using the statip package in R software with 100 simulations based on the Bernoulli distribution. The MAF were re-calculated following each round of 100 simulations for all samples. Missing genotypes were also imputed over 100 iterations and the derived haplotypes were used to compute the integrated haplotype score (iHS). This was compared to values obtained for subset of samples with lower levels of missingness and multiplicity to validate the process of imputation. The final SNP dataset was used to extract SNPs at regions of known drug resistance loci (*Pfcrt, Pfmdr1, Pfdhfr, Pfdhps* and *Pfk13*).

To determine signatures of selection, regions of IBD within and between population were scanned, generating the iR index using the isoRelate package in R (Henden et al., 2018). Correction for multiple testing was applied on the resultant *P* values based on the Benjamin-Hochberg procedure with a 5% false discovery rate (FDR) threshold. Further analysis of differentiation at positive selection signatures was done by comparing haplotypes between pairs of Gambian populations (2008 vs 2014-2015) or each Gambian temporal population against Cambodia using Rsb index derived with the REHH software in R. Outlier SNP loci were extracted and their ontology inferred from PlasmoDB annotations. To identify the differentiating loci within the 10K SNP data, the Weir and Cockerham's Fst between population(s) was calculated using wcFst and pFst of the Genotype Phenotype Association Toolkit (GPAT++) (available at https://github.com/zeeev/vcflib).

5.3.3 *Ex vivo* drug susceptibility assay

Leukocyte depleted iRBCs were used to determine the 50% inhibitory concentration of the following drugs: ARM, DHA, LUM and AMD as previously described (Amambua-Ngwa et al., 2017). Assays were set up in duplicates at 0.5% parasitaemia and 2% haematocrit. The concentration ranges tested were 150 to 0.6nM for DHA and ARM, 2,000 to 8 nM for LUM and 100 to 0.4 nM for AMD. The procedure outlined in section 4.4.3 was used, data acquired using the BD Accuri™ C6 flow cytometer. One hundred thousand (100,000) events were acquired and data analysed using the FlowJo software (Tree Star, Inc.). Synchronised Dd2 and 3D7 laboratory-adapted strains at ring stages were used as controls.

5.3.4 Association analysis of *in vitro* drug sensitivity with genome-wide SNPs and regions of IBD

Genotype-phenotype association was carried out using Genomic Association and Prediction Integrated Tool (GAPIT) in the R package (RStudio v1.2) (Zhiwu Zhang Laboratory, 2020). Drug susceptibility profiles of 57 isolates collected from western Gambia in the 2014/15 malaria season were determined for four antimalarial drugs: AMD, LUM, ARM and DHA. A total of 9291 SNPs that passed the data filtration process were used for this analysis. T-test was used to compare the mean difference between SNPs after logarithmic transformation of the phenotype data. The output obtained was adjusted for multiple comparison using Bonferroni method.

Phenotype-genotype association was obtained using the mixed linear model (MLM) algorithm implemented in GAPIT. Additionally, an R tool for network analysis: Network-based Genome-Wide Association Studies (netGWAS) was used to build a SNP-drug phenotype network map to model LUM and ARM interactions with SNPs across the parasite genome.

5.4 Results

5.4.1 Highly related regions of the genomes of recent *P. falciparum* population

The dataset used for this study consist of 10765 SNPs genotyped from 685 *P. falciparum* isolates, including 96 and 72 isolates from western Gambia in 2008 and 2014/15 respectively, and 517 publicly available whole genome sequences from Cambodia. Relatedness between and within parasite populations was estimated and segments of the parasite genome that are in IBD between all pairs of isolates identified. A 5% FDR allowed for the detection of 139; 115 and 142 loci with significant excess of IBD in western Gambia 2008 and 2014/15 populations as well as Cambodia respectively (Figure 5.1, Table A.1). Pairwise population relatedness analysis also resulted in the identification of 124 SNPs with excess IBD between spatial Gambian populations, 58 SNPs between Gambia 2008 and Cambodia and 52 loci between Gambia 2014/15 and Cambodia (Figure 5.2, Table A.2).

iR was higher within individual populations and between temporal populations from western Gambia. Loci with high excess of IBDs were seen on chromosomes 7 and 10 between western Gambia and Cambodia. The largest number of loci under positive selection was observed within Cambodia. Overall, positive selection was stronger within individual populations and between temporal populations from western Gambia. Several loci under positive selection were detected between isolates from Cambodia and western Gambia on chromosome 10 in genomic regions harbouring merozoite surface protein (*Pfmsp*) genes (Figure 5.2a and 5.2b, Table A.2).

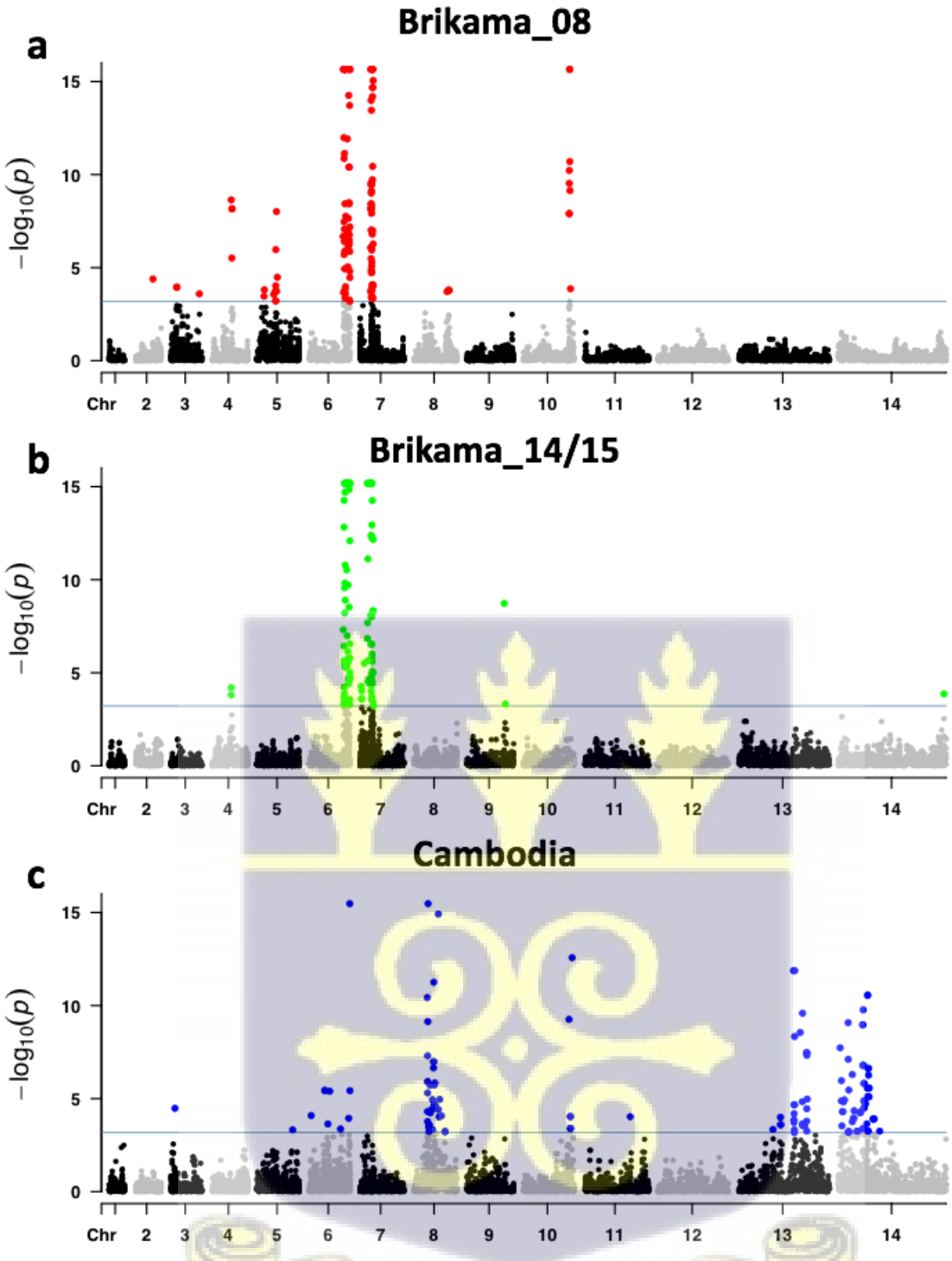

Figure 5.1: -log10 *P* value of calculated iR using isoRelate within each population. The grey and black sections represent individual chromosomes and each point on the plot is a SNP. The horizontal line represents the significant threshold of -log10 values of a. 3.186, b. 3.217 and c. 3.174. Blue, red and green colours represent significant loci on each chromosome from pairwise comparisons.

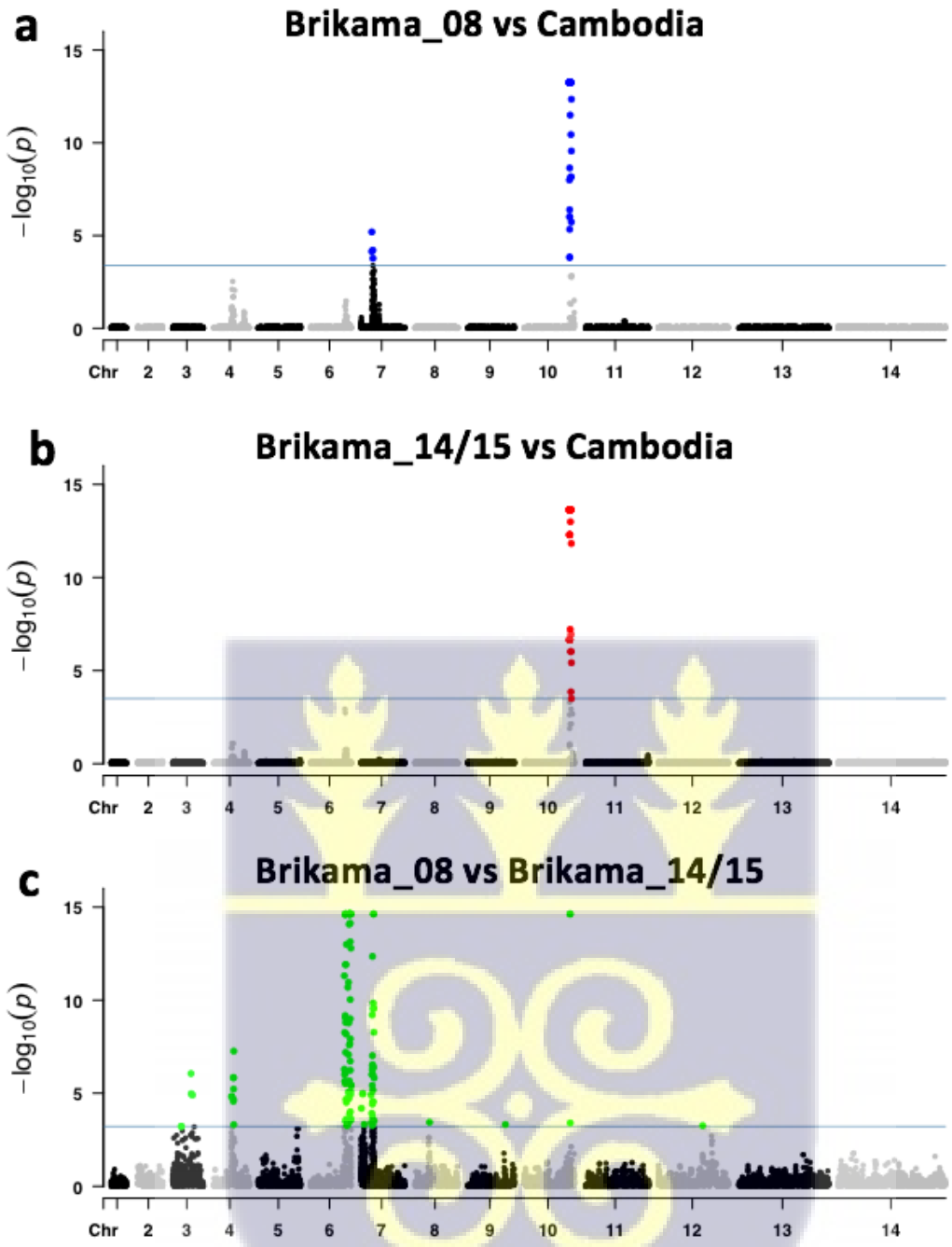

Figure 5.2: -log10 *P* value of calculated iR using isoRelate between population pairs. The grey and black sections represent individual chromosomes and each point on the plot is a SNP. The horizontal line represents the significant threshold of -log10 values of a.3.219, b. 3.378 and c, 3.497. Blue, red and green colours represent significant loci on each chromosome from pairwise comparisons.

5.4.2 Drug resistant allele frequencies from western Gambia in 2008 and 2014/15

Genotypes of 80 and 56 samples from western Gambia in 2008 and 2014/15 respectively were obtained for the drug resistant alleles: *Pfcrt* C72/M74/N75/K76, *Pfmdr1* N86, *Pfdhps* S436/A437, *Pfdhfr* N51/C59 and *Pfk13* C580. Similar frequencies were observed for the two populations with higher mutant haplotype obtained in 2014/15 increasing from 67% to 76%. Higher frequencies of the *Pfmdr1* N86 wild-type allele in 2014/15, increasing by 10%. Wild-type haplotypes for *Pfdhps* and *Pfdhfr* were similar between the two populations. The proportion of mixed parasites was higher in 2008 (34%) than 2014/15 (16%).

Table 5.1: Allele frequencies of known drug resistance genes for 56 *P. falciparum* isolates collected from 2014 and 2015 malaria transmission seasons.

Gene	Alleles	Codons	Gam2008	Gam2014/15
Pfcrt	C72/M74/N75/K76	CMNK (wild-type)	0.23	0.21
		CIET (mutant)	0.67	0.76
		CMNK/CIET (mixed)	0.08	0.11
Pfmdr1	N86	N (wild-type)	0.79	0.89
		Y (mutant)	0.21	0.07
		N/Y (mixed)	0	0.04
Pfdhps	S436/A437	SA (wild-type)	0.13	0.13
		SG (mutant)	0.63	0.74

		FG (mutant)	0.02	0.07
		AA (mutant)	0.06	-
		SA/SG (mixed)	0.23	0.04
		FG/SA/SG (mixed)	0.11	0.02
Pfdhfr	N51/C59	NC (wild-type)	0.06	0.07
		IR (mutant)	0.78	0.77
		IT/NC (mixed)	0.04	0.02
		IR/NR (mixed)	0.06	0.12
		NR/NC (mixed)	0.06	0.02
Pfk13	C580	C (wild-type)	-	1
		Y (mutant)	-	0

Pfcrt = *P. falciparum* chloroquine resistance transporter; *Pfmdr1* = *P. falciparum* multidrug resistance gene 1; *Pfdhps* = *P. falciparum* dihydropteroate synthase; *Pfdhfr* = *P. falciparum* dihydrofolate reductase; *Pfk13*= *P. falciparum* kelch 13

5.4.3 Genome-wide association analysis

A total number of 9291 SNPs were tested for association with the activities of AMD, LUM, DHA and ARM tested against 56 isolates in 2014/15 transmission season. The drug phenotype distribution is represented in Table 5.2. IC_{50} concentrations of AMD ranged from -1.47 nM to 5.87 nM with a mean IC_{50} of 2.19 nM. LUM had the widest distribution of IC_{50} concentrations ranging between 1.25 nM and 8.66 nM with a mean of 5.49 nM. The ART derivatives, DHA

and ARM had distributions ranging from -2.47 nM to 4.90 nM; and -1.25 nM to 5.03 nM with mean IC_{50}s of 0.38 nM and 1.46 nM respectively.

Using t-test to compare the mean difference between SNPs after logarithmic transformation of the data resulted in a total of 16, 27, 59 and 13 SNPs significantly associated with ARM, DHA, LUM and AMD respectively using a significant threshold of -log10 *P* value of 5 (Figure 5.3a, Table A.3). The MLM model integrated in GAPIT resulted in no significant loci detected, however, a number of SNPs were identified as outliers (Figure 5.3b). With these observations, a threshold at -log10 *P* value of 3 was introduced to capture the loci with relatively high associations. These SNPs are listed in Table A.4.

Table 5.2: IC_{50} values of 56 samples assayed against AMD, LUM, DHA and ARM in 2014/15 transmission season.

Drug	**Mean IC_{50} (nM)**	**95% CI (nM)**	**Range (nM)**	
			Min	**Max**
AMD	2.19	1.70 – 2.70	-1.47	5.87
LUM	5.49	5.00 – 5.98	1.25	8.66
ARM	1.47	1.08 – 1.85	-1.25	5.03
DHA	0.38	-0.11 – 0.86	-2.47	4.90

IC_{50} = 50% inhibitory concentration; CI = confidence interval; Mean = geometric mean; min = minimum; max = maximum

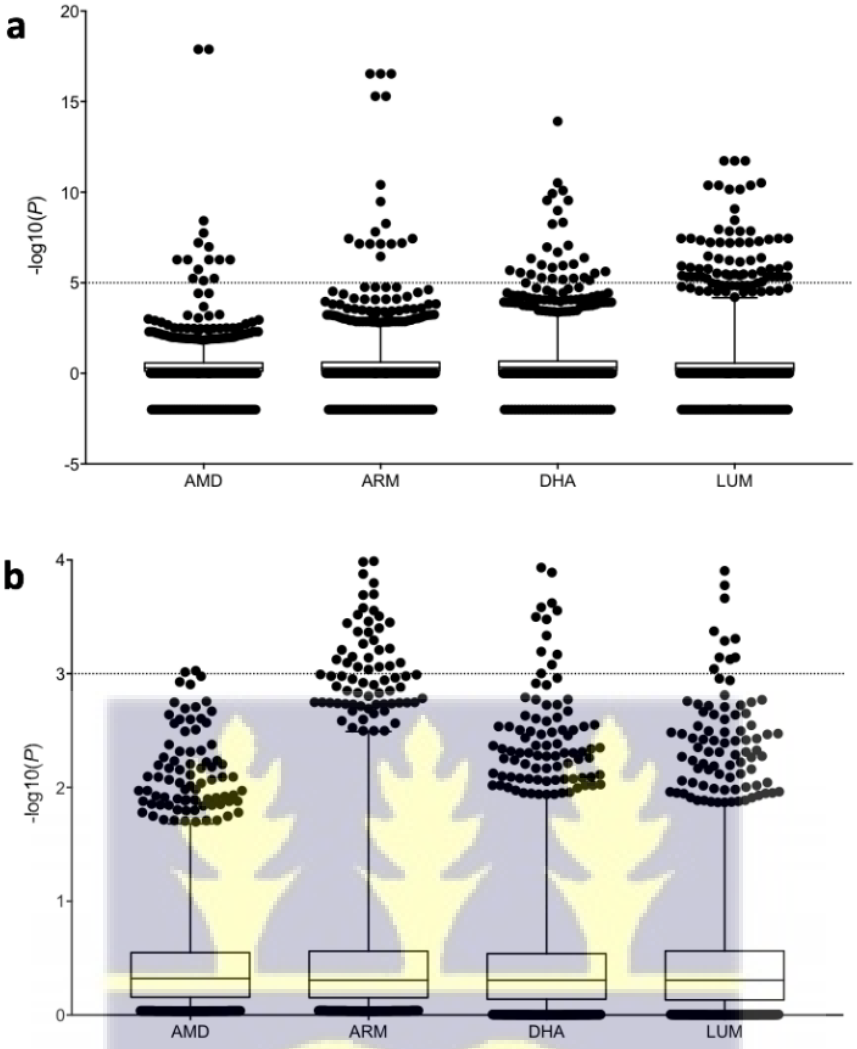

Figure 5.3: Box and whisker plots of -log10 *P* values of genome-wide SNP association with 4 antimalarial drugs using (a) MLM model in GAPIT and (b) t-test to compare the mean difference between SNPs. The mean and 1-99 percentile range are shown on these plots. The dotted horizontal line gives a cut-off at -log10 *P* value of 3 using the MLM model and -log10 *P* value of 5 with the parametric test. Each point on the plots represents an allele.

5.4.4 Relatedness and linkage between markers of selection with phenotypes

A genotype-phenotype network of highly related SNPs was generated, with connections to ARM and LUM, identified as phenotypes, with direct association between them (Figure 5.4). ARM is directly associated with two SNPs both on chromosome 14 of the parasite genome

found in the genes: PF3D7_1465800 (dynein beta chain, putative) and PF3D7_1477600 (surface-associated interspersed protein (SURFIN)-14.1). LUM has direct interactions with 12 SNPs found on chromosomes 7, 9 and 14. Most of the SNPs in the network map interact with each other including those on chromosomes 4, 5, 6 and 12 which are not directly associated with drug phenotypes.

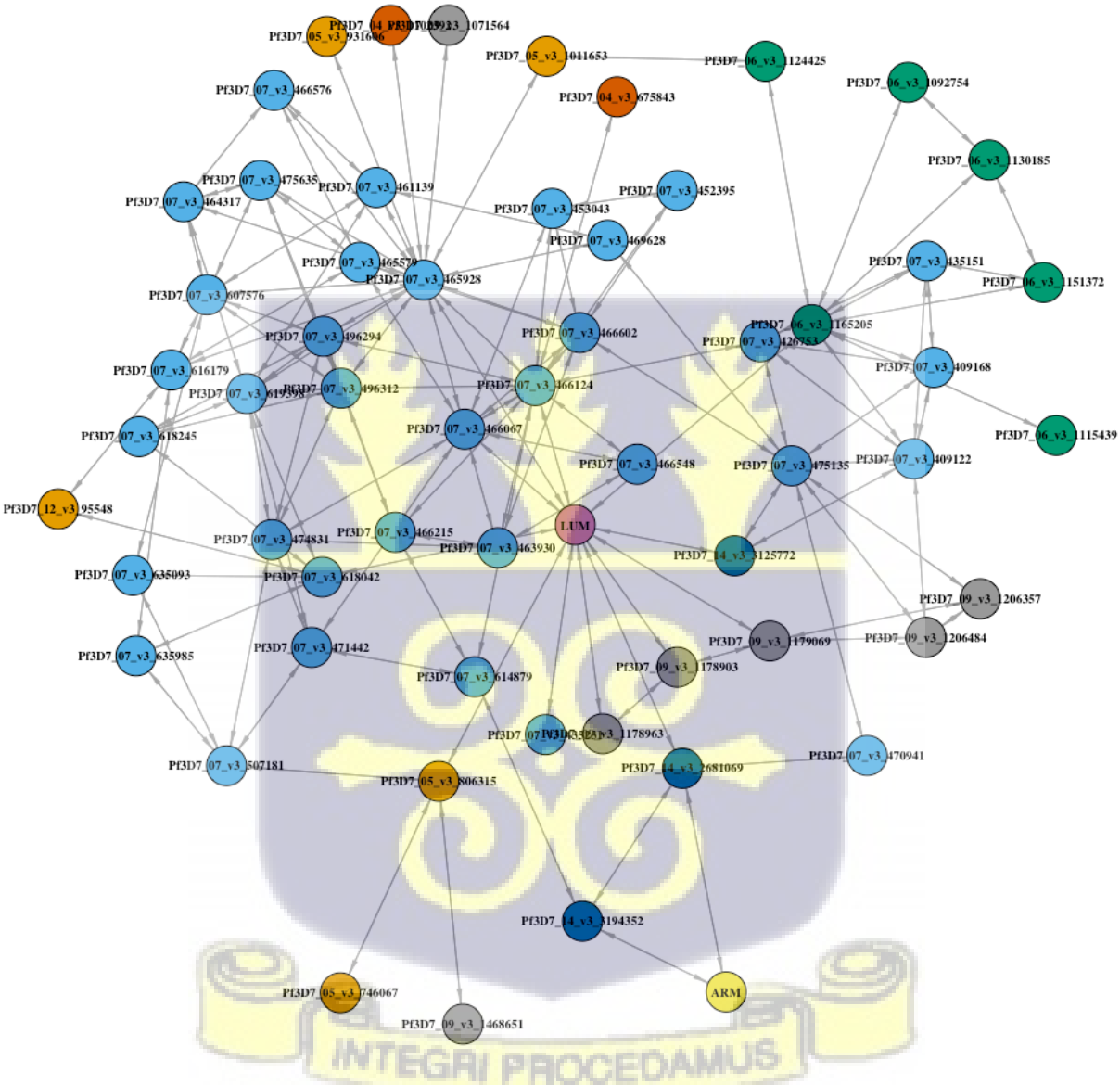

Figure 5.4: Genotype-phenotype interaction networks across the *P. falciparum* genome. Yellow and pink nodes show ARM and LUM phenotypes respectively. Dark orange, orange, green, blue, grey and dark blue- coloured nodes represent chromosomes 4, 5, 6, 7, 9 and 14 respectively. Chromosome 12 is also represented with a mustard-coloured node.

5.5 Discussion

A comprehensive understanding of the genetic basis of drug resistance is essential to determine the molecular mechanisms involved which can guide the development of novel strategies to prevent the spread of drug resistant parasites (Wicht et al., 2020). In this study, population genetic approaches were used to determine recent signatures of selection between temporal parasite populations from western Gambia and show relatedness from ancestry using publicly available whole genome sequences from Cambodia. Isolates from western Gambia in 2008 when ACTs were deployed, were used as baseline population and in 2014/15 transmission season to detect regions with high IBD.

Genome-wide maps of recent positive selection for parasite populations from Cambodia and temporal populations from western Gambia were generated separately. Within each population, many loci that were under positive selection were detected which could be as a result of the immense drug pressure imposed on parasites. Relatedness analysis between temporal populations from western Gambia showed numerous loci under recent positive selection. The candidate drug resistance loci *Pfaat1* on chromosome 6 and the merozoite surface protein (MSP) family are among the loci detected with high IBD proportions between temporal western Gambian populations. The findings indicate that within the Gambian population, there is low frequency of genetic variations which can easily result in the emergence of resistant parasites (Amato et al., 2018). Given that malaria prevalence in The Gambia have declined tremendously with increased monoclonal infections, pressure from drugs will continuously increase.

The *in vitro* drug susceptibility screens showed minimal variations in response to the four drugs used: AMD, DHA, LUM and ARM. Because of this and the dominance of either wild-type or mutant alleles observed for drug resistant genes, correlations between the drug phenotypes

observed could not be established with their corresponding genotypes. As expected, mutant alleles and haplotypes were higher for *Pfmdr1*, *Pfdhps* and *Pfdhfr* with a small proportion of mixed infections. High frequencies of mutant haplotype in *Pfcrt* was observed as CQ is still available in private pharmacies in The Gambia (not published). Mutant allele for *Pfk13* C580 was not detected in any of the isolates.

Association analysis of whole genome sequenced isolates with drug phenotypes using both GWAS and regression analysis resulted in several loci associated with drug phenotypes. Outliers with relatively stronger associations using the MLM model were identified as no significant associations were obtained. Although the analysis did not detect the known drug resistant genes, a number of genes overlapped with drug resistant associated SNPs previously identified in The Gambia (Amambua-Ngwa et al., 2019). These include SURFINS and other surface proteins which could be involved in transportation of drugs into the parasite (Kagaya et al., 2015). Some genes including numerous conserved *Plasmodium* genes showed high associations with both models, which could result from linkage disequilibrium with known resistance-associated genes. These genes should therefore be investigated further.

Pathways and interaction analysis were used to test for the concerted effects of multiple variants, associating genes with drugs. A significant number of loci associated with changes in drug response were obtained using LUM and ARM. However, detected loci associated with drug profiles should be further verified because of the small sample size and relatively low numbers of isolates with minor allele frequencies. The sample size used is small which affected the power of the study. Studies with larger sample sizes, sufficient to conduct a GWAS may result in the identification of novel variants associated with drug resistance.

CHAPTER 6

6.0 Functional validation of *Plasmodium falciparum* cysteine desulfurase gene for its involvement in lumefantrine tolerance

6.1 Abstract

Functional genomic tools permit the validation of markers implicated in drug resistance. Decreased efficacy and increased parasite tolerance to LUM have been reported in sSA, a component of the most widely used ACT: AL. Hypothetically, genetic variants evolving in local *P. falciparum* population under AL pressure could serve as markers of increased LUM tolerance. The *Pfnfs1* gene was previously identified to have the strongest temporal differentiation on the parasite genome and strongly correlated with *ex vivo* LUM tolerance in The Gambia. Characterising this gene could help strategies in preventing the emergence and spread of LUM resistant parasites.

In this study, the CRISPR Cas9 genome editing tool was used to introduce a site-specific mutation on the *Pfnfs1* gene at amino acid position 65 (K65Q) A single plasmid approach was used, carrying a customised donor template, a codon optimised Cas9 enzyme, selection cassettes and restriction sites to allow for efficient cloning. Four plasmids were designed using two guide RNAs and both variance of the allele. Plasmids were transfected in duplicates into 3D7 and Dd2 wild-type laboratory adapted parasite lines, each carrying a variant allele resulting in a total of four transfections for each parasite line.

Recombinant parasites were generated for one and four transfected lines using 3D7 and Dd2 respectively giving a recovery rate of 62.5%. Sequencing of the recombinant parasites revealed that only the control transfections with synonymous mutations were successfully edited and all

other recombinant parasites were partially edited. The reason for this could be due to lack of fitness cost that might be associated with editing a non-synonymous mutation. Additionally, there is evidence of two other alleles in linkage disequilibrium with the K/K65 allele and replacing all three alleles might be needed for successful editing which could be the basis of future work.

6.2 Introduction

Reports on decreased efficacy to AL could be as a result of reduced susceptibility to LUM also observed in a number of studies (Dama et al., 2017; Fukuda et al., 2021). Resistance to LUM is expected to emerge before resistance to ARM in high endemic regions of Africa as parasites are exposed to sub-therapeutic concentrations of LUM for much longer (Conrad et al., 2019). As a consequence, residual sub-therapeutic drug concentrations can exert selective pressure on parasites resulting in the development of drug resistance (Wells et al., 2015). Reduced susceptibility to LUM has been associated with variations in *Pfmdr1* (N86, 184F and D1246 haplotype) and increase in *Pfmdr1* copy numbers (Acharya et al., 2018; Malmberg, Ngasala, et al., 2013; Okell et al., 2018). A better understanding of the molecular mechanisms of LUM tolerance is needed to prevent resistance development and sustain its efficacy.

From a study that was conducted in The Gambia, *Pfnfs1* showed clear signs of temporal differentiation with samples collected pre- and post- the introduction of AL, which strongly correlated with increased LUM tolerance (Amambua-Ngwa et al., 2018). As a result, it was important to prioritise the validation of *Pfnfs1* as a potential marker of LUM tolerance. *Pfnfs1* is composed of the enzymatic subunit NFS1, found in the mitochondria and apicoplast of *P. falciparum*. It functions by catalysing the conversion of cysteine into alanine and elemental sulfur for Fe-S biogenesis. Fe-S clusters are essential for apicoplast maintenance in the

erythrocytic stages of *P. falciparum* and are involved in a variety of other biochemical processes (Gisselberg et al., 2013; Turowski et al., 2012). Moreover, iron homeostasis, which is essential in erythrocytic development, is involved in the mechanism of action of quinolines the family of antimalarial drug where LUM belongs (Lalève et al., 2016). It was therefore necessary to determine the association between *Pfnfs1* and LUM tolerance, crucial to prevent the development of resistance in Africa.

In this study, a forward genetic approach was used to generate site-specific mutations on the *Pfnfs1* gene. The CRISPR-Cas9 genome editing tool was used to precisely introduce a DSB and incorporate a SNP on the *Pfnfs1* gene (PF3D7_0727200) at amino acid position 65 (K65Q). This may potentially lead to its validation as a marker for LUM tolerance and increase our understanding of LUM tolerance mechanisms and ways to prevent or delay resistance development.

6.3 Materials and methods

6.3.1 Guide RNA design and cloning

gRNAs were designed *in silico* for the *Pfnfs1* gene using the CRISPR analysis tool within Benchling (www.benchling.com) (Figure 6.2). *P. falciparum* was selected as organism with the NFS gene ID: PF3D7_0727200. The selection parameters were set for a wild-type Cas9, single gRNA, guide length of 20 bp and an 'NGG' PAM site. gRNAs were selected based on high on and off target scores which represents Cas9 cleavage efficiency and the inverse probability of off- target binding respectively. Complementary oligos were designed for each selected guide and 5' TATT and 3'AAAC overhangs added to each oligo to facilitate annealing and cloning into the pDC2-cam-coCas9-U6.2-hDHFR expression vector (Figure 6.1). The final

guide oligo pairs were synthesised and stored at 100 μM stock solution using 1x TE buffer (10 mM Tris, 1mM EDTA at pH 8.0).

Guide oligos (100 μM) were phosphorylated and annealed in a thermocycler using 10x T4 ligation buffer (66 mM Tris-HCl with 10 mM $MgCl_2$, 1 mM dithiothreitol, 1 mM ATP and 7.5% polyethylene glycol at pH 7.6) (New England Biolabs, UK) and 5 Richardson units of T4 polynucleotide kinase (New England Biolabs, UK) at 37°C for 30 minutes to facilitate efficient ligation to the plasmid. The temperature was then ramped up to 94°C for 5 minutes, followed by a gradual cooling to 25°C at a rate of 5°C per minute for annealing of the oligos to obtain double stranded guide DNA.

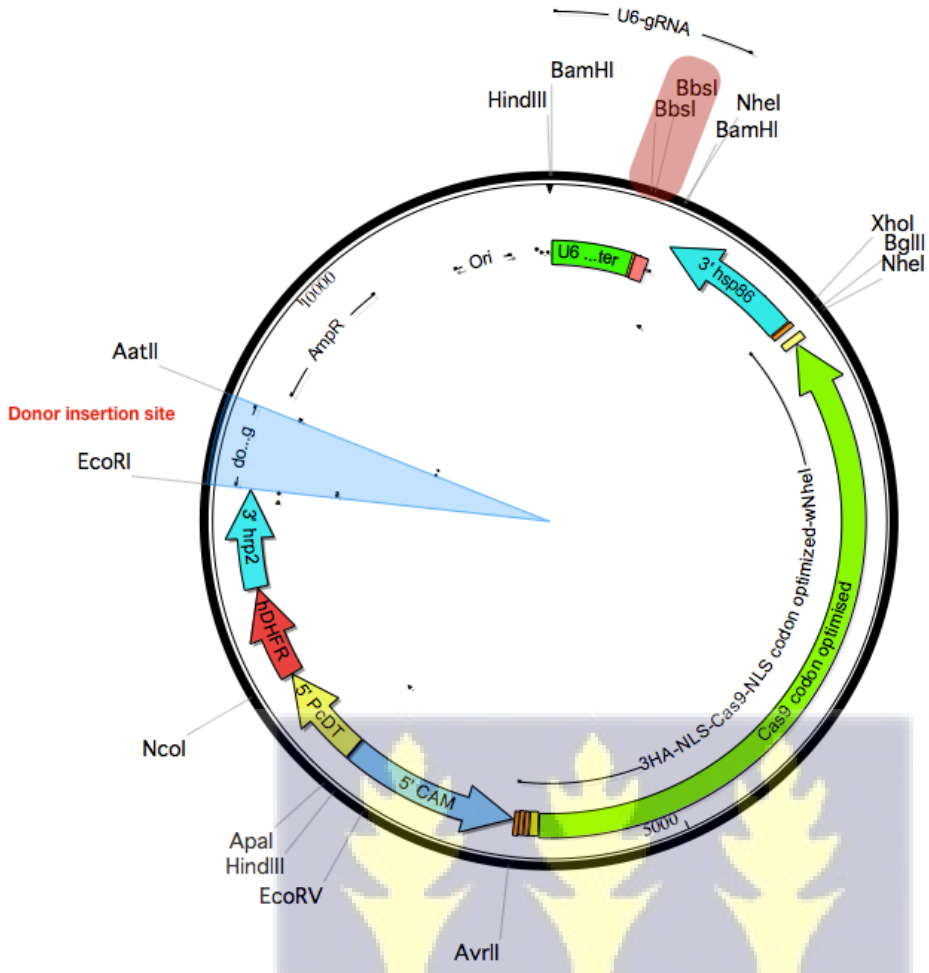

Figure 6.1: pDC2-cam-coCas9-U6.2-hDHFR plasmid. The 11.5kb plasmid was kindly provided by Dr. Marcus Lee of the Wellcome Sanger Institute.The plasmid consists of a codon optimised Cas9 (coCas9) with its expression driven by the 5' CAM and a heat shock protein 86 terminator (3' hsp86). The plasmid has EcoRI and AatII restriction sites for the assembly of a customised donor template and Bbs1 sites to enable cloning of gRNAs, driven by the RNA polymerase III dependent U6 small nuclear RNA (snRNA) component of the spliceosome promoter. It also has an ampicillin resistance gene (AmpR) for prokaryotic propagation and selection, and a hDHFR selectable marker which confers resistance to the antifolate inhibitor WR99210 post-transfection.

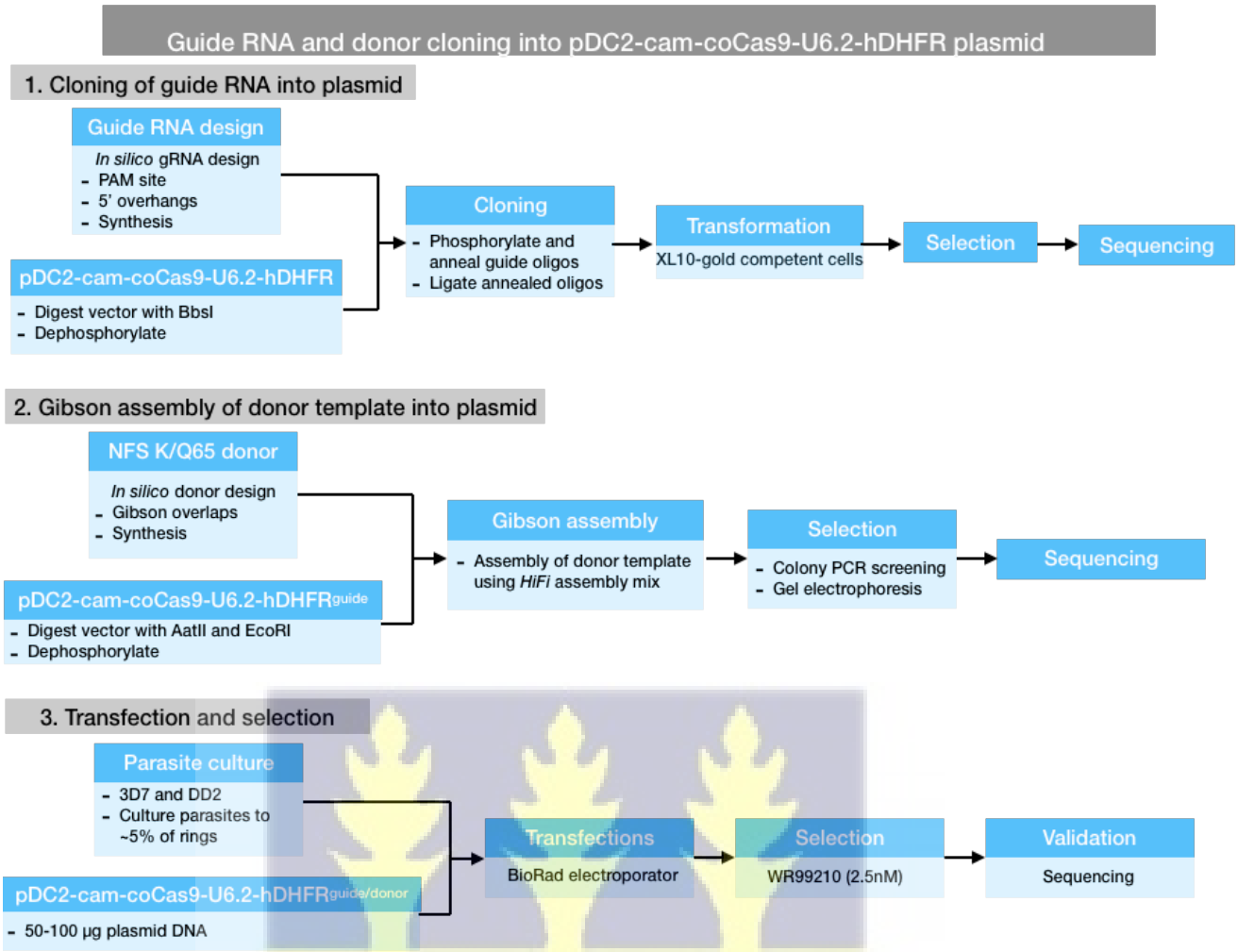

Figure 6.2: CRISPR Cas-9 gene editing strategy used for *Pfnfs1* gene editing including 1. Guide RNA cloning, 2. Assembly of donor template and 3. Transfections into wild-type laboratory strains and selection of recombinant parasites.

The pDC2-cam-coCas9-U6.2-hDHFR expression vector was propagated and purified from *E. coli* XL10-Gold competent bacterial cells. Approximately 4 µg of the Cas9 vector was digested with 4U BbsI restriction enzyme (New England Biolabs, UK) at 37°C for 1 hour. The plasmid was then treated with 2 U Shrimp alkaline phosphatase (rSAP) (New England Biolabs, UK) at 37°C for 1 hour to dephosphorylate the 5' end and maintain linearity, heat inactivated at 65°C for 5 minutes, and column purified using the NucleoSpin Gel and PCR clean-up kit (Macherey-Nagel GmbH & Co.KG, Germany). The annealed oligos were diluted in 1 in 200 nuclease-free

H_2O for ligation with 50 ng of BbsI pre-digested Cas9 vector using T4 ligation buffer and T4 Polynucleotide kinase (New England Biolabs, UK), incubated at room temperature for 1 hour.

Ligated constructs were incubated on ice for 20 minutes with 40 µL of XL10-gold competent cells. Cells were heat-shocked at 42°C for 30 seconds then placed on ice for 1 minute. Four hundred and fifty microliters (450 µL) of S.O.C. media (2% tryptone, 0.5% yeast extract, 10 mM NaCl, 2.5 mM KCl, 10 mM $MgCl_2$, 10 mM $MgSO_4$, and 20 mM glucose) was added to cells and allowed to recover at 37°C for 30 minutes. This was then plated onto Luria-Bertani (LB) with 100 µg/ml of ampicillin (Amp) agar plates and incubated overnight at 37°C.

Single colonies were picked and inoculated in LB+Amp broth, incubated overnight at 37°C while shaking at 180 rpm. Plasmid DNA was isolated from the overnight cultures and purified using the NucleoSpin Plasmid Isolation kit (Macherey-Nagel GmbH & Co.KG, Germany) following manufacturer's instructions. Concentration and purity of the final eluted DNA was quantified with a Nanodrop ND-1000 spectrophotometer at A_{260}/A_{280} and A_{260}/A_{230} respectively. The resultant constructs were sequenced at GATC Biotech (Germany) using an ABI 3730x1 DNA Analyser to confirm successful cloning. Sequences were analysed and aligned to the plasmid consensus sequence using Lasergene 17 SeqMan Pro multiple sequence alignment. Constructs with successfully cloned guides (pDC2-cam-coCas9-U6.2-hDHFR^{guide}) were selected for donor assembly.

6.3.2 Donor design and assembly

A 0.672 kb donor with a variation on the *Pfnfs1* gene at amino acid position 65 (K65Q) was designed using Benchling (Figure 6.2). Single nucleotide changes were made on the PAM site and seed region of the gRNA binding sites on the donor template creating silent shield

mutations (re-codonisation). A control donor template with shield mutations but lacking the SNP of interest was also designed. All donors were synthesised, and PCR amplified using gene-specific primers with additional 20 nucleotide overhangs at the 5'end which are complementary to the sequence of the digested plasmid for efficient Gibson assembly. Four micrograms (4 µg) of the pDC2-cam-coCas9-U6.2-hDHFR^{guide} plasmid was digested overnight with AatII and EcoRI at 37°C and phosphatase treated using 1 µL of rSAP, incubated at 37°C for 30 minutes.

The digest was purified by running products on a 1% agarose gel using Gel Loading Dye Purple (6X) (New England Biolabs, UK) and 1 kb HyperLadder (Bioline, UK) for 45 minutes. Expected band size of about 1000 kb was cut out, weighed and purified using the NucleoSpin Gel and PCR Clean-up kit. Concentration and purity of the final purified plasmid DNA was determined using the Nanodrop ND-1000. Gibson assembly of 12.5 ng of synthesised donor and 100 ng of pDC2-cam-coCas9-U6.2-hDHFR^{guide} plasmid was done using NEBuilder HiFi DNA Assembly Master Mix (New England Biolabs, UK) for a final volume of 10 µL using manufacturer's instructions. The mix was incubated at 50°C for 15 minutes after which the assembly reaction was transformed into XL10 gold competent cells and incubated overnight at 37°C while shaking at 180 rpm.

Colony PCR was carried out to screen for successful Gibson assembly. Primer pairs specific to the donor insert (P282) and plasmid (P283) were used for amplification. PCR products were analysed on a 1% agarose gel for 45 minutes and band sizes assessed. These were then submitted for sequencing using the primer P282 and analysed using Lasergene 14 SeqMan Pro (v.15). Successful constructs were cultured in 200 mL of LB+Amp broth overnight while shaking at 180 rpm. Plasmid DNA was isolated from saturated cultures using the NucleoBond Xtra Midi/Maxi purification kit (Macherey-Nagel GmbH & Co.KG, Germany) following manufacturer's instructions. The final DNA was reconstituted with Cytomix (120 mM KCl,

0.15mM $CaCl_2$, 2mM EGTA, 5mM $MgCl_2$, 10mM K_2PO_4, 25mM HEPES, at pH 7.6) at 1 µg/µL and stored at -20°C.

6.3.3 *In vitro P. falciparum* parasite culture

Dd2 and 3D7 *P. falciparum* laboratory clones were continuously cultured using standard parasite growth media as described (Trager et al., 1976) and an atmospheric condition of 1% O_2, 3% CO_2 and 96% N_2 at 37°C. Cultures were maintained at 3% haematocrit and 2% parasitaemia using O+ uRBCs from healthy donors through the National Health Services (NHS), UK, after obtaining informed consent. Parasitaemia was determined using Giemsa-stained thin blood smears and assessed with standard light microscopy.

6.3.4 Parasite transfections and drug selection

Parasites were cultured and synchronised using sorbitol to obtain > 5% ring stages. These parasites were harvested by centrifugation at 1500 rpm for 3 minutes and the resultant pellet of approximately 100 µL washed with Cytomix. Fifty micrograms (50 µg) of the plasmid construct was added to the uRBC pellet and reconstituted with cytomix for a final volume of 400 µL. The suspension was transferred into a chilled electroporation cuvette and electroporated using a BioRad Gene Pulser Xcell electroporator set at a voltage of 0.31kV, maximum capacitance (950F) and an optimal time constant of 10-15 ms.

One millilitre (1 mL) of pre-warmed growth media (RPMI 1640 (Sigma-Aldrich, UK) supplemented with 35 mM HEPES (Sigma, St. Louis, MO), 24 mM NaHCO3, 1 mg/l of hypoxanthine (Sigma), 5µg/ml of gentamicin (Gibco-BRL) and 0.5% Albumax (Gibco-BRL)

was immediately added to electroporated cells and transferred to a 15 mL tube with 4 mL complete media, incubated at 37°C for 1 hour for parasite recovery. Recovered transfected cells were centrifugated at 13,500 rpm for 3 minutes and pellet resuspended in 5 mL complete media with 150 µL of fresh uRBCs at 50% haematocrit. The suspension was incubated at 37°C and cultures maintained.

At day 1 post transfection, parasites were maintained under 5 nM and 1 nM WR99210 selection for Dd2 and 3D7 transfected parasites respectively for 10 days (Figure 6.2). Media was changed every 24 hours for the first 8 to 10 days and three times weekly thereafter. Growth was monitored using standard microscopy and transfected parasites maintained until parasites recovered or for 45 days.

6.3.5 DNA extraction and screening of recombinant parasites

The transfected parasites were expanded once they reached 1% parasitaemia and allowed to reach 2 to 3% parasitaemia in a culture volume of 20 mL for genomic DNA (gDNA) extraction. Excess media was removed from the cultures for a final volume of <15 ml and 150 µL of saponin added to it. Once lysis started to take place, the cultures were centrifuged at 3000 rpm for 5 minutes. The resultant pellet was washed once with 10 mL of PBS and transferred to a 2 mL Eppendorf tube. DNeasy Blood and Tissue Qiagen kit was used for gDNA extraction following manufacturer's instructions.

Primers were designed to genotype the transfected parasites for validation (P1829/P1830: Table 6.2). These primers were designed to amplify the whole donor segment. Template DNA at 50 to 100 ng was used with CloneAmp HiFi PCR Premix (Takara Bio Inc.) for amplification. PCR products were analysed on a 1% agarose gel and DNA purified from expected band sizes using NucleoSpin Gel and PCR clean-up kit for sequencing with the primer P1829.

6.3.6 Drug susceptibility assays

Synchronised *P. falciparum* cultures with >80 rings were used to determine the 50% drug inhibitory concentrations of LUM and CQ. Wild-type and recombinant parasites were assayed at 1% haematocrit and 1% parasitaemia for 72 hours in 96-well microtiter plates. One hundred microliters (100 µL) of cultures were dispensed in wells pre-coated with 50 µL of serially diluted drugs. The concentration ranges tested for LUM and CQ were 100 to 0.04 nM and 2000 to 0.9 nM respectively. The plates were incubated at standard conditions for 72 hours. Cells were then stained by dispensing 100 µL of 2x SYBR green I intercalating dye in lysis buffer in each well. This was incubated in the dark at 37°C for 30 minutes and fluorescence measured using a microplate reader with an excitation and emission filter of 485nm and 535nm respectively.

6.4 Results

6.4.1 gRNA design and validated cloning into pDC2-cam-coCas9-U6.2-hDHFR plasmid

Two gRNAs of 20 bp upstream of the NGG PAM sequence were selected (Table 6.1, Figure 6.4b). On-target and off-target scores were lower for gRNA-1. Both gRNAs on the *Pfnfs1* gene were close to the target mutation site at positions 244-246. gRNA-1 and gRNA-2 had a 5'-AGG-3' and 5'-TGG-3' PAM motif respectively downstream of their sequences with both gRNAs overlapping at 4 nucleotide positions. Both gRNAs are on the sense strand and their GC contents are 30% and 35% for gRNA-1 and gRNA-2 respectively.

Table 6.1: Guide oligonucleotide sequences designed for *Pfnfs1* gene modification.

	Guide sequence	PAM	Gene position	Strand	On-target score	Off-target score
gRNA 1	CAATAACTTTAGTTCCACGA	AGG	168-187	+1	49.2	99.9
gRNA 2	ACGAAGGAACATTCTGAACA	TGG	184-203	+1	56.6	99.0

6.4.2 Cloning of guide oligonucleotides into pDC2-cam-coCas9-U6.2-hDHFR plasmid

Following ligation of the guide oligos to the pDC2-cam-coCas9-U6.2-hDHFR plasmid, the purified plasmid DNA concentration yield was 144.9 ng/µL and 189.7 ng/µL respectively for guides 1 and 2, with purity ranging between 1.73-1.91. To insert the donor, the plasmid was digested with EcoRI and AatII and separated by agarose gel electrophoresis. The plasmid backbone with cloned guides, which is approximately 11 kb in size (Figure 6.3a), was purified from the gel, yielding 28.5 ng/µL and 37.1 ng/µL for plasmids with cloned guide 1 and 2

respectively. A 500 bp DNA fragment corresponding to the excised fragment for subsequent donor insertion was also seen on the gel image (Figure 6.3a). Capillary sequencing confirmed successful cloning of the guide oligos into the plasmid (pDC2-cam-coCas9-U6.2-hDHFR^{guide}: Figure 6.3b).

6.4.3 Gibson assembly of donor into pDC2-cam-coCas9-U6.2-hDHFR^{guide} plasmid

Two donor templates were designed, one carrying the wild-type allele (K65K) and the other carrying the mutant allele (K65Q) relative to the reference 3D7 sequence. Additional shield mutations were included on both the PAM site and seed region of gRNA-1 and on the seed region of gRNA-2, to decrease the chances of Cas9 recutting once an edit has occurred. Following Gibson assembly of the donor and plasmid, the DNA concentrations and purity obtained ranged between 111.5 -234.8 ng/µL and 1.53-1.86 respectively. Capillary sequencing confirmed successful assembly of the donor and plasmid (Figure 6.3b). In the reference 3D7 sequence on PlasmoDB, the nucleotides that code for lysine at position 65 (K65) of the *Pfnfs1* gene is AAA (shown in Figure 6.3c and 6.4b), which was re-codonised to G: "AAG" for the wild-type K65K donor, a silent shield mutation. The edited donor has the nucleotides "CAA", coding for Glutamine (Q65). This resulted to a single nucleotide change from A to C at position 244 of the *Pfnfs1* gene (Figure 6.3c).

Table 6.2: List of primers used for genotyping and sequencing

Primer ID	Sequence	Description
P35	5'-AAGCACCGACTCGGTGCCAC-3'	U6 guide RNA sequencing primer for pDC2-cam-coCas9-U6.2-hDHFR plasmid
P282	5'-AACATATGTTAAATATTTATTTCTC-3'	HRP2 3'UTR forward primer to sequence into donor
P283	5'-AGGGTTATTGTCTCATGAGCGG-3'	Sequencing primer towards AatII site on pDC2-cam-coCas9-U6.2-hDHFR plasmid to sequence donor
P1829	5'-ATCAGCATCTTAATGTATCT-3'	Forward primer to genotype NFS editing (upstream of donor)
P1830	5'-CAATATTCATCTTTTGTACATC-3'	Reverse primer to genotype NFS editing (downstream of donor)

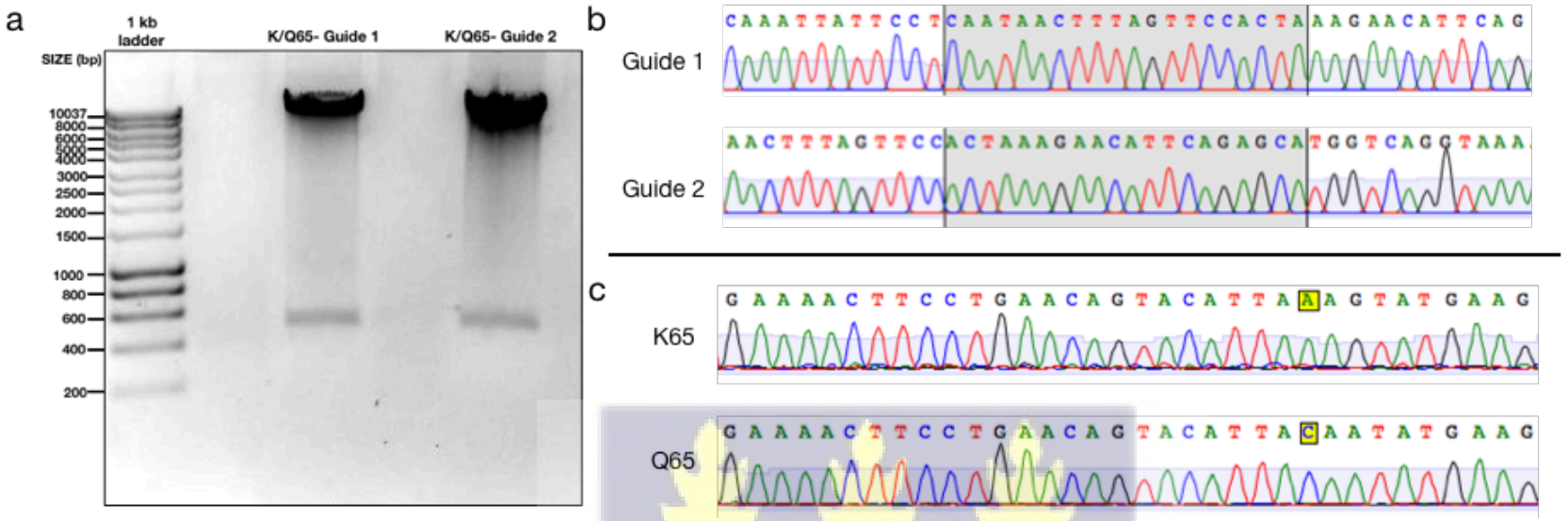

Figure 6.3: a. One percent (1%) agarose gel electrophoresis showing restriction digest patterns of the validated pDC2-cam-coCas9-U6.2-hDHFR^{guide} plasmids cut using AatII and EcoRI. Chromatograms showing (b) cloned guide sequences in the shaded segments and (c) the mutations of interest incorporated in the donor template highlight in yellow.

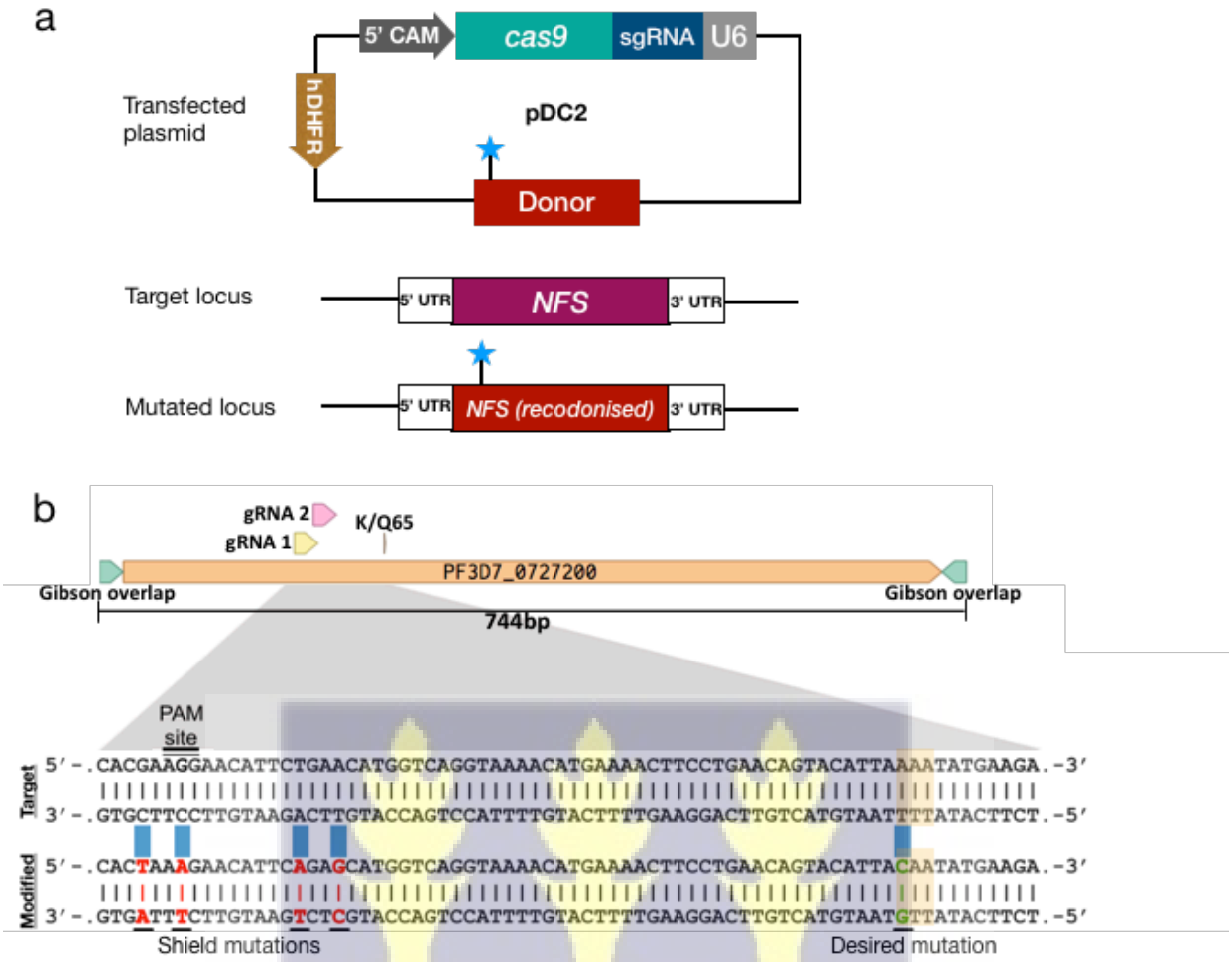

Figure 6.4: a. Schematic representation of targeted gene editing of *Pfnfs1* using CRISPR-Cas9. The pDC2 plasmid expresses the Cas9 endonuclease driven by 5' CAM, a sgRNA expression cassette driven by RNA polymerase III dependent U6 promoter (U6), a hDHFR selectable marker and a re-codonised donor template. b. Donor segment of 744 bp with Gibson overlaps on the 5' and 3' ends, and two guide RNAs with 4bp overlapping sequences. A segment of the donor sequence showing the target gene locus with PAM site downstream of the guide sequence and modified sequence designed as donor template with the desired mutation at amino acid position 65 (K65Q) highlighted and desired mutation in green. The shield mutations on the PAM site and seed region of the guide sequence are in red.

6.4.4 Recovery of 3D7 and Dd2 *P. falciparum* parasite transfections

Dd2 and 3D7 wild-type parasite cultures had high parasitaemias of 7.2% and 6.5% respectively with >80% of ring stages present at the time of transfection. Each parasite line was transfected with plasmids carrying each donor and each guide (K65-g1, K65-g2, Q65-g1 and Q65-g2) giving a total of 8 transfections (Table 6.3). The parasitaemia for all transfections dropped rapidly following electroporation resulting in a median parasitaemia of 2.7% and 1.8% respectively for Dd2 and 3D7 transfected parasites. Parasites were undetectable at day 3 following drug selection with WR99210. All four transfected parasites with Dd2 backbone successfully recovered and were visible at days 25 (Dd2 K65-g2), 27 (Dd2 K65-g1 and Dd2 Q65-g1) and 33 (Dd2 Q65-g2) post-transfection. Only one out of four transfected parasites with 3D7 backbone recovered at day 36 (3D7 K65-g1) giving a total recovery rate of 62.5%. All recovered transgenic parasites had a steady increase in parasitaemia.

6.4.5 Confirmation of successful *Pfnfs1* K/Q65 editing

Genomic DNA extraction from successfully recovered parasites and non-transfected wild-type strains gave the following yield (Table 6.3). Amplification of the transfected parasites and wild-type controls with corresponding primers resulted in DNA fragment sizes of approximately 1200 bp (Figure 6.5).

Table 6.3: Dd2 and 3D7 transfected parasites using both guides (gRNA-1 and gRNA-2) and both donors (K65 and Q65) of the *Pfnfs1* gene.

Dd2				**3D7**			
Mutation	**Type**	**Recovered**	**gDNA yield (ng/µL)**	**Mutation**	**Type**	**Recovered**	**gDNA yield (ng/µL)**
Q65Q-g1	Silent control	Yes	76.7	**K65K-g1**	Silent control	Yes	158.9
Q65Q-g2	Silent control	Yes	88.4	**K65K-g2**	Silent control	No	-
Q65K-g1	Mutant	Yes	90.2	**K65Q-g1**	Mutant	No	-
Q65K-g2	Mutant	Yes	101.6	**K65Q-g2**	Mutant	No	-
-	Wild-type control	-	98.5	-	Wild-type control	-	96.9

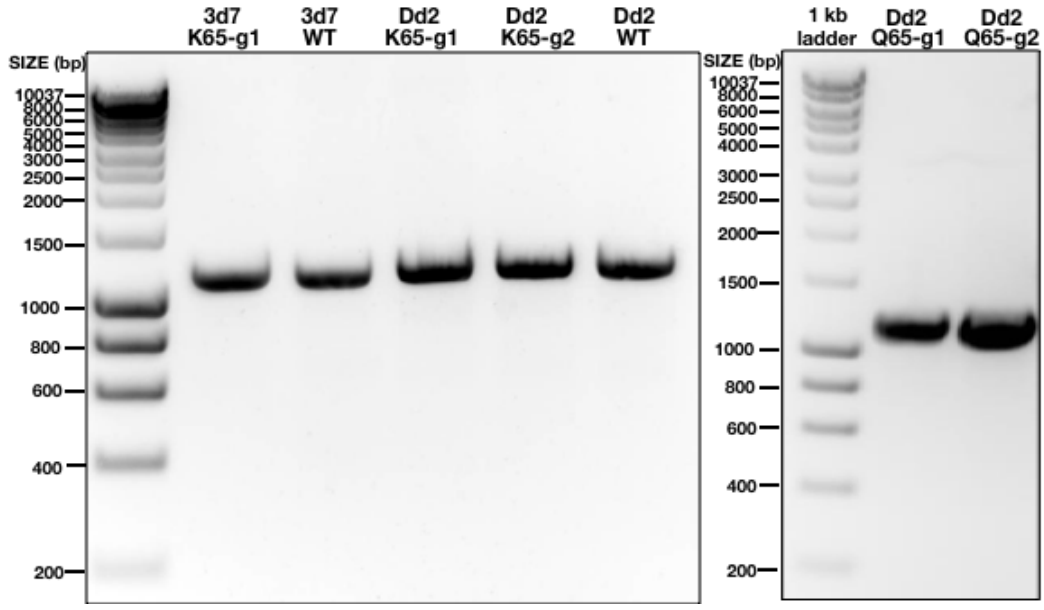

Figure 6.5: PCR amplification of *Pfnfs1* gene fragment using gDNA of transfected parasites and wild-type control strains. The expected DNA fragment sizes of approximately 1200 bp were visualized with a 1% agarose gel.

6.4.6 Confirmation of recombinant parasite

Sequence results confirmed a 40% success in gene editing of K/Q 65 allele on *Pfnfs1*, with 2 successfully edited out of 5 recovered parasites (Figure 6.6). Only one of the edited parasites with 3D7 backbone recovered and capillary sequencing confirmed successful editing. The silent control 3D7 K65K-g1 with shield and synonymous mutations showed the integration of all shield mutations from the donor including the silent mutation at amino acid 65 (AAA to AAG) coding for lysine (K65K). Editing of Dd2 Q65Q was also successful for one guide (Dd2 Q65Q- g2). Both the wild-type and edited Dd2 carry the same nucleotides that code for the amino acid glutamine (Q) however, the shield mutations on the donor were present in the edited parasite confirming successful editing (Figure 6.6). Dd2 Q65K-g1, Q65K-g2 and Q65Q-g1 was partially edited with only the first two shield mutations incorporated. All other mutations on the donor template including those on amino acid 65 were not integrated (Figure 6.6).

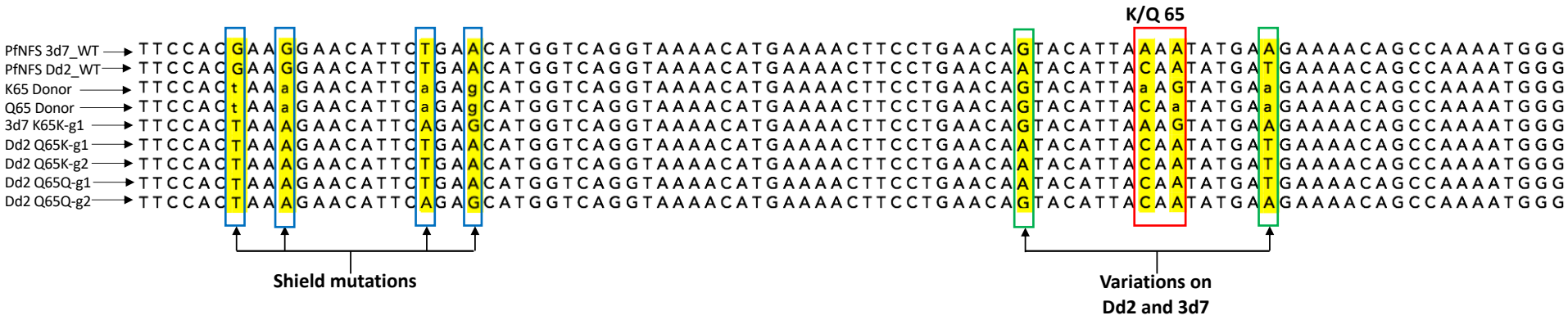

Figure 6.6: Sequence analysis of wild-type and recombinant parasites. Dd2 and 3D7 wild-type sequences are used as references. Designed K65 and Q65 donor sequences and sequences of recovered parasites following transfections are shown. All variations on the sequences are highlighted. Shield mutations on the seed region of the guides and PAM sites are shown in blue outlines. Also shown are variations found on Dd2 and 3D7 reference sequences (green outline) surrounding the target desired mutation at amino acid 65 of *Pfnfs1* (red outline).

6.4.7 Susceptibility of recombinant parasites to antimalarial drugs

In vitro susceptibility test of the parent and recovered parasites to LUM and CQ was performed to estimate their IC_{50} values (Table 6.4, Figure 6.7). No significant differences were observed comparing the wild-type parent isolates and the edited isolates. This is the same for both 3D7 and Dd2 parasite lines and both drug treatments (Figure 6.7).

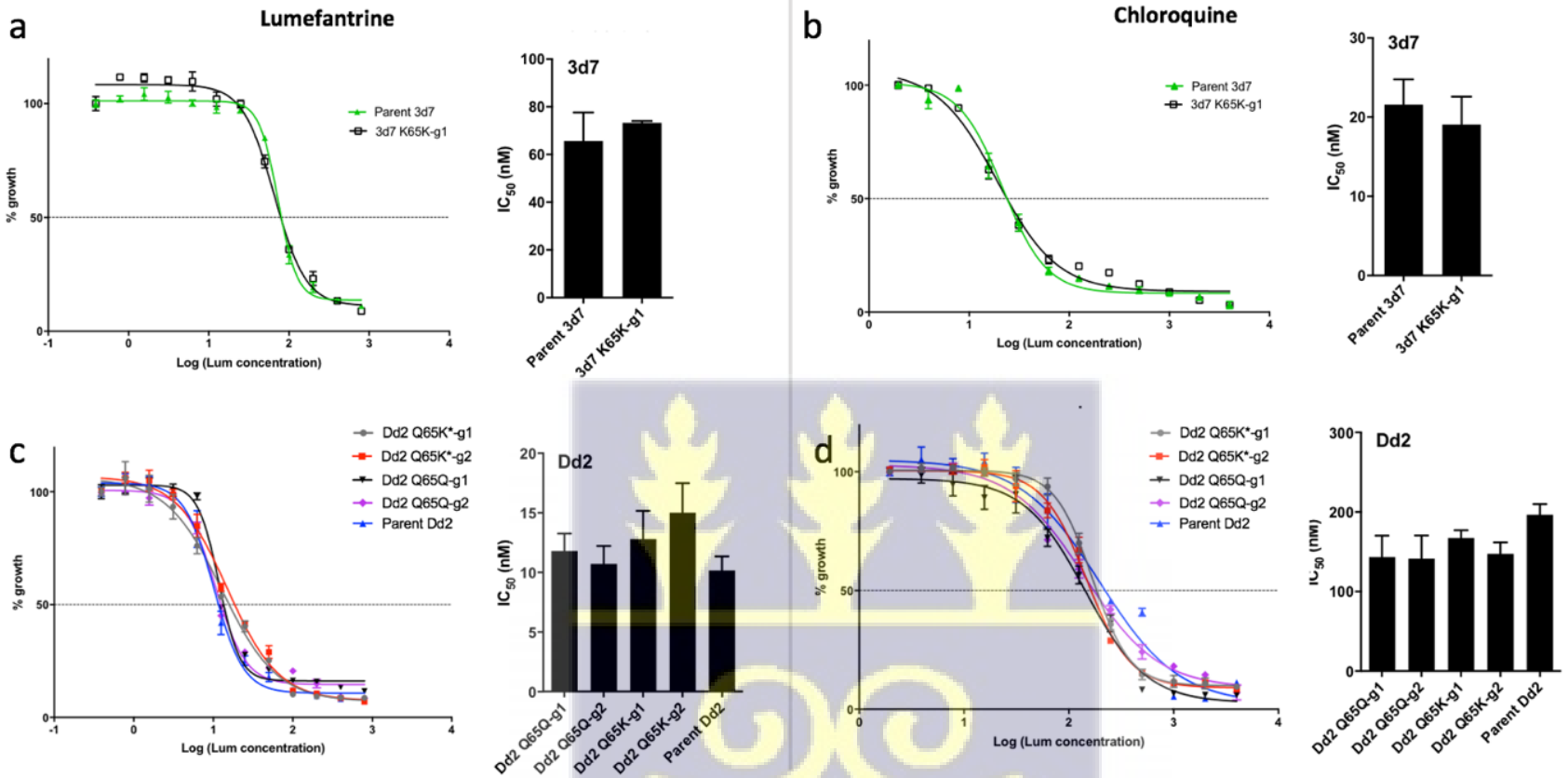

Figure 6.7: IC_{50} estimates for *P. falciparum* wild-type (Parent) and recombinant parasites following 72 hours exposure to LUM and CQ. IC_{50} values of parent 3D7 and the control edited 3D7 (K65K) following exposure to a. LUM and b. CQ. IC_{50} estimates of Dd2 parent and edited lines following exposure to c. LUM and d. CQ. *Note: these recombinant lines were only edited for the silent mutations but retained the wild-type Q65 codon.

Table 6.4: IC_{50} values of parent and recombinant parasite lines

	Drugs	3D7 Parent	3D7 K65K-g1	Dd2 Parent	Dd2 Q65K-g1	Dd2 Q65K-g2	Dd2 Q65Q-g1	Dd2 Q65Q-g2
Mean IC_{50} values (nM)	LUM	65.65	73.23	10.16	12.80	15.02	11.79	10.70
	CQ	21.59	19.06	196.5	167.4	147.4	143.3	141.4

6.5 Discussion

In The Gambia, an increase in parasite tolerance to LUM, used in combination with ARM as the first-line treatment for uncomplicated malaria, strongly correlated with increase in frequency of K65 allele on *Pfnfs1* that was shown to be under positive selection (Amambua-Ngwa et al., 2018). It was therefore important to validate the relationship between *Pfnfs1* and LUM tolerance as LUM pressure is maintained.

In this study, a site-specific DSB was created and a SNP incorporated in the *Pfnfs1* gene to generate the K/Q65 recombinant parasites. The CQ-sensitive 3D7 strain carries the canonical wild-type K65 allele associated with LUM tolerance and CQ-resistant Dd2 strain carries the K65Q mutation, sensitive to LUM. Previous *in vitro* drug analysis of these two isolates in our laboratory showed that 3D7 consistently has higher IC_{50} than Dd2. In this study, successful editing of the K/Q65 allele was confirmed for some of the recovered parasite clones with both 3D7 and Dd2 genomic backgrounds. However, these were the control transfections with synonymous mutations on the target locus: K65K for 3D7 and Q65Q for Dd2. Isolates with the Dd2 genomic background that recovered other than the control transfection all showed integration of only the synonymous shield mutations on the PAM site and seed region of the gRNAs. Recombinant parasites with the mutation of interest did not recover. The reason for partial editing and failure to recover recombinant parasites is not known and could be multifactorial.

The complex genome of *P. falciparum* parasite makes it challenging to identify unique gRNA sites with the -NGG PAM site downstream and high on- and off- target scores for successful gene editing (Kudyba et al., 2018). A major limitation that prevents the design of suitable guides is the AT rich genome of the parasite which can result in guides with Poly-T stretches with the potential of inducing premature termination when RNA Pol III or T7 RNAP are used

(Roy et al., 2018). It is important to consider guides with high on- and off- target scores (closer to 100) that ascertain more efficient cleavage and the inverse likelihood of binding to other genomic regions other than the target site (Ribeiro et al., 2018). Studies by Ribeiro et al., proved that high on-target scores predict successful editing. Another possible factor that can contribute to unsuccessful editing is if the gRNAs and shield mutations on the donor template lie further than 100bp away from the target mutation site. Successful editing of shield mutations and not the target mutation could occur due to homology in the sequence immediately after the shield mutations, halting the repair process (Kudyba et al., 2018).

Although the gRNAs designed are less than 60bp away from the target mutation site, a similar issue was observed. This can be resolved by performing transfections in replicates though a better alternative would be to re-codonise the entire region between the guide sequence and the target mutation site by incorporating silent mutations on the donor template, ensuring a continuous repair process from the guide to the target mutation site (Lee et al., 2019). Another factor which could be the most probable one is the potential fitness cost associated with editing a single non-synonymous mutation. In addition to the K65 allele, other alleles may be associated with LUM tolerance in The Gambia. An increase in frequency was seen by at least two other alleles surrounding K65: S62 and E67, suggesting that these three alleles are in linkage disequilibrium (unpublished). Consequently, LUM tolerance could be caused by a triple mutation in *Pfnfs1*.

While this study has not been successful in generating recombinant parasites with the desired mutation, it should be noted that an efficient method was used to introduce a point mutation in *Pfnfs1*, which opens a platform to effectively study this gene. More studies are required to validate the involvement of *Pfnfs1* K65 with LUM tolerance. Editing of the K65 allele should be repeated taking into consideration effective gRNA and donor design. A publicly accessible

list of 662,795 potential gRNA sites across the whole genome with on- and off- target scores by Ribeiro et al. makes gRNA selection easier and more efficient (Ribeiro et al., 2018). Successful functional validation of *Pfnfs1* will be beneficial for understanding the role of the gene in drug resistance and consequently prevent its development. Potentially replacing the entire haplotype may be required for full functionality or fitness, and this could be the basis of future work.

CHAPTER 7

7.0 General discussion, conclusion, limitations and recommendation

7.1 General discussion

The renewed efforts of malaria elimination require more research to focus on malaria chemotherapy as antimalarial drug resistance is one of the impediments to achieving the goal of elimination. Parasite resistance to antimalarial drugs result in drugs becoming ineffective and therefore lack the ability to clear infections from the circulation of human hosts (WHO, 2015b). Drug resistance is associated with an increase in malaria-related clinical cases and deaths which is a major concern for global health (Kumar et al., 2018). Drug resistance can be mitigated by continuous surveillance with *in vivo* TES, *in vitro/ex vivo* drug efficacy studies and molecular genotyping tools.

To effectively assess the efficacy of antimalarial drugs currently in use and monitor the emergence and spread of drug resistance, highly sensitive *in vitro*/*ex vivo* tools are needed. The drugs used in combination in ACTs are of different potencies making it complex to simultaneously compare their efficacy using currently available drug assays (Tse et al., 2019). Hence, the first objective in chapter 3 was to develop the PSRA to assess parasite survival and re-invasion potential following 72 hours of exposure to DHA (the active component in all ART derivatives) and the partner drug, LUM. Seventy-two hours (72 hours) of drug exposure was used to mimic ACT drug course which lasts for 3 days (Tun et al., 2018). The drug concentrations used here were identified to be optimal, enabling the determination of the rate at which parasites were inhibited over time. Results from this analysis showed four and three isolates that persistently grew in the presence of DHA and LUM respectively with one isolate surviving in the presence of both drugs. These isolates were considered to be tolerant and could be driving towards a state of resistance, a worrying finding. MRA-1241, a laboratory-adapted

strain characterised as resistant to DHA showed to have a delayed clearance phenotype with almost all parasites inhibited at 48 hours using PSRA. The PSRA, unlike the commonly used IC_{50} assay or RSA can allow for a more sensitive detection of tolerant isolates even for infections with very low levels of parasitaemia. Its reliance on growth and re-invasion by first generation rings following drug exposure, provides an indirect measure of viability. Surviving parasites were therefore considered to possess genomic or other mechanisms that drive drug tolerance and evolution to resistance.

Molecular surveillance of genes associated with antimalarial drug resistance was also carried out in this objective to assess the circulating genotypes and determine their association with observed phenotypes if any. Genotyping was carried out for alleles associated with quinoline, antifolate and ART resistance at *Pfcrt*, *Pfmdr1*, *Pfdhfr*, *Pfdhps* and *Pfk13* loci in assayed samples. Surprisingly, over 80% of isolates carried the *Pfcrt* 72-76 mutant haplotype, denoting that there is ongoing drug pressure from CQ and AMD, though CQ had been discontinued for the treatment of malaria for many years now (Dieye et al., 2016). We are however aware that CQ is still available in the private sector and the use of AMD in ASAQ in neighbouring Senegal might also be contributing to increased mutant variants. However, the reversal to wild-type *Pfcrt* variants is due to massive use of AL (Maiga et al., 2021). As expected high levels of the wild-type *Pfmdr1* N86/184F/D1246 haplotype was observed as this is selected for by LUM (Raman et al., 2019). High frequencies of resistant loci were observed for *Pfdhfr* and *Pfdhps* which could be explained by the use of SP for SMC and IPTp (Ndiaye et al., 2021). Finally, as expected, only wild-type alleles were present for *Pfk13* loci. With the high mutant and wild-type alleles observed for drug resistant genes, associations with drug phenotypes could not be derived. Though surveying these validated molecular markers of resistance remain useful for monitoring drug resistant *P. falciparum* parasites in real time, they are less informative in case of alternative mechanisms of resistance to ACTs in different populations (Ashley et al., 2014;

Chenet et al., 2016). Therefore, there is the need to continuously characterise the molecular mechanisms in emerging tolerant parasites.

Multiple reports of ACT failure and increasing *ex vivo* tolerance to LUM for example, prompted the testing of available compound libraries to aid discovery and development of novel antimalarial drugs. Identifying potent compounds from the MMV pathogen box with antimalarial activities that could progress in the drug development pipeline was the focus of chapter 4. Firstly, 125 compounds were screened against CQ - sensitive 3D7 laboratory isolate using the IC_{50} determination assay. A number of compounds more potent than CQ where identified and out of these, the top seven compounds with the lowest IC_{50}s, putatively considered to be highly potent were further analysed. Following confirmation that these were the most potent compounds with antimalarial activities in the MMV pathogen box, three of them were selected to assess their efficacy against parasite isolates from the field with different genetic backgrounds and have undergone selection after years of being exposed to different drugs (Leba et al., 2015). These isolates will most definitely generate in different responses, and as a result give a better assessment of the potencies of these compounds. Adding to this, the newly developed PSRA assay was used to confirm its application to compounds with different potencies. The results generated revealed that these candidate compounds are highly efficacious in killing both laboratory and field *P. falciparum* isolates with MMV667494, a quinoline-carboxamides (Baragana et al., 2016) performing better than the highly potent DHA even at 6 hours post exposure. MMV010576, a 2-amino pyridine derivative (Paquet et al., 2017) was also observed to be more potent than DHA at 72 hours and appeared to be a slower acting compound. Finally, another quinoline-carboxamide, MMV634140 (Baragana et al., 2016) showed the survival of four isolates above the threshold of 0.2% even after 72 hours post- exposure. Of note is the cross resistance observed between LUM and MMV634140 which could be explained by similarities in the drug classes of these two, for which more attention

should be paid. These three compounds have previously been characterised and their targets identified which opens opportunities for further exploration to determine their pharmacokinetic and toxicity properties.

The prevalence of known drug resistance markers was determined earlier in the study, however, the identification of novel markers of antimalarial drug resistance was not done, which was the focus of my second objective in Chapter 5. The identification of novel molecular markers of resistance has mainly been done in SEA, where drug resistance mostly emerges, making it possible to perform genomic surveillance of drug resistance (Reviewed by (Ippolito et al., 2021)). This has resulted in the identification of most drug resistance genes, including Pfk13 which remains rare in Africa (WHO, 2020b). The recent observations of mutations in Pfk13 in isolates from Rwanda and Uganda suggests that resistance to ARTs might emerge independently in Africa (Maniga et al., 2021; Uwimana et al., 2020). Mutations in other genes such as the *Pfap2-mu* on chromosome 12 have also been identified to be associated with tolerance to ACTs (Reviewed by (Siddiqui et al., 2021)). In western Gambia, *Pfmdr1* molecular markers associated with LUM tolerance are increasing and *ex vivo* tolerant isolates are also seen in this same population, shown in chapter3 (Amambua-Ngwa et al., 2017). While ACTs remain highly efficacious, strong signatures of selection at drug resistant loci and recent directional selection in temporal populations have previously been reported (Henriques et al., 2014). Hence, this objective sought to gain insights on loci affecting drug response phenotypes, specifically for LUM.

Whole genome relatedness analysis of isolates from 2008, when AL was just introduced and 7 years later from 2015, identified regions in the *P. falciparum* genome that have undergone recent positive selection probably from constant drug pressure exerted on the parasites. The dominant regions identified in this study have previously been described in genome scans of

Gambian populations for signatures of selection. These included regions around known markers of resistance such as *Pfcrt* on chromosome 7 but also a sweep around *Pfaat1* in chromosome 6 which is not well characterised (Amambua-Ngwa et al., 2016). This region shows a population haplotype structure similar to that around *Pfcrt*, with haplotypes related to those in Cambodia, evidence of likely introgression. These SEA related haplotypes were not identified in the recent 2014/2015 isolates despite the persistence of *Pfcrt* 76T mutant variant associated with CQ resistance. The use of AL for 7 years in The Gambia had not selected for mutations and a selective signature on *Pfk13* which had evidence of positive selection in Cambodian samples as expected. A strong region of selection common to Gambian and Cambodian population was around a cluster of MSP3/6 and Duffy binding proteins on chromosome 10. This region has not been shown to be under selection from drugs, though the presence of shared haplotypes between Gambia and Cambodia leads us to speculate that it may be driving a common unknown phenomenon.

Several mixed linear model regression approaches were used for association between genomic loci in 2014/2015 isolates and their *in vitro* drug susceptibility phenotypes however, this was not powered to result in significantly associated SNPs. Nevertheless, a number of outliers were identified, including CG1 proteins and SURFIN 14.1 associated with responses to LUM, and the multidrug resistance-associated protein 2 and SURFIN 4.2 associated with DHA. Three SNPs around the chromosome 10 region of recent selection had low *P* values in association with both DHA and LUM but these did not reach genome-wide significance. Validating these genes for their role in drug resistance will be a starting point to understanding the mechanisms of resistance. Furthermore, emerging ACT tolerant isolates should be prioritised for screening candidate compound libraries to facilitate the identification of novel potent drugs.

The final objective of this study was to functionally validate SNPs in *Pfnfs1* as a marker of LUM tolerance. Markedly, a recent study conducted in The Gambia, mutations in the cysteine desulfurase gene (*Pfnfs1*- PF3D7_0727200) at amino acid position 65 (K65Q) showed the strongest temporal differentiation following 6 years of AL use with a steady increase in allele frequency within a four-year span (Amambua-Ngwa et al., 2018). This strongly correlated with a temporal increase in *P. falciparum* tolerance to LUM observed within the same period, prioritising the validation of *Pfnfs1* as a potential marker of LUM tolerance (Amambua-Ngwa et al., 2018). An increase in frequencies was also seen for two other alleles: S62 and E67, suggesting that they are in linkage disequilibrium. Accordingly, a forward genetic approach was used to generate site specific mutations on the gene using CRISPR-Cas9 genome editing tool. Dd2 and 3D7 laboratory isolates were transfected with plasmids consisting of the customised donor template with the K/Q65 allele, guide RNAs Cas9 enzyme and selection cassettes. Though edited parasites were generated, recombinant parasites with the mutations of interest were not recovered in culture. This could be due to several factors including proximity of gRNAs and shield mutations on the donor template, and potential fitness cost associated with editing non-synonymous mutations (Kudyba et al., 2018). Replacing the entire loci may be required for full functionality or fitness, and this could be the basis of future work.

7.2 General conclusion

In conclusion, this study presents work on the evaluation of parasite susceptibility using the newly developed flow cytometry-based PSRA which provides a significant advancement in approaches for *in vitro/ex vivo* assessment of parasite susceptibility to drugs. This revealed the presence of DHA and LUM tolerant parasites in The Gambia where malaria incidence has significantly declined in recent years (Broekhuizen et al., 2021). The PSRA also identified

three hit compounds from the MMV pathogen box potent against laboratory-adapted and field isolates. These compounds were among the most potent and therefore, the results from this study add to the body of knowledge needed for their further development. Potential markers of association with *ex vivo* drug tolerance, specifically, LUM were also found. Going forward, these markers should be validated for their involvement in LUM tolerance which can then be used as markers of LUM tolerance/resistance for resistance surveillance. Finally, forward genetic approach was explored to characterise a candidate marker of LUM tolerance previously identified. The results obtained suggests the lack of fitness associated with the mutation of interest and should be further explored. With reduced transmission and sustained drug pressure against *P. falciparum* in The Gambia, the results here call for increased molecular and phenotypic surveillance to pre-empt local emergence of clinical resistance to ACTs.

7.3 Limitations and recommendations

The study had several limitations; (i) In Chapter 4, all compounds that were identified as potent could not be further validated using the PSRA due to limited time and resources, hence only three of these were tested. Testing of the remaining potent compounds against field isolates continued, which is beyond this thesis. (ii) The results generated in Chapter 5 were obtained by combining mixed model regression methods, simple parametric t-test, and population genetic analyses because of the small sample size used which did not allow for power to do a strong GWAS analysis. Consequently, a number of genes with relatively stronger associations were identified but no particular gene was significantly associated with tolerance to LUM or any other drug used in this study. Future studies should aim to use a large sample size that will permit the use of well powered genome-wide association approaches to identify drug resistance markers that will enable the monitoring of drug interventions against malaria. (iii) Firm

conclusions could not be drawn following the genome editing of the *Pfnfs1* gene (Chapter 6) due to limited time available. More work is needed to establish the role of *Pfnfs1* in LUM tolerance.

7.0REFERENCES

Abdulla, S., Ashley, E. A., Bassat, Q., Bethell, D., Björkman, A., Borrmann, S., et al. (2015). Baseline data of parasite clearance in patients with falciparum malaria treated with an artemisinin derivative: An individual patient data meta-analysis. *Malaria Journal*, *14*(1), p. 359. Retrieved October 1, 2020, from https://malariajournal.biomedcentral.com/articles/10.1186/s12936-015-0874-1

Achan, J., Mwesigwa, J., Edwin, C. P., & D'alessandro, U. (2018). Malaria medicines to address drug resistance and support malaria elimination efforts. *Expert Review of Clinical Pharmacology*, *11*(1), pp. 61–70.

Achan, J., Talisuna, A. O., Erhart, A., Yeka, A., Tibenderana, J. K., Baliraine, F. N., et al. (2011). Quinine, an old anti-malarial drug in a modern world: Role in the treatment of malaria. *Malaria Journal*, *10*(1), p. 144.

Acharya, A., Bansal, D., Bharti, P. K., Khan, F. Y., Abusalah, S., Elmalik, A., et al. (2018). Molecular surveillance of chloroquine drug resistance markers (Pfcrt and Pfmdr1) among imported Plasmodium falciparum malaria in Qatar. *Pathogens and Global Health*, *112*(2), pp. 57–62.

Achieng, A. O., Muiruri, P., Ingasia, L. A., Opot, B. H., Juma, D. W., Yeda, R., et al. (2015). Temporal trends in prevalence of Plasmodium falciparum molecular markers selected for by artemether-lumefantrine treatment in pre-ACT and post-ACT parasites in western Kenya. *International Journal for Parasitology: Drugs and Drug Resistance*, *5*(3), pp. 92–99. Retrieved from http://dx.doi.org/10.1016/j.ijpddr.2015.05.005

Aftab, T., Ferreira, J. F. S., Khan, M. M. A., & Naeem, M. (2014). *Artemisia annua - Pharmacology and biotechnology*. Springer-Verlag Berlin Heidelberg.

Ahmed, M. A., & Cox-Singh, J. (2015). Plasmodium knowlesi - an emerging pathogen . *ISBT Science Series*, *10*(S1), pp. 134–140.

Alam Saifi, M., Beg, T., Halim Harrath, A., Suleman Hamad Altayalan, F., & Al Quraishy, S. (2013). Antimalarial drugs: Mode of action and status of resistance. *African Journal of Pharmacy and Pharmacology*, *7*(5), pp. 148–156.

Amambua-Ngwa, A., Amenga-Etego, L., Kamau, E., Amato, R., Ghansah, A., Golassa, L., et al. (2019). Major subpopulations of Plasmodium falciparum in sub-Saharan Africa. *Science*, *365*(6455), pp. 813–816. Retrieved December 7, 2020, from http://science.sciencemag.org/

Amambua-Ngwa, A., Danso, B., Worwui, A., Ceesay, S., Davies, N., Jeffries, D., et al. (2016). Exceptionally long-range haplotypes in Plasmodium falciparum chromosome 6 maintained in an endemic African population. *Malaria Journal*, *15*(1). Retrieved December 30, 2020, from https://pubmed.ncbi.nlm.nih.gov/27769292/

Amambua-Ngwa, A., Jeffries, D., Amato, R., Worwui, A., Karim, M., Ceesay, S., et al. (2018). Consistent signatures of selection from genomic analysis of pairs of temporal and spatial Plasmodium falciparum populations from the Gambia. *Scientific Reports*, *8*(1), pp. 1–10.

Amambua-Ngwa, A., Okebe, J., Mbye, H., Ceesay, S., El-Fatouri, F., Joof, F., et al. (2017). Sustained Ex Vivo Susceptibility of Plasmodium falciparum to Artemisinin Derivatives but Increasing Tolerance to Artemisinin Combination Therapy Partner Quinolines in The Gambia. *Antimicrobial agents and chemotherapy*, *61*(12), pp. e00759-17. Retrieved from https://pubmed.ncbi.nlm.nih.gov/28971859

Amaratunga, C., Neal, A. T., & Fairhurst, R. M. (2014). Flow cytometry-based analysis of artemisinin-resistant Plasmodium falciparum in the ring-stage survival assay.

Antimicrobial agents and chemotherapy, *58*(8), pp. 4938–4940.

Amato, R., Pearson, R. D., Almagro-Garcia, J., Amaratunga, C., Lim, P., Suon, S., et al. (2018). Origins of the current outbreak of multidrug-resistant malaria in southeast Asia: a retrospective genetic study. *The Lancet Infectious Diseases*, *18*(3), pp. 337–345. Retrieved June 13, 2022, from http://www.thelancet.com/article/S1473309918300689/fulltext

Ariey, F., Witkowski, B., Amaratunga, C., Beghain, J., Langlois, A. C., Khim, N., et al. (2014). A molecular marker of artemisinin-resistant Plasmodium falciparum malaria. *Nature*, *505*(7481), pp. 50–55.

Arya, A., Kojom Foko, L. P., Chaudhry, S., Sharma, A., & Singh, V. (2021). Artemisinin-based combination therapy (ACT) and drug resistance molecular markers: A systematic review of clinical studies from two malaria endemic regions – India and sub-Saharan Africa. *International Journal for Parasitology: Drugs and Drug Resistance*, *15*, pp. 43–56.

Ashley, E. A., Dhorda, M., Fairhurst, R. M., Amaratunga, C., Lim, P., Suon, S., et al. (2014). Spread of artemisinin resistance in Plasmodium falciparum malaria. *New England Journal of Medicine*, *371*(5), pp. 411–423. Retrieved October 27, 2020, from /pmc/articles/PMC4143591/?report=abstract

Ashley, E. A., & Phyo, A. P. (2018). Drugs in Development for Malaria. *Drugs*, *78*(9), pp. 861–879. Retrieved from https://doi.org/10.1007/s40265-018-0911-9

Awasthi, G., & Das, A. (2013). Genetics of chloroquine-resistant malaria: a haplotypicview. *Memórias do Instituto Oswaldo Cruz*, *108*(8), p. 947. Retrieved June 15, 2022, from /pmc/articles/PMC4005552/

Baliraine, F. N., & Rosenthal, P. J. (2011). Prolonged selection of pfmdr1 polymorphisms

after treatment of falciparum malaria with artemether-lumefantrine in Uganda. *Journal of Infectious Diseases*, *204*(7), pp. 1120–1124. Retrieved December 31, 2020, from https://pubmed.ncbi.nlm.nih.gov/21881128/

Baragana, B., Norcross, N. R., Wilson, C., Porzelle, A., Hallyburton, I., Grimaldi, R., et al. (2016). Discovery of a Quinoline-4-carboxamide Derivative with a Novel Mechanism of Action, Multistage Antimalarial Activity, and Potent in Vivo Efficacy. *Journal of Medicinal Chemistry*, *59*(21), pp. 9672–9685.

Bartoloni, A., & Zammarchi, L. (2012). Clinical Aspects of Uncomplicated and Severe Malaria. *Mediterranean Journal of Hematology and Infectious Diseases*, *4*(1), p. 201. Retrieved June 15, 2022, from /pmc/articles/PMC3375727/

Barua, P., Beeson, J. G., Maleta, K., Ashorn, P., & Rogerson, S. J. (2019). The impact of early life exposure to Plasmodium falciparum on the development of naturally acquired immunity to malaria in young Malawian children. *Malaria Journal*, *18*(1), pp. 1–12. Retrieved June 15, 2022, from https://malariajournal.biomedcentral.com/articles/10.1186/s12936-019-2647-8

Bennink, S., Kiesow, M. J., & Pradel, G. (2016). The development of malaria parasites in the mosquito midgut. *Cellular Microbiology*, *18*(7), p. 905. Retrieved June 15, 2022, from /pmc/articles/PMC5089571/

Bhatt, S., Weiss, D. J., Cameron, E., Bisanzio, D., Mappin, B., Dalrymple, U., et al. (2015). The effect of malaria control on Plasmodium falciparum in Africa between 2000 and 2015. *Nature*, *526*(7572), pp. 207–211.

Bollen, Y., Post, J., Koo, B. K., & Snippert, H. J. G. (2018). How to create state-of-the-art genetic model systems: strategies for optimal CRISPR-mediated genome editing. *Nucleic Acids Research*, *46*(13), pp. 6435–6454. Retrieved June 13, 2022, from

https://academic.oup.com/nar/article/46/13/6435/5046101

Borrmann, S., Sasi, P., Mwai, L., Bashraheil, M., Abdallah, A., Muriithi, S., et al. (2011). Declining responsiveness of plasmodium falciparum infections to Artemisinin-Based combination treatments on the Kenyan coast. *PLoS ONE*, *6*(11).

Bouyou-Akotet, M. K., Mawili-Mboumba, D. P., Kendjo, E., Moutandou Chiesa, S., Tshibola Mbuyi, M. L., Tsoumbou-Bakana, G., et al. (2016). Decrease of microscopic Plasmodium falciparum infection prevalence during pregnancy following IPTp-SP implementation in urban cities of Gabon. *Transactions of the Royal Society of Tropical Medicine and Hygiene*, *110*(6), pp. 333–342.

Bridgford, J. L., Xie, S. C., Cobbold, S. A., Pasaje, C. F. A., Herrmann, S., Yang, T., et al. (2018). Artemisinin kills malaria parasites by damaging proteins and inhibiting the proteasome. *Nature Communications*, *9*(1).

Broekhuizen, H., Fehr, A., Nieto-Sanchez, C., Muela, J., Peeters-Grietens, K., Smekens, T., et al. (2021). Costs and barriers faced by households seeking malaria treatment in the Upper River Region, The Gambia. *Malaria Journal*, *20*(1). Retrieved June 13, 2022, from /pmc/articles/PMC8447575/

Burns, A. L., Dans, M. G., Balbin, J. M., De Koning-Ward, T. F., Gilson, P. R., Beeson, J. G., et al. (2019). Targeting malaria parasite invasion of red blood cells as an antimalarial strategy. *FEMS Microbiology Reviews*, *43*(3), pp. 223–238.

Callaghan, P. S., & Roepe, P. D. (2017). The biochemistry of quinoline antimalarial drug resistance, in: *Handbook of Antimicrobial Resistance*, pp. 289–311. Springer New York.

Camarda, G., Jirawatcharadech, P., Priestley, R. S., Saif, A., March, S., Wong, M. H. L., et al. (2019). Antimalarial activity of primaquine operates via a two-step biochemical relay. *Nature Communications*, *10*(1), pp. 1–9.

Capela, R., Moreira, R., & Lopes, F. (2019). An Overview of Drug Resistance in Protozoal Diseases. *International Journal of Molecular Sciences*, *20*(22). Retrieved June 15, 2022, from /pmc/articles/PMC6888673/

Chawla, J., Oberstaller, J., & Adams, J. H. (2021). Targeting Gametocytes of the Malaria Parasite Plasmodium falciparum in a Functional Genomics Era: Next Steps. *Pathogens*, *10*(3). Retrieved June 15, 2022, from /pmc/articles/PMC7999360/

Chenet, S. M., Akinyi Okoth, S., Huber, C. S., Chandrabose, J., Lucchi, N. W., Talundzic, E., et al. (2016). Independent Emergence of the Plasmodium falciparum Kelch Propeller Domain Mutant Allele C580Y in Guyana. *Journal of Infectious Diseases*, *213*(9), pp. 1472–1475.

Combrinck, J. M., Mabotha, T. E., Ncokazi, K. K., Ambele, M. A., Taylor, D., Smith, P. J., et al. (2013). Insights into the Role of Heme in the Mechanism of Action of Antimalarials. *ACS chemical biology*, *8*(1), p. 133. Retrieved June 15, 2022, from /pmc/articles/PMC3548943/

Conrad, M. D., & Rosenthal, P. J. (2019). Antimalarial drug resistance in Africa: the calm before the storm? *The Lancet. Infectious diseases*, *19*(10), pp. e338–e351. Retrieved June 15, 2022, from https://pubmed.ncbi.nlm.nih.gov/31375467/

Costanzo, M. S., Brown, K. M., & Hartl, D. L. (2011). Fitness Trade-Offs in the Evolution of Dihydrofolate Reductase and Drug Resistance in Plasmodium falciparum. *PLOS ONE*, *6*(5), p. e19636. Retrieved June 13, 2022, from https://journals.plos.org/plosone/article?id=10.1371/journal.pone.0019636

Cowman, A. F., Healer, J., Marapana, D., & Marsh, K. (2016). Malaria: Biology and Disease. *Cell*, *167*(3), pp. 610–624. Retrieved from http://dx.doi.org/10.1016/j.cell.2016.07.055

Crompton, P. D., Moebius, J., Portugal, S., Waisberg, M., Hart, G., Garver, L. S., et al.

(2014). Malaria immunity in man and mosquito: insights into unsolved mysteries of a deadly infectious disease. *Annual review of immunology*, *32*, p. 157. Retrieved June 15, 2022, from /pmc/articles/PMC4075043/

Dama, S., Niangaly, H., Ouattara, A., Sagara, I., Sissoko, S., Traore, O. B., et al. (2017). Reduced ex vivo susceptibility of Plasmodium falciparum after oral artemether-lumefantrine treatment in Mali. *Malaria Journal*, *16*(1), pp. 1–6.

Daniels, R., Ndiaye, D., Wall, M., McKinney, J., Séne, P. D., Sabeti, P. C., et al. (2012). Rapid, field-deployable method for genotyping and discovery of single-nucleotide polymorphisms associated with drug resistance in Plasmodium falciparum. *Antimicrobial agents and chemotherapy*, *56*(6), pp. 2976–2986.

Davlantes, E., Dimbu, P. R., Ferreira, C. M., Joao, M. F., Pode, D., Félix, J., et al. (2018). Efficacy and safety of artemether-lumefantrine, artesunate-amodiaquine, and dihydroartemisinin-piperaquine for the treatment of uncomplicated Plasmodium falciparum malaria in three provinces in Angola, 2017. *Malaria journal*, *17*(1). Retrieved October 1, 2020, from https://pubmed.ncbi.nlm.nih.gov/29615039/

Delves, M. J., Miguel-Blanco, C., Matthews, H., Molina, I., Ruecker, A., Yahiya, S., et al. (2018). A high throughput screen for next-generation leads targeting malaria parasite transmission. *Nature Communications*, *9*(1). Retrieved from http://dx.doi.org/10.1038/s41467-018-05777-2

Delves, M. J., Plouffe, D., Scheurer, C., Meister, S., Wittlin, S., Winzeler, E. A., et al. (2012). The Activities of Current Antimalarial Drugs on the Life Cycle Stages of Plasmodium: A Comparative Study with Human and Rodent Parasites. *PLOS Medicine*, *9*(2), p. e1001169. Retrieved June 13, 2022, from http://www.mmv.org

Deng, C., Huang, B., Wang, Q., Wu, W., Zheng, S., Zhang, H., et al. (2018). Large-scale

Artemisinin-Piperaquine Mass Drug Administration with or Without Primaquine Dramatically Reduces Malaria in a Highly Endemic Region of Africa. *Clinical Infectious Diseases*, *67*(11), pp. 1670–1676.

Diawara, S., Madamet, M., Kounta, M. B., Lo, G., Wade, K. A., Nakoulima, A., et al. (2017). Confirmation of Plasmodium falciparum in vitro resistance to monodesethylamodiaquine and chloroquine in Dakar, Senegal, in 2015. *Malaria Journal*, *16*(1), p. 118. Retrieved October 1, 2020, from http://malariajournal.biomedcentral.com/articles/10.1186/s12936-017-1773-4

Dieye, B., Affara, M., Sangare, L., Joof, F., Ndiaye, Y. D., Gomis, J. F., et al. (2016). West Africa International Centers of Excellence for Malaria Research: Drug Resistance Patterns to Artemether–Lumefantrine in Senegal, Mali, and The Gambia. *The American Journal of Tropical Medicine and Hygiene*, *95*(5), p. 1054. Retrieved June 15, 2022, from /pmc/articles/PMC5094217/

Diouf, I., Adeola, A. M., Abiodun, G. J., Lennard, C., Shirinde, J. M., Yaka, P., et al. (2022). Impact of future climate change on malaria in West Africa. *Theoretical and Applied Climatology*, *147*(3–4), pp. 853–865. Retrieved June 15, 2022, from https://link.springer.com/article/10.1007/s00704-021-03807-6

Djimde, A. A., Makanga, M., Kuhen, K., & Hamed, K. (2015). The emerging threat of artemisinin resistance in malaria: Focus on artemether-lumefantrine. *Expert Review of Anti-Infective Therapy*, *13*(8), pp. 1031–1045.

Draper, S. J., & Higgins, M. K. (2018). A new site of attack for a malaria vaccine. *Nature Medicine*, *24*(4), pp. 382–383.

Duffy, S., Sykes, M. L., Jones, A. J., Shelper, T. B., Simpson, M., Lang, R., et al. (2017). Screening the medicines for malaria venture pathogen box across multiple pathogens

reclassifies starting points for open-source drug discovery. *Antimicrobial Agents and Chemotherapy*, *61*(9), pp. 1–22.

Duru, V., Khim, N., Leang, R., Kim, S., Domergue, A., Kloeung, N., et al. (2015). Plasmodium falciparum dihydroartemisinin-piperaquine failures in Cambodia are associated with mutant K13 parasites presenting high survival rates in novel piperaquine in vitro assays: Retrospective and prospective investigations. *BMC Medicine*, *13*(1), pp. 1–11.

Eastman, R. T., Dharia, N. V., Winzeler, E. A., & Fidock, D. A. (2011). Piperaquine resistance is associated with a copy number variation on chromosome 5 in drug-pressured Plasmodium falciparum parasites. *Antimicrobial Agents and Chemotherapy*, *55*(8), pp. 3908–3916.

Ebohon, O., Irabor, F., Ebohon, L. O., & Omoregie, E. S. (2019). Therapeutic failure after regimen with artemether-lumefantrine combination therapy: A report of three cases in Benin city, Nigeria. *Revista da Sociedade Brasileira de Medicina Tropical*, *52*.

Ecker, A., Lehane, A. M., Clain, J., & Fidock, D. A. (2012). PfCRT and its role in antimalarial drug resistance. *Trends in parasitology*, *28*(11), p. 504. Retrieved June 15, 2022, from /pmc/articles/PMC3478492/

Ehrlich, H. Y., Bei, A. K., Weinberger, D. M., Warren, J. L., & Parikh, S. (2021). Mapping partner drug resistance to guide antimalarial combination therapy policies in sub-Saharan Africa. *Proceedings of the National Academy of Sciences of the United States of America*, *118*(29). Retrieved June 13, 2022, from /pmc/articles/PMC8307356/

Ehrlich, H. Y., Jones, J., & Parikh, S. (2020). Molecular surveillance of antimalarial partner drug resistance in sub-Saharan Africa: a spatial-temporal evidence mapping study. *The Lancet Microbe*, *1*(5), pp. e209–e217. Retrieved June 13, 2022, from

http://www.thelancet.com/article/S266652472030094X/fulltext

Fairhurst, R. M., & Dondorp, A. M. (2016). Artemisinin-resistant Plasmodium falciparum malaria. *Microbiol Spectr*, *4*(3).

Faurant, C. (2011). From bark to weed: The history of artemisinin. *Parasite*, *18*(3), pp. 215–218.

Faye, S., Cico, A., Gueye, A. B., Baruwa, E., Johns, B., Ndiop, M., et al. (2018). Scaling up malaria intervention "packages" in Senegal: Using cost effectiveness data for improving allocative efficiency and programmatic decision-making. *Malaria Journal*, *17*(1).

Fidock, D. A., Nomura, T., Talley, A. K., Cooper, R. A., Dzekunov, S. M., Ferdig, M. T., et al. (2000). Mutations in the P. falciparum digestive vacuole transmembrane protein PfCRT and evidence for their role in chloroquine resistance. *Molecular Cell*, *6*(4), pp. 861–871. Retrieved September 28, 2020, from https://pubmed.ncbi.nlm.nih.gov/11090624/

Flannery, E. L., Chatterjee, A. K., & Winzeler, E. A. (2013). Antimalarial drug discovery-approaches and progress towards new medicines. *Nature Reviews Microbiology*, *11*(12), pp. 849–862. Retrieved December 8, 2020, from /pmc/articles/PMC3941073/?report=abstract

Fukuda, N., Tachibana, S. I., Ikeda, M., Sakurai-Yatsushiro, M., Balikagala, B., Katuro, O. T., et al. (2021). Ex vivo susceptibility of Plasmodium falciparum to antimalarial drugs in Northern Uganda. *Parasitology International*, *81*, p. 102277.

Gao, F. (2020). Iron–Sulfur Cluster Biogenesis and Iron Homeostasis in Cyanobacteria. *Frontiers in Microbiology*, *11*. Retrieved October 1, 2020, from /pmc/articles/PMC7058544/?report=abstract

Gardner, M. J., Hall, N., Fung, E., White, O., Berriman, M., Hyman, R. W., et al. (2002).

Genome sequence of the human malaria parasite Plasmodium falciparum. *Nature*, *419*(6906), pp. 498–511.

Ghorbal, M., Gorman, M., MacPherson, C. R., Martins, R. M., Scherf, A., & Lopez-Rubio, J. J. (2014). Genome editing in the human malaria parasite Plasmodium falciparum using the CRISPR-Cas9 system. *Nature Biotechnology*, *32*(8), pp. 819–821. Retrieved November 12, 2020, from https://pubmed.ncbi.nlm.nih.gov/24880488/

Gil, J. P., & Fançony, C. (2021). Plasmodium falciparum Multidrug Resistance Proteins (pfMRPs). *Frontiers in Pharmacology*, *12*, p. 2896.

Gisselberg, J. E., Dellibovi-Ragheb, T. A., Matthews, K. A., Bosch, G., & Prigge, S. T. (2013). The Suf Iron-Sulfur Cluster Synthesis Pathway Is Required for Apicoplast Maintenance in Malaria Parasites. *PLoS Pathogens*, *9*(9).

Grais, R. F., Laminou, I. M., Woi-Messe, L., Makarimi, R., Bouriema, S. H., Langendorf, C., et al. (2018). Molecular markers of resistance to amodiaquine plus sulfadoxine-pyrimethamine in an area with seasonal malaria chemoprevention in south central Niger. *Malaria journal*, *17*(1), p. 98.

Greenwood, B., & Doumbo, O. K. (2016). Implementation of the malaria candidate vaccine RTS,S/AS01. *The Lancet*, *387*(10016), pp. 318–319.

Greenwood, D. (1992). The quinine connection. *Journal of Antimicrobial Chemotherapy*, *30*(4), pp. 417–427. Retrieved December 29, 2020, from https://pubmed.ncbi.nlm.nih.gov/1490916/

Guttery, D. S., Holder, A. A., & Tewari, R. (2012). Sexual Development in Plasmodium: Lessons from Functional Analyses (K. Laura J., Ed.). *PLoS Pathogens*, *8*(1), p. e1002404.

Hamilton, W. L., Amato, R., van der Pluijm, R. W., Jacob, C. G., Quang, H. H., Thuy-Nhien,

N. T., et al. (2019). Evolution and expansion of multidrug-resistant malaria in southeast Asia: a genomic epidemiology study. *The Lancet. Infectious diseases*, *19*(9), pp. 943–951.

Han, L., Hudgens, M. G., Emch, M. E., Juliano, J. J., Keeler, C., Martinson, F., et al. (2017). RTS,S/AS01 Malaria Vaccine Efficacy is Not Modified by Seasonal Precipitation: Results from a Phase 3 Randomized Controlled Trial in Malawi. *Scientific Reports*, *7*(1), pp. 1–8.

Heller, L. E., & Roepe, P. D. (2019). Artemisinin-Based Antimalarial Drug Therapy: Molecular Pharmacology and Evolving Resistance. *Tropical Medicine and Infectious Disease*, *4*(2). Retrieved June 15, 2022, from /pmc/articles/PMC6631165/

Hemingway, J., Ranson, H., Magill, A., Kolaczinski, J., Fornadel, C., Gimnig, J., et al. (2016). Averting a malaria disaster: Will insecticide resistance derail malaria control? *The Lancet*, *387*(10029), pp. 1785–1788.

Henden, L., Lee, S., Mueller, I., Barry, A., & Bahlo, M. (2018). Identity-by-descent analyses for measuring population dynamics and selection in recombining pathogens. *PLoS Genetics*, *14*(5). Retrieved December 7, 2020, from https://pubmed.ncbi.nlm.nih.gov/29791438/

Henrici, R. C., van Schalkwyk, D. A., & Sutherland, C. J. (2019). Modification of pfap2mu and pfubp1 Markedly Reduces Ring- Stage Susceptibility of Plasmodium falciparum to Artemisinin In Vitro. *Antimicrobial agents and chemotherapy*, *64*(1), pp. 1–9.

Henriques, G., Hallett, R. L., Beshir, K. B., Gadalla, N. B., Johnson, R. E., Burrow, R., et al. (2014). Directional Selection at the pfmdr1, pfcrt, pfubp1, and pfap2mu Loci of Plasmodium falciparum in Kenyan Children Treated With ACT. *The Journal of Infectious Diseases*, *210*(12), p. 2001. Retrieved June 15, 2022, from

/pmc/articles/PMC4241946/

Herraiz, T., Guillén, H., González-Peña, D., & Arán, V. J. (2019). Antimalarial Quinoline Drugs Inhibit β-Hematin and Increase Free Hemin Catalyzing Peroxidative Reactions and Inhibition of Cysteine Proteases. *Scientific Reports*, *9*(1). Retrieved June 15, 2022, from /pmc/articles/PMC6817881/

Ippolito, M. M., Moser, K. A., Jean-Bertin, &, Kabuya, B., Cunningham, C., & Juliano, J. J. (2021). Antimalarial Drug Resistance and Implications for the WHO Global Technical Strategy. *Current Epidemiology Reports 2021 8:2*, *8*(2), pp. 46–62. Retrieved June 15, 2022, from https://link.springer.com/article/10.1007/s40471-021-00266-5

Joice, R., Nilsson, S. K., Montgomery, J., Dankwa, S., Egan, E., Morahan, B., et al. (2014). Plasmodium falciparum transmission stages accumulate in the human bone marrow. *Science Translational Medicine*, *6*(244), pp. 244re5-244re5.

Kafsack, B. F. C., Rovira-Graells, N., Clark, T. G., Bancells, C., Crowley, V. M., Campino, S. G., et al. (2014). A transcriptional switch underlies commitment to sexual development in malaria parasites. *Nature*, *507*(7491), pp. 248–252.

Kagaya, W., Miyazaki, S., Yahata, K., Ohta, N., & Kaneko, O. (2015). The Cytoplasmic Region of Plasmodium falciparum SURFIN4.2 Is Required for Transport from Maurer's Clefts to the Red Blood Cell Surface. *Tropical Medicine and Health*, *43*(4), p. 265. Retrieved June 15, 2022, from /pmc/articles/PMC4689606/

Kateera, F., Nsobya, S. L., Tukwasibwe, S., Hakizimana, E., Mutesa, L., Mens, P. F., et al. (2016). Molecular surveillance of Plasmodium falciparum drug resistance markers reveals partial recovery of chloroquine susceptibility but sustained sulfadoxine-pyrimethamine resistance at two sites of different malaria transmission intensities in Rwanda. *Acta Tropica*, *164*, pp. 329–336.

Katsoulis, O., Georgiadou, A., & Cunnington, A. J. (2021). Immunopathology of Acute Kidney Injury in Severe Malaria. *Frontiers in Immunology*, *12*, p. 1391.

Kaushansky, A., & Kappe, S. H. I. (2015). Selection and refinement: 0The malaria parasite's infection and exploitation of host hepatocytes. *Current Opinion in Microbiology*, *26*, pp. 71–78.

Killeen, G. F., Tatarsky, A., Diabate, A., Chaccour, C. J., Marshall, J. M., Okumu, F. O., et al. (2017). Developing an expanded vector control toolbox for malaria elimination. *BMJ Global Health*, *2*(2), p. 211.

Krungkrai, J., & Krungkrai, S. R. (2016). Antimalarial qinghaosu/artemisinin: The therapy worthy of a Nobel Prize. *Asian Pacific Journal of Tropical Biomedicine*, *6*(5), pp. 371–375. Retrieved from http://dx.doi.org/10.1016/j.apjtb.2016.03.010

Kudyba, H. M., Cobb, D. W., Florentin, A., Krakowiak, M., & Muralidharan, V. (2018). CRISPR/Cas9 Gene Editing to Make Conditional Mutants of Human Malaria Parasite P. falciparum. *Journal of Visualized Experiments : JoVE*, *2018*(139), p. 57747. Retrieved June 13, 2022, from /pmc/articles/PMC6235188/

Kumar, S., Bhardwaj, T. R., Prasad, D. N., & Singh, R. K. (2018). Drug targets for resistant malaria: Historic to future perspectives. *Biomedicine & Pharmacotherapy*, *104*, pp. 8–27.

Lalève, A., Vallières, C., Golinelli-Cohen, M. P., Bouton, C., Song, Z., Pawlik, G., et al. (2016). The antimalarial drug primaquine targets Fe-S cluster proteins and yeast respiratory growth. *Redox Biology*, *7*, pp. 21–29.

Leba, L. J., Musset, L., Pelleau, S., Estevez, Y., Birer, C., Briolant, S., et al. (2015). Use of Plasmodium falciparum culture-adapted field isolates for in vitro exflagellation-blocking assay. *Malaria Journal*, *14*(1), pp. 1–4. Retrieved June 4, 2022, from

https://malariajournal.biomedcentral.com/articles/10.1186/s12936-015-0752-x

Lee, M. C. S., Lindner, S. E., Lopez-Rubio, J. J., & Llinás, M. (2019). Cutting back malaria: CRISPR/Cas9 genome editing of Plasmodium. *Briefings in Functional Genomics*, *18*(5), pp. 281–289.

Lehane, A. M., Van Schalkwyk, D. A., Valderramos, S. G., Fidock, D. A., & Kirk, K. (2011). Differential drug efflux or accumulation does not explain variation in the chloroquine response of Plasmodium falciparum strains expressing the same isoform of mutant PfCRT. *Antimicrobial Agents and Chemotherapy*, *55*(5), pp. 2310–2318.

Leroy, D., Macintyre, F., Adoke, Y., Ouoba, S., Barry, A., Mombo-Ngoma, G., et al. (2019). African isolates show a high proportion of multiple copies of the Plasmodium falciparum plasmepsin - 2 gene , a piperaquine resistance marker. *Malaria Journal 2019 18:1*, *18*(1), pp. 1–11. Retrieved December 29, 2020, from https://malariajournal.biomedcentral.com/articles/10.1186/s12936-019-2756-4

Linares, M., Viera, S., Crespo, B., Franco, V., Gómez-Lorenzo, M. G., Jiménez-Díaz, M. B., et al. (2015). Identifying rapidly parasiticidal anti-malarial drugs using a simple and reliable in vitro parasite viability fast assay. *Malaria journal*, *14*, p. 441.

Lindsay, S. W., Thomas, M. B., & Kleinschmidt, I. (2021). Threats to the effectiveness of insecticide-treated bednets for malaria control: thinking beyond insecticide resistance. *The Lancet Global Health*, *9*(9), pp. e1325–e1331. Retrieved June 15, 2022, from http://www.thelancet.com/article/S2214109X21002163/fulltext

Liu, Z., Miao, J., & Cui, L. (2011). Gametocytogenesis in malaria parasite: Commitment, development and regulation. *Future Microbiology*, *6*(11), pp. 1351–1369.

Lopera-Mesa, T. M., Doumbia, S., Chiang, S., Zeituni, A. E., Konate, D. S., Doumbouya, M., et al. (2013). Plasmodium falciparum clearance rates in response to artesunate in Malian

children with malaria: Effect of acquired immunity. *Journal of Infectious Diseases*, *207*(11), pp. 1655–1663. Retrieved September 28, 2020, from http://www.wwarn.org/research/parasite-clearance-estimator

Lu, F., Culleton, R., Zhang, M., Ramaprasad, A., von Seidlein, L., Zhou, H., et al. (2017). Emergence of Indigenous Artemisinin-Resistant Plasmodium falciparum in Africa . *New England Journal of Medicine*, *376*(10), pp. 991–993.

De Lucia, S., Tsamesidis, I., Pau, M. C., Kesely, K. R., Pantaleo, A., & Turrini, F. (2018). Induction of high tolerance to artemisinin by sub-lethal administration: A new in vitro model of P. falciparum. *PloS one*, *13*(1), pp. e0191084–e0191084. Retrieved from https://pubmed.ncbi.nlm.nih.gov/29342187

Lukens, A. K., Ross, L. S., Heidebrecht, R., Gamo, F. J., Lafuente-Monasterio, M. J., Booker, M. L., et al. (2014). Harnessing evolutionary fitness in Plasmodium falciparum for drug discovery and suppressing resistance. *Proceedings of the National Academy of Sciences of the United States of America*, *111*(2), pp. 799–804. Retrieved June 13, 2022, from www.pnas.org/cgi/doi/10.1073/pnas.1320886110

Maiga, H., Grivoyannis, A., Sagara, I., Traore, K., Traore, O. B., Tolo, Y., et al. (2021). Selection of pfcrt k76 and pfmdr1 n86 coding alleles after uncomplicated malaria treatment by artemether-lumefantrine in mali. *International Journal of Molecular Sciences*, *22*(11). Retrieved June 15, 2022, from /pmc/articles/PMC8200001/

Maio, N., & Rouault, T. A. (2016). Mammalian Fe-S proteins: definition of a consensus motif recognized by the co-chaperone HSC20. *Metallomics : integrated biometal science*, *8*(10), p. 1032. Retrieved June 13, 2022, from /pmc/articles/PMC5240853/

Malmberg, M., Ferreira, P. E., Tarning, J., Ursing, J., Ngasala, B., Björkman, A., et al. (2013). Plasmodium falciparum drug resistance phenotype as assessed by patient

antimalarial drug levels and its association with pfmdr1 polymorphisms. *The Journal of infectious diseases*, *207*(5), pp. 842–847.

Malmberg, M., Ngasala, B., Ferreira, P. E., Larsson, E., Jovel, I., Hjalmarsson, A., et al. (2013). Temporal trends of molecular markers associated with artemether- lumefantrine tolerance/resistance in Bagamoyo district, Tanzania. *Malaria Journal*, *12*(1), pp. 1–7.

Maniga, J. N., Akinola, S. A., Odoki, M., Odda, J., & Adebayo, I. A. (2021). Limited Polymorphism in Plasmodium falciparum Artemisinin Resistance Kelch13-Propeller Gene Among Clinical Isolates from Bushenyi District, Uganda. *Infection and Drug Resistance*, *14*, p. 5153. Retrieved June 15, 2022, from /pmc/articles/PMC8665267/

Mata-Cantero, L., Lafuente, M. J., Sanz, L., & Rodriguez, M. S. (2014). Magnetic isolation of Plasmodium falciparum schizonts iRBCs to generate a high parasitaemia and synchronized in vitro culture. *Malaria Journal*, *13*, pp. 1–9. Retrieved June 13, 2022, from http://www.malariajournal.com/content/13/1/112

Mbaye, A., Dieye, B., Ndiaye, Y. D., Bei, A. K., Muna, A., Deme, A. B., et al. (2016). Selection of N86F184D1246 haplotype of Pfmrd1 gene by artemether-lumefantrine drug pressure on Plasmodium falciparum populations in Senegal. *Malaria journal*, *15*(1), p. 433.

Mbugi, E. V., Mutayoba, B. M., Malisa, A. L., Balthazary, S. T., Nyambo, T. B., & Mshinda, H. (2006). Drug resistance to sulphadoxine-pyrimethamine in Plasmodium falciparum malaria in Mlimba, Tanzania. *Malaria Journal*, *5*(1), p. 94.

Mbye, H., Bojang, F., Jawara, A. S., Njie, B., Mohammed, N. I., Okebe, J., et al. (2020). Tolerance of Gambian Plasmodium falciparum to Dihydroartemisinin and Lumefantrine detected by Ex vivo Parasite Survival Rate Assay (PSRA) . *Antimicrobial Agents and Chemotherapy*, (October).

Menard, D., & Ariey, F. (2015). Towards real-time monitoring of artemisinin resistance. *The Lancet Infectious Diseases*, *15*(4), pp. 367–368. Retrieved October 1, 2020, from http://dx.doi.org/10.1016/

Menard, D., & Dondorp, A. (2017). Antimalarial Drug Resistance: A Threat to Malaria Elimination. *Cold Spring Harbor Perspectives in Medicine*, *7*(7), pp. 1–24. Retrieved June 15, 2022, from /pmc/articles/PMC5495053/

Ménard, D., Khim, N., Beghain, J., Adegnika, A. A., Shafiul-Alam, M., Amodu, O., et al. (2016). A Worldwide Map of Plasmodium falciparum K13-Propeller Polymorphisms. *The New England journal of medicine*, *374*(25), pp. 2453–2464.

Miotto, O., Almagro-garcia, J., Manske, M., Macinnis, B., Campino, S., Rockett, K. A., et al. (2013). Multiple populations of artemisinin-resistant Plasmodium falciparum in Cambodia. *Nature Publishing Group*, *45*(6), pp. 648–655. Retrieved from http://dx.doi.org/10.1038/ng.2624

Miotto, O., Amato, R., Ashley, E. A., Macinnis, B., Almagro-Garcia, J., Amaratunga, C., et al. (2015). Genetic architecture of artemisinin-resistant Plasmodium falciparum. *Nature Genetics*, *47*(3), pp. 226–234.

Mishra, M., Mishra, V. K., Kashaw, V., Iyer, A. K., & Kashaw, S. K. (2017). Comprehensive review on various strategies for antimalarial drug discovery. *European Journal of Medicinal Chemistry*, *125*, pp. 1300–1320.

Müller, O., Lu, G. Y., & Von Seidlein, L. (2019). Geographic expansion of artemisinin resistance. *Journal of Travel Medicine*, *26*(4). Retrieved September 28, 2020, from https://pubmed.ncbi.nlm.nih.gov/30995310/

Muralidharan, V., Oksman, A., Iwamoto, M., Wandless, T. J., & Goldberg, D. E. (2011). Asparagine repeat function in a Plasmodium falciparum protein assessed via a

regulatable fluorescent affinity tag. *Proceedings of the National Academy of Sciences of the United States of America*, *108*(11), pp. 4411–4416. Retrieved December 29, 2020, from www.pnas.org/cgi/doi/10.1073/pnas.1018449108

Murray, L., Stewart, L. B., Tarr, S. J., Ahouidi, A. D., Diakite, M., Amambua-Ngwa, A., et al. (2017). Multiplication rate variation in the human malaria parasite Plasmodium falciparum. *Scientific reports*, *7*(1), p. 6436.

Mwai, L., Diriye, A., Masseno, V., Muriithi, S., Feltwell, T., Musyoki, J., et al. (2012). Genome wide adaptations of Plasmodium falciparum in response to Lumefantrine selective drug pressure. *PLoS ONE*, *7*(2).

Mwendera, C., Jager, C. de, Longwe, H., Phiri, K., Hongoro, C., & Mutero, C. M. (2016). Malaria research and its influence on anti-malarial drug policy in Malawi: a case study. *Health Research Policy and Systems 2016 14:1*, *14*(1), pp. 1–14. Retrieved December 2, 2020, from https://link.springer.com/articles/10.1186/s12961-016-0108-1

Mwesigwa, J., Achan, J., Affara, M., Wathuo, M., Worwui, A., Mohammed, N. I., et al. (2019). Mass Drug Administration With Dihydroartemisinin-piperaquine and Malaria Transmission Dynamics in The Gambia: A Prospective Cohort Study. *Clinical Infectious Diseases*, *69*(2), pp. 278–286. Retrieved June 13, 2022, from https://academic.oup.com/cid/article/69/2/278/5125954

Naing, C., Whittaker, M. A., Nyunt Wai, V., & Mak, J. W. (2014). Is Plasmodium vivax Malaria a Severe Malaria?: A Systematic Review and Meta-Analysis. *PLoS Neglected Tropical Diseases*, *8*(8). Retrieved October 27, 2020, from /pmc/articles/PMC4133404/?report=abstract

Nájera, J. A., González-Silva, M., & Alonso, P. L. (2011). Some Lessons for the Future from the Global Malaria Eradication Programme (1955–1969). *PLoS Medicine*, *8*(1).

Retrieved June 13, 2022, from /pmc/articles/PMC3026700/

Ndiaye, D., Dieye, B., Ndiaye, Y. D., Tyne, D. Van, Daniels, R., Bei, A. K., et al. (2013). Polymorphism in dhfr/dhps genes, parasite density and ex vivo response to pyrimethamine in plasmodium falciparum malaria parasites in thies, senegal. *International Journal for Parasitology: Drugs and Drug Resistance*, *3*, pp. 135–142.

Ndiaye, Y. D., Hartl, D. L., McGregor, D., Badiane, A., Fall, F. B., Daniels, R. F., et al. (2021). Genetic surveillance for monitoring the impact of drug use on Plasmodium falciparum populations. *International Journal for Parasitology: Drugs and Drug Resistance*, *17*, pp. 12–22.

Ng, C. L., & Fidock, D. A. (2019). Plasmodium falciparum in vitro drug resistance selections and gene editing, in: *Methods in Molecular Biology*, pp. 123–140. Humana Press Inc. Retrieved November 12, 2020, from /pmc/articles/PMC6756925/?report=abstract

Ngotho, P., Soares, A. B., Hentzschel, F., Achcar, F., Bertuccini, L., & Marti, M. (2019). Revisiting gametocyte biology in malaria parasites. *FEMS Microbiology Reviews*, *43*(4), p. 401. Retrieved June 13, 2022, from /pmc/articles/PMC6606849/

Nguetse, C. N., & Egan, E. S. (2019). Host Genetic Predisposition to Malaria, in: *Encyclopedia of Malaria*, pp. 1–25. Springer New York. Retrieved December 28, 2020, from https://link.springer.com/referenceworkentry/10.1007/978-1-4614-8757-9_139-1

Nilsson, S. K., Childs, L. M., Buckee, C., & Marti, M. (2015). Targeting Human Transmission Biology for Malaria Elimination. *PLoS Pathogens*, *11*(6).

Nixon, C. P. (2016). Plasmodium falciparum gametocyte transit through the cutaneous microvasculature: A new target for malaria transmission blocking vaccines? *Human Vaccines & Immunotherapeutics*, *12*(12), p. 3189. Retrieved June 15, 2022, from /pmc/articles/PMC5215481/

Noedl, H., Wongsrichanalai, C., & Wernsdorfer, W. H. (2003). Malaria drug-sensitivity testing: new assays, new perspectives. *Trends in Parasitology*, *19*(4), pp. 175–181.

Nsanzabana, C. (2019). Resistance to artemisinin combination therapies (ACTs): Do not forget the partner Drug! *Tropical Medicine and Infectious Disease*, *4*(1).

Nsanzabana, C., Ariey, F., Beck, H. P., Ding, X. C., Kamau, E., Krishna, S., et al. (2018). Molecular assays for antimalarial drug resistance surveillance: A target product profile. *PLoS ONE*, *13*(9), pp. 1–18.

Nsanzabana, C., Djalle, D., Guérin, P. J., Ménard, D., & González, I. J. (2018). Tools for surveillance of anti-malarial drug resistance: an assessment of the current landscape. *Malaria Journal 2018 17:1*, *17*(1), pp. 1–16. Retrieved June 22, 2022, from https://malariajournal.biomedcentral.com/articles/10.1186/s12936-018-2185-9

Nzila, A. (2006). The past, present and future of antifolates in the treatment of Plasmodium falciparum infection. *Journal of Antimicrobial Chemotherapy*, *57*(6), pp. 1043–1054. Retrieved September 15, 2020, from https://academic.oup.com/jac/article/57/6/1043/731405

O'Flaherty, K., Maguire, J., Simpson, J. A., & Fowkes, F. J. I. (2017). Immunity as a predictor of anti-malarial treatment failure: A systematic review. *Malaria Journal*, *16*(1), p. 158.

Ocan, M., Akena, D., Nsobya, S., Kamya, M. R., Senono, R., Kinengyere, A. A., et al. (2019). Persistence of chloroquine resistance alleles in malaria endemic countries: a systematic review of burden and risk factors. *Malaria journal*, *18*(1), p. 76.

Ojuka, P., Boum, Y., Denoeud-Ndam, L., Nabasumba, C., Muller, Y., Okia, M., et al. (2015). Early biting and insecticide resistance in the malaria vector Anopheles might compromise the effectiveness of vector control intervention in Southwestern Uganda.

Malaria Journal, *14*(1), pp. 1–8.

Okell, L. C., Reiter, L. M., Ebbe, L. S., Baraka, V., Bisanzio, D., Watson, O. J., et al. (2018). Emerging implications of policies on malaria treatment: Genetic changes in the Pfmdr-1 gene affecting susceptibility to artemether–lumefantrine and artesunate–amodiaquine in Africa. *BMJ Global Health*, *3*(5), pp. 1–12.

Osier, F. H., Mackinnon, M. J., Crosnier, C., Fegan, G., Kamuyu, G., Wanaguru, M., et al. (2014). Malaria: New antigens for a multicomponent blood-stage malaria vaccine. *Science Translational Medicine*, *6*(247).

Packard, R. M. (2014). The Origins of Antimalarial-Drug Resistance. *New England Journal of Medicine*, *371*(5), pp. 397–399. Retrieved October 22, 2020, from http://www.nejm.org/doi/10.1056/NEJMp1403340

Paquet, T., Le Manach, C., Cabrera, D. G., Younis, Y., Henrich, P. P., Abraham, T. S., et al. (2017). Antimalarial efficacy of MMV390048, an inhibitor of Plasmodium phosphatidylinositol 4-kinase. *Science Translational Medicine*, *9*(387).

Parida, P., Sarma, K., Borkakoty, B., & Mohapatra, P. K. (2016). Structure and Functional Differentiation of PfCRT Mutation in Chloroquine Resistance (CQR) in Plasmodium falciparum Malaria. *Current Topics in Malaria*. Retrieved June 15, 2022, from undefined/state.item.id

Patel, P., Bharti, P. K., Bansal, D., Ali, N. A., Raman, R. K., Mohapatra, P. K., et al. (2017). Prevalence of mutations linked to antimalarial resistance in Plasmodium falciparum from Chhattisgarh, Central India: A malaria elimination point of view. *Scientific Reports*, *7*(1), pp. 1–8.

Patra, A. T., Hingmire, T. B., Belekar, M., Xiong, A., Subramanian, G., Bozdech, Z., et al. (2019). Whole Cell Phenotypic Screening Of MMV Pathogen Box identifies Specific

Inhibitors of Plasmodium falciparum merozoite maturation and egress. *bioRxiv*.

Pérez-Moreno, G., Cantizani, J., Sánchez-Carrasco, P., Ruiz-Pérez, L. M., Martín, J., El Aouad, N., et al. (2016). Discovery of New Compounds Active against Plasmodium falciparum by High Throughput Screening of Microbial Natural Products. *PLoS ONE*, *11*(1). Retrieved June 13, 2022, from /pmc/articles/PMC4703298/

Perrin, A. J., Bisson, C., Faull, P. A., Renshaw, M. J., Lees, R. A., Fleck, R. A., et al. (2021). Malaria parasite schizont egress antigen-1 plays an essential role in nuclear segregation during schizogony. *mBio*, *12*(2), pp. 1–16. Retrieved June 13, 2022, from https://journals.asm.org/doi/full/10.1128/mBio.03377-20

Phillips, M. A., Burrows, J. N., Manyando, C., Van Huijsduijnen, R. H., Van Voorhis, W. C., & Wells, T. N. C. (2017). Malaria. *Nature Reviews Disease Primers*, *3*(1), p. 17050.

Pinichpongse, S., Doberstyn, E. B., Cullen, J. R., Yisunsri, L., Thongsombun, Y., & Thimasarn, K. (1982). An evaluation of five regimens for the outpatient therapy of falciparum malaria in Thailand 1980-81. *Bulletin of the World Health Organization*, *60*(6), pp. 907–912. Retrieved September 28, 2020, from https://www.ncbi.nlm.nih.gov/pmc/articles/pmid/6761005/?tool=EBI

Plucinski, M. M., Talundzic, E., Morton, L., Dimbu, P. R., Macaia, A. P., Fortes, F., et al. (2015). Efficacy of artemether-lumefantrine and dihydroartemisinin-piperaquine for treatment of uncomplicated malaria in children in Zaire and Uíge provinces, Angola. *Antimicrobial Agents and Chemotherapy*, *59*(1), pp. 437–443. Retrieved October 27, 2020, from /pmc/articles/PMC4291383/?report=abstract

Portugaliza, H. P., Miyazaki, S., Geurten, F. J. A., Pell, C., Rosanas-Urgell, A., Janse, C. J., et al. (2020). Artemisinin exposure at the ring or trophozoite stage impacts Plasmodium falciparum sexual conversion differently. *eLife*, *9*, pp. 1–22.

Raman, J., Kagoro, F. M., Mabuza, A., Malatje, G., Reid, A., Frean, J., et al. (2019). Absence of kelch13 artemisinin resistance markers but strong selection for lumefantrine-tolerance molecular markers following 18 years of artemisinin-based combination therapy use in Mpumalanga Province, South Africa (2001-2018). *Malaria Journal*, *18*(1), pp. 1–12. Retrieved from https://doi.org/10.1186/s12936-019-2911-y

Raphemot, R., Posfai, D., & Derbyshire, E. R. (2016). Current therapies and future possibilities for drug development against liver-stage malaria. *Journal of Clinical Investigation*, *126*(6), pp. 2013–2020.

Ray, S., Das, S., & Suar, M. (2017). Molecular mechanism of drug resistance. *Drug Resistance in Bacteria, Fungi, Malaria, and Cancer*, pp. 47–110. Retrieved June 15, 2022, from https://link.springer.com/chapter/10.1007/978-3-319-48683-3_3

Reader, J., Botha, M., Theron, A., Lauterbach, S. B., Rossouw, C., Engelbrecht, D., et al. (2015). Nowhere to hide: Interrogating different metabolic parameters of Plasmodium falciparum gametocytes in a transmission blocking drug discovery pipeline towards malaria elimination. *Malaria Journal*, *14*(1), p. 213. Retrieved December 4, 2020, from http://www.malariajournal.com/content/14/1/213

Reiling, S. J., & Rohrbach, P. (2015). Monitoring PfMDR1 transport in Plasmodium falciparum. *Malaria Journal*, *14*(1), p. 270. Retrieved June 15, 2022, from /pmc/articles/PMC4501111/

Ribeiro, J. M., Garriga, M., Potchen, N., Crater, A. K., Gupta, A., Ito, D., et al. (2018). Guide RNA selection for CRISPR-Cas9 transfections in Plasmodium falciparum. *International Journal for Parasitology*, *48*(11), pp. 825–832. Retrieved from https://doi.org/10.1016/j.ijpara.2018.03.009

Rishi, G., & Subramaniam, V. N. (2017). The relationship between systemic iron

homeostasis and erythropoiesis. *Bioscience Reports*, *37*(6), p. 20170195. Retrieved June 13, 2022, from /pmc/articles/PMC5705776/

Rodriguez-Barraquer, I., Arinaitwe, E., Jagannathan, P., Boyle, M. J., Tappero, J., Muhindo, M., et al. (2016). Quantifying Heterogeneous Malaria Exposure and Clinical Protection in a Cohort of Ugandan Children, in: *Journal of Infectious Diseases*, pp. 1072–1080. Oxford University Press.

Roepe, P. D. (2014). To kill or not to kill, that is the question: Cytocidal antimalarial drug resistance. *Trends in Parasitology*, *30*(3), pp. 130–135.

Ross, L. S., & Fidock, D. A. (2019). Elucidating Mechanisms of Drug-Resistant Plasmodium falciparum. *Cell Host & Microbe*, *26*(1), pp. 35–47.

Roy, K. R., Smith, J. D., Vonesch, S. C., Lin, G., Szu Tu, C., Lederer, A. R., et al. (2018). Multiplexed precision genome editing with trackable genomic barcodes in yeast HHS Public Access Author manuscript. *Nat Biotechnol*, *36*(6), pp. 512–520.

RTS S Clinical Trials Partnership. (2015). Efficacy and safety of RTS,S/AS01 malaria vaccine with or without a booster dose in infants and children in Africa: Final results of a phase 3, individually randomised, controlled trial. *The Lancet*, *386*(9988), pp. 31–45.

Sáenz, F. E., Mutka, T., Udenze, K., Oduola, A. M. J., & Kyle, D. E. (2012). Novel 4-aminoquinoline analogs highly active against the blood and sexual stages of Plasmodium in vivo and in vitro. *Antimicrobial agents and chemotherapy*, *56*(9), pp. 4685–4692. Retrieved June 13, 2022, from https://pubmed.ncbi.nlm.nih.gov/22710117/

Sanz, L. M., Crespo, B., De-Cózar, C., Ding, X. C., Llergo, J. L., Burrows, J. N., et al. (2012). P. falciparum in vitro killing rates allow to discriminate between different antimalarial mode-of-action. *PloS one*, *7*(2), pp. e30949–e30949.

Saunders, D. L., Vanachayangkul, P., & Lon, C. (2014). Dihydroartemisinin–Piperaquine

Failure in Cambodia. *New England Journal of Medicine*, *371*(5), pp. 484–485. Retrieved January 3, 2021, from https://www.nejm.org/doi/full/10.1056/NEJMc1403007

Schrum, J. E., Crabtree, J. N., Dobbs, K. R., Kiritsy, M. C., Reed, G. W., Gazzinelli, R. T., et al. (2018). Plasmodium falciparum induces trained innate immunity. *Journal of immunology (Baltimore, Md. : 1950)*, *200*(4), p. 1243. Retrieved June 15, 2022, from /pmc/articles/PMC5927587/

Von Seidlein, L., Olaosebikan, R., Hendriksen, I. C. E., Lee, S. J., Adedoyin, O. T., Agbenyega, T., et al. (2012). Predicting the clinical outcome of severe falciparum malaria in African children: Findings from a large randomized trial. *Clinical Infectious Diseases*, *54*(8), pp. 1080–1090.

Siddiqui, F. A., Liang, X., & Cui, L. (2021). Plasmodium falciparum resistance to ACTs: Emergence, mechanisms, and outlook. *International Journal for Parasitology: Drugs and Drug Resistance*, *16*, p. 102. Retrieved June 15, 2022, from /pmc/articles/PMC8188179/

Simon, C. S., Stürmer, V. S., & Guizetti, J. (2021). How Many Is Enough? - Challenges of Multinucleated Cell Division in Malaria Parasites. *Frontiers in Cellular and Infection Microbiology*, *11*. Retrieved June 13, 2022, from /pmc/articles/PMC8137892/

Sinha, S., Sarma, P., Sehgal, R., & Medhi, B. (2017). Development in Assay Methods for in Vitro Antimalarial Drug Efficacy Testing: A Systematic Review. *Frontiers in pharmacology*, *8*, p. 754.

Sologub, L., Kuehn, A., Kern, S., Przyborski, J., Schillig, R., & Pradel, G. (2011). Malaria proteases mediate inside-out egress of gametocytes from red blood cells following parasite transmission to the mosquito. *Cellular Microbiology*, *13*(6), pp. 897–912.

Sougoufara, S., Ottih, E. C., & Tripet, F. (2020). The need for new vector control approaches

targeting outdoor biting anopheline malaria vector communities. *Parasites & Vectors 2020 13:1*, *13*(1), pp. 1–15. Retrieved June 13, 2022, from https://parasitesandvectors.biomedcentral.com/articles/10.1186/s13071-020-04170-7

Straimer, J., Lee, M. C. S., Lee, A. H., Zeitler, B., Williams, A. E., Pearl, J. R., et al. (2012). Site-Specific Editing of the Plasmodium falciparum Genome Using Engineered Zinc-Finger Nucleases. , *9*(10), pp. 993–998.

Sutherland, C. J., Lansdell, P., Sanders, M., Muwanguzi, J., Van Schalkwyk, D. A., Kaur, H., et al. (2017). pfk13-independent treatment failure in four imported cases of Plasmodium falciparum malaria treated with artemether-lumefantrine in the United Kingdom. *Antimicrobial Agents and Chemotherapy*, *61*(3).

Takala-Harrison, S., Jacob, C. G., Arze, C., Cummings, M. P., Silva, J. C., Dondorp, A. M., et al. (2015). Independent emergence of artemisinin resistance mutations among Plasmodium falciparum in Southeast Asia. *Journal of Infectious Diseases*, *211*(5), pp. 670–679. Retrieved September 28, 2020, from https://pubmed.ncbi.nlm.nih.gov/25180241/

Taylor, S. M., Parobek, C. M., DeConti, D. K., Kayentao, K., Coulibaly, S. O., Greenwood, B. M., et al. (2015). Absence of putative artemisinin resistance mutations among Plasmodium falciparum in Sub-Saharan Africa: a molecular epidemiologic study. *The Journal of infectious diseases*, *211*(5), pp. 680–688.

The Ivermectin Roadmappers. (2020). A roadmap for the development of ivermectin as a complementary malaria vector control tool. *American Journal of Tropical Medicine and Hygiene*, *102*(2 Suppl), pp. 3–24. Retrieved December 28, 2020, from /pmc/articles/PMC7008306/?report=abstract

Theron, M., Hesketh, R. L., Subramanian, S., & Rayner, J. C. (2010). An adaptable two-color

flow cytometric assay to quantitate the invasion of erythrocytes by Plasmodium falciparum parasites. *Cytometry. Part A : the journal of the International Society for Analytical Cytology*, *77*(11), pp. 1067–1074.

Thu, A. M., Phyo, A. P., Landier, J., Parker, D. M., & Nosten, F. H. (2017). Combating multidrug-resistant Plasmodium falciparum malaria. *FEBS Journal*, *284*(16), pp. 2569–2578. Retrieved October 26, 2020, from /pmc/articles/PMC5575457/?report=abstract

Tilley, L., Straimer, J., Gnädig, N. F., Ralph, S. A., & Fidock, D. A. (2016). Artemisinin Action and Resistance in Plasmodium falciparum. *Trends in parasitology*, *32*(9), pp. 682–696.

Trager, W., & Jensen, J. B. (1976). Human malaria parasites in continuous culture. *Science*, *193*(4254), pp. 673–675.

Tse, E. G., Korsik, M., & Todd, M. H. (2019). The past, present and future of anti-malarial medicines. *Malaria Journal 2019 18:1*, *18*(1), pp. 1–21. Retrieved June 13, 2022, from https://malariajournal.biomedcentral.com/articles/10.1186/s12936-019-2724-z

Tun, K. M., Jeeyapant, A., Myint, A. H., Kyaw, Z. T., Dhorda, M., Mukaka, M., et al. (2018). Effectiveness and safety of 3 and 5 day courses of artemether-lumefantrine for the treatment of uncomplicated falciparum malaria in an area of emerging artemisinin resistance in Myanmar. *Malaria journal*, *17*(1). Retrieved June 15, 2022, from https://pubmed.ncbi.nlm.nih.gov/29996844/

Turowski, V. R., Busi, M. V., & Gomez-Casati, D. F. (2012). Structural and functional studies of the mitochondrial cysteine desulfurase from arabidopsis thaliana. *Molecular Plant*, *5*(5), pp. 1001–1010.

van Tyne, D., Park, D. J., Schaffner, S. F., Neafsey, D. E., Angelino, E., Cortese, J. F., et al. (2011). Identification and functional validation of the novel antimalarial resistance locus

PF10_0355 in plasmodium falciparum. *PLoS Genetics*, *7*(4).

Uwimana, A., Legrand, E., Stokes, B. H., Ndikumana, J. L. M., Warsame, M., Umulisa, N., et al. (2020). Emergence and clonal expansion of in vitro artemisinin-resistant Plasmodium falciparum kelch13 R561H mutant parasites in Rwanda. *Nature Medicine*.

Vaughan, A. M., & Kappe, S. H. I. (2017). Malaria parasite liver infection and exoerythrocytic biology. *Cold Spring Harbor Perspectives in Medicine*, *7*(6).

Vaughan, A. M., Mikolajczak, S. A., Wilson, E. M., Grompe, M., Kaushansky, A., Camargo, N., et al. (2012). Complete Plasmodium falciparum liver stage development in liver-chimeric mice. *Journal of Clinical Investigation*, *122*(10), pp. 3618–3628.

Veiga, M. I., Dhingra, S. K., Henrich, P. P., Straimer, J., Gnädig, N., Uhlemann, A. C., et al. (2016). Globally prevalent PfMDR1 mutations modulate Plasmodium falciparum susceptibility to artemisinin-based combination therapies. *Nature Communications*, *7*. Retrieved October 1, 2020, from https://pubmed.ncbi.nlm.nih.gov/27189525/

Venkatesan, M., Gadalla, N. B., Stepniewska, K., Dahal, P., Nsanzabana, C., Moriera, C., et al. (2014). Polymorphisms in Plasmodium falciparum chloroquine resistance transporter and multidrug resistance 1 genes: parasite risk factors that affect treatment outcomes for P. falciparum malaria after artemether-lumefantrine and artesunate-amodiaquine. *The American journal of tropical medicine and hygiene*, *91*(4), pp. 833–843. Retrieved October 27, 2020, from /pmc/articles/PMC4183414/?report=abstract

Venugopal, K., Hentzschel, F., Valkiūnas, G., & Marti, M. (2020). Plasmodium asexual growth and sexual development in the haematopoietic niche of the host. *Nature Reviews Microbiology 2020 18:3*, *18*(3), pp. 177–189. Retrieved June 13, 2022, from https://www.nature.com/articles/s41579-019-0306-2

Verhoef, H., Veenemans, J., Mwangi, M. N., & Prentice, A. M. (2017). Safety and benefits of

interventions to increase folate status in malaria-endemic areas. *British Journal of Haematology*, *177*(6), p. 905. Retrieved June 13, 2022, from /pmc/articles/PMC5485039/

Weiss, D. J., Lucas, T. C. D., Nguyen, M., Nandi, A. K., Bisanzio, D., Battle, K. E., et al. (2019). Mapping the global prevalence, incidence, and mortality of Plasmodium falciparum, 2000–17: a spatial and temporal modelling study. *The Lancet*, *394*(10195), pp. 322–331. Retrieved November 11, 2020, from http://dx.doi.org/10.1016/

Wells, T. N. C., Van Huijsduijnen, R. H., & Van Voorhis, W. C. (2015). Malaria medicines: A glass half full? *Nature Reviews Drug Discovery*, *14*(6), pp. 424–442.

White, N. J. (2017). Malaria parasite clearance. *Malaria journal*, *16*(1), p. 88.

White, N. J., Hien, T. T., & Nosten, F. H. (2015). A Brief History of Qinghaosu. *Trends in Parasitology*, *31*(12), pp. 607–610.

White, N. J., Pukrittayakamee, S., Hien, T. T., Faiz, M. A., Mokuolu, O. A., & Dondorp, A. M. (2014). Malaria. *The Lancet*, *383*(9918), pp. 723–735.

WHO. (2009). *Methods for surveillance of antimalarial drug efficacy*. World Health Organization. Retrieved March 29, 2020, from https://www.who.int/docs/default-source/documents/publications/gmp/methods-for-surveillance-of-antimalarial-drug-efficacy.pdf?sfvrsn=29076702_2

WHO. (2012a). *Management of severe malaria – A practical handbook*. Geneva: World Health Organization. Retrieved December 11, 2020, from https://www.who.int/publications/i/item/9789241548526

WHO. (2012b). *Global plan for Insecticide Resistance Management in Malaria Vectors*. Geneva: World Health Organization. Retrieved March 16, 2020, from https://apps.who.int/iris/handle/10665/44846

WHO. (2013). *Seasonal malaria chemoprevention with sulfadoxine-pyrimethamine plus amodiaquine in children: A field guide*. Geneva: WHO. Retrieved October 28, 2020, from http://www.who.int/malaria/publications/atoz/9789241504737/en/

WHO. (2014a). *WHO policy brief for the Implementation of Intermittent Preventive Treatment of Malaria in Pregnancy Using Sulfadoxine-Pyrimethamine (IPTp-SP)*. Retrieved from http://www.who.int/malaria/publications/atoz/iptp-sp-updated-policy-brief-24jan2014.pdf?ua=1

WHO. (2014b). *Emergence and spread of artemisinin resistance calls for intensified efforts to withdraw oral artemisinin-based monotherapy from the market (archived)*. World Health Organization. Retrieved October 28, 2020, from http://www.who.int/malaria/publications/atoz/policy-brief-withdrawal-of-oral-artemisinin-based-monotherapies/en/

WHO. (2014c). *World Malaria Report 2014*. Geneva. Retrieved from https://www.who.int/publications/i/item/9789241564830

WHO. (2015a). *Global technical strategy for malaria 2016-2030*. Geneva. Retrieved from https://www.who.int/docs/default-source/documents/global-technical-strategy-for-malaria-2016-2030.pdf

WHO. (2015b). *Guidelines for the treatment of malaria*. Geneva. Retrieved from https://apps.who.int/iris/handle/10665/162441

WHO. (2016). *Eliminating Malaria*. Geneva. Retrieved from https://apps.who.int/iris/bitstream/handle/10665/205565/WHO_HTM_GMP_2016.3_eng.pdf

WHO. (2017). *World malaria report 2017*. Geneva. Retrieved from https://www.who.int/publications/i/item/9789241565523

WHO. (2018). *Artemisinin and artemisinin-based combination therapy resistance: status report*. Geneva. Retrieved from https://apps.who.int/iris/handle/10665/274362

WHO. (2019). *World malaria report 2019*. Geneva. Retrieved from https://www.who.int/publications/i/item/9789241565721

WHO. (2020a). *World Malaria Report: 20 years of global progress and challenges*. Geneva.

WHO. (2020b). *Report on antimalarial drug efficacy, resistance and response: 10 years of surveillance (2010-2019)*. Geneva. Retrieved from https://www.who.int/publications/i/item/9789240012813

Wicht, K. J., Mok, S., & Fidock, D. A. (2020). Molecular Mechanisms of Drug Resistance in Plasmodium falciparum Malaria. *Annual review of microbiology*, *74*, p. 431. Retrieved June 13, 2022, from /pmc/articles/PMC8130186/

Witkowski, B., Amaratunga, C., Khim, N., Sreng, S., Chim, P., Kim, S., et al. (2013). Novel phenotypic assays for the detection of artemisinin- resistant Plasmodium falciparum malaria in Cambodia: in-vitro and ex-vivo drug-response studies. *Lancet Indect Dis.*, *13*(12), pp. 1043–1049.

Witkowski, B., Khim, N., Chim, P., Kim, S., Ke, S., Kloeung, N., et al. (2013). Reduced artemisinin susceptibility of Plasmodium falciparum ring stages in western Cambodia. *Antimicrobial agents and chemotherapy*, *57*(2), pp. 914–923.

Zekar, L., & Sharman, T. (2021). Plasmodium Falciparum Malaria. *StatPearls*. Retrieved June 13, 2022, from https://www.ncbi.nlm.nih.gov/books/NBK555962/

Zhao, Y., Liu, Z., Myat Thu Soe, Wang, L., Soe, T. N., Wei, Huanping, et al. (2019). Genetic Variations Associated with Drug Resistance Markers in Asymptomatic Plasmodium falciparum Infections in Myanmar. *Genes*, *10*(9). Retrieved June 13, 2022, from /pmc/articles/PMC6770986/

Zhiwu Zhang Laboratory. (2020). *User Manual for GAPIT: Genomic Association and Prediction Integrated Tool (Version 3)*. Washington State University.

(2020). MMV-supported projects. Retrieved December 11, 2020, from https://www.mmv.org/research-development/mmv-supported-projects

8.0 APPENDICES

Table 8.1: Loci with significant IBD within populations

Location	Gene ID	Position	Function
Gambia 2008	PF3D7_0209000	373697	6-cysteine protein P230
Gambia 2008	PF3D7_0316200	657140	conserved *Plasmodium* protein, unknown function
Gambia 2008	PF3D7_0301300	82459	epoxide hydrolase 1
Gambia 2008	PF3D7_0301600	92152	*Plasmodium* exported protein (hyp1), unknown function
Gambia 2008	PF3D7_0425200	1137276	conserved *Plasmodium* protein, unknown function
Gambia 2008	PF3D7_0425200	1137318	conserved *Plasmodium* protein, unknown function
Gambia 2008	PF3D7_0410800	488769	conserved *Plasmodium* protein, unknown function
Gambia 2008	PF3D7_0411200	506375	PP-loop family protein, putative
Gambia 2008	PF3D7_0411200	507063	PP-loop family protein, putative
Gambia 2008	PF3D7_0411800	519867	conserved *Plasmodium* protein, unknown function
Gambia 2008	PF3D7_0508900	368020	conserved *Plasmodium* protein, unknown function
Gambia 2008	PF3D7_0509400	396039	RNA polymerase I

Gambia 2008	PF3D7_0509600	404759	asparagine--tRNA ligase
Gambia 2008	PF3D7_0509800	410338	phosphatidylinositol 4-kinase
Gambia 2008	PF3D7_0509800	415296	phosphatidylinositol 4-kinase
Gambia 2008	PF3D7_0510000	419065	conserved *Plasmodium* protein, unknown function
Gambia 2008	PF3D7_0510100	428493	conserved protein, unknown function
Gambia 2008	PF3D7_0511200	472369	stearoyl-CoA desaturase
Gambia 2008	PF3D7_0511300	475055	MORN repeat protein, putative
Gambia 2008	PF3D7_0511300	476551	MORN repeat protein, putative
Gambia 2008	PF3D7_0624600	1002835	SNF2 helicase, putative
Gambia 2008	PF3D7_0624800	1011446	conserved *Plasmodium* protein, unknown function
Gambia 2008	PF3D7_0624800	1013440	conserved *Plasmodium* protein, unknown function
Gambia 2008	PF3D7_0624800	1014250	conserved *Plasmodium* protein, unknown function
Gambia 2008	PF3D7_0624900	1018087	GAS8-like protein, putative
Gambia 2008	PF3D7_0625100	1023829	sphingomyelin synthase 2, putative
Gambia 2008	PF3D7_0625300	1027653	DNA polymerase 1, putative
Gambia 2008	PF3D7_0625300	1028380	DNA polymerase 1, putative

Gambia 2008	PF3D7_0625400	1033118	conserved *Plasmodium* protein, unknown function
Gambia 2008	PF3D7_0625500	1036233	conserved *Plasmodium* membrane protein, unknown function
Gambia 2008	PF3D7_0625600	1040344	poly(A) polymerase PAP, putative
Gambia 2008	PF3D7_0625900	1047188	conserved *Plasmodium* protein, unknown function
Gambia 2008	PF3D7_0625900	1047197	conserved *Plasmodium* protein, unknown function
Gambia 2008	PF3D7_0626100	1056479	oxidoreductase, short-chain dehydrogenase family, putative
Gambia 2008	PF3D7_0626400	1065491	CRAL/TRIO domain-containing protein, putative
Gambia 2008	PF3D7_0627200	1095748	myosin light chain, putative
Gambia 2008	PF3D7_0627800	1114564	acetyl-CoA synthetase, putative
Gambia 2008	PF3D7_0627800	1114587	acetyl-CoA synthetase, putative
Gambia 2008	PF3D7_0627800	1115372	acetyl-CoA synthetase, putative
Gambia 2008	PF3D7_0628100	1124087	HECT-domain (ubiquitin-transferase), putative
Gambia 2008	PF3D7_0628100	1124576	HECT-domain (ubiquitin-transferase), putative
Gambia 2008	PF3D7_0628100	1125190	HECT-domain (ubiquitin-transferase), putative
Gambia 2008	PF3D7_0628100	1129048	HECT-domain (ubiquitin-transferase), putative
Gambia 2008	PF3D7_0628100	1130185	HECT-domain (ubiquitin-transferase), putative

Gambia 2008	PF3D7_0619800	833114	conserved *Plasmodium* membrane protein, unknown function
Gambia 2008	PF3D7_0619800	833321	conserved *Plasmodium* membrane protein, unknown function
Gambia 2008	PF3D7_0619800	834400	conserved *Plasmodium* membrane protein, unknown function
Gambia 2008	PF3D7_0619800	834464	conserved *Plasmodium* membrane protein, unknown function
Gambia 2008	PF3D7_0620200	847198	conserved *Plasmodium* protein, unknown function
Gambia 2008	PF3D7_0620400	851783	merozoite surface protein 10
Gambia 2008	PF3D7_0620500	855744	cleavage stimulation factor subunit 1, putative
Gambia 2008	PF3D7_0621000	863830	conserved *Plasmodium* protein, unknown function
Gambia 2008	PF3D7_0621100	866478	conserved *Plasmodium* protein, unknown function
Gambia 2008	PF3D7_0621100	869327	conserved *Plasmodium* protein, unknown function
Gambia 2008	PF3D7_0621100	869387	conserved *Plasmodium* protein, unknown function
Gambia 2008	PF3D7_0621100	869396	conserved *Plasmodium* protein, unknown function
Gambia 2008	PF3D7_0621300	873824	mRNA-binding protein PUF3
Gambia 2008	PF3D7_0621300	874163	mRNA-binding protein PUF4
Gambia 2008	PF3D7_0621300	875619	mRNA-binding protein PUF5
Gambia 2008	PF3D7_0621400	879279	Pf77 protein

Gambia 2008	PF3D7_0621700	887805	conserved *Plasmodium* protein, unknown function
Gambia 2008	PF3D7_0622100	900278	conserved *Plasmodium* protein, unknown function
Gambia 2008	PF3D7_0622100	902078	conserved *Plasmodium* protein, unknown function
Gambia 2008	PF3D7_0622200	905617	radical SAM protein, putative
Gambia 2008	PF3D7_0622700	916177	conserved *Plasmodium* membrane protein, unknown function
Gambia 2008	PF3D7_0622800	921841	leucine--tRNA ligase, putative
Gambia 2008	PF3D7_0623000	938238	chorismate synthase
Gambia 2008	PF3D7_0623300	947981	EGF-like membrane protein, putative
Gambia 2008	PF3D7_0623300	948047	EGF-like membrane protein, putative
Gambia 2008	PF3D7_0623800	970157	tyrosine kinase-like protein, putative
Gambia 2008	PF3D7_0623800	970261	tyrosine kinase-like protein, putative
Gambia 2008	PF3D7_0705200	260654	conserved *Plasmodium* protein, unknown function
Gambia 2008	PF3D7_0705500	270957	inositol-phosphate phosphatase, putative
Gambia 2008	PF3D7_0705500	271472	inositol-phosphate phosphatase, putative
Gambia 2008	PF3D7_0705500	278066	inositol-phosphate phosphatase, putative
Gambia 2008	PF3D7_0705600	282766	RNA helicase, putative

Gambia 2008	PF3D7_0706000	296804	importin-7, putative
Gambia 2008	PF3D7_0706100	298651	conserved *Plasmodium* protein, unknown function
Gambia 2008	PF3D7_0706100	298916	conserved *Plasmodium* protein, unknown function
Gambia 2008	PF3D7_0706100	299971	conserved *Plasmodium* protein, unknown function
Gambia 2008	PF3D7_0706700	325321	DNA mismatch repair protein MSH2, putative
Gambia 2008	PF3D7_0707200	332638	conserved *Plasmodium* protein, unknown function
Gambia 2008	PF3D7_0707200	332719	conserved *Plasmodium* protein, unknown function
Gambia 2008	PF3D7_0707200	333053	conserved *Plasmodium* protein, unknown function
Gambia 2008	PF3D7_0707200	333407	conserved *Plasmodium* protein, unknown function
Gambia 2008	PF3D7_0707200	333500	conserved *Plasmodium* protein, unknown function
Gambia 2008	PF3D7_0707500	349162	conserved *Plasmodium* protein, unknown function
Gambia 2008	PF3D7_0707500	349267	conserved *Plasmodium* protein, unknown function
Gambia 2008	PF3D7_0707500	353008	conserved *Plasmodium* protein, unknown function
Gambia 2008	PF3D7_0708200	374738	conserved *Plasmodium* protein, unknown function
Gambia 2008	PF3D7_0708200	374834	conserved *Plasmodium* protein, unknown function
Gambia 2008	PF3D7_0708200	375818	conserved *Plasmodium* protein, unknown function

Gambia 2008	PF3D7_0708200	376423	conserved *Plasmodium* protein, unknown function
Gambia 2008	PF3D7_0708200	376425	conserved *Plasmodium* protein, unknown function
Gambia 2008	PF3D7_0708400	384293	heat shock protein 90
Gambia 2008	PF3D7_0709000	405362	chloroquine resistance transporter
Gambia 2008	PF3D7_0709000	405600	chloroquine resistance transporter
Gambia 2008	PF3D7_0709300	415245	Cg2 protein
Gambia 2008	PF3D7_0709300	415250	Cg2 protein
Gambia 2008	PF3D7_0709300	415543	Cg2 protein
Gambia 2008	PF3D7_0709300	416615	Cg2 protein
Gambia 2008	PF3D7_0709300	417360	Cg2 protein
Gambia 2008	PF3D7_0709300	417622	Cg2 protein
Gambia 2008	PF3D7_0709300	417661	Cg2 protein
Gambia 2008	PF3D7_0709300	417700	Cg2 protein
Gambia 2008	PF3D7_0709300	418726	Cg2 protein
Gambia 2008	PF3D7_0709300	419603	Cg2 protein
Gambia 2008	PF3D7_0709400	424982	Cg7 protein

Gambia 2008	PF3D7_0709600	431181	ribonucleases P/MRP protein subunit POP1, putative
Gambia 2008	PF3D7_0709600	431257	ribonucleases P/MRP protein subunit POP1, putative
Gambia 2008	PF3D7_0709600	431287	ribonucleases P/MRP protein subunit POP1, putative
Gambia 2008	PF3D7_0709600	432784	ribonucleases P/MRP protein subunit POP1, putative
Gambia 2008	PF3D7_0709600	433519	ribonucleases P/MRP protein subunit POP1, putative
Gambia 2008	PF3D7_0709700	435151	prodrug activation and resistance esterase
Gambia 2008	PF3D7_0709700	435368	prodrug activation and resistance esterase
Gambia 2008	PF3D7_0710000	449042	conserved *Plasmodium* protein, unknown function
Gambia 2008	PF3D7_0710000	449571	conserved *Plasmodium* protein, unknown function
Gambia 2008	PF3D7_0710000	450032	conserved *Plasmodium* protein, unknown function
Gambia 2008	PF3D7_0710000	450424	conserved *Plasmodium* protein, unknown function
Gambia 2008	PF3D7_0710000	450711	conserved *Plasmodium* protein, unknown function
Gambia 2008	PF3D7_0710000	451727	conserved *Plasmodium* protein, unknown function
Gambia 2008	PF3D7_0710000	452331	conserved *Plasmodium* protein, unknown function
Gambia 2008	PF3D7_0710000	452339	conserved *Plasmodium* protein, unknown function
Gambia 2008	PF3D7_0710200	467225	conserved *Plasmodium* protein, unknown function

Gambia 2008	PF3D7_0710200	467610	conserved *Plasmodium* protein, unknown function
Gambia 2008	PF3D7_0710200	468471	conserved *Plasmodium* protein, unknown function
Gambia 2008	PF3D7_0824400	1063363	nucleoside transporter 2
Gambia 2008	PF3D7_0825800	1104061	conserved protein, unknown function
Gambia 2008	PF3D7_0826100	1120456	HECT-like E3 ubiquitin ligase, putative
Gambia 2008	PF3D7_0826100	1123101	HECT-like E3 ubiquitin ligase, putative
Gambia 2008	PF3D7_1036000	1427674	merozoite surface protein 11
Gambia 2008	PF3D7_1036300	1434109	duffy binding-like merozoite surface protein 2
Gambia 2008	PF3D7_1036300	1434129	duffy binding-like merozoite surface protein 3
Gambia 2008	PF3D7_1036300	1434271	duffy binding-like merozoite surface protein 4
Gambia 2008	PF3D7_1036300	1434553	duffy binding-like merozoite surface protein 5
Gambia 2008	PF3D7_1036500	1443005	conserved *Plasmodium* protein, unknown function
Gambia 2008	PF3D7_1036800	1449646	acetyl-CoA transporter, putative
Gambia 2008	PF3D7_1036900	1453956	conserved *Plasmodium* protein, unknown function
Gambia 2008	PF3D7_1037100	1470239	pyruvate kinase 2
Gambia 2015	PF3D7_0414400	653046	conserved *Plasmodium* protein, unknown function

Gambia 2015	PF3D7_0414400	653266	conserved *Plasmodium* protein, unknown function
Gambia 2015	PF3D7_0627100	1092754	ankyrin-repeat protein, putative
Gambia 2015	PF3D7_0627400	1100815	mitochondrial import inner membrane translocase subunit TIM22, putative
Gambia 2015	PF3D7_0627700	1110574	transportin
Gambia 2015	PF3D7_0627800	1115311	acetyl-CoA synthetase, putative
Gambia 2015	PF3D7_0627800	1116101	acetyl-CoA synthetase, putative
Gambia 2015	PF3D7_0627800	1116117	acetyl-CoA synthetase, putative
Gambia 2015	PF3D7_0627800	1116574	acetyl-CoA synthetase, putative
Gambia 2015	PF3D7_0627800	1117447	acetyl-CoA synthetase, putative
Gambia 2015	PF3D7_0627800	1117519	acetyl-CoA synthetase, putative
Gambia 2015	PF3D7_0628100	1128748	HECT-domain (ubiquitin-transferase), putative
Gambia 2015	PF3D7_0628100	1132174	HECT-domain (ubiquitin-transferase), putative
Gambia 2015	PF3D7_0628100	1133865	HECT-domain (ubiquitin-transferase), putative
Gambia 2015	PF3D7_0628100	1134020	HECT-domain (ubiquitin-transferase), putative
Gambia 2015	PF3D7_0628100	1136295	HECT-domain (ubiquitin-transferase), putative

Gambia 2015	PF3D7_0628100	1138697	HECT-domain (ubiquitin-transferase), putative
Gambia 2015	PF3D7_0628100	1140090	HECT-domain (ubiquitin-transferase), putative
Gambia 2015	PF3D7_0628100	1142668	HECT-domain (ubiquitin-transferase), putative
Gambia 2015	PF3D7_0628100	1142857	HECT-domain (ubiquitin-transferase), putative
Gambia 2015	PF3D7_0628100	1143755	HECT-domain (ubiquitin-transferase), putative
Gambia 2015	PF3D7_0628100	1148415	HECT-domain (ubiquitin-transferase), putative
Gambia 2015	PF3D7_0628100	1149046	HECT-domain (ubiquitin-transferase), putative
Gambia 2015	PF3D7_0628100	1151372	HECT-domain (ubiquitin-transferase), putative
Gambia 2015	PF3D7_0628900	1193017	RAP protein, putative
Gambia 2015	PF3D7_0628900	1193139	RAP protein, putative
Gambia 2015	PF3D7_0629100	1197298	nicotinate phosphoribosyl transferase, putative
Gambia 2015	PF3D7_0629300	1206227	phospholipase, putative
Gambia 2015	PF3D7_0629300	1206442	phospholipase, putative
Gambia 2015	PF3D7_0629500	1214350	amino acid transporter AAT1
Gambia 2015	PF3D7_0629700	1221991	SET domain protein, putative
Gambia 2015	PF3D7_0629700	1226823	SET domain protein, putative

Gambia 2015	PF3D7_0629700	1237460	SET domain protein, putative
Gambia 2015	PF3D7_0629700	1238196	SET domain protein, putative
Gambia 2015	PF3D7_0629700	1238724	SET domain protein, putative
Gambia 2015	PF3D7_0629700	1238829	SET domain protein, putative
Gambia 2015	PF3D7_0629700	1239644	SET domain protein, putative
Gambia 2015	PF3D7_0629700	1240560	SET domain protein, putative
Gambia 2015	PF3D7_0629700	1241113	SET domain protein, putative
Gambia 2015	PF3D7_0630100	1255482	alpha/beta hydrolase, putative
Gambia 2015	PF3D7_0630100	1255840	alpha/beta hydrolase, putative
Gambia 2015	PF3D7_0630300	1261391	DNA polymerase epsilon catalytic subunit A, putative
Gambia 2015	PF3D7_0630300	1266297	DNA polymerase epsilon catalytic subunit A, putative
Gambia 2015	PF3D7_0630300	1267353	DNA polymerase epsilon catalytic subunit A, putative
Gambia 2015	PF3D7_0630400	1272518	conserved *Plasmodium* protein, unknown function
Gambia 2015	PF3D7_0630700	1285573	bifunctional methylenetetrahydrofolate dehydrogenase/cyclohydrolase, putative
Gambia 2015	PF3D7_0630800	1288904	TPH domain-containing protein, putative

Gambia 2015	PF3D7_0630800	1289571	TPH domain-containing protein, putative
Gambia 2015	PF3D7_0630800	1289915	TPH domain-containing protein, putative
Gambia 2015	PF3D7_0630800	1290024	TPH domain-containing protein, putative
Gambia 2015	PF3D7_0630800	1290444	TPH domain-containing protein, putative
Gambia 2015	PF3D7_0630800	1290486	TPH domain-containing protein, putative
Gambia 2015	PF3D7_0630800	1290718	TPH domain-containing protein, putative
Gambia 2015	PF3D7_0630900	1291481	ATP-dependent RNA helicase HAS1
Gambia 2015	PF3D7_0630900	1292764	ATP-dependent RNA helicase HAS2
Gambia 2015	PF3D7_0630900	1292928	ATP-dependent RNA helicase HAS3
Gambia 2015	PF3D7_0702600	110031	chitinase, fragment
Gambia 2015	PF3D7_0703200	123301	conserved *Plasmodium* protein, unknown function
Gambia 2015	PF3D7_0703200	125579	conserved *Plasmodium* protein, unknown function
Gambia 2015	PF3D7_0703200	125921	conserved *Plasmodium* protein, unknown function
Gambia 2015	PF3D7_0704400	205197	phosphoinositide-binding protein, putative
Gambia 2015	PF3D7_0706000	294698	importin-7, putative
Gambia 2015	PF3D7_0706100	298978	conserved *Plasmodium* protein, unknown function

Gambia 2015	PF3D7_0706100	301758	conserved *Plasmodium* protein, unknown function
Gambia 2015	PF3D7_0706500	310181	conserved *Plasmodium* protein, unknown function
Gambia 2015	PF3D7_0706500	310356	conserved *Plasmodium* protein, unknown function
Gambia 2015	PF3D7_0706500	312348	conserved *Plasmodium* protein, unknown function
Gambia 2015	PF3D7_0706500	313313	conserved *Plasmodium* protein, unknown function
Gambia 2015	PF3D7_0707400	344469	AAA family ATPase, putative
Gambia 2015	PF3D7_0708700	392078	Cg8 protein
Gambia 2015	PF3D7_0708800	396910	heat shock protein 110
Gambia 2015	PF3D7_0708800	397135	heat shock protein 111
Gambia 2015	PF3D7_0709000	403625	chloroquine resistance transporter
Gambia 2015	PF3D7_0709100	408434	Cg1 protein
Gambia 2015	PF3D7_0709100	408439	Cg1 protein
Gambia 2015	PF3D7_0709100	408743	Cg1 protein
Gambia 2015	PF3D7_0709100	408982	Cg1 protein
Gambia 2015	PF3D7_0709100	409108	Cg1 protein
Gambia 2015	PF3D7_0709100	409122	Cg1 protein

Gambia 2015	PF3D7_0709100	409168	Cg1 protein
Gambia 2015	PF3D7_0709100	410132	Cg1 protein
Gambia 2015	PF3D7_0709100	410698	Cg1 protein
Gambia 2015	PF3D7_0709100	411244	Cg1 protein
Gambia 2015	PF3D7_0709100	411281	Cg1 protein
Gambia 2015	PF3D7_0709100	411301	Cg1 protein
Gambia 2015	PF3D7_0709100	411352	Cg1 protein
Gambia 2015	PF3D7_0709200	412735	glutaredoxin-like protein
Gambia 2015	PF3D7_0709200	412821	glutaredoxin-like protein
Gambia 2015	PF3D7_0709300	416827	Cg2 protein
Gambia 2015	PF3D7_0709300	416897	Cg2 protein
Gambia 2015	PF3D7_0709300	418378	Cg2 protein
Gambia 2015	PF3D7_0709300	418830	Cg2 protein
Gambia 2015	PF3D7_0709400	425729	Cg7 protein
Gambia 2015	PF3D7_0709600	430421	ribonucleases P/MRP protein subunit POP1, putative
Gambia 2015	PF3D7_0709600	430538	ribonucleases P/MRP protein subunit POP1, putative

Gambia 2015	PF3D7_0709600	431080	ribonucleases P/MRP protein subunit POP1, putative
Gambia 2015	PF3D7_0709600	431194	ribonucleases P/MRP protein subunit POP1, putative
Gambia 2015	PF3D7_0709600	431302	ribonucleases P/MRP protein subunit POP1, putative
Gambia 2015	PF3D7_0709600	431440	ribonucleases P/MRP protein subunit POP1, putative
Gambia 2015	PF3D7_0709600	432561	ribonucleases P/MRP protein subunit POP1, putative
Gambia 2015	PF3D7_0709600	432566	ribonucleases P/MRP protein subunit POP1, putative
Gambia 2015	PF3D7_0709600	433609	ribonucleases P/MRP protein subunit POP1, putative
Gambia 2015	PF3D7_0709700	435413	prodrug activation and resistance esterase
Gambia 2015	PF3D7_0709900	438767	conserved protein, unknown function
Gambia 2015	PF3D7_0709900	444875	conserved protein, unknown function
Gambia 2015	PF3D7_0709900	444911	conserved protein, unknown function
Gambia 2015	PF3D7_0710000	455345	conserved *Plasmodium* protein, unknown function
Gambia 2015	PF3D7_0710200	464718	conserved *Plasmodium* protein, unknown function
Gambia 2015	PF3D7_0710200	464800	conserved *Plasmodium* protein, unknown function
Gambia 2015	PF3D7_0710200	466386	conserved *Plasmodium* protein, unknown function
Gambia 2015	PF3D7_0710200	466676	conserved *Plasmodium* protein, unknown function

Gambia 2015	PF3D7_0711000	487758	AAA family ATPase, CDC48 subfamily
Gambia 2015	PF3D7_0929700	1186104	conserved *Plasmodium* protein, unknown function
Gambia 2015	PF3D7_0930600	1219780	peptidyl-prolyl cis-trans isomerase
Gambia 2015	PF3D7_1477500	3189316	*Plasmodium* exported protein (PHISTb), unknown function
Cambodia	PF3D7_0215300	630150	acyl-CoA synthetase
Cambodia	PF3D7_0525100	1043474	acyl-CoA synthetase
Cambodia	PF3D7_0532400	1313555	lysine-rich membrane-associated PHISTb protein
Cambodia	PF3D7_0532500	1316719	*Plasmodium* exported protein, unknown function
Cambodia	PF3D7_0514900	619538	conserved *Plasmodium* protein, unknown function
Cambodia	PF3D7_0602600	108761	SAC3 domain-containing protein, putative
Cambodia	PF3D7_0603600	148827	AT-rich interactive domain-containing protein, putative
Cambodia	PF3D7_0611800	496580	conserved *Plasmodium* protein, unknown function
Cambodia	PF3D7_0619300	803476	conserved *Plasmodium* protein, unknown function
Cambodia	PF3D7_0619800	834448	conserved *Plasmodium* membrane protein, unknown function
Cambodia	PF3D7_0620400	851736	merozoite surface protein 10
Cambodia	PF3D7_0809400	476280	conserved protein, unknown function

Cambodia	PF3D7_0809400	477797	conserved protein, unknown function
Cambodia	PF3D7_0809600	480016	peptidase family C50, putative
Cambodia	PF3D7_0809600	480159	peptidase family C50, putative
Cambodia	PF3D7_0809600	482147	peptidase family C50, putative
Cambodia	PF3D7_0809600	486805	peptidase family C50, putative
Cambodia	PF3D7_0809600	486841	peptidase family C50, putative
Cambodia	PF3D7_0809600	489196	peptidase family C50, putative
Cambodia	PF3D7_0809600	491157	peptidase family C50, putative
Cambodia	PF3D7_0809600	495550	peptidase family C50, putative
Cambodia	PF3D7_0809600	495730	peptidase family C50, putative
Cambodia	PF3D7_0809700	501042	RuvB-like helicase 1
Cambodia	PF3D7_0809800	503483	conserved *Plasmodium* protein, unknown function
Cambodia	PF3D7_0809800	503494	conserved *Plasmodium* protein, unknown function
Cambodia	PF3D7_0809900	509018	JmjC domain-containing protein, putative
Cambodia	PF3D7_0810300	526923	protein phosphatase PPM5, putative
Cambodia	PF3D7_0810500	535807	protein phosphatase PPM7, putative

Cambodia	PF3D7_0811600	585854	conserved protein, unknown function
Cambodia	PF3D7_0811700	592262	conserved *Plasmodium* protein, unknown function
Cambodia	PF3D7_0811700	592892	conserved *Plasmodium* protein, unknown function
Cambodia	PF3D7_0812100	605294	proteasome activator complex subunit 4, putative
Cambodia	PF3D7_0812100	612596	proteasome activator complex subunit 4, putative
Cambodia	PF3D7_0812200	615922	trypsin-like serine protease, putative
Cambodia	PF3D7_0812500	626266	RNA-binding protein, putative
Cambodia	PF3D7_0812900	639308	conserved *Plasmodium* protein, unknown function
Cambodia	PF3D7_0813000	643788	protein KIC7
Cambodia	PF3D7_0813500	666328	PUB domain-containing protein, putative
Cambodia	PF3D7_0814200	687615	DNA/RNA-binding protein Alba 1
Cambodia	PF3D7_0814500	702404	conserved protein, unknown function
Cambodia	PF3D7_0815800	740134	vacuolar protein sorting-associated protein 9, putative
Cambodia	PF3D7_0815800	740768	vacuolar protein sorting-associated protein 9, putative
Cambodia	PF3D7_0816600	765093	chaperone protein ClpB1
Cambodia	PF3D7_0817700	810629	rhoptry neck protein 5

Cambodia	PF3D7_0818600	846225	BEM46-like protein, putative
Cambodia	PF3D7_0822200	983577	phosphorylated CTD interacting factor 1 WW domain-containing protein, putative
Cambodia	PF3D7_0822400	991389	conserved *Plasmodium* protein, unknown function
Cambodia	PF3D7_1035700	1414440	duffy binding-like merozoite surface protein
Cambodia	PF3D7_1036900	1456037	conserved *Plasmodium* protein, unknown function
Cambodia	PF3D7_1036900	1456547	conserved *Plasmodium* protein, unknown function
Cambodia	PF3D7_1037000	1467904	DNA polymerase zeta catalytic subunit, putative
Cambodia	PF3D7_1037100	1471050	pyruvate kinase 2
Cambodia	PF3D7_1038300	1513542	conserved *Plasmodium* protein, unknown function
Cambodia	PF3D7_1136900	1457009	subtilisin-like protease 2
Cambodia	PF3D7_1326500	1103578	conserved *Plasmodium* protein, unknown function
Cambodia	PF3D7_1331500	1314283	conserved *Plasmodium* protein, unknown function
Cambodia	PF3D7_1332100	1330092	conserved protein, unknown function
Cambodia	PF3D7_1332200	1333253	conserved protein, unknown function
Cambodia	PF3D7_1343400	1717461	DNA repair protein RAD5, putative

Cambodia	PF3D7_1343400	1718905	DNA repair protein RAD5, putative
Cambodia	PF3D7_1343700	1726432	kelch protein K13
Cambodia	PF3D7_1343700	1726643	kelch protein K13
Cambodia	PF3D7_1343800	1734260	conserved *Plasmodium* protein, unknown function
Cambodia	PF3D7_1343800	1734578	conserved *Plasmodium* protein, unknown function
Cambodia	PF3D7_1343800	1734757	conserved *Plasmodium* protein, unknown function
Cambodia	PF3D7_1343800	1737057	conserved *Plasmodium* protein, unknown function
Cambodia	PF3D7_1343800	1743222	conserved *Plasmodium* protein, unknown function
Cambodia	PF3D7_1343800	1745609	conserved *Plasmodium* protein, unknown function
Cambodia	PF3D7_1343800	1750965	conserved *Plasmodium* protein, unknown function
Cambodia	PF3D7_1343800	1751205	conserved *Plasmodium* protein, unknown function
Cambodia	PF3D7_1347700	1910058	ethanolamine-phosphate cytidylyltransferase
Cambodia	PF3D7_1349300	1981018	tyrosine kinase-like protein
Cambodia	PF3D7_1349300	1981673	tyrosine kinase-like protein
Cambodia	PF3D7_1349500	1986165	conserved *Plasmodium* protein, unknown function
Cambodia	PF3D7_1349500	1986698	conserved *Plasmodium* protein, unknown function

Cambodia	PF3D7_1351200	2046191	conserved *Plasmodium* protein, unknown function
Cambodia	PF3D7_1352700	2104131	intron-binding protein aquarius, putative
Cambodia	PF3D7_1352700	2107756	intron-binding protein aquarius, putative
Cambodia	PF3D7_1352800	2110844	vacuolar fusion protein MON1, putative
Cambodia	PF3D7_1352900	2114339	*Plasmodium* exported protein, unknown function
Cambodia	PF3D7_1352900	2114498	*Plasmodium* exported protein, unknown function
Cambodia	PF3D7_1352900	2115117	*Plasmodium* exported protein, unknown function
Cambodia	PF3D7_1352900	2115118	*Plasmodium* exported protein, unknown function
Cambodia	PF3D7_1352900	2115578	*Plasmodium* exported protein, unknown function
Cambodia	PF3D7_1427300	1065485	conserved *Plasmodium* protein, unknown function
Cambodia	PF3D7_1427500	1082949	DNA mismatch repair protein MSH2, putative
Cambodia	PF3D7_1428400	1111084	WD and tetratricopeptide repeats protein 1, putative
Cambodia	PF3D7_1432300	1272402	conserved *Plasmodium* protein, unknown function
Cambodia	PF3D7_1403500	130979	dynein light chain, putative
Cambodia	PF3D7_1403600	133144	selenoprotein
Cambodia	PF3D7_1404000	144382	DNA-directed RNA polymerase II subunit RPB4, putative

Cambodia	PF3D7_1404800	165436	conserved *Plasmodium* protein, unknown function
Cambodia	PF3D7_1404900	170404	conserved *Plasmodium* protein, unknown function
Cambodia	PF3D7_1405400	189520	DNA mismatch repair protein, putative
Cambodia	PF3D7_1406200	221707	transcription elongation factor SPT6, putative
Cambodia	PF3D7_1408700	334976	conserved protein, unknown function
Cambodia	PF3D7_1408700	337415	conserved protein, unknown function
Cambodia	PF3D7_1408700	339650	conserved protein, unknown function
Cambodia	PF3D7_1408700	341123	conserved protein, unknown function
Cambodia	PF3D7_1408700	344754	conserved protein, unknown function
Cambodia	PF3D7_1408800	350181	conserved *Plasmodium* protein, unknown function
Cambodia	PF3D7_1409000	353747	WD repeat-containing protein, putative
Cambodia	PF3D7_1411200	453738	rhomboid protease ROM8
Cambodia	PF3D7_1411300	459931	DnaJ protein, putative
Cambodia	PF3D7_1412400	495491	conserved *Plasmodium* protein, unknown function
Cambodia	PF3D7_1412400	504067	conserved *Plasmodium* protein, unknown function
Cambodia	PF3D7_1412500	508547	actin II

Cambodia	PF3D7_1414700	595585	ubiquitin carboxyl-terminal hydrolase, putative
Cambodia	PF3D7_1415100	610371	conserved protein, unknown function
Cambodia	PF3D7_1416600	674689	conserved *Plasmodium* protein, unknown function
Cambodia	PF3D7_1417100	690978	conserved *Plasmodium* protein, unknown function
Cambodia	PF3D7_1417200	704109	NOT family protein, putative
Cambodia	PF3D7_1418100	762777	liver specific protein 1, putative
Cambodia	PF3D7_1418100	766801	liver specific protein 1, putative
Cambodia	PF3D7_1418100	771553	liver specific protein 1, putative
Cambodia	PF3D7_1418100	771557	liver specific protein 1, putative
Cambodia	PF3D7_1418100	771571	liver specific protein 1, putative
Cambodia	PF3D7_1418900	784555	ATP-dependent RNA helicase DBP4, putative
Cambodia	PF3D7_1419100	796205	ATP-dependent RNA helicase DDX55
Cambodia	PF3D7_1419300	803248	glutathione S-transferase
Cambodia	PF3D7_1419400	808765	conserved *Plasmodium* membrane protein, unknown function
Cambodia	PF3D7_1419400	809210	conserved *Plasmodium* membrane protein, unknown function
Cambodia	PF3D7_1419400	809810	conserved *Plasmodium* membrane protein, unknown function

Cambodia	PF3D7_1419400	809986	conserved *Plasmodium* membrane protein, unknown function
Cambodia	PF3D7_1419400	810165	conserved *Plasmodium* membrane protein, unknown function
Cambodia	PF3D7_1402100	83469	pseudouridine synthase, putative
Cambodia	PF3D7_1420500	851498	protein GPR89, putative
Cambodia	PF3D7_1421400	883173	DNA-directed RNA polymerase III subunit RPC6, putative
Cambodia	PF3D7_1422500	907527	ERAD-associated E3 ubiquitin-protein ligase HRD1
Cambodia	PF3D7_1422600	911819	conserved *Plasmodium* protein, unknown function
Cambodia	PF3D7_1422700	914614	conserved *Plasmodium* protein, unknown function
Cambodia	PF3D7_1422700	914742	conserved *Plasmodium* protein, unknown function
Cambodia	PF3D7_1422800	918771	actin-related protein, putative
Cambodia	PF3D7_1422800	919132	actin-related protein, putative
Cambodia	PF3D7_1422900	923274	14-3-3 protein, putative
Cambodia	PF3D7_1422900	923791	14-3-3 protein, putative
Cambodia	PF3D7_1423200	934323	peptidyl-prolyl cis-trans isomerase
Cambodia	PF3D7_1423400	942445	conserved *Plasmodium* membrane protein, unknown function
Cambodia	PF3D7_1423400	945185	peptidyl-prolyl cis-trans isomerase

Cambodia	PF3D7_1423500	949947	conserved *Plasmodium* protein, unknown function
Cambodia	PF3D7_1423500	949991	conserved *Plasmodium* protein, unknown function
Cambodia	PF3D7_1423500	951534	conserved *Plasmodium* protein, unknown function

Table 8.2: Loci with significant IBD between populations

Populations	Gene ID	Position	Description
Gambia2008 vs Gambia2014/15	PF3D7_0307700	331330	conserved *Plasmodium* protein, unknown function
Gambia2008 vs Gambia2014/15	PF3D7_0315200	621090	circumsporozoite- and TRAP-related protein
Gambia2008 vs Gambia2014/15	PF3D7_0315300	627740	conserved *Plasmodium* protein, unknown function
Gambia2008 vs Gambia2014/15	PF3D7_0316400	664726	CS domain-containing protein, putative
Gambia2008 vs Gambia2014/15	PF3D7_0413600	617166	26S protease regulatory subunit 6B, putative
Gambia2008 vs Gambia2014/15	PF3D7_0414000	626901	structural maintenance of chromosomes protein 3
Gambia2008 vs Gambia2014/15	PF3D7_0415100	671047	conserved protein, unknown function
Gambia2008 vs Gambia2014/15	PF3D7_0415100	671646	conserved protein, unknown function
Gambia2008 vs Gambia2014/15	PF3D7_0415200	677292	conserved *Plasmodium* protein, unknown function
Gambia2008 vs Gambia2014/15	PF3D7_0415200	677321	conserved *Plasmodium* protein, unknown function
Gambia2008 vs Gambia2014/15	PF3D7_0415200	677644	conserved *Plasmodium* protein, unknown function
Gambia2008 vs Gambia2014/15	PF3D7_0415300	683801	cdc2-related protein kinase 3
Gambia2008 vs Gambia2014/15	PF3D7_0415300	684059	cdc2-related protein kinase 4

Gambia2008 vs Gambia2014/15	PF3D7_0627100	1091436	ankyrin-repeat protein, putative
Gambia2008 vs Gambia2014/15	PF3D7_0627100	1092754	ankyrin-repeat protein, putative
Gambia2008 vs Gambia2014/15	PF3D7_0627300	1098313	E3 ubiquitin-protein ligase RNF5, putative
	PF3D7_0627400	1100815	mitochondrial import inner membrane translocase subunit
Gambia2008 vs Gambia2014/15			TIM22, putative
Gambia2008 vs Gambia2014/15	PF3D7_0627500	1102052	protein DJ-1
Gambia2008 vs Gambia2014/15	PF3D7_0627700	1110574	transportin
Gambia2008 vs Gambia2014/15	PF3D7_0627800	1115311	acetyl-CoA synthetase, putative
Gambia2008 vs Gambia2014/15	PF3D7_0627800	1116101	acetyl-CoA synthetase, putative
Gambia2008 vs Gambia2014/15	PF3D7_0627800	1116117	acetyl-CoA synthetase, putative
Gambia2008 vs Gambia2014/15	PF3D7_0627800	1116574	acetyl-CoA synthetase, putative
Gambia2008 vs Gambia2014/15	PF3D7_0628100	1124087	HECT-domain (ubiquitin-transferase), putative
Gambia2008 vs Gambia2014/15	PF3D7_0628100	1124576	HECT-domain (ubiquitin-transferase), putative
Gambia2008 vs Gambia2014/15	PF3D7_0628100	1125190	HECT-domain (ubiquitin-transferase), putative
Gambia2008 vs Gambia2014/15	PF3D7_0628100	1128748	HECT-domain (ubiquitin-transferase), putative

Gambia2008 vs Gambia2014/15	PF3D7_0628100	1129048	HECT-domain (ubiquitin-transferase), putative
Gambia2008 vs Gambia2014/15	PF3D7_0628100	1129620	HECT-domain (ubiquitin-transferase), putative
Gambia2008 vs Gambia2014/15	PF3D7_0628100	1130064	HECT-domain (ubiquitin-transferase), putative
Gambia2008 vs Gambia2014/15	PF3D7_0628100	1130185	HECT-domain (ubiquitin-transferase), putative
Gambia2008 vs Gambia2014/15	PF3D7_0628100	1130698	HECT-domain (ubiquitin-transferase), putative
Gambia2008 vs Gambia2014/15	PF3D7_0628100	1132174	HECT-domain (ubiquitin-transferase), putative
Gambia2008 vs Gambia2014/15	PF3D7_0628100	1138697	HECT-domain (ubiquitin-transferase), putative
Gambia2008 vs Gambia2014/15	PF3D7_0628100	1142857	HECT-domain (ubiquitin-transferase), putative
Gambia2008 vs Gambia2014/15	PF3D7_0628100	1146646	HECT-domain (ubiquitin-transferase), putative
Gambia2008 vs Gambia2014/15	PF3D7_0628100	1148415	HECT-domain (ubiquitin-transferase), putative
Gambia2008 vs Gambia2014/15	PF3D7_0628100	1149142	HECT-domain (ubiquitin-transferase), putative
Gambia2008 vs Gambia2014/15	PF3D7_0628100	1151372	HECT-domain (ubiquitin-transferase), putative
Gambia2008 vs Gambia2014/15	PF3D7_0628200	1160911	eukaryotic translation initiation factor 2-alpha kinase
Gambia2008 vs Gambia2014/15	PF3D7_0628700	1184506	conserved *Plasmodium* protein, unknown function
Gambia2008 vs Gambia2014/15	PF3D7_0628800	1187117	glutamyl-tRNA(Gln) amidotransferase subunit B

Gambia2008 vs Gambia2014/15	PF3D7_0628900	1193017	RAP protein, putative
Gambia2008 vs Gambia2014/15	PF3D7_0629300	1206442	phospholipase, putative
Gambia2008 vs Gambia2014/15	PF3D7_0629500	1214350	amino acid transporter AAT1
Gambia2008 vs Gambia2014/15	PF3D7_0629500	1215233	amino acid transporter AAT2
Gambia2008 vs Gambia2014/15	PF3D7_0629700	1223570	SET domain protein, putative
Gambia2008 vs Gambia2014/15	PF3D7_0629700	1224777	SET domain protein, putative
Gambia2008 vs Gambia2014/15	PF3D7_0629700	1226823	SET domain protein, putative
Gambia2008 vs Gambia2014/15	PF3D7_0629700	1234246	SET domain protein, putative
Gambia2008 vs Gambia2014/15	PF3D7_0629700	1237460	SET domain protein, putative
Gambia2008 vs Gambia2014/15	PF3D7_0629700	1238196	SET domain protein, putative
Gambia2008 vs Gambia2014/15	PF3D7_0629701	1238724	SET domain protein, putative
Gambia2008 vs Gambia2014/15	PF3D7_0629700	1238829	SET domain protein, putative
Gambia2008 vs Gambia2014/15	PF3D7_0629700	1239644	SET domain protein, putative
Gambia2008 vs Gambia2014/15	PF3D7_0629700	1240560	SET domain protein, putative
Gambia2008 vs Gambia2014/15	PF3D7_0629700	1241113	SET domain protein, putative

Gambia2008 vs Gambia2014/15	PF3D7_0629800	1245738	cullin-like protein, putative
Gambia2008 vs Gambia2014/15	PF3D7_0630100	1255840	alpha/beta hydrolase, putative
Gambia2008 vs Gambia2014/15	PF3D7_0630300	1266213	DNA polymerase epsilon catalytic subunit A, putative
Gambia2008 vs Gambia2014/15	PF3D7_0630300	1266255	DNA polymerase epsilon catalytic subunit A, putative
Gambia2008 vs Gambia2014/15	PF3D7_0630301	1266297	DNA polymerase epsilon catalytic subunit A, putative
Gambia2008 vs Gambia2014/15	PF3D7_0630300	1266308	DNA polymerase epsilon catalytic subunit A, putative
Gambia2008 vs Gambia2014/15	PF3D7_0630300	1266600	DNA polymerase epsilon catalytic subunit A, putative
Gambia2008 vs Gambia2014/15	PF3D7_0630300	1267260	DNA polymerase epsilon catalytic subunit A, putative
Gambia2008 vs Gambia2014/15	PF3D7_0630300	1267353	DNA polymerase epsilon catalytic subunit A, putative
Gambia2008 vs Gambia2014/15	PF3D7_0630300	1268187	DNA polymerase epsilon catalytic subunit A, putative
Gambia2008 vs Gambia2014/15	PF3D7_0630300	1268325	DNA polymerase epsilon catalytic subunit A, putative
Gambia2008 vs Gambia2014/15	PF3D7_0630300	1268688	DNA polymerase epsilon catalytic subunit A, putative
Gambia2008 vs Gambia2014/15	PF3D7_0630300	1268778	DNA polymerase epsilon catalytic subunit A, putative
Gambia2008 vs Gambia2014/15	PF3D7_0630300	1268898	DNA polymerase epsilon catalytic subunit A, putative
Gambia2008 vs Gambia2014/15	PF3D7_0630300	1268919	DNA polymerase epsilon catalytic subunit A, putative

Gambia2008 vs Gambia2014/15	PF3D7_0630300	1268973	DNA polymerase epsilon catalytic subunit A, putative
Gambia2008 vs Gambia2014/15	PF3D7_0630400	1272518	conserved *Plasmodium* protein, unknown function
Gambia2008 vs Gambia2014/15	PF3D7_0630400	1272582	conserved *Plasmodium* protein, unknown function
Gambia2008 vs Gambia2014/15	PF3D7_0630400	1273022	conserved *Plasmodium* protein, unknown function
Gambia2008 vs Gambia2014/15	PF3D7_0630700	1285497	bifunctional methylenetetrahydrofolate dehydrogenase/cyclohydrolase, putative
Gambia2008 vs Gambia2014/15	PF3D7_0630700	1286801	bifunctional methylenetetrahydrofolate dehydrogenase/cyclohydrolase, putative
Gambia2008 vs Gambia2014/15	PF3D7_0630700	1286911	bifunctional methylenetetrahydrofolate dehydrogenase/cyclohydrolase, putative
Gambia2008 vs Gambia2014/15	PF3D7_0630800	1290718	TPH domain-containing protein, putative
Gambia2008 vs Gambia2014/15	PF3D7_0630900	1292928	ATP-dependent RNA helicase HAS1
Gambia2008 vs Gambia2014/15	PF3D7_0702000	85504	*Plasmodium* exported protein (hyp12), unknown function
Gambia2008 vs Gambia2014/15	PF3D7_0703200	123301	conserved *Plasmodium* protein, unknown function
Gambia2008 vs Gambia2014/15	PF3D7_0703200	125579	conserved *Plasmodium* protein, unknown function

	PF3D7_0704000	169933	conserved *Plasmodium* membrane protein, unknown
Gambia2008 vs Gambia2014/15			function
Gambia2008 vs Gambia2014/15	PF3D7_0708200	374738	conserved *Plasmodium* protein, unknown function
Gambia2008 vs Gambia2014/15	PF3D7_0708400	384188	heat shock protein 90
Gambia2008 vs Gambia2014/15	PF3D7_0708800	397135	heat shock protein 110
Gambia2008 vs Gambia2014/15	PF3D7_0709100	408434	Cg1 protein
Gambia2008 vs Gambia2014/15	PF3D7_0709100	408439	Cg1 protein
Gambia2008 vs Gambia2014/15	PF3D7_0709100	408982	Cg1 protein
Gambia2008 vs Gambia2014/15	PF3D7_0709100	410132	Cg1 protein
Gambia2008 vs Gambia2014/15	PF3D7_0709100	410698	Cg1 protein
Gambia2008 vs Gambia2014/15	PF3D7_0709100	411301	Cg1 protein
Gambia2008 vs Gambia2014/15	PF3D7_0709300	415245	Cg2 protein
Gambia2008 vs Gambia2014/15	PF3D7_0709300	415250	Cg2 protein
Gambia2008 vs Gambia2014/15	PF3D7_0709300	415529	Cg2 protein
Gambia2008 vs Gambia2014/15	PF3D7_0709300	415543	Cg2 protein

Gambia2008 vs Gambia2014/15	PF3D7_0709300	415625	Cg2 protein
Gambia2008 vs Gambia2014/15	PF3D7_0709300	415775	Cg2 protein
Gambia2008 vs Gambia2014/15	PF3D7_0709300	416897	Cg2 protein
Gambia2008 vs Gambia2014/15	PF3D7_0709300	417622	Cg2 protein
Gambia2008 vs Gambia2014/15	PF3D7_0709300	417700	Cg2 protein
Gambia2008 vs Gambia2014/15	PF3D7_0709300	418720	Cg2 protein
Gambia2008 vs Gambia2014/15	PF3D7_0709300	418726	Cg2 protein
Gambia2008 vs Gambia2014/15	PF3D7_0709300	419603	Cg2 protein
Gambia2008 vs Gambia2014/15	PF3D7_0709600	431287	ribonucleases P/MRP protein subunit POP1, putative
Gambia2008 vs Gambia2014/15	PF3D7_0709600	431302	ribonucleases P/MRP protein subunit POP1, putative
Gambia2008 vs Gambia2014/15	PF3D7_0709700	435231	prodrug activation and resistance esterase
Gambia2008 vs Gambia2014/15	PF3D7_0709900	438767	conserved protein, unknown function
Gambia2008 vs Gambia2014/15	PF3D7_0709900	443052	conserved protein, unknown function
Gambia2008 vs Gambia2014/15	PF3D7_0709900	444875	conserved protein, unknown function
Gambia2008 vs Gambia2014/15	PF3D7_0710000	447544	conserved *Plasmodium* protein, unknown function

Gambia2008 vs Gambia2014/15	PF3D7_0710000	453645	conserved *Plasmodium* protein, unknown function
Gambia2008 vs Gambia2014/15	PF3D7_0710000	454103	conserved *Plasmodium* protein, unknown function
Gambia2008 vs Gambia2014/15	PF3D7_0710100	460943	conserved protein, unknown function
Gambia2008 vs Gambia2014/15	PF3D7_0710200	467155	conserved *Plasmodium* protein, unknown function
Gambia2008 vs Gambia2014/15	PF3D7_0710200	468471	conserved *Plasmodium* protein, unknown function
Gambia2008 vs Gambia2014/15	PF3D7_0810200	522796	ABC1 family, putative
Gambia2008 vs Gambia2014/15	PF3D7_0930300	1202285	merozoite surface protein 1
Gambia2008 vs Gambia2014/15	PF3D7_1036500	1443005	conserved *Plasmodium* protein, unknown function
Gambia2008 vs Gambia2014/15	PF3D7_1036800	1449581	acetyl-CoA transporter, putative
Gambia2008 vs Gambia2014/15	PF3D7_1036800	1450767	acetyl-CoA transporter, putative
Gambia2008 vs Gambia2014/15	PF3D7_1233600	1391451	asparagine and aspartate rich protein 1
Gambia2008 vs Cambodia	PF3D7_0628100	1146646	HECT-domain (ubiquitin-transferase), putative
Gambia2008 vs Cambodia	PF3D7_0629700	1240560	SET domain protein, putative
Gambia2008 vs Cambodia	PF3D7_0630300	1268688	DNA polymerase epsilon catalytic subunit A, putative
Gambia2008 vs Cambodia	PF3D7_0630300	1268778	DNA polymerase epsilon catalytic subunit A, putative

Gambia2008 vs Cambodia	PF3D7_0630300	1268898	DNA polymerase epsilon catalytic subunit A, putative
Gambia2008 vs Cambodia	PF3D7_0705500	271717	inositol-phosphate phosphatase, putative
Gambia2008 vs Cambodia	PF3D7_0708000	370875	cytoskeleton associated protein, putative
Gambia2008 vs Cambodia	PF3D7_0708200	375770	conserved *Plasmodium* protein, unknown function
Gambia2008 vs Cambodia	PF3D7_1035300	1399259	glutamate-rich protein GLURP
Gambia2008 vs Cambodia	PF3D7_1035300	1399269	glutamate-rich protein GLURP
Gambia2008 vs Cambodia	PF3D7_1035300	1399377	glutamate-rich protein GLURP
Gambia2008 vs Cambodia	PF3D7_1035300	1399594	glutamate-rich protein GLURP
Gambia2008 vs Cambodia	PF3D7_1035300	1399613	glutamate-rich protein GLURP
Gambia2008 vs Cambodia	PF3D7_1035300	1399634	glutamate-rich protein GLURP
Gambia2008 vs Cambodia	PF3D7_1035300	1399656	glutamate-rich protein GLURP
Gambia2008 vs Cambodia	PF3D7_1035300	1399681	glutamate-rich protein GLURP
Gambia2008 vs Cambodia	PF3D7_1035300	1399819	glutamate-rich protein GLURP
Gambia2008 vs Cambodia	PF3D7_1035300	1400719	glutamate-rich protein GLURP
Gambia2008 vs Cambodia	PF3D7_1035300	1400727	glutamate-rich protein GLURP

Gambia2008 vs Cambodia	PF3D7_1035300	1401754	glutamate-rich protein GLURP
Gambia2008 vs Cambodia	PF3D7_1035300	1402417	glutamate-rich protein GLURP
Gambia2008 vs Cambodia	PF3D7_1035400	1404315	merozoite surface protein 3
Gambia2008 vs Cambodia	PF3D7_1035400	1405061	merozoite surface protein 4
Gambia2008 vs Cambodia	PF3D7_1035400	1405094	merozoite surface protein 5
Gambia2008 vs Cambodia	PF3D7_1035400	1405160	merozoite surface protein 6
Gambia2008 vs Cambodia	PF3D7_1035500	1407780	merozoite surface protein 6
Gambia2008 vs Cambodia	PF3D7_1035500	1407783	merozoite surface protein 7
Gambia2008 vs Cambodia	PF3D7_1035500	1407784	merozoite surface protein 8
Gambia2008 vs Cambodia	PF3D7_1035500	1407955	merozoite surface protein 9
Gambia2008 vs Cambodia	PF3D7_1035500	1408292	merozoite surface protein 10
Gambia2008 vs Cambodia	PF3D7_1035600	1410035	merozoite surface protein
Gambia2008 vs Cambodia	PF3D7_1035600	1410327	merozoite surface protein
Gambia2008 vs Cambodia	PF3D7_1035700	1413638	duffy binding-like merozoite surface protein
Gambia2008 vs Cambodia	PF3D7_1035700	1413652	duffy binding-like merozoite surface protein

Gambia2008 vs Cambodia	PF3D7_1035700	1413659	duffy binding-like merozoite surface protein
Gambia2008 vs Cambodia	PF3D7_1035700	1413669	duffy binding-like merozoite surface protein
Gambia2008 vs Cambodia	PF3D7_1035700	1414133	duffy binding-like merozoite surface protein
Gambia2008 vs Cambodia	PF3D7_1035700	1414244	duffy binding-like merozoite surface protein
Gambia2008 vs Cambodia	PF3D7_1035700	1414253	duffy binding-like merozoite surface protein
Gambia2008 vs Cambodia	PF3D7_1035700	1414265	duffy binding-like merozoite surface protein
Gambia2008 vs Cambodia	PF3D7_1035700	1414274	duffy binding-like merozoite surface protein
Gambia2008 vs Cambodia	PF3D7_1035700	1414286	duffy binding-like merozoite surface protein
Gambia2008 vs Cambodia	PF3D7_1035700	1414316	duffy binding-like merozoite surface protein
Gambia2008 vs Cambodia	PF3D7_1035700	1414332	duffy binding-like merozoite surface protein
Gambia2008 vs Cambodia	PF3D7_1035700	1414333	duffy binding-like merozoite surface protein
Gambia2008 vs Cambodia	PF3D7_1035700	1414440	duffy binding-like merozoite surface protein
Gambia2008 vs Cambodia	PF3D7_1035700	1414537	duffy binding-like merozoite surface protein
Gambia2008 vs Cambodia	PF3D7_1035700	1414598	duffy binding-like merozoite surface protein
Gambia2008 vs Cambodia	PF3D7_1035700	1414617	duffy binding-like merozoite surface protein

Gambia2008 vs Cambodia	PF3D7_1035700	1414838	duffy binding-like merozoite surface protein
Gambia2008 vs Cambodia	PF3D7_1035700	1415066	duffy binding-like merozoite surface protein
Gambia2008 vs Cambodia	PF3D7_1035700	1415182	duffy binding-like merozoite surface protein
Gambia2008 vs Cambodia	PF3D7_1036300	1433436	duffy binding-like merozoite surface protein 2
Gambia2008 vs Cambodia	PF3D7_1036300	1433586	duffy binding-like merozoite surface protein 3
Gambia2008 vs Cambodia	PF3D7_1036300	1433757	duffy binding-like merozoite surface protein 4
Gambia2008 vs Cambodia	PF3D7_1036300	1433921	duffy binding-like merozoite surface protein 5
Gambia2008 vs Cambodia	PF3D7_1036300	1433950	duffy binding-like merozoite surface protein 6
Gambia2008 vs Cambodia	PF3D7_1037200	1476249	conserved *Plasmodium* protein, unknown function
Gambia2014/15 vs Cambodia	PF3D7_1036000	1427333	merozoite surface protein 11
Gambia2014/15 vs Cambodia	PF3D7_1036000	1427595	merozoite surface protein 12
Gambia2014/15 vs Cambodia	PF3D7_1036000	1427674	merozoite surface protein 13
Gambia2014/15 vs Cambodia	PF3D7_1036300	1432783	duffy binding-like merozoite surface protein 2
Gambia2014/15 vs Cambodia	PF3D7_1036300	1433599	duffy binding-like merozoite surface protein 3
Gambia2014/15 vs Cambodia	PF3D7_1036300	1433613	duffy binding-like merozoite surface protein 4

Gambia2014/15 vs Cambodia	PF3D7_1036300	1433619	duffy binding-like merozoite surface protein 5
Gambia2014/15 vs Cambodia	PF3D7_1036300	1433627	duffy binding-like merozoite surface protein 6
Gambia2014/15 vs Cambodia	PF3D7_1036300	1433638	duffy binding-like merozoite surface protein 7
Gambia2014/15 vs Cambodia	PF3D7_1036300	1433650	duffy binding-like merozoite surface protein 8
Gambia2014/15 vs Cambodia	PF3D7_1036300	1433694	duffy binding-like merozoite surface protein 9
Gambia2014/15 vs Cambodia	PF3D7_1036300	1433766	duffy binding-like merozoite surface protein 10
Gambia2014/15 vs Cambodia	PF3D7_1036300	1433812	duffy binding-like merozoite surface protein 11
Gambia2014/15 vs Cambodia	PF3D7_1036300	1433871	duffy binding-like merozoite surface protein 12
Gambia2014/15 vs Cambodia	PF3D7_1036300	1433893	duffy binding-like merozoite surface protein 13
Gambia2014/15 vs Cambodia	PF3D7_1036300	1433926	duffy binding-like merozoite surface protein 14
Gambia2014/15 vs Cambodia	PF3D7_1036300	1434014	duffy binding-like merozoite surface protein 15
Gambia2014/15 vs Cambodia	PF3D7_1036300	1434023	duffy binding-like merozoite surface protein 16
Gambia2014/15 vs Cambodia	PF3D7_1036300	1434028	duffy binding-like merozoite surface protein 17
Gambia2014/15 vs Cambodia	PF3D7_1036300	1434038	duffy binding-like merozoite surface protein 18
Gambia2014/15 vs Cambodia	PF3D7_1036300	1434045	duffy binding-like merozoite surface protein 19

Gambia2014/15 vs Cambodia	PF3D7_1036300	1434069	duffy binding-like merozoite surface protein 20
Gambia2014/15 vs Cambodia	PF3D7_1036300	1434072	duffy binding-like merozoite surface protein 21
Gambia2014/15 vs Cambodia	PF3D7_1036300	1434077	duffy binding-like merozoite surface protein 22
Gambia2014/15 vs Cambodia	PF3D7_1036300	1434080	duffy binding-like merozoite surface protein 23
Gambia2014/15 vs Cambodia	PF3D7_1036300	1434089	duffy binding-like merozoite surface protein 24
Gambia2014/15 vs Cambodia	PF3D7_1036300	1434091	duffy binding-like merozoite surface protein 25
Gambia2014/15 vs Cambodia	PF3D7_1036300	1434092	duffy binding-like merozoite surface protein 26
Gambia2014/15 vs Cambodia	PF3D7_1036300	1434096	duffy binding-like merozoite surface protein 27
Gambia2014/15 vs Cambodia	PF3D7_1036300	1434098	duffy binding-like merozoite surface protein 28
Gambia2014/15 vs Cambodia	PF3D7_1036300	1434103	duffy binding-like merozoite surface protein 29
Gambia2014/15 vs Cambodia	PF3D7_1036300	1434106	duffy binding-like merozoite surface protein 30
Gambia2014/15 vs Cambodia	PF3D7_1036300	1434109	duffy binding-like merozoite surface protein 31
Gambia2014/15 vs Cambodia	PF3D7_1036300	1434129	duffy binding-like merozoite surface protein 32
Gambia2014/15 vs Cambodia	PF3D7_1036300	1434268	duffy binding-like merozoite surface protein 33
Gambia2014/15 vs Cambodia	PF3D7_1036300	1434271	duffy binding-like merozoite surface protein 34

Gambia2014/15 vs Cambodia	PF3D7_1036300	1434553	duffy binding-like merozoite surface protein 35
Gambia2014/15 vs Cambodia	PF3D7_1036500	1443005	conserved *Plasmodium* protein, unknown function
Gambia2014/15 vs Cambodia	PF3D7_1036800	1449581	acetyl-CoA transporter, putative
Gambia2014/15 vs Cambodia	PF3D7_1036800	1449646	acetyl-CoA transporter, putative
Gambia2014/15 vs Cambodia	PF3D7_1036900	1453956	conserved *Plasmodium* protein, unknown function
Gambia2014/15 vs Cambodia	PF3D7_1036900	1456037	conserved *Plasmodium* protein, unknown function
Gambia2014/15 vs Cambodia	PF3D7_1036900	1456547	conserved *Plasmodium* protein, unknown function
Gambia2014/15 vs Cambodia	PF3D7_1037000	1467904	DNA polymerase zeta catalytic subunit, putative
Gambia2014/15 vs Cambodia	PF3D7_1037000	1468031	DNA polymerase zeta catalytic subunit, putative
Gambia2014/15 vs Cambodia	PF3D7_1037000	1468943	DNA polymerase zeta catalytic subunit, putative
Gambia2014/15 vs Cambodia	PF3D7_1037100	1470239	pyruvate kinase 2
Gambia2014/15 vs Cambodia	PF3D7_1037100	1471050	pyruvate kinase 3
Gambia2014/15 vs Cambodia	PF3D7_1037200	1475201	conserved *Plasmodium* protein, unknown function
Gambia2014/15 vs Cambodia	PF3D7_1037400	1481988	conserved *Plasmodium* protein, unknown function
Gambia2014/15 vs Cambodia	PF3D7_1037400	1484939	conserved *Plasmodium* protein, unknown function

Gambia2014/15 vs Cambodia	PF3D7_1037400	1485068	conserved *Plasmodium* protein, unknown function

Table 8.3: Loci significantly associated with drugs using parametric test

Gene ID	Position	Drug	*P* value	Description
PF3D7_0622800	923440	lumefantrine	1.85E-12	leucine--tRNA ligase, putative
PF3D7_0929400	1180235	lumefantrine	1.85E-12	high molecular weight rhoptry protein 2
PF3D7_1362800	2524059	lumefantrine	1.85E-12	conserved *Plasmodium* protein, unknown function
PF3D7_1112300	473653	lumefantrine	3.04E-11	conserved *Plasmodium* protein, unknown function
PF3D7_0615900	662585	lumefantrine	4.21E-11	protein phosphatase, putative
PF3D7_1115700	593492	lumefantrine	4.21E-11	cysteine proteinase falcipain 2a
PF3D7_1454200	2223179	lumefantrine	4.21E-11	conserved *Plasmodium* protein, unknown function
PF3D7_0113800	530379	lumefantrine	6.97E-11	DBL containing protein, unknown function
PF3D7_1462400	2535489	lumefantrine	6.97E-11	conserved *Plasmodium* protein, unknown function
PF3D7_1112600	479878	lumefantrine	8.43E-10	ATPase, putative
PF3D7_0619100	798471	lumefantrine	3.52E-09	conserved *Plasmodium* protein, unknown function
PF3D7_0617300	720582	lumefantrine	1.11E-08	conserved *Plasmodium* protein, unknown function
PF3D7_1422400	904801	lumefantrine	1.40E-08	conserved *Plasmodium* protein, unknown function

PF3D7_0721600	931663	lumefantrine	1.42E-08	40S ribosomal protein S5, putative
PF3D7_0821100	953603	lumefantrine	1.42E-08	protein kinase 1
PF3D7_0613600	555968	lumefantrine	3.58E-08	conserved *Plasmodium* protein, unknown function
PF3D7_0613900	585834	lumefantrine	3.58E-08	myosin E, putative
PF3D7_1029100	1192814	lumefantrine	3.58E-08	conserved *Plasmodium* membrane protein, unknown function
PF3D7_1133400	1295032	lumefantrine	3.58E-08	apical membrane antigen 1
PF3D7_0306100	92778	lumefantrine	4.03E-08	conserved *Plasmodium* protein, unknown function
PF3D7_0909100	416478	lumefantrine	4.50E-08	conserved *Plasmodium* membrane protein, unknown function
PF3D7_1473100	2976440	lumefantrine	5.09E-08	GTPase-activating protein, putative
PF3D7_0615400	637100	lumefantrine	5.93E-08	ribonuclease, putative
PF3D7_0615900	664695	lumefantrine	5.93E-08	protein phosphatase, putative
PF3D7_0620000	842964	lumefantrine	5.93E-08	PIMMS43 protein
PF3D7_0826500	1155838	lumefantrine	5.93E-08	ubiquitin conjugation factor E4 B, putative
PF3D7_1319200	792970	lumefantrine	6.21E-08	conserved Plasmodium protein, unknown function
PF3D7_0809600	489196	lumefantrine	3.39E-07	peptidase family C50, putative
PF3D7_1457700	2368133	lumefantrine	4.17E-07	large ribosomal subunit nuclear export factor, putative

PF3D7_0807900	403762	lumefantrine	4.63E-07	tyrosine--tRNA ligase
PF3D7_1352300	2084135	lumefantrine	5.84E-07	conserved *Plasmodium* protein, unknown function
PF3D7_1312400	523206	lumefantrine	5.85E-07	translation initiation factor IF-2, putative
PF3D7_0511300	477900	lumefantrine	7.07E-07	MORN repeat protein, putative
PF3D7_1343800	1746601	lumefantrine	1.19E-06	conserved *Plasmodium* protein, unknown function
PF3D7_1477500	3189316	lumefantrine	1.19E-06	*Plasmodium* exported protein (PHISTb), unknown function
PF3D7_0708400	384293	lumefantrine	1.43E-06	heat shock protein 90
PF3D7_0709100	411244	lumefantrine	1.71E-06	Cg1 protein
PF3D7_0709100	411281	lumefantrine	1.71E-06	Cg1 protein
PF3D7_0709100	411301	lumefantrine	1.71E-06	Cg1 protein
PF3D7_0709100	411352	lumefantrine	1.71E-06	Cg1 protein
PF3D7_0419500	868072	lumefantrine	2.29E-06	conserved *Plasmodium* membrane protein, unknown function
PF3D7_1362700	2510569	lumefantrine	3.01E-06	conserved *Plasmodium* protein, unknown function
PF3D7_0311200	476185	lumefantrine	3.34E-06	valine--tRNA ligase, putative
PF3D7_0311600	501133	lumefantrine	3.34E-06	dolichyl-diphosphooligosaccharide-protein glycosyltransferase subunit OST1, putative

PF3D7_0313900	563004	lumefantrine	3.34E-06	conserved *Plasmodium* protein, unknown function
PF3D7_0301600	563543	lumefantrine	3.34E-06	*Plasmodium* exported protein (hyp1), unknown function
PF3D7_0107800	324294	lumefantrine	3.98E-06	double-strand break repair protein MRE11
PF3D7_1021800	900216	lumefantrine	3.98E-06	schizont egress antigen-1
PF3D7_0306100	290609	lumefantrine	4.05E-06	conserved *Plasmodium* protein, unknown function
PF3D7_1338700	1561299	lumefantrine	4.72E-06	conserved protein, unknown function
PF3D7_1339700	1592828	lumefantrine	4.72E-06	conserved *Plasmodium* protein, unknown function
PF3D7_1341500	1640137	lumefantrine	4.72E-06	inner membrane complex suture component, putative
PF3D7_1347200	1891015	lumefantrine	4.72E-06	nucleoside transporter 1
PF3D7_1350700	2023349	lumefantrine	4.72E-06	N6-adenine-specific methylase, putative
PF3D7_1351800	2066138	lumefantrine	4.72E-06	conserved *Plasmodium* protein, unknown function
PF3D7_1474200	3030786	lumefantrine	4.72E-06	conserved *Plasmodium* membrane protein, unknown function
PF3D7_1475200	3082620	lumefantrine	4.72E-06	conserved protein, unknown function
PF3D7_1477600	3199459	lumefantrine	4.72E-06	surface-associated interspersed protein 14.1 (SURFIN 14.1)
PF3D7_1402700	96603	lumefantrine	5.82E-06	U2 snRNP-associated SURP motif-containing protein, putative
PF3D7_0216900	702777	dihydroartemisinin	4.62E-09	conserved *Plasmodium* protein, unknown function

PF3D7_0303700	191556	dihydroartemisinin	3.00E-06	lipoamide acyltransferase component of branched-chain alpha-keto acid dehydrogenase complex
PF3D7_0307900	350260	dihydroartemisinin	5.78E-06	conserved *Plasmodium* protein, unknown function
PF3D7_0309900	414557	dihydroartemisinin	1.44E-06	conserved *Plasmodium* protein, unknown function
PF3D7_0418100	813649	dihydroartemisinin	2.75E-06	protein SOC1, putative
PF3D7_0420000	897099	dihydroartemisinin	8.11E-11	zinc finger protein, putative
PF3D7_0531100	1278385	dihydroartemisinin	4.16E-07	conserved *Plasmodium* protein, unknown function
PF3D7_0501000	56432	dihydroartemisinin	5.18E-06	*Plasmodium* exported protein, unknown function
PF3D7_0514200	599322	dihydroartemisinin	4.60E-07	conserved *Plasmodium* protein, unknown function
PF3D7_0518100	754696	dihydroartemisinin	2.86E-10	protein AMR2
PF3D7_0619800	835044	dihydroartemisinin	3.05E-11	conserved *Plasmodium* membrane protein, unknown function
PF3D7_0728700	1226141	dihydroartemisinin	5.68E-06	alpha/beta hydrolase, putative
PF3D7_0731500	1358730	dihydroartemisinin	1.13E-06	erythrocyte binding antigen-175
PF3D7_0711500	506669	dihydroartemisinin	2.37E-06	regulator of chromosome condensation, putative
PF3D7_0825900	1107895	dihydroartemisinin	1.03E-06	conserved *Plasmodium* protein, unknown function
PF3D7_0826100	1115815	dihydroartemisinin	1.09E-07	HECT-like E3 ubiquitin ligase, putative

PF3D7_0925800	1037823	dihydroartemisinin	1.19E-10	regulator of nonsense transcripts 2, putative
PF3D7_0924500	996462	dihydroartemisinin	3.38E-06	conserved *Plasmodium* membrane protein, unknown function
PF3D7_1031600	1277622	dihydroartemisinin	5.66E-09	protein GEXP15
PF3D7_1037100	1471050	dihydroartemisinin	8.56E-08	pyruvate kinase 2
PF3D7_1131400	1204563	dihydroartemisinin	5.24E-06	conserved *Plasmodium* protein, unknown function
PF3D7_1108000	354205	dihydroartemisinin	2.04E-07	IWS1-like protein, putative
PF3D7_1356800	2256607	dihydroartemisinin	2.07E-06	serine/threonine protein kinase ARK3, putative
PF3D7_1361300	2462918	dihydroartemisinin	9.41E-07	conserved Plasmodium protein, unknown function
PF3D7_1444800	1844839	dihydroartemisinin	2.86E-10	fructose-bisphosphate aldolase
PF3D7_1464500	2611458	dihydroartemisinin	1.22E-14	conserved *Plasmodium* membrane protein, unknown function
PF3D7_1409600	375235	dihydroartemisinin	1.04E-09	conserved *Plasmodium* protein, unknown function
PF3D7_0415800	694287	artemether	3.61E-08	RING zinc finger protein, putative
PF3D7_0518100	754696	artemether	5.02E-16	protein AMR2
PF3D7_0721000	905988	artemether	3.89E-11	conserved *Plasmodium* membrane protein, unknown function
PF3D7_0804300	242815	artemether	7.17E-08	zinc finger protein, putative
PF3D7_0924600	1005253	artemether	3.49E-07	conserved *Plasmodium* protein, unknown function

PF3D7_0928200	1140161	artemether	7.17E-08	conserved *Plasmodium* protein, unknown function
PF3D7_1140600	1619808	artemether	6.36E-08	conserved *Plasmodium* protein, unknown function
PF3D7_1149200	1976796	artemether	2.92E-17	ring-infected erythrocyte surface antigen
PF3D7_1149200	1976807	artemether	2.92E-17	ring-infected erythrocyte surface antigen
PF3D7_1149200	1977194	artemether	2.92E-17	ring-infected erythrocyte surface antigen
PF3D7_1356000	2221832	artemether	7.01E-08	conserved *Plasmodium* protein, unknown function
PF3D7_1369400	2767112	artemether	7.17E-08	conserved *Plasmodium* protein, unknown function
PF3D7_1439300	1598494	artemether	5.37E-09	Sad1/UNC domain-containing protein, putative
PF3D7_1444800	1844839	artemether	5.02E-16	fructose-bisphosphate aldolase
PF3D7_1453400	2189487	artemether	3.61E-08	gamma-tubulin complex component, putative
PF3D7_1420500	851461	artemether	1.53E-08	protein GPR89, putative
PF3D7_0210300	423435	amodiaquine	6.14E-08	monocarboxylate transporter, putative
PF3D7_0310000	420780	amodiaquine	3.73E-09	50S ribosomal protein L9, apicoplast, putative
PF3D7_0319400	812699	amodiaquine	1.29E-18	kinesin-8X
PF3D7_0501800	91908	amodiaquine	1.04E-07	chromatin assembly factor 1 subunit A
PF3D7_0604600	202296	amodiaquine	5.80E-06	DNA helicase, putative

PF3D7_0918700	770345	amodiaquine	5.28E-07	conserved *Plasmodium* protein, unknown function
PF3D7_1032900	1318709	amodiaquine	1.78E-08	RNA polymerase II-associated protein 1, putative
PF3D7_1009600	387813	amodiaquine	5.28E-07	protein phosphatase PPM10, putative
PF3D7_1009800	397765	amodiaquine	5.28E-07	conserved *Plasmodium* membrane protein, unknown function
PF3D7_1140900	1639674	amodiaquine	1.29E-18	conserved *Plasmodium* protein, unknown function
PF3D7_1105900	254794	amodiaquine	5.80E-06	conserved *Plasmodium* membrane protein, unknown function
PF3D7_1403300	124379	amodiaquine	5.28E-07	tetratricopeptide repeat protein, putative
PF3D7_1447800	1952994	amodiaquine	1.82E-06	calponin homology domain-containing protein, putative

Table 8.4: Loci presented as outliers with association to drugs using the MLM (GWAS) model

Gene ID	Position	Drug	*P* value	Description
PF3D7_0113800	529726	lumefantrine	3.70E-05	DBL containing protein, unknown function
PF3D7_0409000	433629	lumefantrine	0.000719182	conserved *Plasmodium* protein, unknown function
PF3D7_0409000	433645	lumefantrine	0.000719182	conserved *Plasmodium* protein, unknown function
PF3D7_0504800	192222	lumefantrine	0.000907289	conserved *Plasmodium* protein, unknown function
PF3D7_0727000	1193645	lumefantrine	2.36E-05	vacuolar protein sorting-associated protein 53, putative
PF3D7_0727800	844728	lumefantrine	0.000422861	cation transporting ATPase, putative
PF3D7_0728100	1179033	lumefantrine	0.000492275	anaphase-promoting complex subunit 1, putative
PF3D7_0717600	1148859	lumefantrine	0.000515814	conserved *Plasmodium* protein, unknown function
PF3D7_0719300	761656	lumefantrine	0.000747392	actin-related protein, putative
PF3D7_1035100	1413638	lumefantrine	9.32E-05	probable protein, unknown function
PF3D7_1035700	1392698	lumefantrine	0.000124777	duffy binding-like merozoite surface protein
PF3D7_1035700	1413652	lumefantrine	0.000167075	duffy binding-like merozoite surface protein
PF3D7_1124500	968081	lumefantrine	0.000217357	pyruvate dehydrogenase E1 component subunit alpha

PF3D7_1313800	595379	lumefantrine	9.93E-05	conserved *Plasmodium* membrane protein, unknown function
PF3D7_1402800	101422	lumefantrine	9.67E-05	conserved *Plasmodium* protein, unknown function
PF3D7_0113800	527210	dihydroartemisinin	0.00099502	DBL containing protein, unknown function
PF3D7_0424400	1106026	dihydroartemisinin	7.70E-05	surface-associated interspersed protein 4.2 (SURFIN 4.2)
PF3D7_0511500	510223	dihydroartemisinin	0.00067754	RNA pseudouridylate synthase, putative
PF3D7_0724900	1052943	dihydroartemisinin	0.00031724	kinesin-20, putative
PF3D7_0929700	1186104	dihydroartemisinin	0.00012898	conserved Plasmodium protein, unknown function
PF3D7_1134000	1321097	dihydroartemisinin	3.11E-05	heat shock protein 70
PF3D7_1139300	1558936	dihydroartemisinin	0.00083209	AP2 domain transcription factor, putative
PF3D7_1228900	1185255	dihydroartemisinin	0.0002608	conserved *Plasmodium* protein, unknown function
PF3D7_1229100	1196073	dihydroartemisinin	0.00046236	multidrug resistance-associated protein 2
PF3D7_1339700	1596082	dihydroartemisinin	0.00063903	conserved *Plasmodium* protein, unknown function
PF3D7_1345200	1813639	dihydroartemisinin	0.0001168	rhomboid protease ROM6, putative
PF3D7_1322300	945088	dihydroartemisinin	0.00033281	conserved *Plasmodium* protein, unknown function
PF3D7_1430600	1208789	dihydroartemisinin	0.00023906	endonuclease/exonuclease/phosphatase family protein, putative
PF3D7_1418100	771557	dihydroartemisinin	0.00027874	liver specific protein 1, putative

PF3D7_0104300	196981	artemether	0.00034698	ubiquitin carboxyl-terminal hydrolase 1, putative
PF3D7_0308100	360645	artemether	0.00010422	zinc finger protein, putative
PF3D7_0405000	270767	artemether	0.00087152	ATP-dependent RNA helicase DDX51, putative
PF3D7_0414100	635669	artemether	0.00015963	conserved *Plasmodium* membrane protein, unknown function
PF3D7_0506000	256454	artemether	2.82E-05	conserved *Plasmodium* protein, unknown function
PF3D7_0604600	202296	artemether	0.00091826	DNA helicase, putative
PF3D7_0609300	396298	artemether	0.00054504	conserved *Plasmodium* protein, unknown function
PF3D7_0707700	358324	artemether	0.00031264	E3 ubiquitin-protein ligase, putative
PF3D7_0718800	834393	artemether	0.00020047	conserved *Plasmodium* protein, unknown function
PF3D7_0824800	1079292	artemether	2.44E-05	conserved *Plasmodium* membrane protein, unknown function
PF3D7_0824900	1082495	artemether	2.37E-05	conserved *Plasmodium* protein, unknown function
PF3D7_0826200	1143515	artemether	0.00027853	alpha/beta hydrolase, putative
PF3D7_0805800	323295	artemether	0.00060047	conserved *Plasmodium* protein, unknown function
PF3D7_0902600	115178	artemether	0.0004322	serine/threonine protein kinase, FIKK family
PF3D7_0911300	520326	artemether	0.00074947	cysteine repeat modular protein 1
PF3D7_0902000	90178	artemether	0.00087152	serine/threonine protein kinase, FIKK family

PF3D7_1027300	1141473	artemether	1.07E-05	peroxiredoxin
PF3D7_1027600	1149278	artemether	2.82E-05	meiotic recombination protein SPO11-2, putative
PF3D7_1034500	1374986	artemether	7.45E-05	conserved *Plasmodium* protein, unknown function
PF3D7_1037200	1475201	artemether	5.28E-05	conserved *Plasmodium* protein, unknown function
PF3D7_1039000	1569809	artemether	2.07E-05	serine/threonine protein kinase, FIKK family
PF3D7_1018000	720024	artemether	1.86E-05	tRNA pseudouridine synthase, putative
PF3D7_1127800	1078263	artemether	0.00050827	TFIIS central domain-containing protein, putative
PF3D7_1138800	1539483	artemether	0.00026401	WD repeat-containing protein, putative
PF3D7_1139300	1559197	artemether	0.00039713	AP2 domain transcription factor, putative
PF3D7_1113000	501783	artemether	0.00020321	conserved *Plasmodium* protein, unknown function
PF3D7_1121300	802610	artemether	0.00013269	tyrosine kinase-like protein
PF3D7_1121700	822260	artemether	0.00061755	protein GCN20
PF3D7_1231800	1316485	artemether	0.00035431	asparagine-rich protein, putative
PF3D7_1245200	1890235	artemether	0.00072335	conserved *Plasmodium* membrane protein, unknown function
PF3D7_1203900	195381	artemether	0.00061858	ubiquitin-conjugating enzyme E2
PF3D7_1218200	712024	artemether	5.30E-05	symplekin domain-containing protein, putative

PF3D7_1328400	1200911	artemether	0.00030311	conserved protein, unknown function
PF3D7_1331100	1300835	artemether	5.28E-05	DNA polymerase theta, putative
PF3D7_1303300	163562	artemether	0.00035972	conserved *Plasmodium* protein, unknown function
PF3D7_1351700	2061301	artemether	0.00079989	inner membrane complex protein 1f, putative
PF3D7_1359400	2360342	artemether	2.80E-06	CUGBP Elav-like family member 1
PF3D7_1359600	2372908	artemether	2.80E-06	conserved *Plasmodium* protein, unknown function
PF3D7_1308400	386554	artemether	0.00085634	conserved *Plasmodium* protein, unknown function
PF3D7_1313500	577753	artemether	0.00070827	conserved *Plasmodium* membrane protein, unknown function
PF3D7_1313800	594841	artemether	0.00010264	conserved *Plasmodium* membrane protein, unknown function
PF3D7_1440500	1654114	artemether	0.00080188	allantoicase, putative
PF3D7_1417100	690978	artemether	0.00042617	conserved *Plasmodium* protein, unknown function
PF3D7_0527600	1147408	amodiaquine	0.000968428	conserved *Plasmodium* protein, unknown function
PF3D7_0807700	398723	amodiaquine	0.000941268	serine protease DegP